Technische Universität Berlin

Fakultät II
Institut für theoretische Physik

Zertifikat seit 2008
audit familiengerechte
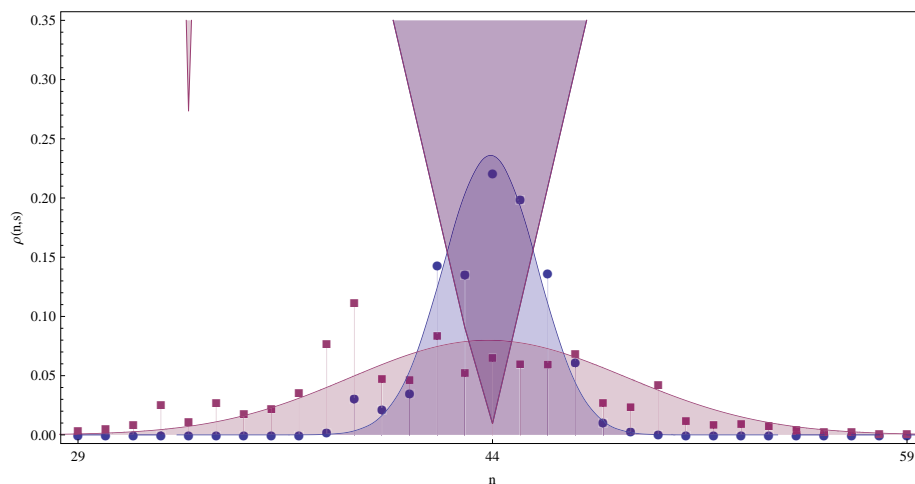hochschule

berlin

DIPLOMARBEIT

Full Counting Statistics

in the time independent Quantum Master Equation approach

Supervisor: Prof. Dr. Tobias Brandes
Author: Moritz Schubotz
Date: March 29, 2011

Moritz Schubotz
(Matrikel Nummer 232 996)
Institut für theoretische Physik
Technische Universität Berlin
Hardenbergstr. 36
D-10623 Berlin

The formal frame of this thesis i.e. management summary, acknowledge was written in german. The english content part starts with the table of contents on page xiii.

Der formale Rahmen dieser Diplomarbeit, bestehend aus Zusammenfassung, Danksagung, Selbstständigkeitserlärung und Vorwort ist gemäß der Bestimmungen des Prüfungsamts der Technischen Universität Berlin in deutscher Sprache verfasst worden.

Dieser Teil endet unmittelbar vor dem Inhaltsverzeichnis auf Seite xiii.

Da sich der inhaltliche Teil an ein internationales Fachpublikum richtet, wurde dieser in Englisch verfasst.

Diese Diplomarbeit ist der Einheit von
Lehre und Forschung
gewidmet.

Zusammenfassung

Der heutige Alltag wird dominiert von elektrischen und elektronischen Geräten, deren Funktionsweise auf dem Fluss von elektrischem Strom basiert. Stromfluss wird in Ampere gemessen. Ein Stromfluss von einem Ampere bedeutet, dass sich 6.241.509.647.120.418.000 Elektronen pro Sekunde durch ein Kabel oder Ähnliches bewegen. Selbst bei Geräten, denen umgangssprachlich ein geringer Stromverbrauch zugeschrieben wird, beispielsweise der Standby-Leuchtdiode eines Fernsehers, liegt ein Stromfluss im Bereich von einigen mA vor. Dies bedeutet, dass sich die Anzahl der durch die Leuchtdiode fließenden Elektronen auf einige Billiarden Elektronen pro Sekunde, also ein Tausendstel der oben angegebenen Zahl, reduziert. Bei derart großen Stromflüssen sind selbst Schwankungen um einige Millionen Elektronen pro Sekunde kaum messbar. Sie haben folglich auch keine Auswirkungen auf die Funktionsweise der Geräte.

Die rasanten Fortschritte in Nanotechnologie und Messtechnik haben es jedoch ermöglicht, sehr kleine Strukturen herzustellen und den Stromfluss in extrem kurzen Zeitintervallen zu messen. Dabei ist es sogar möglich die Elektronen einzeln zu detektieren.

Bei dieser detaillierten Betrachtung der speziellen Nanostrukturen liefert die Angabe des Stroms eine unzureichende Beschreibung der Gegebenheiten, da sich hier Schwankungen des Stroms stark bemerkbar machen. Um eine geeignete Beschreibung zu finden, wurde in den letzten Jahrzehnten die Methode der **Full Counting Statistics** entwickelt.

Hierbei werden neben dem Erwartungswert der geflossenen Elektronen, welcher für die Berechnung des klassischen Stroms hinreichend war, zusätzlich noch die Standardabweichung, die Schiefheit, die Steilheit sowie weitere Verteilungsmomente der geflossenen Elektronen angegeben. Demzufolge entsteht eine vollständige Wahrscheinlichkeitsverteilung (Full Counting Statistics) für die Anzahl der geflossenen Teilchen nach einer bestimmten Zeit.

Diese Wahrscheinlichkeitsverteilung wurde auch von Seiten der theoretischen Physik erklärt, wobei folgendes Modell angenommen wurde.

Elektronen fließen aus einem klassischen, makroskopischen Reservoir, durch eine Nanostruktur, in ein anderes makroskopisches Reservoir. Dabei ist die Nanostruktur als so klein anzusehen, dass hier quantenmechanische Effekte berücksichtigt werden müssen. Zur einfacheren Orientierung bezeichnet man

die Quelle der Elektronen als linkes Bad, das Ziel als rechtes Bad und die Nanostruktur in der Mitte als System.

In der üblichen theoretischen Beschreibung wird die Verbindung zwischen System und Bad durch eine konstante Tunnelrate beschrieben. Diese Tunnelrate gibt an, wie viele Elektronen in einer bestimmten Zeit vom Bad ins System tunneln.

In der vorliegenden Arbeit wird hingegen angenommen, dass diese Tunnelraten sich nach jedem Tunnelvorgang ändern können. Die Tunnelraten sind demzufolge nicht länger konstant.

Aus dieser neuen Betrachtung wird im ersten Teil der Arbeit eine verallgemeinerte Mastergleichung hergeleitet, die für konstante Tunnelraten, mit der bekannten n-aufgelösten Mastergleichung übereinstimmt. Diese hergeleitete Mastergleichung beschreibt das Verhalten des Systems und ermöglicht es, unter Verwendung von bekannten Rechenverfahren, auf den Strom und die Wahrscheinlichkeitsverteilung der geflossenen Teilchen zu schließen. Diese Rechenverfahren werden im ersten Teil diskutiert und für ihre Anwendung im zweiten Teil der Arbeit optimiert.

Im zweiten Teil der Arbeit wird, die in der Festkörperphysik übliche Annahme getroffen, dass die Tunnelraten statistisch verteilt sind. Nach jedem Tunnelprozess wird quasi eine neue Rate 'gewürfelt'. Unter dieser Annahme wird dann die Full Counting Statistic für die bekannten Nanostrukturen Quantenpunktkontakt, Quantenpunkt und Doppelquantenpunkt berechnet.

Dabei stellt sich heraus, dass für Systeme ohne relevante interne Dynamik (Quantenpunkt und Quantenpunktkontakt) die Bekannte Formel für den Strom verwendet werden kann. Allerdings müssen in dieser bekannten Formel für konstante Tunnelraten die inversen Tunnelraten durch den Mittelwert der inversen Tunnelraten ersetzt werden. Der Mittelwert der inversen Rate, der mathematisch als erstes negatives Verteilungsmoment definiert werden kann, wird aus Gründen der Anschaulichkeit als **Wartezeit** bezeichnet. Dieses erste wichtige Ergebnis, für den Strom bei Systemen ohne relevante interne Systemdynamik, kann mit folgendem Beispiel aus dem Alltag verglichen werden:

> Stellt man sich beispielsweise eine Fertigungslinie in einer Fabrik vor und betrachtet dort einen Fertigungsprozess, der aus mehreren sequentiell ablaufenden Schritten besteht. Der Erwartungswert der für den Fertigungsprozess benötigten Zeit, ist gleich der Summe der Erwartungswerte der Zeiten für die Teilschritte. Der Kehrwert dieser Zeit die zu erwartende Fertigungsrate. Die Berechnung der mittlere Fertigungsrate aus den mittleren Raten für die Teilschritte ist offensichtlich unmöglich.

Bezogen auf den Elektronenstrom bedeutet dies, dass die Wartezeiten (und nicht die Tunnelraten) die kanonischen Größen zur Beschreibung des Stroms darstellen.

Im Fall des Doppelquantenpunkts, bei dem die interne Systemdynamik eine entscheidende Rolle spielt und quantenmechanische Effekte berücksichtigt werden

müssen, stellt man fest, dass der Strom nicht mehr alleine durch die Mittelwerte der Wartezeiten ausgedrückt werden kann.

Hier müssen sowohl negative als auch positive Verteilungsmomente zur Berechnung verwendet werden, da sehr kleine Tunnelraten zu sehr großen Wartezeiten führen und umgekehrt. Betrachtet man Verteilungen, die in der Nähe der Rate null (entspricht einer sehr langen Wartezeit) einen messbar großen Wert annehmen, so wird der Stromfluss zunehmend geringer. Für bestimmte Verteilungen kann es sogar dazu kommen, dass der Erwartungswert des Stroms null wird, also der Stromfluss stoppt.

Dies ist ein deutlicher Unterschied zum Fall der Systeme ohne interne Dynamik, bei denen der Erwartungswert des Stroms selbst bei endlichen Wahrscheinlichkeiten für beliebig große, aber endliche, Wartezeiten konstant bleibt.

Im dritten Teil der Arbeit wird, die im ersten Teil hergeleitete, verallgemeinerte Mastergleichung auf spezielle Fälle für deterministische Tunnelraten angewendet. Es wird beispielsweise untersucht, wie sich ein System verhält, bei dem bis auf eine alle Tunnelraten konstant sind. Weiterhin wird ein System mit alternierenden Tunnelraten untersucht.

Abschließend wird eine Simulation vorgestellt, bei der Verfahren der Rückkopplungskontrolle auf das Quantenpunktkontaktsystem mit zufällig verteilten Tunnelraten angewendet werden.

Danksagung

Selbstständigkeitserklärung

Vorwort

Der inhaltliche Teil der Diplomarbeit ist in englischer Sprache verfasst.

Dabei wurde auf eine ausführliche Einführung der verwendeten theoretischen Konzepte verzichtet, da diese größenteils ausführlich in den Hauptdiplomsvorlesungen[1] zur theoretischen Physik behandelt werden. Die für das Verständnis der Arbeit wichtigsten Methoden sind jedoch im Anhang knapp zusammengefasst.

Bei der Gliederung der Arbeit wurde die Priorität auf die inhaltliche Struktur gelegt und nicht (wie allgemein üblich) auf Kapitel gleicher Länge. Dies soll den offenen Charakter der Fragestellung widerspiegeln.

Der inhaltliche Schwerpunkt dieser Arbeit liegt auf einer ausführlichen Diskussion der Beispiele für zufällige Tunnelraten (Kapitel 5).

Die Ausgestaltung der einzelnen Kapitel variiert erheblich. Insbesondere der Teil III der Arbeit ist weniger ausführlich gestaltet. Dem Author war es jedoch wichtig, dass auch die Überlegungen in der Diplomarbeit dokumentiert werden, die zum aktuellen Zeitpunkt nur peripher bedeutsam sind. Diese können als gute Basis für zukünftige Arbeiten dienen.

Kapitel 6.2 fasst die Teile I und II zusammen. Eine Veröffentlichung dieses Kapitels in Form eines Papers ist geplant. Ein Beginn mit Kapitel 6.2 oder dem Beispiels des Single Dots (Kapitel 5.2) bietet sich somit als Quereinstieg an.

Der Text sowie die Mathematica Quelltexte und Animationen stehen zusätzlich unter https://fcs.physikerwelt.de als Onlineversion zur Verfügung. Derzeit sind diese Inhalte nicht öffentlich einsehbar. Für interessierte Leser besteht jedoch die Möglichkeit einen Zugang einzurichten.

Kapitel die für den weiteren Verlauf der Arbeit nicht entscheidend sind, sind mit einem * gekennzeichnet.

---

[1] Eine Mitschrift der Vorlesungsreihe von *Prof. Dr. E. Schöll*, die mit Methoden des semantischen Internets aufgearbeitet wurde, kann auf der Webseite http://wiki.physikerwelt.de eingesehen und weiterbearbeitet werden.

Außerdem finden sich an dieser Stelle Ausschnitte aus Mitschschriften zu einer Vorlesung zur fortgeschrittenen Quantemechanikvorlesung von *Prof. Dr. T. Brandes* und zur Thermodynamikvorlesung von *Prof. Dr. A. Knorr*.

Das Projekt befindet sich derzeit in ein einem Teststadium. Die dort zu findenden Informationen sind nicht authorisiert.

Contents

Appendix   127

Part I

Full Counting Statistics in Master Equations

Chapter 1

Introduction

Nowadays electrical and electronic devices are an integral part of daily life. Their function is based on current flow, which is measured in Ampere. The current of one Ampere is equal to 6.241.509.647.120.418.000 electrons passing a conductor in the time interval of one second. Charge transport in electrical components, which can be seen as macroscopic systems, is described by the current. For these types of systems a repeating current measurement reading will not change if the overall setup is not being changed. So far this is a known fact.

Investigating smaller systems, where quantum effects occur, measurement readings of the current will fluctuate, even if the setup is not being changed. Therefore, it is no longer sufficient to characterize the current with a single value, like the average current. A more detailed description is required, based on single counts of electrons. From those counts, probabilities can be derived with regard to the amount of transported electrons per time interval. This method is called **Full Counting Statistic** (FCS).

Based on such investigations the field of Full Counting Statistics has been developed over the past decades [Levitov et al., 1996]. Full Counting Statistics investigates setups, where one ore more macroscopic reservoirs of electrons are connected to a microscopic quantum system. The main focus of recent investigations was to determine the connection between the macroscopic and microscopic system. As a result a constant tunneling rate was defined, which is the most effective way of description so far. This was done with respect to the assumption that the macroscopic system can not be influenced by the microscopic system.

In this thesis, the hypothesis that the tunneling rate is a constant value, was dropped. It is being assumed that the rate might change, when an electron has jumped from the reservoir to the microscopic system.

As a first step of the new approach, a **generalized** version of the **Quantum Master Equation** is derived. This equation describes the behavior of the quantum system and is the corner stone to obtain current and higher cumulants. Afterwards, a proceeding to calculate the Full Counting Statistics of random distributed rates is developed. As a prove of concept this new calcu-

lation method was applied to three microscopic systems setups. The results converged to the known case for tunnel rate distributions with a small variance.

It turns out that the inverse of the tunneling rate, which is called waiting time here, plays a fundamental role in this context, and is the canonical formalism to describe the Full Counting Statistics of mesoscopic systems with random behavior. For systems without internal dynamics, i.e. Tunneling Junction and Single Quantum Dot, the mean value of the average current is proportional to the inverse of the sum of the mean of the waiting times. This result is also obtained by replacing the waiting times in the formula for the constant rate current by their means. This leads to a false result. At this point it has to be mentioned that the calculations are done in sequential tunneling limit. With the consequence that there is always only one particle in the system. For these systems without internal dynamics, a comparison with the classical assembly line problem is possible. Thinking of one process, which consists of several sub processes. The average time for the process (which is the inverse of the average flow) is the sum of the averages for the sub processes. It is not possible to gain the average time (or rate) from a combination of the average rates.

Even more exciting are the results for the Double Quantum Dot, which involves internal system dynamics. It concludes that electrons can jump 'backwards and forwards' and enter coherent states. Here the results are separated from the case of constant rates. The current no longer only depends on the average waiting times, but rather on the relationship of negative and positive distribution moment of the waiting time, respectively inverse tunneling rate distribution. Especially, if the probability for small rates raises and the expectation value is fixed, the current decreases.

In the last part of this thesis, there are some considerations, how the formalism can be applied to special setups of deterministic tunneling rates. For example the influence of an impurity for a process with constant rates is investigated and the expected result is obtained.

Overview

The thesis consists of three parts, which are structured in nine chapters.

Part I treats the problem on a formal and abstract level.

In chapter 1 a general introduction to Full Counting Statistics and mesoscopic physics is given. The wide field of application of Full Counting Statistics is sketched and the economic relevance of its application in mesoscopic physics is pointed out.

In chapter 2 a new derivation for the n-resolved Quantum Master Equation with n-dependent transmission rates is developed. Therefore the Nakajima-Zwanzig Projection operator technique is used. Furthermore the Born-Markov Approximation is applied.

Independently from the derivation the n-dependent Quantum Master Equation is formally defined in chapter 3. The forms and representations of this equation are presented and the counting field is introduced. It is discussed, which approximations lead to good results in the long-time limit. Furthermore the known formulas for n-independent rates are derived as special case.

More demonstrative is part II. Random and uncorrelated tunneling rates are handled with explicit calculations there.

Chapter 4 shows, how to deal with random tunneling rates or waiting times in general. The proposed way, to replace the current and the higher cumulants by their expectation values, allows a procedure analogically to the case of constant rates.

The 5'th chapter is representing the main focus of this thesis. The procedure, developed in the former chapter, is applied to simple example setups with known results for constant rates.

Concluding, a summary of part I and II with a comparison between the systems follows in chapter 6.2. This summary is planned to be published in a paper and addresses the advanced reader.

Part III is the creative portion of this thesis.

In chapter 7 Tunneling Junction with constant rates, with the exception of one impurity, is described and the time-resolved Full Counting Statistics is explicitly calculated.

Chapter 8 comes up with the idea to use a Tunneling Junction with alternating rates to simulate the behavior of a Quantum Dot.

Finally, the 9'th chapter is said to be a thought provoking impuls to apply the methods of feedback control to random distributions. Therefore, a numerical simulation is deployed, which opens the question of the maximal feedback strength.

Dictionary

In the following a very brief explanation of some important terms is given in dictionary style.

Mesoscopics The default physics canon handles macroscopic objects as for example planets or billiard balls in the context of classical mechanics. Microscopic objects like the hydrogen atom are handled in the context of quantum mechanics.

This raises the question about the boundaries between both fields and creates the field of mesoscopic physics. In mesoscopic physics one is aware of quantum mechanical features, which occur, if a macroscopic object is scaled down to microscopic length scales. The length scale, where quantum mechanics effect occur, is about 100 nm. Consequently this field of research stands in connection to nanotechnology that has developed to a new branch of economical interest [BMB, 2011].

Transport In this thesis the transport of charge through a mesoscopic structure is investigated. In the macroscopic, classical case this charge transfer is described by the (average) current. In the mesoscopic regime this description is too rough. A more detailed view is required, which is provided by Full Counting Statistics.

Full Counting Statistics 'Full Counting Statistics is the theory of quantum statistical properties of transport phenomena' [Belzig, 2005].

Full Counting Statistic (FCS) has attracted worldwide attention in the theoretical [Levitov et al., 1996] an experimental [Reulet et al., 2003] examination over the last decades. Not only in the mesoscopic physics, but also in other physical fields, as well as in chemistry or biology, Full Counting Statistics now plays a decisive role. With its historical roots in quantum optics the terminology was adopted by Levito and coworkers to mesocopic transport problems [Nazarov and Division, 2003, Büttiker, 1992, Datta, 1997, Lenstra, 1982, Emary, 2009, Brandes, 2007].

Investigated setup In this work one will regard quantum mechanical systems, which are connected to a classical electron reservoir.

Experiment The investigated systems are not only theoretically consideration, but exist in reality. It should be pointed out that, especially the Single and Double Quantum Dot, where the calculations in chapter 5 base on, were build up experimentally e.g. by [Hanson et al., 2006]. For the physical implementation Hanson an coworkers used a two dimensional electron gas (cf. figure 1.1) .

For <u>further information</u> on nanostructures see [Skobel'tsyn and Wood, 1972, Nazarov and Blanter, 2009, Schöll, 1998, Sohn et al., 1997, Datta, 1995, J.Jacack, 1998, Jäckle, 1978] as well as [Emary, 2009], which was the base for this thesis.
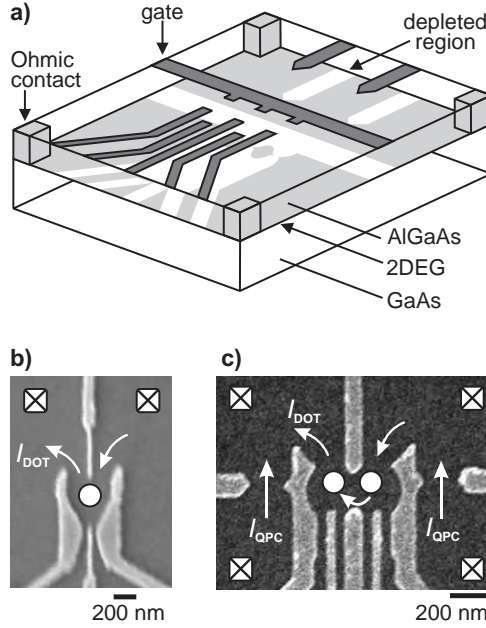
FIG. 2 Lateral quantum dot device defined by metal surface electrodes. (a) Schematic view. Negative voltages applied to metal gate electrodes (dark gray) lead to depleted regions (white) in the 2DEG (light gray). Ohmic contacts (light gray columns) enable bonding wires to make electrical contact to the 2DEG reservoirs. (b)-(c) Scanning electron micrographs of a few-electron single-dot device (b) and a double-dot device (c), showing the gate electrodes (light gray) on top of the surface (dark gray). The white dots indicate the location of the quantum dots. Ohmic contacts are shown in the corners. White arrows outline the path of current I_{DOT} from one reservoir through the dot(s) to the other reservoir. For the device in (c) the two gates on the side can be used to create two quantum point contacts, which can serve as electrometers by passing a current I_{QPC}. Note that this device can also be used to define a single dot. Image in (b) courtesy of A. Sachrajda.

Figure 1.1: Lateral quantum dot device defined by metal surface electrodes.
(a) Schematic view. Negative voltages applied to metal gate electrodes
(dark gray) lead to depleted regions shown in white; make the 2DEG.
Ohmic contacts (light gray columns) enable bonding wires to
make electrical contact to the 2DEG reservoirs (light gray)
(b)-(c) Scanning electron micrographs of a few-electron single-dot device
(b) and a double-dot device (c), showing the gate electrodes (light gray)
on top of the surface (dark gray). The white dots indicate the location
of the quantum dots. Ohmic contacts are shown in the corners. White
arrows outline the path of current I_{DOT} from one reservoir through the
dot(s) to the other reservoir. For the device in (c), the two gates on the
side can be used to create two quantum point contacts, which can serve as
electrometers by passing a current I_{QPC}. Note that this device can also
be used to define a single dot. Image in (b) courtesy of A. Sachrajda.
Image and description from [Hanson et al., 2006]

become the standard for lateral coupled quantum dots and is used with minor adaptions by several research groups (Petta *et al.*, 2004; Pioro-Ladrière *et al.*, 2005); one noticable improvement has been the electrical isolation of the charge sensing part of the circuit from the reservoirs that connect to the dot (Hanson *et al.*, 2005).

C. Measurement techniques

In this review, two all-electrical measurement techniques are discussed: i) measurement of the current due to transport of electrons through the dot, and ii) detection of changes in the number of electrons on the dot with a nearby electrometer, so-called *charge sensing*. With the latter technique, the dot can be probed *non-invasively* in the sense that no current needs to be sent through the dot.

The potential of charge sensing was first demonstrated in the early 1990s (Ashoori *et al.*, 1992; Field *et al.*, 1993). But whereas current measurements were already used extensively in the first experiments on quantum dots (Kouwenhoven *et al.*, 1997), charge sensing has only recently been fully developed as a spectroscopic tool (Elzerman *et al.*, 2004a; Johnson *et al.*, 2005a). Several implementations of electrometers coupled to a quantum dot have been demonstrated: a single-electron transistor fabricated on top of the heterostructure (Ashoori *et al.*, 1992; Lu *et al.*, 2003), a second electrostatically defined quantum dot (Fujisawa *et al.*, 1995) and a quantum point contact (QPC) (Field *et al.*, 1993; Sprinzak *et al.*, 2002). The QPC is the most widely used because of its ease of fabrication and experimental operation. We discuss the QPC operation and charge sensing techniques in more detail in section V.

Why is it worth while to use charge sensing to electron transport measurements. The smallest currents that can be resolved in optimized setups and devices are roughly 10 fA, which sets a lower bound of order 10 fA/$e \approx$ 60 kHz on the tunnel rate to the reservoir, Γ, for which transport experiments are possible (see e.g. Vandersypen *et al.* (2004) for a discussion on noise sources). For $\Gamma < 100$ kHz the charge detection technique can be used to resolve electron tunneling in real time. Because the coupling to the leads is a source of decoherence and relaxation (most notably via cotunneling), charge detection is preferred for quantum information purposes since it still functions for very small couplings to a (single) reservoir.

Measurements using either technique are conveniently understood with the Constant Interaction model. In the next section we use this model to describe the physics of single dots and show how relevant spin parameters can be extracted from measurements.

Applying the same gate design principle to a double quantum dot, Elzerman *et al.* demonstrated in 2003 control over the electron number in both dots while maintaining tunable tunnel coupling to the reservoir (Elzerman *et al.*, 2003). Their design is shown in Fig. 2c (for more details on design considerations and related versions of this gate design, see Hanson (2005)). In addition to the coupled dots, two quantum point contacts (QPCs) are incorporated in this device to serve as charge sensors. The QPCs are placed close to the dots, thus ensuring a good charge sensitivity. This design has

Chapter 2

n-dependent Master Equation: Derivation

In this chapter the **n-resolved Quantum Master Equation** with **n-dependent tunneling rates** (nQME) is derived. At first the nQME is motivated and distinguished from the ordinary n-resolved Quantum Master Equation in section 2.1. In a second step the Nakajima- Zwanzig Equation is used to derive a general form of the nQME in section 2.2. Finally, a Lindblad similar form of the nQME is obtained, by performing a wide range of assumptions in section 2.3.

2.1   Motivation and configuration

The derivation of the n-resolved Quantum Master Equation

$$\partial_t \rho^{(n)}(t) = \mathcal{L}\rho^{(n)}(t) + \mathcal{J}\rho^{(n-1)}(t) \tag{2.1}$$

for constant tunneling rates Γ is well known and is an integral part of many physic lectures [Brandes, 2007, Emary, 2009, Breuer and Petruccione, 2002].

For these derivations the system bath theory is used, in which the world is divided into two parts:

- the **system**, whereon the investigations are made
- the rest, the **bath**, which is assumed to be constant and influences the system in a specific way

In this work one additional external parameter, the *number of particles* in the reservoirs (bath) N_α, is taken into account. This additional information will cause n-dependent tunneling rates $\Gamma^{(n)}$, which cause the n-resolved Quantum Master Equation with n-dependent tunneling rates (**nQME**)

$$\partial_t \rho^{(n)}(t) = \mathcal{L}_0^{(n)} \rho^{(n)}(t) + \mathcal{J}_{n-1} \rho^{(n-1)}(t). \tag{2.2}$$

To achieve a comfortable access to the derivation and a demonstrative model, the following assumptions are made. Not all assumptions are really needed. They can be neglected later on, if they where not used, for achieving more general statements.

The following setup is given for this thesis:

- There are *two reservoirs* (called left and right), which are not interacting with each other.

- There is *a system*, which interacts with the reservoirs in the following way:

  Particles (particularly electrons) can jump from the left reservoir to the system. This process happens with the rate $\Gamma_L^{(n)}$. The number of particles in the left reservoir changes from N_L to $N_L - 1$.

  Particles can jump from the system to the right reservoir with the rate $\Gamma_R^{(n)}$ and the number of particles in the right reservoir changes to $N_R + 1$.

- At one instant of time, there can be only *one particle* in the system.[1]

- The reservoirs do not change their particle number aside from an interaction with the system. Therefore the numbers N_L and N_R are in a fixed relationship (cf. figure 2.1).

- A new number **n** is introduced, which stands for the number of particles transported through the system. This variable is used as index for the rates and the system density matrix.

left reservoir	$\xrightarrow{\text{jump}}$	system	$\xrightarrow{\text{jump}}$	right reservoir
(N_L, N_R, n)	$\xrightarrow{\Gamma_L^{(n)}}$	$(N_L - 1, N_R, n)$	$\xrightarrow{\Gamma_R^{(n)}}$	$(N_L - 1, N_R + 1, n + 1)$
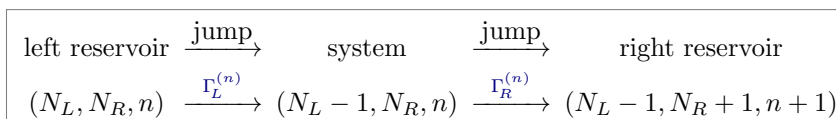
Figure 2.1: Abstract model with
N_L: number of particles in the left reservoir
N_R: number of particles in the right reservoir
n: number of particles transported through the system

---

[1] This assumption was not explicitly used in the derivation. However, all system in this thesis fulfill that requirement.

$$\Gamma_L^{(N_L)} \qquad \Gamma_R^{(N_R)}$$

$$\mu_L$$

$$\varrho_{B,L}^{(N_L)} \qquad \rho^{(n)}(t) \qquad \varrho_{B,R}^{(N_R)}$$

source | system | target

$$\mu_R$$
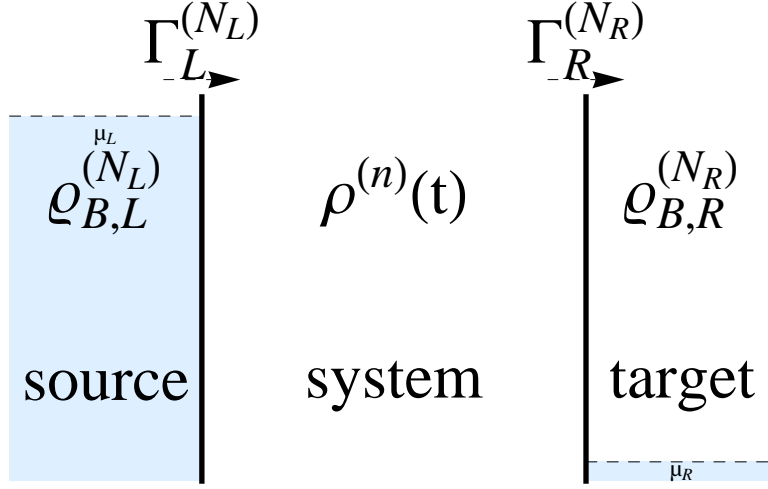
Figure 2.2: Scheme of the setup

Content of this chapter

This chapter might be observed apart from the other chapters of this thesis. As it is not necessary for the comprehension of the following chapters, it can be skipped.

In the following the derivation of the n-resolved Quantum Master Equation is started on a microscopic level. Then the Nakajima-Zwanzig Formalism is applied. The knowledge of the superoperator-formalism (cf. appendix B.3, p. 138) and a basic understanding of the projection operator technique are the precondition for the comprehension of the following chapter compare with perturbation theory [Brandes, 2009, 3.7.1].

2.2   Nakajima-Zwanzig Projection

As already mentioned before the new aspect, proposed in this thesis, is the variability of the tunneling rates, which depend on the number of particles that tunneled through the system. For the default approach [Brandes, 2007, Pöltl, 2008] for constant tunneling rates the Quantum Master Equation is derived by using the common **system bath theory**. After that the complete system density matrix is transformed to the n-resolved (conditioned) system density matrix by an procedure called 'decomposition into histories'. This procedure originally comes from quantum jump approaches [Lambert, 2005, 5.27-5.37].

In contrast the derivation, developed in this thesis, arises from the **projection operator technique** proposed by Nakajima and Zwanzig [Kühne and Reineker, 1978, Zwanzig, 1960, Nakajima, 1958].

For variable tunneling rates the bath cannot be assumed as constant, because some information of the system influences the bath. Therefore, the point of view has changed.

From now on the partition of the world is no longer done with regard to geometric properties like in thermodynamics. The approach is based on information theory. All information of interest are projected into the subspace of the relevant information [Breuer and Petruccione, 2002, Kato, 2004]. In the investigated case the part of interest is the system-density-operator and the information of the quantity of particles, which have been transported through the system.

2.2.1   Projection operator

The complete density operator ϱ describes the behavior of the system (i.e. the Quantum Dot) and the environment (i.e. the left and the right reservoir). This information is much and can hardly be described or managed.

By applying an projection (super) operator (P), this density operator is simplified by disregarding the information, which is not in focus of interest. The precise form of this operator will be discussed later on. At first some general properties of this projection operator will be pointed out.

$$\mathsf{P}^2 \equiv \mathsf{P} \tag{2.3}$$

$$\mathsf{Q} \equiv \mathbb{1}^2 - \mathsf{P} \tag{2.4}$$

$$\Rightarrow \mathsf{Q}^2 = \mathsf{Q} \tag{2.5}$$

$$\Rightarrow \mathsf{QP} = \mathsf{PQ} = 0 \tag{2.6}$$

---

[2]Identity-superoperator

2.2.2 Nakajima-Zwanzig Equation

The Liouville-von Neumann Equation, which describes the dynamics of the density matrix [3] $\partial_t \varrho = \mathcal{L}\varrho$, can be rewritten by splitting ϱ into the two parts $\varrho = (\mathsf{P} + \mathsf{Q})\varrho$:

$$\frac{d}{dt}\begin{pmatrix}\mathsf{P}\\\mathsf{Q}\end{pmatrix}\varrho = \begin{pmatrix}\mathsf{P}\\\mathsf{Q}\end{pmatrix}\mathcal{L}\begin{pmatrix}\mathsf{P}\\\mathsf{Q}\end{pmatrix}\varrho + \begin{pmatrix}\mathsf{P}\\\mathsf{Q}\end{pmatrix}\mathcal{L}\begin{pmatrix}\mathsf{Q}\\\mathsf{P}\end{pmatrix}\varrho. \tag{2.7}$$

The second row is formally solved by

$$\mathsf{Q}\varrho = \mathcal{U}^\dagger(t,t_0)\varrho(t_0) + \int_{t_0}^t dt'\mathcal{U}^\dagger(t,t')\mathsf{Q}\mathcal{L}'\mathsf{P}\varrho(t') \tag{2.8}$$

with $\mathcal{U}^\dagger(t,t') := T_\leftarrow e^{\int_{t'}^t ds\,\mathcal{Q}\mathcal{L}(s)}$, where $T_\leftarrow$ is the chronological time ordering[4] operator. For the special case of a time independent $\mathcal{L}$, this operator can be simplified to $\mathcal{U}^\dagger(t') = e^{\mathcal{Q}\mathcal{L}t'}$.

Inserting this into the first row leads to the Nakajima-Zwanzig Equation:

$$\partial_t\mathsf{P}\varrho = \mathsf{P}\mathcal{L}\mathsf{P}\varrho + \underbrace{\mathsf{P}\mathcal{L}\mathcal{U}^\dagger(t,t')\mathsf{Q}\varrho(t_0)}_{=0} + \mathsf{P}\mathcal{L}\int_{t_0}^t dt'\mathcal{U}^\dagger(t,t')\mathsf{Q}\mathcal{L}'\mathsf{P}\varrho(t'). \tag{2.9}$$

The assumption that the inhomogeneous term disappears[5], the short hand notation for the integral kernel $\mathcal{K}(t,t') = \mathsf{P}\mathcal{L}\mathcal{U}^\dagger(t,t')\mathsf{Q}\mathcal{L}'\mathsf{P}$ and the projector property $\mathsf{P}^2 = \mathsf{P}$ are used to derive the final form of the **Nakajima-Zwanzig Equation**

$$\partial_t\mathsf{P}\varrho = \mathsf{P}\mathcal{L}\mathsf{P}\varrho + \int_{t_0}^t dt'\mathcal{K}(t,t')\mathsf{P}\varrho(t'). \tag{2.10}$$

---

[3]For details cf. appendix (B.14).
[4]For details cf. [Breuer and Petruccione, 2002]
[5]This can be realized by assuming that at the start $\mathsf{P}\varrho = \varrho \Rightarrow \mathsf{Q}\varrho = 0$, which is sometimes called **factorizing initial condition**.

2.2.3   Interaction picture

In accordance to the assumption that the interaction between system and bath is *weak*, a transformation is performed in this subsection, which corresponds to the transformation to the interaction picture.[6]

The Liouvillian can be split into three parts[7]

$$\mathcal{L} = (\mathcal{P} + \mathcal{Q})\mathcal{L}(\mathcal{P} + \mathcal{Q}) \tag{2.11}$$

$$\mathcal{L} = \underbrace{\mathcal{PLP}}_{\mathcal{L}_S} + \underbrace{\mathcal{QLQ}}_{\mathcal{L}_B} + \underbrace{\mathcal{PLQ} + \mathcal{QLP}}_{\mathcal{L}_I} \tag{2.12}$$

$$\mathcal{L} = \underbrace{\mathcal{L}_S + \mathcal{L}_B}_{\mathcal{L}_0} + \lambda\mathcal{L}_I \, \lambda = 1 \tag{2.13}$$

$$\mathcal{L} = \mathcal{L}_0 + \lambda\mathcal{L}_I \tag{2.14}$$

The subscript reminds of the standard system bath approach, where H_S is the system path, which describes the system dynamics. In words of the projector-approach, $\mathcal{L}_S$ describes the dynamics in the **relevant** part. The bath part corresponds to the **irrelevant** part $\mathcal{L}_B$. The **interaction** part $\mathcal{L}_I$ describe the interaction between relevant and irrelevant parts. This interaction part is assumed to be small, which is indicated by the scalar parameter λ. Nevertheless, this was derived without an explicit use of system or bath properties and is only based on the definition of the projector.

With the help of $PQ = 0$, the following rules are simply derived

$$P\mathcal{L}P = P\mathcal{L}_0P \qquad\qquad Q\mathcal{L}Q = Q\mathcal{L}_0Q \tag{2.15}$$

$$Q\mathcal{L}P = Q\mathcal{L}_IP \qquad\qquad P\mathcal{L}Q = P\mathcal{L}_IQ. \tag{2.16}$$

This rules are useful to rewrite the Nakajima-Zwanzig Equation

$$\partial_t P\varrho = P\mathcal{L}_0 P\varrho + \int\limits_{t_0}^{t} dt' \mathcal{K}(t,t') P\varrho(t'). \tag{2.17}$$

The kernel $\mathcal{K}$ can be simplified to

$$\mathcal{K}(t,t') = P\mathcal{L}\sum_{k=0}^{\infty} T_{\leftarrow}\frac{(\int_{t'}^{t} ds Q\mathcal{L}(s))^k}{k!}Q\mathcal{L}'P = P\mathcal{L}Q\sum_{k=0}^{\infty} T_{\leftarrow}\frac{(\int_{t'}^{t} ds Q\mathcal{L}(s)Q)^k}{k!}Q\mathcal{L}'P$$

$$= P\mathcal{L}_IQ(Q\underbrace{T_{\leftarrow}e^{\int_{t'}^{t} ds\mathcal{L}_0(s)}}_{\mathcal{U}_0^\dagger(t,t_0)} \underbrace{Q}_{Q+0})\underbrace{Q\mathcal{L}_I'P}_{(Q+P)\mathcal{L}_IP} = P\mathcal{L}_I\mathcal{U}_0^\dagger(t,t_0)\mathcal{L}_I'P. \tag{2.18}$$

Switching to the *interaction picture* via

$$\tilde{\varrho} := \mathcal{U}_0^\dagger(t,t_0)\varrho \quad \tilde{\mathcal{L}} = \mathcal{U}_0^\dagger(t,t_0)\mathcal{L}\mathcal{U}_0(t,t_0), \tag{2.19}$$

---

[6] Transformation to the interaction or Dirac picture is a default approach in scattering theory (cf. appendix B.3.1).

[7] As well as the Hamiltonian ([Brandes, 2009, 3.120])

leads to

$$\partial_t \tilde{\varrho} = (\partial_t \mathcal{U}_0^\dagger(t,t_0))\varrho + \mathcal{U}_0^\dagger(t,t_0)\partial_t \varrho$$

$$\partial_t \mathsf{P}\tilde{\varrho} = -\mathsf{P}\mathcal{L}\mathcal{U}_0^\dagger(t,t_0)\varrho + \mathcal{U}_0^\dagger(t,t_0)\left(\mathsf{P}\mathcal{L}_0\varrho + \int\limits_0^t dt'\mathcal{K}(t,t')\mathsf{P}\varrho(t-t')\right) \quad (2.20)$$

$$\partial_t \mathsf{P}\tilde{\varrho} = \mathcal{U}_0^\dagger(t,t_0)\int\limits_{t_0}^t dt'\mathcal{K}(t,t')\mathsf{P}\mathcal{U}_0(t,t')\tilde{\varrho}(t'). \quad (2.21)$$

The Nakajima-Zwanzig Equation can be simplified by assuming $\mathsf{P}\tilde{\mathcal{L}}\mathsf{P} = 0$ to

$$\mathrm{d}_t\mathsf{P}\tilde{\varrho} = \lambda^2 \int{}' \tilde{\mathcal{K}}'\mathsf{P}\tilde{\varrho}'. \quad (2.22)$$

$\tilde{\mathcal{K}}$ becomes up to first order in t' $\tilde{\mathcal{K}}(t',t) = \mathsf{P}\tilde{\mathcal{L}}\tilde{\mathcal{L}}'\mathsf{P}$,

$$\mathrm{d}_t\mathsf{P}\tilde{\varrho} = +\lambda^2 \int{}' \mathsf{P}\tilde{\mathcal{L}}\tilde{\mathcal{L}}'\mathsf{P}\tilde{\varrho}'. \quad (2.23)$$

2.2.4 Hilbert Space

In a former step the Hilbert Space is investigated and the projection operator is explicitly defined.

The complete Hilbert Space [8] reads

$$\mathcal{H} = \mathcal{H}_S \otimes \left(\bigoplus_\alpha \mathcal{H}_{B,\alpha}\right) \quad (2.24)$$

$$\mathcal{H}_{B,\alpha} = \bigoplus_{N_\alpha} \mathsf{S}_\alpha \mathcal{H}^{\otimes N_\alpha}, \quad (2.25)$$

where S_α is the operator that (anti) symmetrises the space. In our case we only treat fermionic systems, so $\mathsf{S}_\alpha = \mathsf{S}$. The commutativity of tensor and direct product yields

$$\mathcal{H} = \mathcal{H}_S \otimes \bigoplus_N \mathsf{S}\mathcal{H}^{\otimes N} = \bigoplus_N \mathcal{H}_S \otimes \mathsf{S}\mathcal{H}^{\otimes N}, \quad (2.26)$$

where $N = (N_L, N_R, \dots)$ is a vector, representing one combination of particles quantities in the bath α. One can think of the setup of figure 2.2 (p. 11), where $\alpha \in \{R, L\}$ represents the left or right bath. The default approach is to 'trace out the bath part'. In the default manner all information about the bath, i.e. the number of particles, is destroyed. Therefore in the present case, where the number of particles is important, this information will be kept.

---

[8] Describing 'system and bath' in words of system bath theory.

Table 2.1: Comparison: n-resolved and default approach

default projection	n-resolved projection
$\mathcal{P}'\varrho = \mathrm{Tr_B}\left[\varrho\right] \otimes \varrho_B$	$\mathcal{P}\varrho = \bigoplus_N \mathrm{Tr_B^{(N)}}\left(\varrho\right) \otimes \varrho_B^{(N)}$

With $\mathrm{Tr_B^{(N)}}\left(\boxed{x}\right) = \sum \langle N_\alpha; k_{\alpha 1}, \ldots, k_{\alpha N} | \boxed{x} | N_\alpha; k_{\alpha 1}, \ldots, k_{\alpha N}\rangle$ and the assumption that the part $\varrho_B^{(N)}$ or ϱ_B is constant, the goal to retain the number of particles can be archived. One can imagine that $\varrho_B^{(N)}$, as the grand canonical statistical operator for reservoir α, is

$$\varrho_B^{(N)} = \bigoplus_\alpha \frac{e^{-\beta_\alpha(\mathrm{H}_{B,\alpha} - \mu_\alpha N_\alpha)}}{\mathrm{Tr_B}\left[e^{-\beta_\alpha(\mathrm{H}_{B,\alpha} - \mu_\alpha N_\alpha)}\right]}. \tag{2.27}$$

But in the following the concrete representation of $\varrho_B^{(N)}$ is not needed. A comparison between the n-resolved and default approach projector can be seen in table 2.1.

Partial trace

If one assumes unidirectional, sequential tunneling, the vector N only depends on one scalar parameter, which is called n. The physical interpretation of n is the number of particles, transported through the system. The partial trace over the bath, a function, which sums over all possible bath vectors, can be split into a sum of traces for every subspace.

$$\mathrm{Tr_B^{(n)}}\left(\boxed{x}\right) \equiv \sum_\alpha \langle N(n,\alpha)k_{\alpha 1}, \ldots, k_{\alpha N} | \boxed{x} | N(n,\alpha); k_{\alpha 1}, \ldots, k_{\alpha N}\rangle \tag{2.28}$$

If one regards $\tilde{\mathrm{V}}$ as a perturbation, it is self-evident that a perturbative expansion makes sense.

$$\tilde{\varrho} = \tilde{\varrho}_0 + \mathrm{i}\int' \left[\tilde{\varrho}_0, \tilde{\mathrm{V}}'\right] + O(\tilde{\mathrm{V}})^2. \tag{2.29}$$

Inserting the definition for the projector

$$\mathcal{P}\varrho = \bigoplus_n \mathrm{Tr_B^{(n)}}\left(\varrho\right) \otimes \varrho_B^{(n)} \tag{2.30}$$

with the short hand notation $\mathrm{Tr_B^{(n)}}\left(\varrho\right) = \varrho_S^{(n)}$ leads to

$$\partial_t \mathsf{P}\tilde{\varrho} = -\bigoplus_n \int \mathrm{Tr_B^{(n)}}\left(\left[\left[\bigoplus_{n'} \tilde{\varrho}_S'^{(n')} \otimes \varrho_B^{(n')}, \tilde{\mathrm{V}}'\right], \tilde{\mathrm{V}}\right]\right) \otimes \varrho_B^{(n)} + O(\tilde{\mathrm{V}})^2. $$

$$\tag{2.31}$$

Investigating the system path of the density matrix leads to

$$\partial_t \mathrm{Tr}_{\mathrm{B}}^{(\mathrm{n})}\left(\mathsf{P}\tilde{\varrho}\right) = -\bigoplus_n \int' \mathrm{Tr}_{\mathrm{B}}^{(\mathrm{n})}\left(\left[\left[\bigoplus_{n'}\tilde{\varrho'}_S^{(n')}\otimes\varrho_B^{(n')},\tilde{\mathsf{V}}'\right],\tilde{\mathsf{V}}\right]\right)\otimes\underbrace{\mathrm{Tr}_{\mathrm{B}}^{(\mathrm{n})}\left(\varrho_B^{(n)}\right)}_{=1}+O(\tilde{\mathsf{V}})^2.$$

(2.32)

In component notation, with $\rho^{(n)}(t)$ as the n-th entry of the direct sum, it leads to

$$\partial_t \tilde{\rho}_t^{(n)} = -\int' \mathrm{Tr}_{\mathrm{B}}^{(\mathrm{n})}\left(\left[\left[\bigoplus_{n'}\tilde{\varrho'}_S^{(n')}\otimes\varrho_B^{(n')},\tilde{\mathsf{V}}'\right],\tilde{\mathsf{V}}\right]\right)+O(\tilde{\mathsf{V}})^2.$$

(2.33)

The explicit expression for $\rho^{(n)}(t)$ reads

$$\bigoplus_n \varrho_S^{(n)} \equiv \begin{pmatrix}\rho^{(0)}(t)\\\rho^{(1)}(t)\\\vdots\end{pmatrix}.$$

(2.34)

2.2.5 Formal solution

The expressiveness of (2.31) is quite low if no additional information on the Interaction Hamiltonian V is given. Therefore one can use the Schmidt Decomposition to express V in the style of [Brandes, 2007, 1.2.20]

$$\mathsf{V} = \sum_{k,n,\alpha} S_k \otimes B_k^{N(n,\alpha)}$$

(2.35)

and to collect terms with the same system part S_k

$$= \sum_m S_l \otimes \sum_{k,\alpha,n} c_{l,k,n,\alpha} B_k^{N(n,\alpha)}$$

(2.36)

with S_l as an element of the system Hilbert space, $B_l^{N(k,\alpha)}$ as a part of the bath Hilbert Space and $c_{l,k,n,\alpha}$ as scalar parameters from the system part. This notation underlines that interactions with more than one bath Hilbert Space ($\mathcal{H}_{B\alpha,1}\otimes\mathcal{H}_{B\alpha,2}$) are not regarded.

Formally the expression $\mathrm{Tr}_{\mathrm{B}}^{(\mathrm{n})}\left(\left[\left[\mathsf{P}\tilde{\varrho}',\tilde{\mathsf{V}}'\right],\tilde{\mathsf{V}}\right]\right)$ can be rewritten as

$$\mathrm{Tr}_{\mathrm{B}}^{(\mathrm{n})}\left(\left[\left[\mathsf{P}\tilde{\varrho}',\tilde{\mathsf{V}}'\right],\tilde{\mathsf{V}}\right]\right) = \sum_{n',l',l}\underline{\gamma}(t,t',n,n',l',l).\left[\left[\rho^{(n')}(t'),S_{l'}\right],S_l\right],$$

(2.37)

where $\underline{\gamma}(t,t',n,n',l',l)$ is said to be a four component vector, which is multiplied with the four components of the double commutator.

With the Markov Assumption (see below) the memory of this equation is dropped and the nQME becomes

$$\partial_t\rho^{(n)}(t) = \mathcal{L}_s\rho^{(n)}(t) - \sum_{n',l',l}\underline{\Gamma}(n',l',l).\left[\left[\rho^{(n')}(t),S_{l'}\right],S_l\right].$$

(2.38)

2.2.6   Bath correlation functions

The form of equation (2.38) is still general. Especially $\underline{\Gamma}(n', l', l)$ is not a very useful vector, because it involves all bath information. The next subsection explains how the bath information is reduced by using bath correlation functions [Gardiner et al., 1986]. In the n-independent case the bath correlation functions of the bath can be introduced in the following form[9]:

$$C_{k,k'}(t,t') = \mathrm{Tr_B}\left[\tilde{B}'_{k'}\tilde{B}_k \varrho_{B,0}\right]. \tag{2.39}$$

On a more atomic level for fermions this reads

$$\mathrm{Tr_B}\left[\mathrm{b^\dagger}_{k'}\mathrm{b}_k \varrho_{B,0}\right] = \delta_{k,k'} f_k(\epsilon_k). \tag{2.40}$$

The same applies to cyclic permutations, respectively $\mathrm{Tr_B}\left[\mathrm{b}_k \mathrm{b^\dagger}_k \varrho_{B,0}^{(N')}\right] = \delta_{k,k'}(1 - f_k(\epsilon_k))$ for odd numbers of permutations. f_k denotes the Fermi Functions. In the n-dependent case it works slightly different, because the creation and annihilation operators $\mathrm{b}_k, \mathrm{b}_k^\dagger$ change the number of particles in the bath, which is connected to a different bath density matrix.

Explicitly spoken this means that

$$\mathrm{Tr_B^{(N)}}\left(\mathrm{b^\dagger}_{k'}\mathrm{b}_k \varrho_{B,0}^{(N')(N')}\right) = \mathrm{Tr_B^{(N)}}\left(\varrho_{B,0}^{(N')(N')}\mathrm{b^\dagger}_{k'}\mathrm{b}_k\right) = \delta_{k,k'}\delta_{N,N'} f_k(\epsilon_k) \tag{2.41}$$

does not change the particle number, but

$$\mathrm{Tr_B^{(N)}}\left(b_k \varrho_{B,0}^{(N')(N')}\mathrm{b^\dagger}_{k'}\right) = \delta_{k,k'}\delta_{N,N'+1} f_k(\epsilon_k) \tag{2.42}$$

involves a change in N'.

$$\mathrm{Tr_B^{(N)}}\left(\mathrm{b}_k \mathrm{b^\dagger}_k \varrho_{B,0}^{(N')(N')}\right) = \mathrm{Tr_B^{(N)}}\left(\varrho_{B,0}^{(N')(N')}\mathrm{b}_k \mathrm{b^\dagger}_k\right) = \delta_{k,k'}\delta_{N,N'}(1 - f_k(\epsilon_k)) \tag{2.43}$$

$$\mathrm{Tr_B^{(N)}}\left(\mathrm{b^\dagger}_k \varrho_{B,0}^{(N')(N')}\mathrm{b}_{k'}\right) = \delta_{k,k'}\delta_{N,N'-1}(1 - f_k(\epsilon_k)). \tag{2.44}$$

is analogically computed. As this is an useful result for calculating $\underline{\gamma}(t,t',n,n',l',l)$, the result will be summed up (see table 2.2, p. 22).

---

[9] $\varrho_{B,0} = R_0$ [Brandes, 2007]

2.3 Assumptions and limits

To receive explicit solvable results and produce simple solutions some assumptions are useful. The important assumptions and approximations are

- Born-Markov Approximation

- Limitation to two bath reservoirs

- Unidirectional tunneling

- Sequential tunneling limit

- Infinite bias limit

2.3.1 Born-Markov Approximation

The Born-Markov Approximation is a serious restriction. Thereby, it is assumed that there are no memory effects in the system. This reminds to Hamilton mechanics, where a state in the phase-space had specified the complete system dynamics. In (2.31) the system state depends on the complete history. This fact is expressed by $\int'$, which stands for $\int_0^t dt'$. In the Born-Markov Approximation it is assumed that the integral kernel is strongly peaked around $t - t' \approx 0$. Roughly spoken that means that events, which happened longer time ago, are increasingly forgotten by the system.

Strongly peaked means that the width of the peak $\delta(t - t') \ll \tau$, where τ is the inverse of the rate of change of $\tilde{\rho}(t)$. This restriction has to be kept in mind with regard to numerical simulation, using the discrete time step approach, introduced in chapter 7. That means that one can replace $\tilde{\varrho}' \equiv \tilde{\varrho}(t') \to \tilde{\varrho} \equiv \tilde{\varrho}(t)$, respectively $\varrho(t') \to \varrho(t)$. For (2.17) this reads

$$\partial_t \mathsf{P}\varrho = \left(\mathsf{P}\mathcal{L}_0 + \int_{t_0}^t \mathcal{K}(t, t') dt' \right) \mathsf{P}\varrho. \tag{2.45}$$

As the difference between (2.17) and (2.45) is only one apostrophe, it could be misunderstood as no big change. This is a misapprehension, as (2.17) is a complex integro-differential equation, while (2.45) is a kind of simple first order differential equation. The explicit form of (2.31), after back- transformation into the **Schrödinger picture**, becomes

$$\partial_t \mathsf{P}\varrho = \left(\mathsf{P}\mathcal{L}_0 + \int_{t_0}^t \mathsf{P}\tilde{\mathcal{L}}_I(t - t')\mathcal{L}_I dt' \right) \mathsf{P}\varrho \tag{2.46}$$

or, with expanded double commutator,

$$\partial_t \mathsf{P}\varrho(t) = \mathsf{P}\mathcal{L}_0 \mathsf{P}\varrho(t) - \bigoplus_n \int_0^t dt' \mathrm{Tr}_\mathrm{B}^{(n)} \left(\left[\left[\mathsf{P}\varrho(t), \tilde{\mathsf{V}}(t - t') \right], \mathsf{V} \right] \right) \otimes \varrho_B^{(n)}.$$

(2.47)

It has to be pointed out that only single particle actions were taken into account. This was assumed by the approximation of the integral Kernel $\mathcal{K}$ up to the first order, which ended in a Quantum Master Equation for $\partial_t \mathsf{P}\varrho$ of second order.

This means that the change of $|n - n'|$ is at maximum 1 within each jump [Bagrets and Nazarov, 2003, Nazarov, 1993, Stoof and Nazarov, 1996].

2.3.2   Explicit calculation

In the following section the calculation will be explicitly done. As it involves 16 terms, the calculation is quite long. Therefore in this thesis only some exemplary terms where noted. Nevertheless it might be helpful to compare this section to [Brandes, 2007] or [Pöltl, 2008], where more expressions are described.

Explicitly the Hamiltonian $\mathsf{H} = \mathsf{H}_S + \mathsf{H}_B + \mathsf{H}_{S,B}$ consists of three parts.

$$\mathsf{H}_S = \epsilon_s \mathsf{s}^\dagger \mathsf{s},$$

(2.48)

is the system part of the Hamiltionan in Eigenbasis

$$\mathsf{H}_B = \sum_{k,\alpha} \epsilon_{b,k,\alpha} \mathsf{b}^\dagger_{k,\alpha} \mathsf{b}_{k,\alpha}.$$

(2.49)

H_B is the bath part of the Hamiltonian. The index with $\alpha \in \{R, L\}$ indicates the left or right lead and k labels the channel-index of the bath, where jumps into our out of the system, might occur. And there is the most important part, the interaction part

$$\mathsf{V} = \mathsf{H}_{S,B} = \sum_{k,\alpha,n} \left(T_{k,\alpha,n} \mathsf{b}^\dagger_{k,\alpha} \mathsf{s} + T^*_{k,\alpha,n} \mathsf{s}^\dagger \mathsf{b}_{k,\alpha} \right).$$

(2.50)

This interaction part can be rewritten with regard to the splitting, proposed in (2.36)

$$\mathsf{V} = \mathsf{H}_{S,B} = \mathsf{s}\mathsf{B}^\dagger + \mathsf{s}^\dagger \mathsf{B}, \quad \mathsf{B} = \sum_{k,\alpha,n} T^*_{k,\alpha,n} \mathsf{b}_{k,\alpha}.$$

(2.51)

As stated above, there are no processes, which interact with the right and the left lead at the same time. In the next section $\mathrm{Tr}_\mathrm{B}^{(n)} \left(\left[\left[\mathsf{P}\varrho(t), \tilde{\mathsf{V}}(t - t') \right], \mathsf{V} \right] \right)$ will be obtained and the time integration will be executed afterwards.

Right lead $\alpha = R$

To get rid of the alpha index we first investigate the right side and keep the R index in mind. This makes the text more readable. The trace on the right hand, applied on some object $\boxed{x}$, becomes

$$\mathrm{Tr}_{\mathrm{B}}^{(\mathrm{N})}\left(\boxed{x}\right) = \sum_{k_1,k_2,\ldots k_N} \langle N; k_1, k_2 \ldots k_N| \boxed{x} |N; k_1, k_2 \ldots k_N\rangle \equiv \sum_k \langle N; k| \boxed{x} |N; k\rangle. \tag{2.52}$$

In the interaction picture, $\tilde{\mathrm{V}}$ reads

$$\tilde{\mathrm{V}}(\Upsilon) = \left(e^{-\mathrm{i}\Upsilon\epsilon_s}\mathrm{s}\bar{\mathrm{B}}^\dagger + e^{\mathrm{i}\Upsilon\epsilon_s}\mathrm{s}^\dagger\bar{\mathrm{B}}\right), \quad \bar{\mathrm{B}} = \sum_{\bar{k},\bar{N}} e^{-\mathrm{i}\Upsilon\epsilon_{\bar{k}}} T_{\bar{k},\bar{N}}^* \mathrm{b}_{\bar{k}}. \tag{2.53}$$

One can think of $\Upsilon = t - t'$. Inserting this in $\mathrm{Tr}_{\mathrm{B}}^{(\mathrm{N})}\left(\left[\left[\mathrm{P}\varrho(t), \tilde{\mathrm{V}}(t - t')\right], \mathrm{V}\right]\right)$ leads to[10]

$$\mathrm{Tr}_{\mathrm{B}}^{(\mathrm{N}")}\left(\left[\left[\varrho_B^{(N')}, \bar{\mathrm{B}}^\dagger\right], \mathrm{B}\right] \cdot \left[\left[\varrho_S^{(N')}, e^{-\mathrm{i}\Upsilon\epsilon_S}\mathrm{s}\right], \mathrm{s}^\dagger\right]\right) + h.c., \tag{2.54}$$

where . is a special notation for the scalar product of the four components of the double commutator and h.c. stands for the hermitan conjugate, which means that the $\dagger$ are switched. Inserting the definition for B and $\mathrm{Tr}_{\mathrm{B}}^{(\mathrm{N})}()$ leads to

$$\sum_{k'',\bar{k},k,N',\bar{N},N} \langle N''; k''| . e^{\mathrm{i}\Upsilon\epsilon_{\bar{k}}} T_{\bar{k},\bar{N}} T_{k,N}^* \left[\left[\varrho_B^{(N')}, \mathrm{b}_{\bar{k}}^\dagger\right], \mathrm{b}_k\right] \cdot \left[\left[\varrho_S^{(N')}, e^{-\mathrm{i}\Upsilon\epsilon_S}\mathrm{s}\right], \mathrm{s}^\dagger\right] |N''; k''\rangle \tag{2.55}$$

for the first part. With $N'' \to N$ this expression can be rewritten to

$$\sum_k e^{\mathrm{i}\Upsilon(\epsilon_k - \epsilon_S)} |T_{k,N'}|^2 \mathrm{Tr}_{\mathrm{B}}^{(\mathrm{N})}\left(\left[\left[\varrho_B^{(N')}, \mathrm{b}^\dagger_k\right], \mathrm{b}_k\right]\right) \cdot \left[\left[\varrho_S^{(N')}, \mathrm{s}\right], \mathrm{s}^\dagger\right]. \tag{2.56}$$

As seen in 2.2.6, the Fermi Function always leads to a $\delta\bar{k}, k$. This is a considerable achievement, because the values for $\mathrm{Tr}_{\mathrm{B}}^{(\mathrm{N})}\left(\left[\left[\varrho_B^{(N')}, \mathrm{b}^\dagger_k\right], \mathrm{b}_k\right]\right)$ are known and listed in table 2.2.

---

[10]N was changed to N" to avoid a mixing of the indices.

Table 2.2: Correlation functions

NO.	sign	$\mathrm{Tr}_{\mathrm{B}}^{(\mathrm{N})}([\underline{x}])$	$f(\epsilon_k)$	N	system
1	+	$\varrho_{B,0}^{(N')}\mathrm{b}_k^\dagger \mathrm{b}_k$	$f(\epsilon_k)$	$N' \to N$	$\rho^{(N)}(t)\mathrm{ss}^\dagger$
2,7	-	$\mathrm{b}_k\varrho_{B,0}^{(N')}\mathrm{b}_k^\dagger$	$f(\epsilon_k)$	$N' \to N-1$	$\mathrm{s}^\dagger \rho^{(N-1)}(t)\mathrm{s}$
3,6	-	$\mathrm{b}_k^\dagger \varrho_{B,0}^{(N')}\mathrm{b}_k$	$1 - f(\epsilon_k)$	$N' \to N+1$	$\mathrm{s}\rho^{(N+1)}(t)\mathrm{s}^\dagger$
4	+	$\mathrm{b}_k\mathrm{b}_k^\dagger \varrho_{B,0}^{(N')}$	$1 - f(\epsilon_k)$	$N' \to N$	$\mathrm{s}^\dagger \mathrm{s}\rho^{(N)}(t)$
5	+	$\varrho_{B,0}^{(N')}\mathrm{b}_k\mathrm{b}_k^\dagger$	$1 - f(\epsilon_k)$	$N' \to N$	$\rho^{(N)}(t)\mathrm{s}^\dagger \mathrm{s}$
8	+	$\mathrm{b}_k^\dagger \mathrm{b}_k\varrho_{B,0}^{(N')}$	$f(\epsilon_k)$	$N' \to N$	$\mathrm{ss}^\dagger \rho^{(N)}(t)$

Formally an expression for the right part or $\underline{\gamma}$ can be written down. The accomplishment will be skipped and further simplifications are proceed.

The investigation of the term

$$\sum_k e^{\mathrm{i}\Upsilon\epsilon_k}|T_{k,N'}|^2 = \int_{-\infty}^{\infty} \sum_k |T_{k,N'}|^2 e^{\mathrm{i}\Upsilon\epsilon}\delta(\epsilon - \epsilon_k) \qquad (2.57)$$

reminds to the following property. The delta-distribution can be written as the Inverse Fourier Transformation of its Fourier Transformation

$$\delta(x) = \frac{1}{2\pi} \int_{-\infty}^{\infty} dy\, e^{\mathrm{i}xy}. \qquad (2.58)$$

With the help of (2.58) and the definition

$$\Gamma^{(N')} = 2\pi \sum_k |T_{k,N'}|^2\delta(\epsilon - \epsilon_k), \qquad (2.59)$$

under the assumption that $\Gamma^{(N')}$ is independent from ϵ, the sum is rewritten to

$$\sum_k e^{\mathrm{i}\Upsilon\epsilon_k}|T_{k,N'}|^2 = \delta(\Upsilon)\Gamma^{(N')}. \qquad (2.60)$$

In the consequence, the time integration of the kernel is simple. Thinking about the delta-distribution, as limit of a series without skewness (for example the Uniform Distribution), it is comprehensible that

$$\int_0^t f(t')\delta(t - t')dt' = \frac{f(t)}{2}. \qquad (2.61)$$

Thus the four investigated terms become

$$\frac{\Gamma^{(N')}}{2} \text{Tr}_B^{(N)} \left(\left[\left[\varrho_B^{(N')}, b^\dagger_k \right], b_k \right] \right) \cdot \left[\left[\varrho_S^{(N')}, s \right], s^\dagger \right]. \tag{2.62}$$

A help for evaluating the double commutator can be given by the following rule

$$\begin{aligned}
\left[\left[a_\mp, b^\pm \right], c \right] = \left[\left[c, b^\pm \right], a_\mp \right] &\equiv ab^\dagger c - acb^\dagger - b^\dagger ca + cb^\dagger a \\
&+ a^\dagger bc - a^\dagger cb - bca^\dagger + c,ba^\dagger,
\end{aligned} \tag{2.63}$$

which gives the full expression for the right lead.

Left lead $\alpha = L$ works exactly equal to the right lead.

2.3.3 Infinite bias limit

In the infinite bias limit, the bias on the right side becomes ∞. According to that the Fermi Function gets 1 or 0. That means that half of the terms disappears. With the conversion $N_L(n), N_R(n)$ the Liouville-von Neumann Equation reads

$$\begin{aligned}
\partial_t \rho^{(n)}(t) = \mathcal{L}_S \rho^{(n)}(t) &+ \frac{\Gamma_R^{(n)}}{2} \{ \rho^{(n)}(t), ss^\dagger \} - \Gamma_R^{(n-1)} s^\dagger \rho^{(n-1)}(t) s \\
&+ \frac{\Gamma_L^{(n)}}{2} \{ \rho^{(n)}(t), ss^\dagger \} - \Gamma_L^{(n)} s^\dagger \rho^{(n)}(t) s.
\end{aligned} \tag{2.64}$$

At last the some steps for the jump part are summarized:

$$\cdots = \sum_k \langle N_R; k | \sum_{n'',n''',k'',k'''} T^*_{k''Rn''} T_{k'''Rn'''} s^\dagger b_{k''R} \bigoplus_{n'} \tilde{\varrho}'^{(n')}_S \otimes \varrho_B^{(n')} sb^\dagger_{k'''R} |k; N_R\rangle \tag{2.65}$$

$$= \sum_{kn'} \langle N_R; k | \sum_{n'',n''',k'',k'''} T^*_{k''Rn''} T_{k'''Rn'''} b_{k''R} \varrho_B^{(n')} b^\dagger_{k'''R} |k; N_R\rangle \otimes s^\dagger \tilde{\varrho}'^{(n')}_S s \tag{2.66}$$

$$= \sum_{n'k} T^*_{kRn'} T_{kRn'} \langle N_R; k | b_{kR} \varrho_B^{(n')} b^\dagger_{kR} |k; N_R\rangle \otimes s^\dagger \tilde{\varrho}'^{(n')}_S s \tag{2.67}$$

$$= \sum_{n'k} T^*_{kRn'} T_{kRn'} f_R(\epsilon_{Rk}) \delta(N_R, N_R(n'-1)) e^{\cdots} s^\dagger \tilde{\varrho}'^{(n')}_S s \tag{2.68}$$

$$= \sum_k T^*_{kRn-1} T_{kRn-1} f_R(\epsilon_{Rk}) e^{\cdots} s^\dagger \tilde{\varrho}'^{(n-1)}_S s \tag{2.69}$$

$$\cdots$$

$$= \Gamma_R^{(n-1)} s^\dagger \rho^{(n-1)} s \tag{2.70}$$

Chapter 3

n-dependent Master Equation: Discussion

In the former chapter the n-dependent n-resolved Quantum Master Equation (nQME) was derived. This derivation includes some assumptions, which strongly restrict the field of application.

To extend the field of applications the nQME is formally defined in section 3.1. This general specification can be easily extended to other, even non physical, problems.

In section 3.2 the different forms and representations of the nQME and the transformations between them are explained.

In section 3.3 the Full Counting Statistics is explained that can be derived from the nQME. The two possibilities, regarding either the occupations $P^{(n)}(t)$ or the moments, are discussed. Furthermore the connection between moments and cumulants, as well as their forms in time and Laplace Space, are described. In addition to that current and Fano factor are introduced.

Finally in 3.4 the long-time limit of current, Fano factor and higher cumulants are explained.

3.1   Formal definition

In the style of [Brandes, 2010] the following setting is defined:

Definition 1 (Conditioned Density Operator) $\rho^{(n)}(t)$ *is the reduced system density operator for a system that n electrons have passed in the time frame from 0 to t.*

At this point it might be appropriate to remark that this operator is a vector with d-real components in the superoperator formalism (see appendix B.3, p.138). In this case d is not necessary the square of the system dimensions, because some components might be neglected, as they are zero due to physical reality.

Furthermore it is always possible to represent complex entries of the density matrix with a base change with real numbers in the superoperator (vector). Examples can be seen in chapter 5, where the representation is discussed for the single ($d = 2$) and the Double Quantum Dot ($d = 5$).

From this setting it follows obviously that negative particle numbers or times do not occur.

This can be formulated as

Proposition 1 $t < 0 \vee n < 0 \Rightarrow \rho^{(n)}(t) = 0$.

Furthermore we call the

Definition 2 (Total initial Density Operator) ρ_0, *which is said to be the total system density operator ρ at $t = 0$.*

In contrast to the conditioned density operator, the total system operator obeys the condition 'trace class = 1' (see appendix B.7, p.134).

Therefore the initial condition for the conditioned density operator reads

Proposition 2 $t = 0 \Rightarrow \rho^{(n)}(t) = \delta_{n,0}\rho_0$.

Due to the relationship $\rho \equiv \sum_{n=0}^{\infty} \rho^{(n)}(t)$, arises

Proposition 3 $t > 0 \Rightarrow \sum_{n=0}^{\infty} \mathrm{Tr}\rho^{(n)}(t) = 1$.

It is assumed that $\rho^{(n)}(t)$ is compatible with

Equation 1 (nQME[1] in nt-representation)

$$\partial_t \rho^{(n)}(t) = \mathcal{L}_0^{(n)}\rho^{(n)}(t) + \mathcal{J}_{n-1}\rho^{(n-1)}(t). \tag{3.1}$$

This equation looks similar to the usual n-resolved QME [Gurvitz and Prager, 1996]. The difference is the dependence of the jump and nojump superoperator on the number of transmitted particles n.

Definition 3 (jump superoperator) *$\mathcal{J}^{(n)}$ can be represented as $d\times d$-matrix[2]. It describes processes, wherein particles leave the system and in this manner increase the number n.*

In almost the same manner

Definition 4 (nojump superoperator) *$\mathcal{L}_0^{(n)}$ can be expressed as $d\times d$-matrix.*

$\mathcal{L}_0^{(n)}$ *is the rest of the Liouvillian ($\mathcal{L}$), which describes processes, where the particles remain in a state with same n.*

Remark: $\mathcal{L}_0^{(n)}$ describes processes, where particles jump into the system and as well in internal system dynamics. This interpretation is also compatible with the agreement made in chapter 2, where the jump out process (on the right side) was drawn to change n (compare figure 2.1).

3.2 Forms and representations

Attentive readers might have asked themselves what 'nt-representation' in definition (3.1) stands for.

The following section gives a complete answer to that question. First of all the aim of the different forms of the representations are motivated.

The first glance at the nQME detects an differential equation. Usually an equation for $\rho^{(n)}(t)$ is preferred to a differential equation for $\partial_t\rho^{(n)}(t)$. Due to that, the Laplace Transformation is eye-catching, which turns the derivative into a multiplication.

In figure 3.1 this is described by the $\underset{t\to z}{\text{LT}}$ -arrow from the upper left to the upper right corner. The reason for choosing this way will be explained later on. Alternatively one could have make use of the recursive character of the nQME. This character can be easily discovered by investigating $\rho^{(0)}(t)$. If one regards proposition 1, it becomes clear that $\rho^{(-1)}(t)$ is 0. This implies that $\rho^{(0)}(t) = e^{\mathcal{L}_0^{(0)}t}\rho_0$.[3] This result can be inserted in the differential equation for $\rho^{(1)}(t)$ and recursive continued. Apart from that, it might be a hard job to calculate the average current (and higher current cumulants) as stated in the introduction. The average current is well known as $\partial_t Q(t)$ [Thomsen and Gumlich, 2008] or in other words $e^-\partial_t\langle N\rangle$, where $e^- = 1$ is the elementary charge, which one gets in our unit system.[4] In our case $\langle N\rangle = \text{Tr}N\rho$ can be simplified to $\sum_{n=0}^{\infty} n\text{Tr}\rho^{(n)}(t)$ by inserting the conditioned density matrix, where $N\rho^{(n)}(t) \equiv n$. As this infinite sum is hard to handle, the counting field variable χ is introduced by a Fourier Sequence Transform ($\underset{n\to\chi}{\text{FST}}$).

---

[2]To express the n-resolved jump operator for all n explicit, one would receive a tensor of order 3. Due to the finite system dimension this tensor could be flatted to a matrix. Nevertheless, this becomes only relevant within the vector notation approach (see appendix C.2.1, p. 143), whereon no further investigations were made in the context of this thesis.

[3]$\mathcal{L}_0^{(n)}$ is time independent in our case, so the time order operator and the integral in the exponent disappear.

[4]An exciting discussion about units can be found in [Wilczek, 2007].

Subsequently the moments and cumulants can be derived. The derivation according to the counting variable was already explained in section 3.3 and many other publications concerning Full Counting Statistics [Schaller et al., 2009, Kambly et al., 2010, Flindt et al., 2010a]. The paper of [Belzig, 2005] for example is a adjuvant overview.

To refer to figure 3.1 this action is expressed by the $\underset{n\to\chi}{\mathrm{FST}}$ -arrows from the top to the bottom.

$$
\begin{array}{ccc}
\partial_t \rho^{(n)}(t) = \mathcal{L}_0^{(n)}\rho^{(n)}(t) + \mathcal{J}_{n-1}\rho^{(n-1)}(t) & \xrightarrow{\;\underset{t\to z}{\mathrm{LT}}\;} & \hat\rho_n(z) = \hat{\mathcal{P}}_n(z)\hat{\mathcal{W}}_{\pi,0}^{(n-1)}(z)\rho_0 \\[2mm]
\underset{n\to\chi}{\mathrm{FST}}\Big\downarrow & & \underset{n\to\chi}{\mathrm{FST}}\Big\downarrow \\[2mm]
\partial_t \rho_\chi(t) = \partial_t \sum_{n=0}^{\infty} \rho^{(n)}(t)e^{in\chi} = \partial_t\left(\mathcal{P}_\chi(t) * \mathcal{G}_\chi(t)\rho_0\right) & \xleftarrow{\;\underset{z\to t}{\mathrm{LT}^{-1}}\;} & \hat\rho_\chi(z) = \hat{\mathcal{P}}_\chi(z)\hat{\mathcal{G}}_\chi(z)\rho_0
\end{array}
$$

Figure 3.1: Overview: Forms of the Quantum Master Equation
$*$: convolution integral
$\underset{t\to z}{\mathrm{LT}}$: Laplace Transformation
$\underset{n\to\chi}{\mathrm{FST}}$: Fourier Sequence Transformation

In the following the transformation between the forms are explained in detail:

Step 1: Laplace Transformation from time to z-domain $\;(\underset{t\to z}{\mathrm{LT}})$

The Laplace transformed density matrix is defined as

$$
\hat\rho_n(z) := \underset{t\to z}{\mathrm{LT}}\,\rho^{(n)}(t) = \int_0^\infty e^{-zt}\rho^{(n)}(t)\,\mathrm{d}t, \quad z \in \mathbb{C}. \tag{3.2}
$$

Applying the Laplace Transformation $(\underset{t\to z}{\mathrm{LT}})$ to equation (3.1) yields

$$
z\hat\rho_n(z) - \rho_n(t=0) = \mathcal{L}_0^{(n)}\hat\rho_n(z) + \mathcal{J}^{(n-1)}\hat\rho_{n-1}(z) \tag{3.3}
$$

$$
(z - \mathcal{L}_0^{(n)})\hat\rho_n(z) = \mathcal{J}^{(n-1)}\hat\rho_{n-1}(z) + \rho_n(t=0). \tag{3.4}
$$

In this connection $\rho_n(t=0)$ is the vector, when counting is started.

We write $\rho_n(t=0) =: \delta_{n,0}\rho_0$ and define the **propagator**[5]. $\hat{\mathcal{P}}_n(z) = \left(z - \mathcal{L}_0^{(n)}\right)^{-1}$.

Inserting this definition into the former equation leads to

$$
\hat\rho_n(z) = \hat{\mathcal{P}}_n(z)\left(\mathcal{J}^{(n-1)}\hat\rho_{n-1}(z) + \delta_{n,0}\rho_0\right). \tag{3.5}
$$

This is a recursive relationship for $\hat\rho_n(z)$

$$
\hat\rho_0(z) = \hat{\mathcal{P}}_0(z)\rho_0
$$

$$
\hat\rho_n(z) = \hat{\mathcal{P}}_n(z)\mathcal{J}^{(n-1)}\hat\rho_{n-1}(z). \tag{3.6}
$$

---

[5]Mathematically seen, this is the resolvent of $\mathcal{L}_0^{(n)}$. Compare also [Emary, 2009]

The next step is to get an explicit formula for (3.6). It can be expanded to

$$\hat{\rho}_n(z) = \hat{\mathcal{P}}_n(z)\mathcal{J}^{(n-1)}\ldots\mathcal{J}^{(1)}\hat{\mathcal{P}}_1(z)\mathcal{J}^{(0)}\hat{\mathcal{P}}_0(z)\rho_0. \tag{3.7}$$

By using the short hand notation

$$\hat{\mathcal{W}}_n(z) := \mathcal{J}^{(n)}\hat{\mathcal{P}}_n(z) = \frac{\mathcal{J}^{(n)}}{z - \mathcal{L}_0^{(n)}} \tag{3.8}$$

$$\hat{\mathcal{W}}_{\pi,0}^{(n-1)}(z) := \prod_{k=n-1}^{0} \hat{\mathcal{W}}_k(z) = \ldots \hat{\mathcal{W}}_2(z)\hat{\mathcal{W}}_1(z)\hat{\mathcal{W}}_0(z), \tag{3.9}$$

$\hat{\rho}_n(z)$ can be expressed as[6] [7]

$$\boxed{\hat{\rho}_n(z) = \hat{\mathcal{P}}_n(z)\hat{\mathcal{W}}_{\pi,0}^{(n-1)}(z)\rho_0.} \tag{3.10}$$

Step 2: Fourier Sequence Transformation from particle number to the counting field $\underset{n \to \chi}{(\text{FST})}$

Defining [8]

$$\hat{\rho}_\chi(z) = \sum_{n=0}^{\infty} \hat{\rho}_n(z)e^{\mathrm{i}n\chi} = \left(\sum_{n=0}^{\infty} e^{\mathrm{i}n\chi}\hat{\mathcal{P}}_n(z)\hat{\mathcal{W}}_{\pi,0}^{(n-1)}(z)\right)\rho_0. \tag{3.11}$$

This equation is quite abstract. Therefore, the first terms are explicitly written down (read from right to left).

$$\hat{\rho}_\chi(z) = \ldots e^{\mathrm{i}\chi}\hat{\mathcal{W}}_2(z) + \hat{\mathcal{P}}_2(z)\Big) e^{\mathrm{i}\chi}\hat{\mathcal{W}}_1(z) + \hat{\mathcal{P}}_1(z)\Big) e^{\mathrm{i}\chi}\hat{\mathcal{W}}_0(z) + \hat{\mathcal{P}}_0(z)\Big) \rho_0 \tag{3.12}$$

If there is no additional information about $\hat{\mathcal{W}}_n(z) = \frac{\mathcal{J}^{(n)}}{z - \mathcal{L}_0^{(n)}}$, it seems as there was no general expression for that sum. In forecast to the clean limit and the general case discussed in [Flindt et al., 2008], the formal short hand notation

$$\hat{\mathcal{P}}_\chi(z)\hat{\mathcal{G}}_\chi(z) \equiv \left(\sum_{n=0}^{\infty} e^{\mathrm{i}n\chi}\hat{\mathcal{P}}_n(z)\hat{\mathcal{W}}_{\pi,0}^{(n-1)}(z)\right) \tag{3.13}$$

is introduced and (3.11) reads

$$\boxed{\hat{\rho}_\chi(z) = \hat{\mathcal{P}}_\chi(z)\hat{\mathcal{G}}_\chi(z)\rho_0.} \tag{3.14}$$

The difference between this notation and the notation, used in

$$[\text{Flindt et al., 2008}]: \quad \hat{\rho}(\chi, z) = \hat{\mathcal{G}}(\chi, z)\hat{\rho}(\chi, t = 0), \tag{3.15}$$

---

[6]Notation advice: An empty product $\prod = 1$ and an empty sum $\sum = 0$.

[7]If one does not like the definition with the $\hat{\mathcal{W}}_{\pi,0}^{(n-1)}(z)$ superoperator, one can keep the explicit formulation of equation (3.7) in mind.

[8]Notation advice: From now on χ is the counting field variable. This is independent from the total system matrix.

is that in our case the superoperator $\hat{\mathcal{W}}$ depends explicit on n and not on $n - n'$.

This becomes relevant in chapter 7, where the impurity case is discussed.

For now, we investigate the known case, where the jump operator does not depend on n. From now on this case is called **clean case**.

The same procedure is applied to *random tunneling rates* in part II. The special case of the *simulated Single Quantum Dot* is taken into account in chapter 8, where the simplification of $\hat{\mathcal{P}}_\chi(z)\hat{\mathcal{G}}_\chi(z)$ is slightly different from the procedure for the clean case. The results for n-independent Liouvillian and jump operator, e.g. independent rates $\Gamma_n = \Gamma$, have already been discussed in the previous chapters of this thesis. For comparison we reference back to these results and mark these sections with **clean limit** or clean case.

n-independent nojump operator $(\mathcal{L}_0)$

To demonstrate how to calculate with the introduced superoperators, this step was inserted on the way to the clean case. Nevertheless this should be seen as mathematical example, for which no common physical realization exists. [9] Assuming that the Liovillian is constant $\mathcal{L}_0^{(n)} = \mathcal{L}_0$ and the jump operator $\mathcal{J}^{(n)}$ stays n-dependent, leads to a constant propagator $\hat{\mathcal{P}}(z) = \hat{\mathcal{P}}_n(z)$.

Equation (3.11) gets simplified to

$$\hat{\rho}_\chi(z) = \hat{\mathcal{P}}(z)\left(\sum_{n=0}^{\infty} e^{in\chi}\hat{\mathcal{W}}_{\pi,0}^{(n-1)}(z)\right)\rho_0. \tag{3.16}$$

As above the short hand notation

$$\hat{\mathcal{G}}_\chi(z) = \left(\sum_{n=0}^{\infty} e^{in\chi}\hat{\mathcal{W}}_{\pi,0}^{(n-1)}(z)\right) \tag{3.17}$$

is used and (3.11) reads

$$\hat{\rho}_\chi(z) = \hat{\mathcal{P}}(z)\hat{\mathcal{G}}_\chi(z)\rho_0. \tag{3.18}$$

Clean limit

For the case of the additional restriction of a constant jump operator $\mathcal{J} = \mathcal{J}^{(n)}$, it is eye-catching that $\hat{\mathcal{W}}_n(z) = \hat{\mathcal{W}}(z)$. $\hat{\mathcal{W}}_{\pi,0}^{(n-1)}(z)$ simplifies to $\hat{\mathcal{W}}_{\pi,0}^{(n-1)}(z) = \hat{\mathcal{W}}^n(z)$. Thus, $\hat{\rho}_n(z)$ (3.10) becomes

$$\hat{\rho}_n(z) = \hat{\mathcal{P}}(z)\hat{\mathcal{W}}^n(z)\rho_0 = \hat{\mathcal{M}}^n(z)\hat{\mathcal{P}}(z)\rho_0. \tag{3.19}$$

---

[9] The difficulty is to construct a jump operator, where the entries in the columns sum up to 0. An imaginable process would be a system with two or more targets (on the right side). One possible jump process would be the following case: The electron is in a state, in which it is clear, that it leaves the system in the next step. The degree of freedom is limited to the targets, the electron jumps to. This rate could be n-dependent and would not affect the claim that the sum over the column entries has to be 0.

As it was implied by (3.12), $\hat{\mathcal{G}}_\chi(z)$ becomes a geometric sequence [10], where the limit is known as $\hat{\mathcal{G}}_\chi(z) = \left(1 - \hat{\mathcal{W}}(z)e^{i\chi}\right)^{-1}$. Thus, equation (3.14) can be expanded to

$$\hat{\rho}_\chi(z) = \hat{\mathcal{P}}(z)\frac{1}{1 - \hat{\mathcal{W}}(z)e^{i\chi}}\rho_0. \tag{3.20}$$

For comparison we define $\hat{\mathcal{M}}(z) := \hat{\mathcal{P}}(z)\mathcal{J}$, which allows to rewrite the former equation to

$$\hat{\rho}_\chi(z) = \frac{1}{1 - \hat{\mathcal{M}}(z)e^{i\chi}}\hat{\mathcal{P}}(z)\rho_0. \tag{3.21}$$

With the definition $\hat{\rho}_0(z) := \hat{\mathcal{P}}(z)\rho_0$ we get

$$\hat{\rho}_\chi(z) = \left(1 - e^{i\chi}\hat{\mathcal{M}}(z)\right)^{-1}\hat{\rho}_0(z). \tag{3.22}$$

This is very similar to (3.15), which was expected for the clean case.

Admittedly this is a more descriptively form. However it is not 'compatible' to the n-dependent case, as rates of order n and $n-1$ would be mixed in that case.

Alternative way*

An alternative is to use the other way round in the diagram 3.1. The counting field in the time domain is defined as expected as $\rho_\chi(t) = \sum_{n=0}^\infty \rho^{(n)}(t)e^{in\chi}$. This way was used by [Flindt, 2007] and is adopted in chapter 7. It can be stated that both ways lead to the same result

$$\rho_\chi(t) = \underset{n\to\chi}{\mathrm{FST}}\rho^{(n)}(t) = \underset{z\to t}{\mathrm{LT}}{}^{-1}\underset{n\to\chi}{\mathrm{FST}}\underset{t\to z}{\mathrm{LT}}\rho^{(n)}(t). \tag{3.23}$$

Formally that means that one has to prof the **Commutativity of diagram 3.1**. Therefore, it is sufficient to show that $\left[\underset{n\to\chi}{\mathrm{FST}}, \underset{t\to z}{\mathrm{LT}}\right]\rho^{(n)}(t) = 0$. This can be mathematically shown in the following way. In our formalism $\rho^{(n)}(t)$ is a vector, which depends on the variable t. Writing this vector as $\rho(n,t) \neq \rho(n(t),t)$ shows that the variables n and t are independent and can be transformed independently.

---

[10] $(1 + x(1 + x(1 + x(1 + \dots))))$ with $x = e^{I\chi}\hat{\mathcal{W}}(z)$

3.3   Statistical quantities

In this section it will be discussed how the relevant information of the nQME are filtered out. In general there are two strongly related approaches. On the one hand one could directly take a visual look to the **occupation** of the system by printing a histogram, which specifies the probability distribution that indicates how many particles have passed a system after a certain time. This representation does not necessarily provide clear statements. But it is always possible to get the probability distribution with a numeric simulation. The connection between density matrix and occupation approach is discussed in the first subsection. The possibility to create of an histogram with a numeric simulation stands in connection with a large computational effort.

On the other hand the methods of descriptive statistics can be used, where one describes the histogram with a view variables that specify its outlook. The advantage of this approach is that the information, gained by this proceeding, classifies the system and produces well-defined results.

distrib.	binomial (discrete)			Rayleigh			chi squared		
PDF	$P(x) = \binom{n}{x} p^x (1-p)^{n-x}$			$f(x) = \frac{x}{\sigma^2} e^{-x^2/2\sigma^2}$			$f(x) = \frac{e^{-x/2} 2^{-\sigma/2} x^{\frac{\sigma}{2}-1}}{\Gamma(\frac{\sigma}{2})}$		
param.	$n = 20, p = .5$			$\sigma = 5$			$\sigma = 5$		
mom.	5.	27.5	162.5	1017.5	6.27	50.	470.	5000.	5.	35.	315.	3465.
cum.	5.	2.5	0.	-1.25	6.27	10.73	22.18	28.22	5.	10.	40.	240.
aam.	5.	2.5	0.	2.8	6.27	10.73	0.631	3.245	5.	10.	1.26	5.4
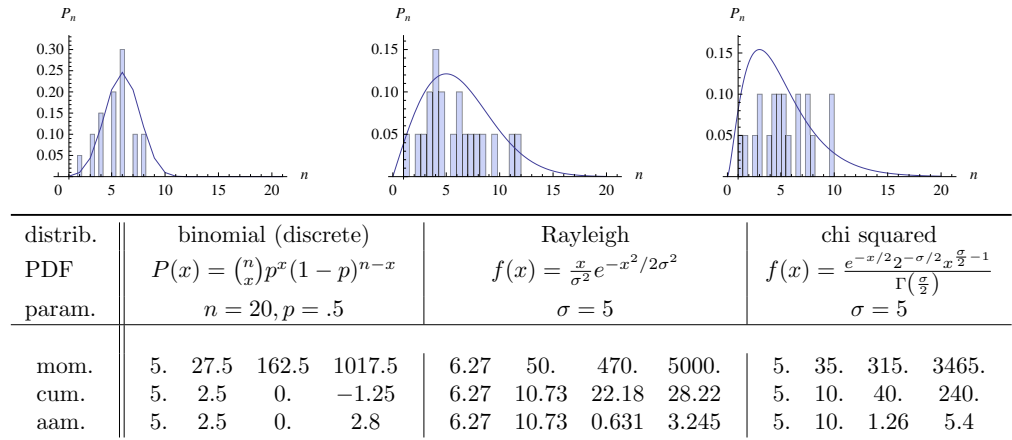
Figure 3.2: Three exemplary Probability-Density-Functions (PDF) and normed histograms for 20 events of certain distributions. In the table details for the distributions are given. The values were calculated with a simple Mathematica Program and only give an imagination of the gathering of image and parameter. The following abbreviations are used.
distrib.:name of the distribution
param.:parameter used for the PDF- and histogram-plot
mom.: moments 1 to 4
cum.: cumulants 1 to 4
nam.: named forms 1 = mean, 2 = variance, 3 = skewness, 4 = kurtosis
(from left to the right)

There are three equal ways of description in means of descriptive statistics.

Moments can be simply derived from the nQME, but are not very intuitive.

Cumulants can be derived directly from the moments and are more intuitive.

Named forms exist for the first crucial parameters

(mean, variance, skewness, kurtosis).

The disadvantage of this approach is that there are only few systems, where these values can be derived analytically. However, even if the values come from a numerical evaluated histogram (first approach), it leads to comparable data. In figure 3.2 this is visualized for some distribution, which are chosen independently from physical models. In the following section the situation is explained, where the density $\hat{\rho}_\chi(z)$ matrix is known as a function of the counting field. For arbitrary n-dependence of the QME this is not the case. In that case this technique would not be applicable and a way to derive $m_n(t)$ directly from $\rho^{(n)}(t)$ would have to be found. However, there is a wide range of cases (clean case, random case (part II), simulated Single Quantum Dot (see chapter 8)), where this technique can be used.

The way from the density matrix $\hat{\rho}_\chi(z)$ to the long-time cumulants is visualized in figure 3.3 and will be explained in the following two sections.

$$\hat{\rho}_\chi(z) \xrightarrow{\text{Tr}} \hat{M}(\mathrm{i}\chi) \xrightarrow{\partial_{\mathrm{i}\chi}^n, \chi \to 0} \hat{m}_n(z) \xrightarrow[z \to t]{\text{LT}^{-1}} m_n(t) \xrightarrow{\sum \binom{n}{k}} c_n(t) \xrightarrow{t \to \infty} c_{n,\infty}$$

$$\underset{z=0}{\succ\!\!\!\prec} \downarrow \qquad\qquad \frac{c_{n,\infty}}{c_{1,\infty}} \to \langle I_\infty \rangle, \langle F_\infty \rangle \dots$$

$$\tilde{m}_n(z) \xrightarrow[z \to t]{\text{LT}^{-1}} \bar{m}_n(t) \xrightarrow{\sum \binom{n}{k}} \bar{c}_n(t) \xrightarrow{t \to \infty} c_{n,\infty}$$

Figure 3.3: Overview: From Density matrix to statistical quantities
This scheme illustrates how the cumulants can be calculated. The values on the bottom are approximated. In the long-time limit this should lead to the same results as the exact calculation for the current ($\langle I_\infty \rangle$) Fano-factor ($\langle F_\infty \rangle$)
LT: Laplace Transformation
FST: Fourier Sequence Transformation
$\underset{z=0}{\succ\!\!\!\prec}$: Taylor Series

The overall concept to derive the cumulants (in time space) from the moments in Laplace Space is the following:

---

1. to calculate the moments $\hat{m}_k(z)$ in Laplace Space
2. to do Inverse Laplace Transform of $\hat{m}_k(z)$ written as $m_k(t)$
3. to calculate the cumulants $c_n = m_n(t) - \sum_{k=1}^{n-1} \binom{n-1}{k-1} c_k m_{n-k}(t)$
4. to normalize c_n to c_1

After that it is possible to derive the long-time limit.

At this point it has to be remarked that this procedure was detailedly discussed by many authors [Flindt et al., 2010a, Belzig, 2005]. Especially the way taken by [Flindt et al., 2010b] is quite similar to the approach in this thesis.

3.3.1   Occupation

The object we are interested in, are not the density matrices themselves, but the sum of the probability of the occupation. For example, the probability distribution concerning the number of transmitted particles at a specific time, is in focus of interest. Examples can be seen in part III, e.g. in figure 9.3.

The connection between probability and density operator is given by

$$\text{P} = \text{Tr}\rho \tag{3.24}$$

in the not n-resolved case $\text{P} = 1$. In the n-resolved case we achieve

$$1 = \sum_n \text{P}_n. \tag{3.25}$$

For $\text{P}_\chi = \sum_n \text{P}_n e^{\mathrm{i}n\chi}$,

$$\text{P}_{\chi=0} = 1. \tag{3.26}$$

P might depend on t or z what is not explicitly marked. In the z-dependent case

$$\hat{\text{P}} := \hat{\text{P}}(z) = \mathop{\text{LT}}_{t \to z} \text{P}(t).$$

3.3.2   Moments

From the mathematical point of view k'th moment (of the occupation probability) in Laplace Space has to be defined as

$$\hat{m}_k(z) := \lim_{\chi \to 0} \partial_\chi^k \hat{M}(\chi) \quad \text{moment,} \tag{3.27}$$

whereby $\hat{M}(\mathrm{i}\chi)$ is **the Moment Generating Function** (MFG). For a single random variable X this function is defined by $M_X(\mathrm{i}\chi) = \left\langle e^{\mathrm{i}\chi X} \right\rangle$ [Ming-Kuei, 1962, Weisstein,], in accordance to our definition of the

Moment **G**enerating **F**unction $\boxed{\hat{M}(\mathrm{i}\chi) = \hat{\text{P}}(\chi) = \text{Tr}\hat{\mathcal{P}}\hat{\mathcal{G}}_\chi(z).}$ \qquad(3.28)

That leads to the same result as in [Emary, 2009, 9.22]. Explicitly spoken the Inverse Laplace Transformation yields

$$\mathop{\text{LT}}_{z \to t}^{-1}\hat{\text{P}}(\chi) = \sum_n \text{P}_n(t)e^{\mathrm{i}n\chi} = M(\chi). \tag{3.29}$$

Computation power

To calculate the moments explicitly we have to compute the derivatives of the Moment Generating Function. The common way is to calculate the Moment Generating Function for a specific given problem and derive the moments henceforward. But it is also possible to derive the moments in general. The advantage within this approach is that one only has to calculate the powers of matrices instead of derivatives. Through that the computational effort decreases. To give an example: For the Double Quantum Dot, the Moment Generating Function approach needs more than 64 seconds to calculate the Fano factor (definition see below) with random tunneling rates. The matrix approach consumes less than 2 seconds.[11]

General formula for moments

In this section the general way is discussed. Therefore theorem 12 (p. 132) is useful.

The application of this theorem with $\hat{\mathcal{G}}_\chi(z) = \frac{1}{1 - \hat{\mathcal{W}}(z)e^{i\chi}} (\leftrightarrow A^{-1})$ leads to

$$\partial_\chi \hat{\mathcal{G}}_\chi(z) = -\hat{\mathcal{G}}_\chi(z).\partial_\chi(1 - \hat{\mathcal{W}}(z)e^{i\chi}).\hat{\mathcal{G}}_\chi(z) \tag{3.30}$$

$$= ie^{i\chi}\hat{\mathcal{G}}_\chi(z).\hat{\mathcal{W}}(z).\hat{\mathcal{G}}_\chi(z). \tag{3.31}$$

The i factor vanishes if one regards the definition of the moment (3.27) (obviously $\partial_{i\chi}^k = \frac{1}{i^k}\partial_\chi^k$). This means for the first moment $\hat{m}_1(z)$

$$\hat{m}_1(z) = -\,i\mathrm{Tr}\hat{\mathcal{P}}(z).\partial_\chi\hat{\mathcal{G}}_\chi(z).\rho_0\Big|_{\chi\to 0}$$

$$= \mathrm{Tr}\hat{\mathcal{P}}(z).\hat{\mathcal{G}}_\chi(z).e^{i\chi}\hat{\mathcal{W}}(z).\hat{\mathcal{G}}_\chi(z).\rho_0\Big|_{\chi\to 0}$$

$$= \mathrm{Tr}\hat{\mathcal{P}}(z).(1 - \hat{\mathcal{W}}(z))^{-1}.\hat{\mathcal{W}}(z).(1 - \hat{\mathcal{W}}(z))^{-1}\rho_0 \tag{3.32}$$

$$= \mathrm{Tr}\hat{\mathcal{P}}(z)\hat{\mathcal{G}}_0(z)\hat{\mathcal{W}}(z)\hat{\mathcal{G}}_0(z)\rho_0 \tag{3.33}$$

with $\hat{\mathcal{G}}_0(z) = (1 - \hat{\mathcal{W}}(z))^{-1}$. The higher moment can be calculated in the same procedure.

The second and third moment read

$$\hat{m}_2(z) = \mathrm{Tr}\hat{\mathcal{P}}(z)\hat{\mathcal{G}}_0(z)\Big(\hat{\mathcal{W}}(z)\hat{\mathcal{G}}_0(z) + 2(\hat{\mathcal{W}}(z)\hat{\mathcal{G}}_0(z))^2\Big)\rho_0 \tag{3.34}$$

$$\hat{m}_3(z) = \mathrm{Tr}\hat{\mathcal{P}}(z)\hat{\mathcal{G}}_0(z)\Big(\hat{\mathcal{W}}(z)\hat{\mathcal{G}}_0(z) + 6(\hat{\mathcal{W}}(z)\hat{\mathcal{G}}_0(z))^2 + 6(\hat{\mathcal{W}}(z)\hat{\mathcal{G}}_0(z))^3\Big)\rho_0. \tag{3.35}$$

For the exact calculation and derivation refer to appendix C.1, p. 141.

---

[11] This is the time needed by the analytical Mathematica Program. A numerical algorithm, e.g. written in C using LaPack, is expected to be much faster.

The general expression for the m'th moment reads

$$\hat{m}_m(z) = \mathrm{Tr}\hat{\mathcal{P}}(z)\hat{\mathcal{G}}_0(z)\left(\sum_{k=1}^{m} c(m,k)(\hat{\mathcal{W}}(z)\hat{\mathcal{G}}_0(z))^m\right)\rho_0. \tag{3.36}$$

$c(m,k)$ is a numeric coefficient that can be calculated numerically in a very short time.

$$c(m,k) = k!\,\tilde{c}(m-k+1,k) \tag{3.37}$$

$$\text{with}\quad \tilde{c}(s,k) = \begin{cases} \sum_{i=1}^{k} i\tilde{c}(s-1,i) & s>1 \\ 1 & \text{else} \end{cases} \tag{3.38}$$

This recursive property was also investigated in [Flindt et al., 2010a] with a different notation explained in [Flindt et al., 2005, Flindt et al., 2004].

Inverse Laplace Transformation

The next step is the Inverse Laplace Transformation $\underset{z\to t}{\mathrm{LT}}^{-1}$ of the moments $\hat{m}_n(z)$. Unfortunately, there are many cases, where this Inverse transformation cannot be calculated analytically. Nevertheless, the key interest is only the long-time limit for the moments, cumulants etc. Therefore the difficulties of the Inverse Laplace Transformation can be avoided by a series approximation. Thus, one makes a series development around the point $z=0$ (denoted as $\underset{z=0}{\bowtie}$), the moments up to the order of $O(z^0)$. This is sufficient, if the long-time limit is in focus of interest. In terms of diagram 3.3 that means that one would take the lower path. The following notation is used

$$\tilde{m}_n(z) = \sum_{b} a_b z^{-b} + O(z)^0 \approx \hat{m}_n(z). \tag{3.39}$$

This function only depends on terms of the form az^{-b}, where the Inverse Laplace Transformation is known as $\underset{z\to t}{\mathrm{LT}}^{-1}az^{-b} = \frac{a}{(b-1)!}t^{b-1}$. At this point it becomes obvious that higher order terms vanish in the long-time limit. For details cf. proposition 8 (p. 130). The moments in time space are called $m_n(t)$ and the series approximation is denoted with $\bar{m}_n(t)$.

3.3.3 Cumulants

Afterwards it is straight forward to derive the cumulants. The relationship between moments and cumulants is given by

$$c_n(t) := m_n(t) - \sum_{k=1}^{n-1} \binom{n-1}{k-1} c_k(t) m_{n-k}(t). \tag{3.40}$$

A special case of this formula is the **displacement law** (theorem 5). The approximated cumulants, which are derived by the approximated moments, are analogy defined as

$$\bar{c}_n(t) := \bar{m}_n(t) - \sum_{k=1}^{n-1} \binom{n-1}{k-1} \bar{c}_k(t) \bar{m}_{n-k}(t). \tag{3.41}$$

At this juncture it has to be discussed what the appropriated order of the series approximation is. Therefore theorem 8, **series of a product of functions**, is helpful. Applying this theorem to the definition of $\bar{c}_n(t)$ shows that, if the order of the Taylor Series for $\bar{m}_n(t)$ is k, the order of $\bar{c}_n(t)$ is k as well. As well as there is a Moment Generating Function for the moment, there is a **Cumulant Generating Function** (CGF) for the cumulants. The CFG is only well defined in time space. The connection between MGF and CGF is simply given by

$$\hat{M}(\mathrm{i}\chi) = e^{F(\chi;t)}. \tag{3.42}$$

In this thesis the CFG will play a minor role. An interesting discussion can be found in [Flindt et al., 2010b, 11], where the identical results are gained in one step

$$e^{S(\chi,t)} = \frac{1}{2\pi\mathrm{i}} \int\limits_{c-\mathrm{i}\infty}^{c+\mathrm{i}\infty} e^{zt} \hat{P} dz. \tag{3.43}$$

3.3.4 Central moments

The representation of moments, cumulants, current and Fano factor in terms of raw moment of waiting $\langle \tau^k \rangle$ is helpful for the clean limit. In that case the density function is a delta function $f(\tau) = \delta(\tau - \tau_0)$, which replaces the waiting time by its value $\langle \tau^k \rangle \to \tau_0^k$. A distribution function, which is given in terms of the expected value and its central moments, is likely in reality, where distributed waiting times appear. Therefore it is convenient to express the results in terms of central moment (e.g. $c_k(t, \langle \tau \rangle, \langle \tau^2 \rangle, \langle \tau^3 \rangle \dots) \to c_k(t, \langle \tau \rangle, \mu_2, \mu_3, \dots)$). The transformation function is given by [Weisstein, 2010a]

$$\mu_n = \sum_{k=0}^{n} \binom{n}{k} (-1)^{n-k} \langle \tau^k \rangle \langle \tau \rangle^{n-k}, \tag{3.44}$$

which implies [Weisstein, 2010b]

$$\langle \tau^n \rangle = \sum_{k=0}^{n} \binom{n}{k} \mu_k \langle \tau \rangle^{n-k}. \tag{3.45}$$

3.3.5   Named forms

Table 3.1: Named statistical quantities

mean	$\langle \mathrm{P} \rangle = m_1(t) = c_1(t)$
variance	$\mathrm{Var}(\mathrm{P}) = c_2(t) = \langle (\mathrm{P} - \langle \mathrm{P} \rangle)^2 \rangle = \langle \mathrm{P}^2 \rangle - \langle \mathrm{P} \rangle^2$
skewness	$\dfrac{\langle (\mathrm{P} - \langle \mathrm{P} \rangle)^3 \rangle}{\mathrm{Var}(\mathrm{P})^{\frac{3}{2}}} = \dfrac{c_3(t)}{c_2(t)^{\frac{3}{2}}}$
kurtosis	$\dfrac{c_4(t)}{c_2(t)}$

Apart from the named forms for statistical properties (listed in table 3.1) there are two named quantities. First of all, the (average) current, which is as expected the time derivative of the first moment.

$$\text{Current} \quad \boxed{I(t) = \partial_t m_1(t)} \tag{3.46}$$

Secondly there is the Fano factor [Fano, 1947], which is defined by

$$\text{Fano factor} \quad \boxed{F(t) = \frac{c_2(t)}{c_1(t)}.} \tag{3.47}$$

Roughly spoken the Fano factor is the common way to describe the quality of the current. A small Fano factor stands for a constant current.

Fano factor in Laplace Space*

A hardly possible way to calculate the second cumulant, is to use a standard Laplace Transformation

$$\hat{c}_2(z) = \hat{m}_2(z) - \frac{1}{2\pi \mathrm{i}} \int_{c-\mathrm{i}\infty}^{c+\mathrm{i}\infty} \hat{m}_1(\sigma) \hat{m}_1(z - \sigma) \, d\sigma. \tag{3.48}$$

In that case one has to be careful with the choice of c, because all poles of $\hat{m}_1(z)$ and not of $\hat{m}_1(\sigma)\hat{m}_1(z - \sigma)$ have to be collected to keep the integral convergent[12].

Afterwards, the Laplace Transformation of the reciprocal of the first moment in time space is needed. Unfortunately there seems to be no easy way to calculate

---

[12]That formula was derived via $\underset{t \to z}{\mathrm{LT}}(m_1(t)^2) = \int_0^t m_1(t)m_1(t)e^{-zt}\,dt$, where one replaces a term $m_1(t)$ by $\int_{c-\mathrm{i}\infty}^{c+\mathrm{i}\infty} \hat{m}_1(\sigma)e^{\sigma t}\,d\sigma$. The pole of $\hat{m}_1(z)$ with the highest real part is called σ_{max}. Now one can choose $c = \sigma_{max} + \epsilon$ with a small $\epsilon > 0$. So $\underset{t \to z}{\mathrm{LT}}(m_1(t)^2) = \int_{c-\mathrm{i}\infty}^{c+\mathrm{i}\infty} \hat{m}_1(\sigma) \int_0^t m_1(t)e^{-(z-\sigma)t},\,dt\,d\sigma$, where $\int_0^t m_1(t)e^{-(z-\sigma)t}\,dt = \hat{m}_1(z - \sigma)$, which only converges if $Re(z - \sigma) > \sigma_{max} \Rightarrow Re(z) > \epsilon$.

the reciprocal in the time domain of a function given in Laplace Space in general. So one would need to transform the first moment into time space, calculate the reciprocal and transform back again. In most cases it will be easier to use the general method presented in the next chapter. For the case that

$$\hat{m}_{1tInv}(z) \equiv \mathop{\mathrm{LT}}_{t \to z} \left(\frac{1}{\mathop{\mathrm{LT}^{-1}}_{z \to t}(\hat{m}_1(z))} \right) \tag{3.49}$$

is known, the Fano factor in Laplace Space can be defined as

$$\hat{F}(z) := \frac{1}{2\pi \mathrm{i}} \int_{c-\mathrm{i}\infty}^{c+\mathrm{i}\infty} \hat{c}_2(z)\hat{m}_{1tInv}(z) \, d\sigma. \tag{3.50}$$

This is the Laplace Transformation of

$$F(t) = \frac{c_2(t)}{c_1(t)}, \tag{3.51}$$

which was the Fano factor, defined by (3.47).

To carry out this integration might involve some difficulties. This will be clarified with the example. In the example this method is used, even though it is not the simplest way to derive the result (see section 5.1).

3.4 Long-time limit

The time evolution of the moments and cumulants is often hard to obtain. The impurity case in chapter 7 is an example for that (see also [Zedler et al., 2009]). In many cases the key interest is in the long-time values and not the behavior of the current on very small time steps. In addition to that the approximations made in the derivation are better for large times. Therefore, one regards the quantities at large times. In mathematical words in the limit for $t \to \infty$.

The long-time limit for current is defined as

$$\text{Long-time Current} \quad \begin{aligned} \langle I_\infty \rangle &\equiv \lim_{t \to \infty} \partial_t m_1(t) \\ &= \lim_{z \to 0} z^2 \hat{m}_1(z). \end{aligned} \tag{3.52} \tag{3.53}$$

The proof of the equality of definition 3.53 is given within theorem 9.

With a known Fano factor in Laplace Space, it would be possible to derive the long-time limit as in the former section.

$$F(t \to \infty) = \lim_{z \to 0} z\hat{F}(z) \tag{3.54}$$

In the regarded cases this does not occur. So one has to use the standard method to calculate the Fano factor in the time space.

$$\text{Long-time Fano factor} \quad \langle F_\infty \rangle \equiv \lim_{t \to \infty} \frac{c_2(t)}{c_1(t)} \tag{3.55}$$

In the same style the long-time limit for higher order cumulants is obtained. A special notation for that is not being introduced. So we write

$$\lim_{t\to\infty} \frac{c_k(t)}{c_1(t)} \tag{3.56}$$

for the **k'th cumulant** normed to the first cumulant in the long-time limit. This normation is helpful, because one otherwise obtains many infinite values for the cumulants.[13]

---

[13]Even the simplest example, the Tunneling Junction in the clean limit and infinite bias limit, leads to infinite long-time cumulants if no feedback loop is applied to the system cf. chapter 9 for details.

Part II

Application to random waiting times

Chapter 4

Formalism

In this part it will be explained, how current, Fano factor and higher order cumulants can be obtained for random tunneling rates. One might ask oneself why the rates should become random in physical reality. Imagining a real system, for example the Single Quantum Dot with n-dependent tunneling rates. If one remembers the derivation, where the bath was described as grand canonical ensemble, one might get the idea of a continuous change of the rates up to a balanced situation. This case has already been discussed.However, the assumption that the bath is constant, does not fit to the real situation, where many fluctuations exist in the bath. Due to the size of the bath, there is no reasonable chance to find an exact expression. Therefore, one assumes that the rates are random variables with a certain statistic. This approach is common in solid state physics, where the system size becomes large soon.

Assumption: statistical independence

With the assumption that all $\Gamma_\alpha^{(n)}$ are statistically independent, one is able to solve the Quantum Master Equation (nQME) equally to the way, taken in the clean limit. The key idea is to **replace the n-independent terms by their expectation values**.

Two way randomness

This random rates read to two types of random processes. On the one hand there is the statistical randomness that is induced by the random rates. On the other hand there is the standard quantum mechanical randomness that occurs in the clean limit as well. In this thesis we will focus on the expectation value of the probability with regard to the tunneling rates. Higher Moments, with regard to the statistical distribution of the rates, are not taken into account. For example the calculation of the Fano factor of the Fano factor is possible, but a reasonable physical interpretation of this value cannot be obtained at the

actual level of considerations. For the nQME (3.1) this means

$$\left\langle \partial_t \rho^{(n)}(t) \right\rangle = \left\langle \mathcal{L}_0^{(n)} \rho^{(n)}(t) + \mathcal{J}_{n-1} \rho^{(n-1)}(t) \right\rangle. \tag{4.1}$$

This equation is no really good starting point as the right hand side depends on $n, n-1$. The use of the solved form in Laplace Space (3.10)

$$\langle \hat{\rho}_n(z) \rangle = \left\langle \hat{\mathcal{W}}_\pi^{(n)}(z) \hat{\mathcal{P}}_0(z) \rho_0 \right\rangle \tag{4.2}$$

is much better, because the rates factorize in this representation. At this point it is helpful to define $\hat{\mathcal{W}}(z) = \left\langle \hat{\mathcal{W}}_n(z) \right\rangle, \hat{\mathcal{P}}(z) = \left\langle \hat{\mathcal{P}}_n(z) \right\rangle$.

Now the **expectation value for the system density matrix in Laplace Space** reads

$$\boxed{\langle \hat{\rho}_n(z) \rangle = \hat{\mathcal{W}}(z)^n \hat{\mathcal{P}}(z) \rho_0.} \tag{4.3}$$

With the discrete Fourier Transformation and the short notation $\rho_\chi(t) = \sum_n \rho^{(n)}(t) e^{in\chi}$ one gets

$$\langle \hat{\rho}_\chi(z) \rangle = \left[1 - e^{i\chi} \hat{\mathcal{W}}(z) \right]^{-1} \hat{\mathcal{P}}(z) \rho_0. \tag{4.4}$$

Defining the k'th moment in Laplace Space as

$$\hat{m}_k(z) := \left. \frac{\text{Tr} \partial_\chi^k \langle \hat{\rho}_\chi(z) \rangle}{i^k} \right|_{\chi \to 0}, \tag{4.5}$$

leads formally to similar moments as in the clean limit. [1]

Time domain

Formally one can transfer back to the **time domain** and derive the $P_n(t)$. Calling $\mathcal{P}(t)$ the Inverse Laplace Transformation of $\hat{\mathcal{P}}(z)$ and $\mathcal{R}_\chi(t)$ the Inverse Laplace Transformation of $\hat{\mathcal{G}}_\chi(z) = [1 - e^{i\chi} \hat{\mathcal{W}}(z)]^{-1}$, leads to the formal definition

$$\langle \rho_\chi(t) \rangle := \mathcal{P}(t) * R_\chi(t). \tag{4.6}$$

In this context $*$ stands for the convolution-integral. If this expression can be calculated analytically, depends on the concrete realization of the system.

----

[1]Strictly one has to write $\langle \hat{m}_k(z) \rangle$ instead of $\hat{m}_k(z)$.

Waiting times

It is often helpful to use waiting times τ instead of tunneling rates Γ. Especially in experiments the measurement results are expected to be waiting times instead of tunneling probabilities. The general relation between **waiting times** and **tunneling rates** is defined by

$$\text{(waiting time)} \quad \tau := \frac{1}{\Gamma}. \tag{4.7}$$

Waiting times and tunneling rates are connected via the following relationship

$$\langle \Gamma \rangle = \int \Gamma f(\Gamma) \, d\Gamma = \int \frac{1}{\tau} \tilde{f}(\tau) \, d\tau \tag{4.8}$$

$$\tilde{f}(\tau) := \int \delta \left(\frac{1}{\Gamma} - \tau \right) f(\Gamma) \, d\Gamma = \left. \frac{f(\Gamma)}{\frac{1}{\Gamma^2}} \right|_{\Gamma = \frac{1}{\tau}} = \frac{1}{\tau^2} f \left(\frac{1}{\tau} \right) \tag{4.9}$$

and the other way round.

Obviously $\tilde{f}(\tau)$ fulfills the same properties as $f(\Gamma)$. Integration, by substitution $(x = \tau^{-1})$ of

$$\int_0^\infty \tilde{f}(\tau) \, d\tau = \int_0^\infty \frac{1}{\tau^2} f \left(\frac{1}{\tau} \right) \, d\tau = \int_{\frac{1}{0}}^{\frac{1}{\infty}} -\frac{x^2}{x^2} f(x) \, dx = \int_0^\infty f(x) \, dx = 1, \tag{4.10}$$

shows the property of norming.

Alternative denotation: Negative moments

Instead of waiting times, $\langle \Gamma^{-k} \rangle$ could have be called k'th negative moment. A disadvantage of this appellation is that waiting times can be mixed up with the waiting time distribution for constant tunneling rates studied in [Brandes, 2008]. The origin of the waiting times is the default quantum mechanical blur. In contrast to that, the waiting time distribution discussed in this thesis, targets the statistical uncertainness of tunneling rates. The investigation of the relationship between this different types of waiting times could be the subject of future research. A brief discussion on that topic can be found in chapter 10.

nQME Mathematica Package

Due to the huge computational effort, which is needed to do the calculations a Mathematica Program was developed. This program is aware to calculate automatically the analytical expressions for current, Fano factor and higher cumulants for the long time limit. The only information needed is the Liouvillian and Jump operator of the system. Furthermore, this Mathematica Package involves a bundle of useful tools for to perform numeric simulations and generate plots and animations. In addition, there is a snipped for the derivation of the Liouvillian for a given Hamiltonian.

Chapter 5

Simple examples

In the following the method, proposed in the former chapter, is applied to simple realistic quantum mechanical systems. It is being started with the simplest system, the Tunneling Junction (5.1). Afterwards the Single Quantum Dot is described in section 5.2. In the following the method, proposed in the former chapter, is applied to simple realistic quantum mechanical systems. It is being started with the simplest system, the Tunneling Junction (5.1). Afterwards the Single Quantum Dot is described in section 5.2.

In the following section this method is being generalized to systems without internal dynamics, transitions in a ring (5.3). Finally an extended discussion of the Double Quantum Dot is performed in section 5.4.

For all cases current and Fano factor are obtained in the long-time limit.

5.1 Tunneling Junction

The simplest, imaginable system is a Tunneling Junction, which is visualized in figure 5.1. On this system the first experimental measurements were performed by [Levitov et al., 1996] (up to the 3rd cumulant) and later on by [Reulet et al., 2003]. In this thesis only the special case of the infinite bias limit is taken into account. So the jump and nojump operators can be easily obtained.

The dimension of the system density operator is 1, which makes Liouvillian and jump operator be 1x1-matrices, which are isomorph to the scalars[1]

$$\mathcal{L}_0^{(n)} = -\Gamma^{(n)}, \mathcal{J}^{(n-1)} = \Gamma^{(n-1)} \tag{5.1}$$

For this system the nQME (3.1) reads

$$\partial_t \rho^{(n)}(t) = \Gamma^{(n-1)} \rho^{(n-1)}(t) - \Gamma^{(n)} \rho^{(n)}(t). \tag{5.2}$$

---

[1]This seems to be a formally negligibility, but plays a decisive role in numerical implementations.
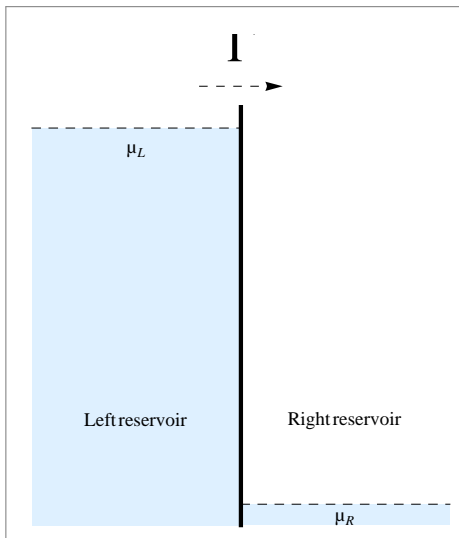
Figure 5.1: Visualization of a Tunneling Junction in infinite bias limit with $\mu_L = -\mu_R = \infty$

The application of the Laplace Transformation $\left(\underset{t\to z}{\text{LT}}\right)$ leads to

$$z\hat{\rho}_n(z) - \rho_n(t=0) = \Gamma^{(n-1)}\hat{\rho}_{n-1}(z) - \Gamma^{(n)}\hat{\rho}_n(z). \tag{5.3}$$

Due to the fact that every density operator has trace-class $\text{Tr}(\rho) = 1$ (see appendix (B.7), p. 134), $\rho_n(t=0) = \delta_{n,0}$ is given.

The recursive equation for $\hat{\rho}_n(z)$ reads

$$\hat{\rho}_n(z) = \frac{1}{z - \Gamma^{(n)}}\left(\Gamma^{(n-1)}\hat{\rho}_{n-1}(z) + \delta_{n,0}\right). \tag{5.4}$$

This equation can be recursively solved (cf. (3.10))

$$\hat{\rho}_n(z) = \left(\prod_{k=n}^{1}\frac{\Gamma^{(k)}}{z + \Gamma^{(k)}}\right)\frac{1}{z - \Gamma^{(0)}}. \tag{5.5}$$

According to the general proceedings we define

$$\hat{\mathcal{P}}_n(z) = \frac{1}{z + \Gamma^{(n)}}, \quad \hat{\mathcal{W}}_n(z) = \frac{\Gamma^{(n)}}{z + \Gamma^{(n)}}, \quad \rho_0 = 1. \tag{5.6}$$

So (3.10) becomes in the

one dimensional case $\boxed{\hat{\rho}_n(z) = \frac{1}{z + \Gamma^{(n)}}\left(\prod_{k=n-1}^{0}\frac{\Gamma^{(k)}}{z + \Gamma^{(k)}}\right).}$ (5.7)

Clean limit

As a first step, we will reproduce the known results for the clean case. With $\Gamma^{(k)} := \Gamma = \text{constant}$, one gets

$$\hat{\rho}_n(z) = \frac{\Gamma^n}{(z + \Gamma)^{n+1}}. \tag{5.8}$$

Applying a discrete Fourier Transformation $\underset{n \to \chi}{\text{FST}}$ to the former equation leads to

$$\hat{\rho}_\chi(z) = \frac{1}{z - \Gamma(e^{i\chi} - 1)}. \tag{5.9}$$

After the Inverse Laplace Transform $\underset{z \to t}{\text{LT}}^{-1}$ the time dependent counting field reads

$$\rho_\chi(t) = e^{-\Gamma(1 - e^{i\chi})t}. \tag{5.10}$$

In this one dimensional case all density matrices are 1x1-matrices. So the trace operation is the identity

$$P_\chi(t) := e^{S_p(\chi, t)} = \rho_\chi(t) \tag{5.11}$$

$$S_p(\chi, t) = \Gamma(e^{i\chi} - 1)t. \tag{5.12}$$

This result is in accordance with the known result of [Flindt, 2007][4.8].

For current, Fano factor and higher cumulants, one gets the (known) results

$$\langle I_\infty \rangle = \lim_{z \to 0} z^2 \lim_{i\chi \to 0} \frac{e^{i\chi} \Gamma}{\left(z - (e^{i\chi} - 1)\Gamma\right)^2} = \lim_{z \to 0} z^2 \frac{\Gamma}{z^2} = \Gamma \tag{5.13}$$

$$\langle F_\infty \rangle = \lim_{t \to \infty} \frac{c_k(t)}{c_1(t)} = 1. \tag{5.14}$$

In other words all cumulants grow linear in time. This result will change, if a control loop is applied to the system. This case is explained in chapter 9.

5.1.1 Current

In the following the current is derived. The first value we are interested in is $\langle \hat{\rho}_n(z) \rangle$. It has being assumed that all Γ_n are statistically independent.

Remembering the definition of the propagator $\hat{\mathcal{P}}_n(z) = \left[z - \mathcal{L}_0^{(n)}\right]^{-1}$ and the definitions

$$\hat{\mathcal{P}}(z) = \left\langle \hat{\mathcal{P}}_0(z) \right\rangle = \left\langle \frac{1}{z + \Gamma^{(n)}} \right\rangle = \left\langle \frac{1}{z + \Gamma} \right\rangle \text{ and} \tag{5.15}$$

$$\hat{\mathcal{W}}(z) = \mathcal{J}\hat{\mathcal{P}}(z) = \left\langle \frac{\Gamma^{(n)}}{z + \Gamma^{(n)}} \right\rangle = \left\langle \frac{\Gamma}{z + \Gamma} \right\rangle = \left\langle \frac{z + \Gamma - z}{z + \Gamma} \right\rangle = 1 - z\hat{\mathcal{P}}(z), \tag{5.16}$$

where the concrete Liouvillian and jump operator for the Tunnel Junction were inserted, according to (5.1).

Consequently (4.3) becomes

$$\langle \hat{\rho}_n(z) \rangle = \left\langle \frac{1}{z + \Gamma^{(n)}} \right\rangle \left(\prod_{i=0}^{n-1} \left\langle \frac{\Gamma^{(i)}}{z + \Gamma^{(i)}} \right\rangle \right)$$

$$= \left\langle \frac{1}{z + \Gamma} \right\rangle \left(\left\langle \frac{\Gamma}{z + \Gamma} \right\rangle \right)^n \tag{5.17}$$

$$= \hat{\mathcal{P}}(z) \left(1 + z\hat{\mathcal{P}}(z) \right)^n. \tag{5.18}$$

The next step it to do the Fourier Transformation $\langle \hat{\rho}_n(z) \rangle \Rightarrow \langle \hat{\rho}_\chi(z) \rangle$.

In accordance to (4.4) this yields to[2]

$$\langle \hat{\rho}_\chi(z) \rangle = \frac{\hat{\mathcal{P}}(z)}{1 + e^{\mathrm{i}\chi} \left(z\hat{\mathcal{P}}(z) - 1 \right)}. \tag{5.19}$$

The first moment $\hat{m}_1(z) := (-\mathrm{i}\partial_\chi)\hat{\rho}_\chi(z)$ at $\chi = 0$ is

$$\hat{m}_1(z) := \frac{1}{z^2\hat{\mathcal{P}}(z)} - \frac{1}{z}. \tag{5.20}$$

For the current that means

$$\langle I_\infty \rangle = \lim_{z \to 0} z^2 \hat{m}_1(z)$$

$$= \lim_{z \to 0} \frac{1}{\hat{\mathcal{P}}(z)} - z. \tag{5.21}$$

A series approximation of $\hat{\mathcal{P}}(z)$ up to the third order of z is

$$\hat{\mathcal{P}}(z) = \left\langle \frac{1}{\Gamma} \right\rangle - z \left\langle \frac{1}{\Gamma^2} \right\rangle + z^2 \left\langle \frac{1}{\Gamma^3} \right\rangle + \mathrm{O}^3(z). \tag{5.22}$$

By using (4.7) the former equation can be rewritten to

$$\hat{\mathcal{P}}(z) = \langle \tau \rangle - z\langle \tau^2 \rangle + z^2 \langle \tau^3 \rangle + \mathrm{O}^3(z). \tag{5.23}$$

For the long term current only the first term of the series development accounts, as the other terms lead to an order below zero in the current and disappear (see theorem 8). Inserting this first order approximation in (5.21) and executing the long-time limit results in the

long-time current $\quad \boxed{ \langle I_\infty \rangle = \left\langle \frac{1}{\Gamma} \right\rangle^{-1} = \langle \tau \rangle^{-1}. } \tag{5.24}$

---

[2]With the geometric sequence.

For the clean case the long-time limit is known as $I_{\infty,\text{cln}} = \Gamma$. This can be also expressed in terms of inverse Tunneling Rates $I_{\infty,\text{cln}} = \frac{1}{\tau}$. For the clean case both formulas describe exactly the same expression, but by using different variables. The question is, due to which physical reasons, the representation in terms of inverse waiting times, is formal equivalent to the random case. On the one hand the rate Γ is microscopically derived from the Interaction Hamiltonian $T_{k\alpha n}\text{sb}_k^\dagger + \ldots$. Therefore, one might think that this is the canonical variable to describe the current. One the other hand the simple definition $I = \dot{Q} \rightsquigarrow \frac{n}{t}$ is an argument for the waiting time interpretation. In conclusion, it can be stated that at this point no convincing physical interpretation can be given. Explanations follow in the c case (see section 5.2) At this point the difference between waiting time and tunneling rate interpretation, respectively the connection between tunneling rate an current, is discussed. In the **tunneling rate picture** the following goal can be formulated: If the exception value for Γ, $\langle\Gamma\rangle$, is known, one would like to receive a formula for the long-time current. Mathematically spoken, an arability function $f(\langle\Gamma\rangle)$ is needed, for which

$$\langle I_\infty\rangle = f(\langle\Gamma\rangle) = \langle\tau\rangle^{-1} \tag{5.25}$$

holds true. $f(\Gamma) = \Gamma$ follows from the clean case, which means a delta distribution for the Probability Distribution of the tunneling rates. At this point no obvious solution for $f(\langle\Gamma\rangle)$ is given.

A budding approach is

$$\langle\tau\rangle\langle\Gamma\rangle = \langle\tau\rangle\left\langle\frac{1}{\tau}\right\rangle \equiv 1 + \alpha. \tag{5.26}$$

α exists for every Probability Density Functions (PDF) of Γ or τ and becomes 0 in the clean limit. In that case it can be shown that $\alpha \geq 0$ is valid. The prove is outlined in the appendix (A.1.1 p. 129).

Thus, the current in the tunneling rate picture reads

$$\langle I_\infty\rangle(\langle\Gamma\rangle, \alpha) = \frac{\langle\Gamma\rangle}{1 + \alpha}. \tag{5.27}$$

A function for $f(\langle\Gamma\rangle)$ could not be found, but a function, which depends on the expectation value and one additional parameter. For this Tunnelling Junction Model it is not traceable, for which reason this parameter is sensible. This will be clarified in the case of the Double Quantum Dot (cf. section 5.4). It has to be again remarked that $\langle\Gamma^{-1}\rangle$ could be called first **negative moment** (cf. chapter 4).

The observation up to this point can be summarized in the following manner:

1. The long-time random current is the inverse of the expectation value of the waiting time, $\langle I_\infty \rangle = \frac{1}{\langle \tau \rangle}$ in the **waiting time picture**.

2. In the **Tunneling rate picture** the long-time random current is smaller than the expectation value of the tunneling rate $\langle I_\infty \rangle \leq \langle \Gamma \rangle$.

3. To calculate the long-time random current in the **tunneling rate picture** one needs an additional information about the distribution of the tunneling rates, beside the mean of the tunneling rate.

From now on the waiting time picture is, therefore, preferred.

5.1.2   Higher moments

The higher moments can be calculated in the same way. Using the developed Mathematica Package nQME leads with $\hat{\mathcal{T}}(z) = \hat{\mathcal{W}}(z)\hat{\mathcal{G}}_0(z) = \frac{1-z\hat{\mathcal{P}}(z)}{1-1+z\hat{\mathcal{P}}(z)} = \frac{1}{z\hat{\mathcal{P}}(z)} - 1$ to

$$\hat{m}_1(z) = \frac{1}{z^2\hat{\mathcal{P}}(z)} - \frac{1}{z} \tag{5.28}$$

$$\hat{m}_2(z) = \frac{2}{z^3\hat{\mathcal{P}}(z)^2} - \frac{3}{z^2\hat{\mathcal{P}}(z)} + \frac{1}{z} \tag{5.29}$$

$$\hat{m}_3(z) = \frac{6}{z^4\hat{\mathcal{P}}(z)^3} - \frac{12}{z^3\hat{\mathcal{P}}(z)^2} + \frac{7}{z^2\hat{\mathcal{P}}(z)} - \frac{1}{z} \tag{5.30}$$

$$\hat{m}_4(z) = \frac{24}{z^5\hat{\mathcal{P}}(z)^4} - \frac{60}{z^4\hat{\mathcal{P}}(z)^3} + \frac{50}{z^3\hat{\mathcal{P}}(z)^2} - \frac{15}{z^2\hat{\mathcal{P}}(z)} + \frac{1}{z} \tag{5.31}$$

$$\hat{m}_5(z) = \frac{120}{z^6\hat{\mathcal{P}}(z)^5} - \frac{360}{z^5\hat{\mathcal{P}}(z)^4} + \frac{390}{z^4\hat{\mathcal{P}}(z)^3} - \frac{180}{z^3\hat{\mathcal{P}}(z)^2} + \frac{31}{z^2\hat{\mathcal{P}}(z)} - \frac{1}{z} \tag{5.32}$$

$$\hat{m}_6(z) = \frac{720}{z^7\hat{\mathcal{P}}(z)^6} - \frac{2520}{z^6\hat{\mathcal{P}}(z)^5} + \frac{3360}{z^5\hat{\mathcal{P}}(z)^4} - \frac{2100}{z^4\hat{\mathcal{P}}(z)^3} + \frac{602}{z^3\hat{\mathcal{P}}(z)^2} - \frac{63}{z^2\hat{\mathcal{P}}(z)} + \frac{1}{z}. \tag{5.33}$$

A way to obtain the long-time limit is to calculate Taylor Series for $\hat{\mathcal{P}}(z)$ at $z = 0$ up to order z^0 to calculate the long-time limit afterwards.

In z space the first three moments read

$$\hat{m}_1(z) = \frac{1}{\langle\tau\rangle z^2} + \frac{\langle\tau^2\rangle}{\langle\tau\rangle^2 z} - \frac{1}{z} + O\left(z^0\right) \tag{5.34}$$

$$\hat{m}_2(z) = \frac{2}{\langle\tau\rangle^2 z^3} + \frac{4\langle\tau^2\rangle - 3\langle\tau\rangle^2}{\langle\tau\rangle^3 z^2} + \frac{\langle\tau\rangle^4 - 3\langle\tau^2\rangle\langle\tau\rangle^2 - 4\langle\tau^3\rangle\langle\tau\rangle + 6\langle\tau^2\rangle^2}{\langle\tau\rangle^4 z} + O\left(z^0\right) \tag{5.35}$$

$$\hat{m}_3(z) = \frac{6}{\langle\tau\rangle^3 z^4} + \frac{6\left(3\langle\tau^2\rangle - 2\langle\tau\rangle^2\right)}{\langle\tau\rangle^4 z^3} + \frac{7\langle\tau\rangle^4 - 24\langle\tau^2\rangle\langle\tau\rangle^2 - 18\langle\tau^3\rangle\langle\tau\rangle + 36\langle\tau^2\rangle^2}{\langle\tau\rangle^5 z^2}$$
$$+ \frac{7\langle\tau^2\rangle\langle\tau\rangle^4 + 24\langle\tau^3\rangle\langle\tau\rangle^3 + 18\left(\langle\tau^4\rangle - 2\langle\tau^2\rangle^2\right)\langle\tau\rangle^2 - 72\langle\tau^2\rangle\langle\tau^3\rangle\langle\tau\rangle + 60\langle\tau^2\rangle^3}{\langle\tau\rangle^6 z}$$
$$- \frac{1}{z} + O\left(z^0\right). \tag{5.36}$$

Higher moments can be calculated similarly. The Inverse Laplace Transformation $\underset{z\to t}{\mathrm{LT}}^{-1}$ is now quiet simple, because only expressions of the form az^{-n} have to be transformed, which leads to $a\frac{t^{n-1}}{(n-1)!}$ (compare theorem 8).

$$m_1(t) = \frac{t}{\langle\tau\rangle} + \frac{\langle\tau^2\rangle}{\langle\tau\rangle^2} - 1 \tag{5.37}$$

$$m_2(t) = \frac{t^2}{\langle\tau\rangle^2} + \frac{t\left(4\langle\tau^2\rangle - 3\langle\tau\rangle^2\right)}{\langle\tau\rangle^3} + \frac{\langle\tau\rangle^4 - 3\langle\tau^2\rangle\langle\tau\rangle^2 - 4\langle\tau^3\rangle\langle\tau\rangle + 6\langle\tau^2\rangle^2}{\langle\tau\rangle^4} \tag{5.38}$$

$$m_3(t) = \frac{t^3}{\langle\tau\rangle^3} - \frac{3t^2\left(2\langle\tau\rangle^2 - 3\langle\tau^2\rangle\right)}{\langle\tau\rangle^4} + \frac{t\left(7\langle\tau\rangle^4 - 24\langle\tau^2\rangle\langle\tau\rangle^2 - 18\langle\tau^3\rangle\langle\tau\rangle + 36\langle\tau^2\rangle^2\right)}{\langle\tau\rangle^5}$$
$$+ \frac{7\langle\tau^2\rangle\langle\tau\rangle^4 + 24\langle\tau^3\rangle\langle\tau\rangle^3 + 18\left(\langle\tau^4\rangle - 2\langle\tau^2\rangle^2\right)\langle\tau\rangle^2 - 72\langle\tau^2\rangle\langle\tau^3\rangle\langle\tau\rangle + 60\langle\tau^2\rangle^3}{\langle\tau\rangle^6} - 1. \tag{5.39}$$

Checking the current in time-domain leads to

$$\langle I_\infty\rangle = \partial_t m_1(t \to \infty) = \frac{1}{\langle\tau\rangle}. \tag{5.40}$$

In this context the long-time has to be taken into account, as within the process of Taylor Series Expansion $\underset{z=0}{\asymp}$, only terms of order t^n were taken into account.

$$c_2(t \to \infty)c_1^{-1} = \frac{2\langle\tau^2\rangle}{\langle\tau\rangle^2} - 1 \tag{5.41}$$

$$c_3(t \to \infty)c_1^{-1} = \frac{\langle\tau\rangle^4 - 6\langle\tau^2\rangle\langle\tau\rangle^2 - 6\langle\tau^3\rangle\langle\tau\rangle + 12\langle\tau^2\rangle^2}{\langle\tau\rangle^4} \tag{5.42}$$

Of special interest is the Fano factor. With help of the displacement-law 5

$\langle \tau^2 \rangle = \langle \tau \rangle^2 + \left\langle \left(\Gamma^{-1} - \langle \tau \rangle \right)^2 \right\rangle$ it can be rewritten to

Fano factor (Tunneling Junction)
$$\langle F_\infty \rangle = \frac{2\langle \tau^2 \rangle}{\langle \tau \rangle^2} - 1 = 1 + \frac{2\langle (\tau - \langle \tau \rangle)^2 \rangle}{\langle \tau \rangle^2}.$$
$$\langle F_\infty \rangle \geq 1$$

$$(5.43)$$

The last inequality holds true, because the standard derivation is always ≥ 0.

5.1.3   Special observations*

In the following section special observations for the Tunneling Junction are summed up. This considerations are facultative and have no influence on the following chapters.

Residual method for the Fano factor

To illustrate the principal introduced in section 3.3.5, the Fano factor will be calculated as mentioned.

First the $\hat{m}_1(z), \hat{m}_2(z)$ can be calculated by (3.27) with the values of (5.9)

$$\hat{m}_1(z) = \frac{\Gamma}{z^2} \tag{5.44}$$

$$\hat{m}_2(z) = \frac{\Gamma}{z^2} + 2\frac{\Gamma^2}{z^3}. \tag{5.45}$$

Now $\hat{c}_1(z)$ can be calculated according to (3.48)

$$\begin{aligned}
\hat{c}_2(z) &= \frac{\Gamma}{z^2} + 2\frac{\Gamma^2}{z^3} - \frac{1}{2\pi i} \int_{c-i\infty}^{c+i\infty} \frac{\Gamma^2}{\sigma^2(z-\sigma)^2} \, d\sigma \\
&= \frac{\Gamma}{z^2} + \Gamma^2 \left(\frac{2}{z^3} - \frac{1}{2\pi i} \int_{c-i\infty}^{c+i\infty} \frac{1}{\sigma^2(z-\sigma)^2} \, d\sigma \right).
\end{aligned} \tag{5.46}$$

So far one has to remind that the choice of c is not arbitrary. $\frac{1}{\sigma^2}$ has one pole at $\sigma = 0$. Therefore, $c = \epsilon$ with $0 < \epsilon < z$ is a applicable choice.

The kernel of the integral has two poles of second order at $\sigma = 0, \sigma = z$. But only the pole at $\sigma = 0$ has to be taken into account.

With the residual theorem $\frac{1}{2\pi i} \int f(\sigma) \, d\sigma = \sum_n Res(f; \sigma_n)$ with $Res(f; \sigma_n) = \lim_{\sigma \to \sigma_n} \frac{1}{(k-1)!} \partial_\sigma^{k-1} \left((\sigma - \sigma_n)^k f(\sigma) \right)$ [Herbort, 2008] the integral can be evaluated with

$$Res\left(\frac{1}{\sigma^2(z-\sigma)^2}; \sigma \to 0 \right) = \frac{1}{1!} \lim_{\sigma \to 0} \partial_\sigma (z-\sigma)^{-2} = \frac{2}{z^3}. \tag{5.47}$$

Thus, the second cumulant in Laplace Space evaluates to

$$\hat{c}_2(z) = \hat{m}_1(z) = \frac{\Gamma}{z^2}. \tag{5.48}$$

Step distribution*

Taking the Uniform Distribution

$$f(\Gamma) = \frac{\Theta(\Gamma - \Gamma_{Min}) - \Theta(\Gamma - \Gamma_{Max})}{\Gamma_{Max} - \Gamma_{Min}} \tag{5.49}$$

as example for a tunneling rate distribution.
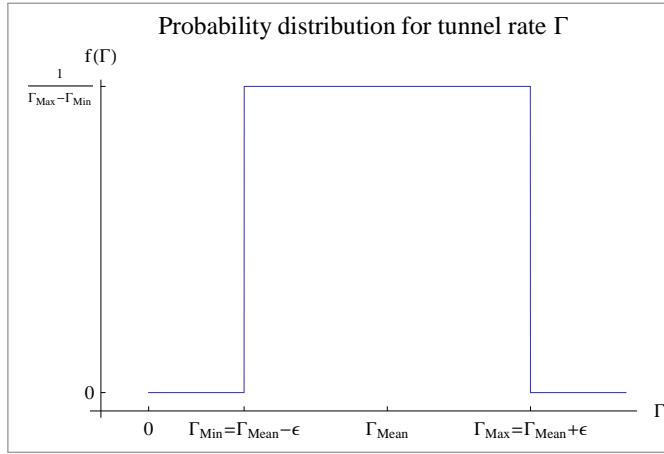
Figure 5.2: Step distribution

With the use of $\partial_\Gamma Log(z + \Gamma) = (\Gamma + z)^{-1}$ and $\partial_\Gamma \Gamma - zLog(\Gamma + z) = \frac{z}{z+\Gamma}$ it is easy to calculate that $\langle \hat{\rho}_n(z) \rangle$ yields, without caring about the poles, to

$$\langle \hat{\rho}_n(z) \rangle = \left(1 - \frac{z}{\Gamma_{Max} - \Gamma_{Min}} Log\left(\frac{z + \Gamma_{Min}}{z + \Gamma_{Max}} \right) \right)^n \frac{1}{\Gamma_{Max} - \Gamma_{Min}} Log\frac{z + \Gamma_{Max}}{z + \Gamma_{Min}}. \tag{5.50}$$

With the use of the short hand notation

$$\hat{\mathcal{P}}(z) := \frac{1}{\Gamma_{Max} - \Gamma_{Min}} Log\left(\frac{z + \Gamma_{Max}}{z + \Gamma_{Min}} \right) = \left\langle \frac{1}{z + \Gamma} \right\rangle, \tag{5.51}$$

the known form

$$\langle \hat{\rho}_n(z) \rangle = \hat{\mathcal{P}}(z) \left(1 + z\hat{\mathcal{P}}(z) \right)^n \tag{5.52}$$

is obtained.

As described above $\underset{n \to \chi}{\text{FST}} : \langle \hat{\rho}_n(z) \rangle \Rightarrow \langle \hat{\rho}_\chi(z) \rangle$

$$\langle \hat{\rho}_\chi(z) \rangle = \frac{\hat{\mathcal{P}}(z)}{1 + e^{i\chi} \left(z\hat{\mathcal{P}}(z) - 1 \right)}. \tag{5.53}$$

The next step is the Inverse Laplace Transformation $\mathrm{LT}^{-1}_{z\to t}$. According to [L

et al., 1966] the Inverse Laplace Transform is known for $Log\frac{z-a}{z-b} \to \frac{e^{bt}-e^{at}}{t}$, but
the Inverse Laplace Transformation of $\frac{1}{c_1+c_2 z Log(\frac{z+c3}{z+c4})}$ is probably unknown.

Defining $l(t)$ as the Inverse Laplace Transformation of $\frac{1}{1+e^{\mathrm{i}\chi}\left(1+z\hat{\mathcal{P}}(z)\right)}$ leads to
the form

$$\langle\rho_\chi(t)\rangle = \frac{e^{-\Gamma_{Max}t} - e^{-\Gamma_{Min}t}}{t} * l(t). \qquad (5.54)$$

In that case * stands for the convolution-integral. As $l(t)$ is not known yet,
another way has to be found. Of course one could investigate the long-time
limit as done for the Single Quantum Dot in the following section. At this point
another possible approach is discussed.

Small bandwidth approach*

A possible approach is to develop $\langle\hat{\rho}_\chi(z)\rangle$ around $\perp \equiv \frac{\Gamma_{Max}+\Gamma_{Min}}{2}$..

The series approximation of $\langle\hat{\rho}_\chi(z)\rangle$ reads

$$\langle\hat{\rho}_\chi(z)\rangle^0 = \frac{1}{z + \perp\left(e^{\mathrm{i}\chi} - 1\right)} \qquad (5.55)$$

$$\langle\hat{\rho}_\chi(z)\rangle^2 = \frac{\epsilon^2\left(e^{\mathrm{i}\chi} - 1\right)}{3(\perp + z)\left(z + \perp\left(e^{\mathrm{i}\chi} - 1\right)\right)^2} \qquad (5.56)$$

$$\langle\hat{\rho}_\chi(z)\rangle^4 = \frac{\left(\epsilon^4\left(e^{\mathrm{i}\chi} - 1\right)\right)\left(9ze^{\mathrm{i}\chi} - 5(\perp\left(e^{\mathrm{i}\chi} - 1\right) + z)\right)}{(\perp + z)^3\left(\perp\left(e^{\mathrm{i}\chi} - 1\right) + z\right)^3} \qquad (5.57)$$

(cf. definition 14). $\perp = \frac{\Gamma_{Max}+\Gamma_{Min}}{2}$ The derivation of the known result $m_{1,t} = \perp t$
for the limit $\Gamma_{Max} \leftarrow \perp, \Gamma_{Min} \to \perp$ could be used as a simple check. Due to the
long terms of the Taylor Series, Mathematica is used.

. . .

$$\langle\hat{\rho}_\chi(z)\rangle^4 = \frac{\epsilon^4\left(-1 + e^{i\chi}\right)\left(9\perp e^{i\chi} - 9\perp + 5ze^{i\chi} - 9z\right)}{45(\perp + z)^3\left(\perp\left(-e^{i\chi}\right) + \perp + z\right)^3}$$
$$- \frac{\epsilon^2\left(-1 + e^{i\chi}\right)}{3(\perp + z)\left(\perp e^{i\chi} - \perp - z\right)^2}$$
$$- \frac{1}{\perp e^{i\chi} - \perp - z} \qquad (5.58)$$

The detailed calculation is to find in the Mathematica Notebook NB:SmallBWBar.
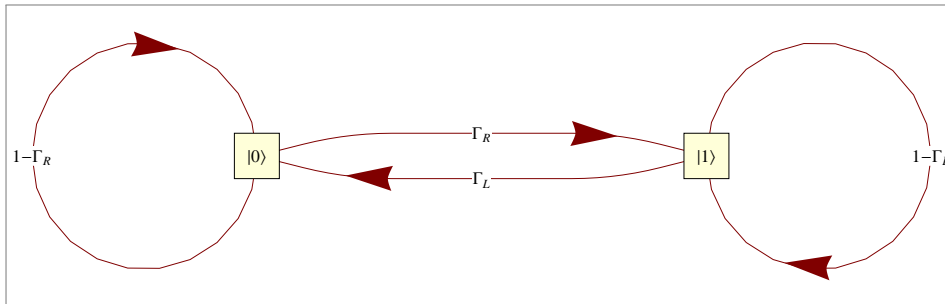
Figure 5.3: Single Quantum Dot with n-independent transmission rates
A simple system with a steady state.
As only the states $|0\rangle\langle0|, |1\rangle\langle1|$ occur, it is sufficient to display the pure states:

$|0\rangle=$ no electron is in the dot

$|1\rangle=$ dot is filled with one electron

To stay in the default notation Γ_α is the rate of change here.

Thus, the probability that an electron tunnels during the time t, is given by $\Gamma_\alpha\Delta t$.

5.2   Single Quantum Dot

The Single Quantum Dot (SD) is a system without relevant internal dynamics. Therefore, it is sufficient to regard the $|0\rangle\langle0|, |1\rangle\langle1|$ elements of the density matrix. Moreover, the Single Quantum Dot is a real physical system, where measurements can be made on [Gustavsson et al., 2005, Lu et al., 2003, Fujisawa et al., 2004]. A picture of a realized Single Quantum Dot can be seen in figure 1.1. Despite this experimental interest, we are in the comfortable situation that it is easy to guess the system description by considering figure 5.4 and transfer the possible processes into a functional scheme (see figure 5.3).
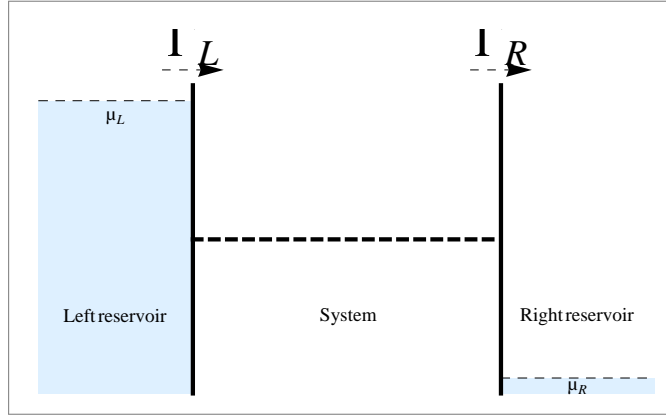
Figure 5.4: Visualization of a Single Quantum Dot in infinite bias limit with $\mu_L = -\mu_R = \infty$

This scheme has to be understood in the following manner: The squares denote the state and the numbers on the arrows denote the probability for a change (or no change). A step in the time evolution looks like

$$\begin{pmatrix} p_0(t + \Delta t) \\ p_1(t + \Delta t) \end{pmatrix} = \begin{pmatrix} 1 - \Gamma_L\Delta t & \Gamma_R\Delta t \\ \Gamma_L\Delta t & 1 - \Gamma_R\Delta t \end{pmatrix} \begin{pmatrix} p_0(t) \\ p_1(t) \end{pmatrix} \qquad (5.59)$$

$$\Rightarrow \partial_t \begin{pmatrix} p_0(t) \\ p_1(t) \end{pmatrix} \equiv \lim_{\Delta t \to 0} \frac{\begin{pmatrix} p_0(t + \Delta t) \\ p_1(t + \Delta t) \end{pmatrix} - \begin{pmatrix} p_0(t) \\ p_1(t) \end{pmatrix}}{\Delta t} = \begin{pmatrix} -\Gamma_L & \Gamma_R \\ \Gamma_L & -\Gamma_R \end{pmatrix}. \qquad (5.60)$$

'That is the Quantum Master Equation!' Alternatively the dynamics of the SD can be expressed via the so called **Lindblad Master Equation** [Breuer and Petruccione, 2002, Lindblad, 1979]. The jump in- and jump out process can be described via $j_\alpha := \begin{cases} \sqrt{\Gamma_L}\,|1\rangle\langle0| & \alpha = L \\ \sqrt{\Gamma_R}\,|0\rangle\langle1| & \alpha = R \end{cases}$ and $j^\dagger_\alpha$ accordingly.

$$\partial_t \rho = \underbrace{i[\rho, H_{int}]}_{0 \text{ for SD}} + \sum_\alpha \left(j_\alpha \rho j^\dagger_\alpha - \frac{1}{2} \left\{ j^\dagger_\alpha j_\alpha, \rho \right\}_+ \right) \qquad (5.61)$$

$$\partial_t \rho = \Gamma_L \left(|1\rangle\langle 0| \, \rho \, |0\rangle\langle 1| - \frac{1}{2} \left\{ |0\rangle\langle 1| \, |1\rangle\langle 0| \, , \rho \right\}_+ \right)$$

$$+ \Gamma_R \left(|0\rangle\langle 1| \, \rho \, |1\rangle\langle 0| - \frac{1}{2} \left\{ |1\rangle\langle 0| \, |0\rangle\langle 1| \, , \rho \right\}_+ \right) \quad (5.62)$$

$$\partial_t \rho = \Gamma_L \left(\rho_{0,0} \, |1\rangle\langle 1| - \rho_{0,0} \, |0\rangle\langle 0| \right) \qquad + \Gamma_R \left(\rho_{1,1} \, |0\rangle\langle 0| - \rho_{1,1} \, |1\rangle\langle 1| \right) \quad (5.63)$$

$$= \begin{pmatrix} -\Gamma_L & \Gamma_R \\ \Gamma_L & -\Gamma_R \end{pmatrix} \rho = \mathcal{L}\rho \quad (5.64)$$

The different forms of possible notation were used here. Especially in the last line, ρ has to be interpreted as superoperator, whereas in the second line, ρ has to be seen as the ordinary density matrix. Obviously the result is equal to the result, derived from the graphical representation of this density matrix (see figure 5.3). In any case by equation (5.64) the time evolution of the total system density matrix is described.

Simplified derivation of n-dependent case

Disregarding the microscopic derivation of chapter 2, a brief prove of feasibility follows. First of all, the n-dependence of the system has to be investigated. Therefore, it has to be examined, which processes changes the n. For convenience, the notation $N_L = N_{L_0} - n - 1, N_R = N_{R_0} - n$ is used here (cf. figure 2.1, p. 10). The relationship between ρ and $\rho^{(n)}(t)$ was given by

$$\rho(t) = \sum_n \rho^{(n)}(t). \quad (5.65)$$

The investigation has to be continued by checking the terms of the Lindblad Form. The constant rate Γ_L, Γ_L will be replaced by $\Gamma_L^{(n)}, \Gamma_R^{(n)}$ and j_α changes to

$$j_\alpha^{(n')} := \begin{cases} \sqrt{\Gamma_L^{(n')}} \, |n'; 1\rangle\langle 0; n'| & \alpha = L \\ \sqrt{\Gamma_R^{(n')}} \, |n' + 1; 0\rangle\langle 1; n'| & \alpha = R \end{cases} \quad [4] \text{ and } \quad {j^\dagger}_\alpha^{(n'')} \quad \text{appropriate and}$$

$\rho^{(n)} = p_{0n} \, |0\rangle\langle 0| + p_{1n} \, |1\rangle\langle 1|.$

For the Lindblad Equation (5.61) this leads to

$$\sum_n \partial_t \rho^{(n)}(t) = \sum_{\alpha,n,n',n''} \left(j_\alpha^{(n')} \rho^{(n)} {j^\dagger}_\alpha^{(n'')} - \frac{1}{2} \left\{ {j^\dagger}_\alpha^{(n'')} j_\alpha^{(n')}, \rho^{(n)} \right\}_+ \right). \quad (5.66)$$

---

[3] In contrast to section 5.3, 1-... was suppressed here

[4] $|n; x\rangle\langle x; n|$ means that n is the number of particles and x the system state

$\partial_t \rho^{(0)}$:

$-\Gamma_L^{(0)}$ $|0;0\rangle\langle0;0|$ $\xrightarrow{\Gamma_L^{(0)}}$ $|0;1\rangle\langle1;0|$ $-\Gamma_R^{(0)}$

$\Gamma_R^{(0)}$

$\partial_t \rho^{(1)}$:

$|1;0\rangle\langle0;1|$ $\xrightarrow{\Gamma_L^{(1)}}$ $|1;1\rangle\langle1;1|$ $-\Gamma_R^{(1)}$

$-\Gamma_L^{(1)}$

$\Gamma_R^{(1)}$

$\partial_t \rho^{(2)}$:

$|2;0\rangle\langle0;2|$ $\xrightarrow{\Gamma_L^{(2)}}$ $|2;1\rangle\langle1;2|$ $-\Gamma_R^{(2)}$

$-\Gamma_L^{(2)}$

$\Gamma_R^{(2)}$
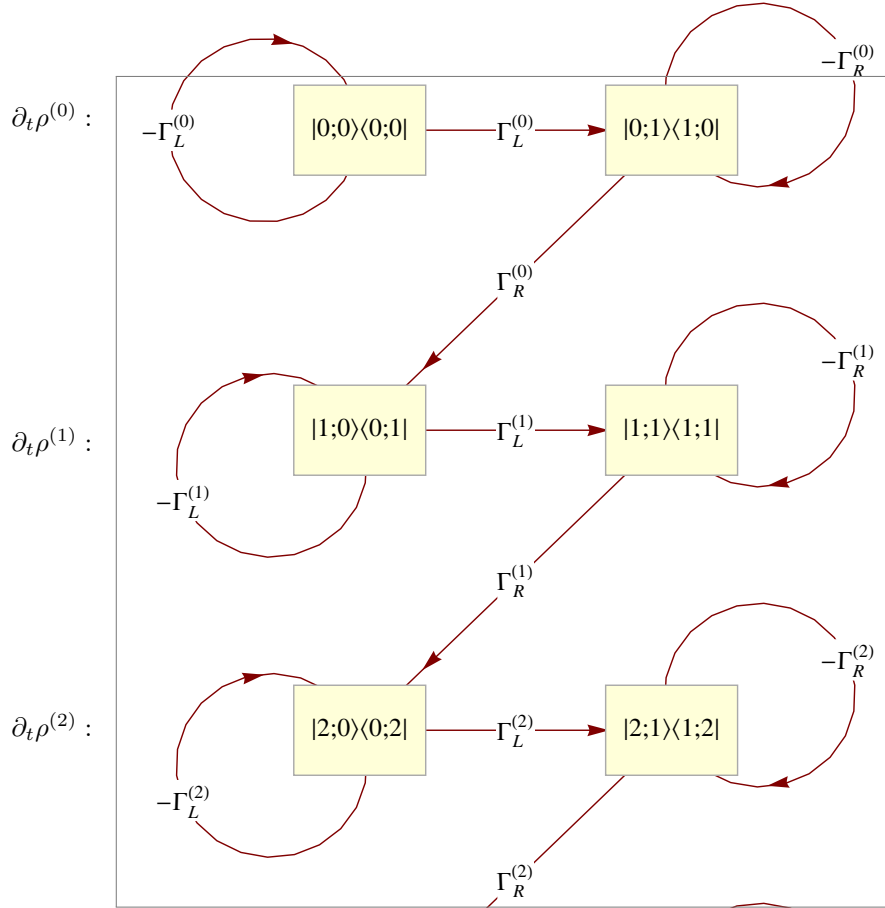
Figure 5.5: Visualization of $\partial_t \rho^{(n)}(t)$ for a Single Quantum Dot with n-dependent
transmission rates $\Gamma_L^{(n)}$, $\Gamma_R^{(n)}$ for $n \in \{0, 1, 2\}$
$|0\rangle$: pure state of the empty dot
$|1\rangle$: pure state of the full dot
Processes, which do not change the number of tunneled electrons (start
and target of the arrow are in the same row) are described with $\mathcal{L}_0^{(n)}$.
The down going arrow corresponds to the jump operator $\mathcal{J}^{(n)}$.[3]

$|3;0\rangle\langle0;3|$ $\xrightarrow{\Gamma_L^{(3)}}$ $|3;1\rangle\langle1;3|$ $-\Gamma_R^{(3)}$

$-\Gamma_L^{(3)}$

$\Gamma_R^{(3)}$

$|4;0\rangle\langle0;4|$
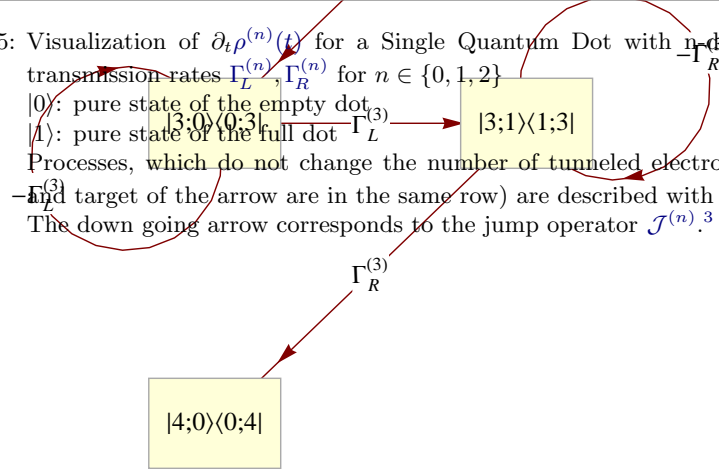
Evaluating the $\alpha = R$ part of the sum

$$\sum_{n,n',n''} \left(\sqrt{\Gamma_R^{(n')}\Gamma_R^{(n'')}} \, |n'+1;0\rangle\langle 1;n'| \, \rho^{(n)} \, |n'';1\rangle\langle 0;n''+1| \right.$$

$$\left. -\frac{\sqrt{\Gamma_R^{(n')}\Gamma_R^{(n'')}}}{2} \left\{ |n'';1\rangle\langle 0;n''+1| \, |n'+1;0\rangle\langle 1;n'| , \rho^{(n)} \right\}_+ \right)$$

$$= \sum_n \Gamma_R^{(n)} p_{1,n} \, |n+1;0\rangle\langle 0;n+1| - \frac{\Gamma_R^{(n)}}{2} \left\{ |n;1\rangle\langle 1;n| , \rho^{(n)} \right\}_+$$

$$= \sum_n \Gamma_R^{(n-1)} p_{1,n-1} \, |n;0\rangle\langle 0;n| - \Gamma_R^{(n)} p_{1,n} \, |n;1\rangle\langle 1;n| \qquad (5.67)$$

$$= \sum_n \begin{pmatrix} 0 & \Gamma_R^{(n-1)} \\ 0 & 0 \end{pmatrix} \rho^{(n-1)} + \begin{pmatrix} 0 & 0 \\ 0 & -\Gamma_R^{(n)} \end{pmatrix} \rho^{(n)} \qquad (5.68)$$

and a similar calculation for $\alpha = L$, leads to

$$\sum_n \partial_t \rho^{(n)}(t) = \sum_n \begin{pmatrix} -\Gamma_L^{(n)} & -\Gamma_R^{(n)} \\ \Gamma_L^{(n)} & 0 \end{pmatrix} \rho^{(n)} + \begin{pmatrix} 0 & \Gamma_R^{(n-1)} \\ 0 & 0 \end{pmatrix} \rho^{(n-1)} \qquad (5.69)$$

$$\Rightarrow \partial_t \rho^{(n)}(t) = \begin{pmatrix} -\Gamma_L^{(n)} & 0 \\ \Gamma_L^{(n)} & -\Gamma_R^{(n)} \end{pmatrix} \rho^{(n)} + \begin{pmatrix} 0 & \Gamma_R^{(n-1)} \\ 0 & 0 \end{pmatrix} \rho^{(n-1)} \qquad (5.70)$$

$$\partial_t \rho^{(n)}(t) = \mathcal{L}_0^{(n)} \rho^{(n)}(t) + \mathcal{J}^{(n-1)} \rho^{(n-1)}(t). \qquad (5.71)$$

In that way the nQME has been motivated for the special case of the Single Quantum Dot. A visual representation of this equation can be found in figure 5.5. If there is internal system dynamics H_{int} (cf. section 5.4), this is simply added to $\mathcal{L}_0^{(n)}$.

5.2.1 Counting field

Transformation to the Laplace Space as discussed in section 3.2, yields $\hat{\rho}_n(z) = \hat{\mathcal{P}}_n(z)\hat{\mathcal{W}}_{\pi,0}^{(n-1)}(z)\rho_0$.

With the assumption that

- all $\Gamma_{R/L}^{(n)}$ are statical independent,

- and no mixed $k, k-1$ from the same side (R, L) appear,

$\hat{\mathcal{W}}_{\pi,0}^{(n-1)}(z)$ gets simplified to $\prod_{k=0}^{n-1} \left\langle \hat{\mathcal{W}}_k(z) \right\rangle$. Remembering that $\hat{\mathcal{W}}(z) = \left\langle \hat{\mathcal{W}}_n(z) \right\rangle$, $\hat{\mathcal{P}}(z) = \left\langle \hat{\mathcal{P}}_n(z) \right\rangle$ leads (in accordance to 3.19) to

$$\langle \hat{\rho}_n(z) \rangle = \hat{\mathcal{P}}(z)\hat{\mathcal{W}}^n(z)\rho_0. \qquad (5.72)$$

With the short hand notation

$$P_\alpha(z) := \left\langle \frac{1}{z+\Gamma_\alpha} \right\rangle, W_\alpha(z) := \left\langle \frac{\Gamma_\alpha}{z+\Gamma_\alpha} \right\rangle, \qquad (5.73)$$

the exception value for the propagator becomes

$$\hat{\mathcal{P}}(z) = \left\langle \left[z - \mathcal{L}_0^{(n)} \right]^{-1} \right\rangle = \begin{pmatrix} P_L(z) & 0 \\ W_L(z)P_R(z) & P_R(z) \end{pmatrix}, \tag{5.74}$$

by inverting the matrix. With a simple matrix multiplication one gets

$$\hat{\mathcal{W}}(z) = \left\langle \mathcal{J}^{(n)}\hat{\mathcal{P}}_n(z) \right\rangle = W_L(z)W_R(z) \begin{pmatrix} 1 & \frac{1}{W_L(z)} \\ 0 & 0 \end{pmatrix} {}^5 \tag{5.75}$$

$$\Rightarrow \hat{\mathcal{W}}^n(z) = (W_L(z)W_R(z))^n \begin{pmatrix} 1 & \frac{1}{W_L(z)} \\ 0 & 0 \end{pmatrix}. \tag{5.76}$$

Thus,

$$\langle \hat{\rho}_n(z) \rangle = \hat{\mathcal{P}}(z)\hat{\mathcal{W}}^n(z)\rho_0 = W_L(z)W_R(z))^n \begin{pmatrix} P_L(z) & \frac{P_L(z)}{W_L(z)} \\ P_R(z)W_L(z) & P_R(z) \end{pmatrix} \rho_0. \tag{5.77}$$

According to $\langle \hat{\rho}_\chi(z) \rangle = \left\langle \sum_{n=0}^{\infty} \hat{\rho}_n(z)e^{\mathrm{i}n\chi} \right\rangle$ one can use the scalar version of the geometric series by regarding that $\hat{\mathcal{W}}^0(z) = 1$ and derive

$$\langle \hat{\rho}_\chi(z) \rangle = \frac{1}{1 - e^{\mathrm{i}\chi}W_L(z)W_R(z)} \begin{pmatrix} P_L(z) & \frac{P_L(z)}{W_L(z)} \\ P_R(z)W_L(z) & P_R(z) \end{pmatrix} \rho_0 - \begin{pmatrix} 0 & \frac{P_L(z)}{W_L(z)} \\ 0 & 0 \end{pmatrix} \rho_0. \tag{5.78}$$

The second term does not depend on χ and has no influence on the moments. At this point it can be remarked that it is a easy to show that the general formalism with $\hat{\mathcal{P}}(z)\hat{\mathcal{G}}_\chi(z) = \hat{\mathcal{P}}(z)\left(1 - e^{\mathrm{i}\chi}\hat{\mathcal{W}}(z)\right)^{-1}$ leads to the same result.

5.2.2   Current

For this subsection we will make use of the short hand notation

$$\hat{\rho}_{0,\mathrm{SD}}(z) = \begin{pmatrix} P_L(z) & \frac{P_L(z)}{W_L(z)} \\ P_R(z)W_L(z) & P_R(z) \end{pmatrix} \rho_0. \tag{5.79}$$

Thus, the χ-dependent part of the Moment Generating Function reads

$$\hat{M}(\mathrm{i}\chi) = \frac{1}{1 - e^{\mathrm{i}\chi}W_\Pi(z)} \mathrm{Tr}\hat{\rho}_{0,\mathrm{SD}}(z) + \mathrm{const.}, \tag{5.80}$$

where $W_\Pi(z) = W_L(z)W_R(z)$.

---

[5] $\hat{\mathcal{W}}(z) \neq 1 - z\hat{\mathcal{P}}(z)$ as in the Tunneling Junction example

Consequently, the first four moments read

$$\hat{m}_1(z) = \frac{W_\Pi(z)}{(W_\Pi(z) - 1)^2} \text{Tr}\hat{\rho}_{0,\text{SD}}(z) \tag{5.81}$$

$$\hat{m}_2(z) = -\frac{W_\Pi(z)(W_\Pi(z) + 1)}{(W_\Pi(z) - 1)^3} \text{Tr}\hat{\rho}_{0,\text{SD}}(z) \tag{5.82}$$

$$\hat{m}_3(z) = \frac{W_\Pi(z)\left(W_\Pi(z)^2 + 4W_\Pi(z) + 1\right)}{(W_\Pi(z) - 1)^4} \text{Tr}\hat{\rho}_{0,\text{SD}}(z) \tag{5.83}$$

$$\hat{m}_4(z) = -\frac{W_\Pi(z)\left(W_\Pi(z)^3 + 11W_\Pi(z)^2 + 11W_\Pi(z) + 1\right)}{(W_\Pi(z) - 1)^5} \text{Tr}\hat{\rho}_{0,\text{SD}}(z). \tag{5.84}$$

In section 3.3.5 the difficulties of the Cumulant Generating Function were already discussed. Of course on could use the scheme, proposed in [Flindt et al., 2010b] and examine the eigenvalues of $\hat{\mathcal{W}}(z)$ or rather $\hat{\mathcal{M}}(z)$. The explicit calculation of the trace $\text{Tr}\hat{\rho}_{0,\text{SD}}(z)$, an explicit expression for the first moment, leads to

$$\hat{m}_1(z) = W_R(z)\frac{P_L(z) + P_R(z)W_L(z)}{(W_L(z)W_R(z) - 1)^2}(\rho_{00}W_L(z) + \rho_{01}). \tag{5.85}$$

Using the norm of the density matrix ($1 = \rho_{00} + \rho_{01}$) and $W_L(z) = 1 - zP_L(z)$ and the same for $W_R(z)$ leads to

$$\hat{m}_1(z) = \frac{zP_R(z) - 1}{z^2(zP_L(z)P_R(z) - P_L(z) - P_R(z))} + \rho_{00}\frac{P_L(z)(1 - zP_R(z))}{z(zP_L(z)P_R(z) - P_L(z) - P_R(z))}$$

$$\Rightarrow \hat{m}_1(z)z^2 = \frac{(zP_R(z) - 1)(zP_L(z)\rho_{00} - 1)}{P_L(z) + P_R(z) - zP_L(z)P_R(z)}. \tag{5.86}$$

For the long-time limit a series expansion for $P_R(z)$ is done that means

$$P_L(z) = \left\langle \frac{1}{\Gamma_L} \right\rangle - z\left\langle \frac{1}{\Gamma_L{}^2} \right\rangle + z^2\left\langle \frac{1}{\Gamma_L{}^3} \right\rangle + \text{O}^3(z), \tag{5.87}$$

which can be rewritten to

$$P_L(z) = \langle \tau_L \rangle - z\langle \tau_L^2 \rangle + z^2\langle \tau_L^3 \rangle + \text{O}^3(z) \tag{5.88}$$

$$\tag{5.89}$$

by using (4.7) and the same procedure for $P_L(z)$.

Inserting this into (5.86) leads, after some sorting [6], to

$$\text{current Single Dot}\quad \boxed{\langle I_\infty \rangle = \lim_{z \to 0} z^2\hat{m}_1(z) = \frac{1}{\langle \tau_L \rangle + \langle \tau_R \rangle}.} \tag{5.90}$$

That means that the average of the current in the long-time limit is related to the inverse of the sum of the waiting times. The comparison to the clean case shows that the former equation

with $I_{\infty,\text{cln}} = \frac{1}{\frac{1}{\Gamma_L} + \frac{1}{\Gamma_R}} = \frac{\Gamma_L\Gamma_R}{\Gamma_L + \Gamma_R}$ is the known result [Emary, 2009].

---

[6]Mathematica is quiet helpful here

Waiting times or tunneling rates?

Regarding the experiment there is no big difference between talking about tunneling rates or waiting times, because both values can be measured in principal.

Even so there are two essential advantages of using waiting times instead of tunneling rates.

- The formular looks easier (even for the clean case)

- The mean of the average long-time current for random rates does only depend on the mean of the waiting time distribution

One can spend some effort on investigating how systems with the same mean rates behave. Everything that is to be done for that, is to compare $\frac{1}{\langle \Gamma_{L,R} \rangle}$ to $\langle \tau_{L,R} \rangle$. According to definition 5.26 the relation reads

$$\langle \tau_{L,R} \rangle = \frac{1 + \alpha_{L,R}}{\langle \Gamma_{L,R} \rangle} \tag{5.91}$$

with $\alpha \geq 0$, which was discussed for the Tunneling Junction. The parameter α can be derived directly from the PDF.

5.2.3   Fano factor

Inserting the definition of $W_L(z), W_R(z)$ to the general formula for $\hat{m}_2(z)$ leads to

$$\hat{m}_2(z) = \frac{(P_R(z)z - 1)\left(P_L(z)P_R(z)z^2 - z(P_L(z) + P_R(z)) + 2\right)(P_L(z)\rho_{00}z - 1)}{z^3(P_L(z)(-P_R(z))z + P_L(z) + P_R(z))^2}. \tag{5.92}$$

A Taylor Series Expansion in first order around $z = 0$ yields

$$P_L(z) = \langle \tau_L \rangle - z\langle \tau_L^2 \rangle + O\left(z^2\right) \tag{5.93}$$

$$P_R(z) = \langle \tau_R \rangle - z\langle \tau_R^2 \rangle + O\left(z^2\right) \tag{5.94}$$

with $\langle \tau_\Sigma \rangle = \langle \tau_R \rangle + \langle \tau_L \rangle$. Equation (5.92) becomes

$$\hat{m}_2(z) = \frac{2}{\langle \tau_\Sigma \rangle^2 z^3} + \frac{4\left(\langle \tau_R^2 \rangle + \langle \tau_L^2 \rangle\right) - 3\langle \tau_R \rangle^2 - \langle \tau_L \rangle^2 - 2\rho_{00}\langle \tau_L \rangle(\langle \tau_R \rangle + \langle \tau_L \rangle)}{\langle \tau_\Sigma \rangle^3 z^2} + O\left(\frac{1}{z}\right). \tag{5.95}$$

The Inverse Laplace Transform $\left(\underset{z \to t}{\mathrm{LT}^{-1}}\right)$ in the time-domain gives

$$m_2 = \frac{t^2}{\langle \tau_\Sigma \rangle^2} + \frac{4t\left(\langle \tau_R^2 \rangle + \langle \tau_L^2 \rangle\right) - 3t\langle \tau_R \rangle^2 - t\langle \tau_L \rangle^2}{\langle \tau_\Sigma \rangle^3} - 2t\rho_{00}\left(\frac{\langle \tau_L \rangle(\langle \tau_R \rangle + \langle \tau_L \rangle)}{\langle \tau_\Sigma \rangle^3}\right). \tag{5.96}$$

That leads to the Fano factor for $t \to \infty$

$$\langle F_\infty \rangle = \lim_{t \to \infty} \frac{m_2(t) - m_1^2(t)}{m_1(t)} = \frac{2\langle \tau_L^2 \rangle - \langle \tau_L \rangle^2 + 2\langle \tau_R^2 \rangle - \langle \tau_R \rangle^2}{(\langle \tau_R \rangle + \langle \tau_L \rangle)^2}. \tag{5.97}$$

There are two useful forms of representations for the Fano factor. The form above (5.97) can be called **moment form**, because the Fano factor is a function of the raw moments of the distribution of waiting times there. The other useful representation is the representation in terms of central moments, hence is can be called **central moment** form.

Using theorem 5 one can express 5.97 via

$$\langle F_\infty \rangle = \frac{\langle \tau_L^2 \rangle + \mathrm{Var}(\tau_L) + \langle \tau_R^2 \rangle + \mathrm{Var}(\tau_R)}{(\langle \tau_R \rangle + \langle \tau_L \rangle)^2}. \tag{5.98}$$

It can be shown that the Fano factor is greater than one if the following inequality is valid.

$$\lim_{t \to \infty} \frac{m_2(t) - m_1^2(t)}{m_1(t)} > 1 \Leftrightarrow \langle (\tau_L - \langle \tau_L \rangle)^2 \rangle \langle (\tau_R - \langle \tau_R \rangle)^2 \rangle > \langle \tau_L \rangle \langle \tau_R \rangle. \tag{5.99}$$

It is easy to see that the Fano factor is greater than one if the product of the variance is greater than the product of the expectation value. This is an intuitive result. The smallest, possible Fano factor occurs in the clean case. This becomes obvious by regarding equation (5.98) and the fact that the variance is always positive.

$$f \geq \frac{1}{2} \tag{5.100}$$

The prove of the inequality (5.100) is basic math and can be found in the appendix (compare theorem 6 p. 128).

5.2.4   Clean limit

In the following subsection the clean limit, which reproduces the known results, is discussed. For the clean limit with

$$\langle \tau_L \rangle = \Gamma_L^{-1}, \langle \tau_R \rangle = \Gamma_R^{-1} \tag{5.101}$$

$$\langle \tau_\Sigma \rangle = \Gamma_L^{-1} + \Gamma_R^{-1} \left(\langle \tau_R^2 \rangle + \langle \tau_L^2 \rangle \right) = \Gamma_L^{-2} + \Gamma_R^{-2}, \tag{5.102}$$

this leads to

$$F_{\infty,\mathrm{cln}} = \frac{\Gamma_L^2 + \Gamma_R^2}{(\Gamma_L + \Gamma_R)^2}. \tag{5.103}$$

This is in accordance to [Emary, 2009, 8.34]. Using waiting times instead of tunneling rates leads to

$$F_{\infty,\mathrm{cln}} = \frac{\langle \tau_L \rangle^2 + \langle \tau_R \rangle^2}{(\langle \tau_L \rangle + \langle \tau_R \rangle)^2}. \tag{5.104}$$

Thus, the random Fano factor can be rewritten to

$$F_{\infty,\text{cln}} = \frac{2\langle\tau_L^2\rangle - \langle\tau_L\rangle^2 + 2\langle\tau_R^2\rangle - \langle\tau_R\rangle^2}{(\langle\tau_R\rangle + \langle\tau_L\rangle)^2} \tag{5.105}$$

$$= \frac{2\langle(\tau_L - \langle\tau_L\rangle)^2)\rangle + \langle\tau_L\rangle^2 + 2\langle(\tau_R - \langle\tau_R\rangle)^2)\rangle + \langle\tau_R\rangle^2}{(\langle\tau_R\rangle + \langle\tau_L\rangle)^2} \tag{5.106}$$

$$= \underbrace{\frac{\langle\tau_L\rangle^2 + \langle\tau_R\rangle^2}{(\langle\tau_L\rangle + \langle\tau_R\rangle)^2}}_{F_{\infty,\text{cln}}} + 2\frac{\langle(\tau_L + \langle\tau_L\rangle)\rangle + \langle(\tau_R - \langle\tau_R\rangle)^2)\rangle}{(\langle\tau_L\rangle + \langle\tau_R\rangle)^2}. \tag{5.107}$$

This can bee seen as third sensible way of representation of the Fano factor and is very similar to the central moment representation.

5.2.5   Steady state

In the case of random rates the description steady state might be misleading. However, investigating the expectation value of the density matrix makes the term 'steady state' well defined. A simple calculation leads to the following result.

$$\langle\rho(t \to \infty)\rangle = \lim_{z \to 0} z \sum_{n=0}^{\infty} \langle\hat{\rho}_n(z)\rangle \tag{5.108}$$

$$= \lim_{z \to 0} z \sum_{n=0}^{\infty} L(z).W(z)^n.\rho_0 \tag{5.109}$$

$$= \lim_{z \to 0} zL(z).\left(\sum_{n=0}^{\infty} W(z)^n\right).\rho_0 \tag{5.110}$$

$$^7 = \lim_{z \to 0} zL(z).\left(\frac{W(z)}{W_L(z)W_R(z) - W_L(z)^2 W_R(z)^2}\right).\rho_0 \tag{5.111}$$

$$= \lim_{z \to 0} \frac{1}{P_L(z) + P_R(z)}\begin{pmatrix} P_L(z) \\ P_R(z) \end{pmatrix} \tag{5.112}$$

$$= \frac{1}{\langle\tau_\Sigma\rangle}\begin{pmatrix} \langle\tau_L\rangle \\ \langle\tau_R\rangle \end{pmatrix}. \tag{5.113}$$

This result was expected analogically to the clean case, where the steady state was

$$\rho_{\text{stat}} = \frac{1}{\Gamma_L + \Gamma_R}\begin{pmatrix} \Gamma_L \\ \Gamma_R \end{pmatrix} \text{[Emary, 2009, 7.123],} \tag{5.114}$$

---

[7] geometric series

5.2.6 Simulation

As in the former sections all results were derived analytically, there is no need for a numeric simulation. Nevertheless, a numerical simulation illustrates the analytical results. In the following a Single Quantum Dot with uniform distributed random rates is regarded. The mean of the distribution was set to $\perp = 5$ and the width of the distribution σ was set to 4. With a discrete time step approach (a detailed explication follows in section 7.1) and the step width of $\Delta_t = \frac{1}{100}$ (figure 5.6) was obtained.

In the upper left picture the dot occupation is visualized for one random sample. In the upper right picture one can see the number of transmitted particles. The particle is counted, when the dot occupation changes from full to empty. By this change new random rates were generated and displayed in the second row. The corresponding waiting times are in the third row. The distribution of this rates or waiting times is visualized in figure 5.7. In the lower left picture the current is visualized. The blue line indicates the moving average current for the real current. The green line indicates the current, which is calculated by using the long-time current formula by the moving average for the waiting times. The red line indicates the same for the tunneling rates. In the lower right picture one can see the same, where the rates were time weighted[8].

---

[8]It has to be discussed, if this makes sense.
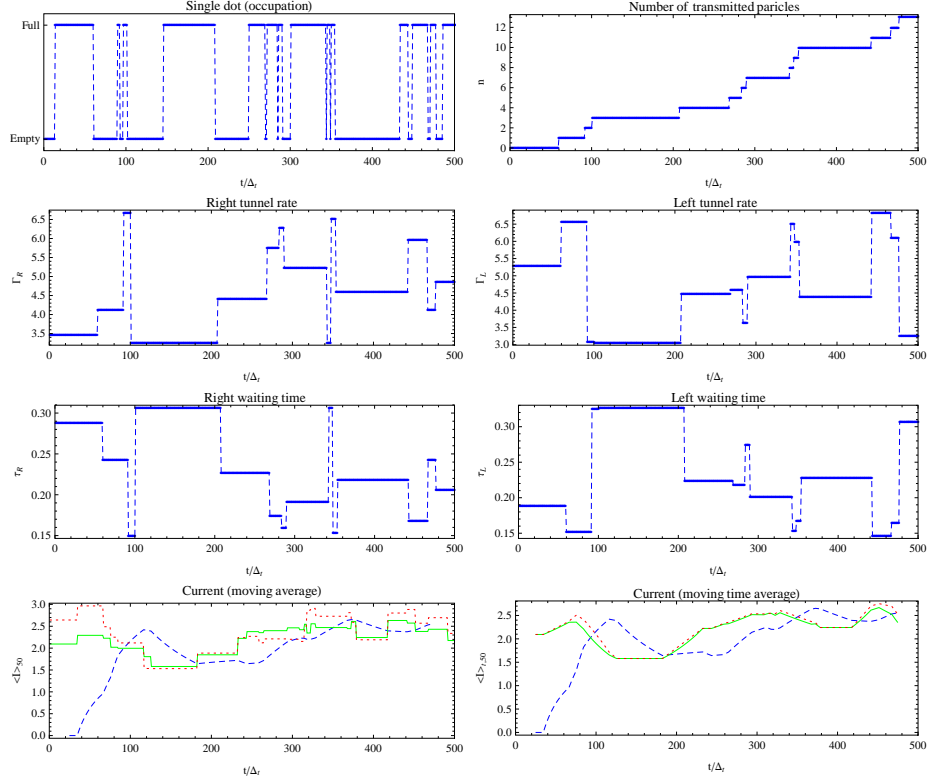
Figure 5.6: Simulation: Single dot with $\perp = 5, \sigma = 4$. Complete description see text. last row: blue simulated current; red wrong current expressed by average tunneling rates; green expected current by making use of the waiting time formula
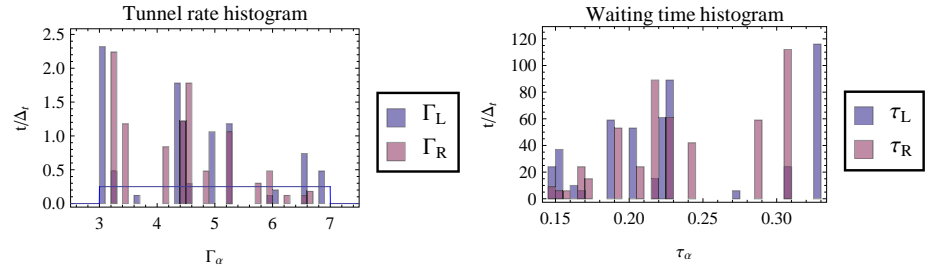
Figure 5.7: Simulation: Histogram $\perp = 5, \sigma = 4$

One can see that no way of calculation leads to good results for the first few time steps. Regarding longer times and replacing the moving average to the average of all recent events leads to figure 5.8. In that situation it becomes clear that the calculation in terms of waiting times leads to the correct result (green line). For comparison the wrong current, which is derived by replacing the tunneling rates by their averages is printed in red.
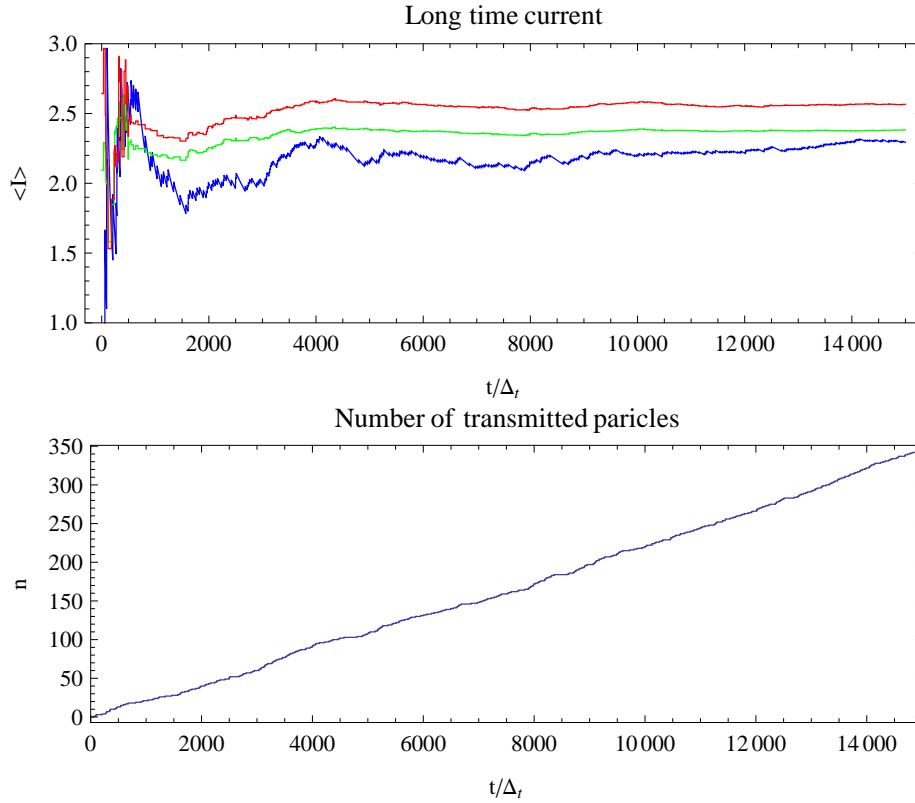
Figure 5.8: Simulation: long-time current $\perp = 5, \sigma = 4, \Delta_t = .01$.
blue simulated current
red wrong current expressed by average tunneling rates
(green expected current by making use of the waiting time formula
Further description see text.

5.3   Transitions in a ring

It could be seen that the results for the Tunneling Junction and the Single
Quantum Dot are congruent. Hence, this class of setups is being extended to a
finite numbers of sequential jumps. At this point it can be remarked that this
system has no essential coherent states.

Regarding a ring with transitions between K states, $1 \to 2 \ldots \to K \to 1$ at rates
$\Gamma_i^{(n)}$. This setup was discussed in [Brandes, 2008, section 3.3]. The step $K \to 0$
is interpreted as jump process and leads to a change in the rates. So Liouvillian
and jump operator read

$$\mathcal{L}_0^{(n)} = \begin{pmatrix} -\Gamma_1^{(n)} & 0 & 0 & \ldots & 0 \\ \Gamma_1^{(n)} & -\Gamma_2^{(n)} & 0 & & 0 \\ 0 & \Gamma_2^{(n)} & -\Gamma_3^{(n)} & & \vdots \\ \vdots & & & \ddots & 0 \\ 0 & 0 & \ldots & \Gamma_{K-1}^{(n)} & -\Gamma_K^{(n)} \end{pmatrix},$$

$$\mathcal{J}^{(n-1)} = \begin{pmatrix} 0 & 0 & 0 & \ldots & \Gamma_K^{(n-1)} \\ 0 & 0 & 0 & & 0 \\ 0 & 0 & 0 & & 0 \\ \vdots & & & \ddots & 0 \\ 0 & 0 & \ldots & 0 & 0 \end{pmatrix}. \tag{5.115}$$

Listing 5.1: Sample code snipped: Generate a ring of size K with the help of our
            nQME-Package

```
 1  Needs["nQME`Random`"](*Initialize tha package*)
    g[i_] := ToExpression["\[CapitalGamma]" <> ToString[i]](*\]*)
    Ring[k_] := ((L0 =
        Normal[SparseArray[{{i_, i_} :> -g[i], {i_, j_} /; i - j == 1 :>
            g[j]}, {k, k}]];
 6  J = Normal[SparseArray[{{1, k} -> g[k]}, {k, k}]];
    vars = Table[g[i], {i, k}];
    TraceFunction[Mat_] :=
     Tr[((Mat.Normal[SparseArray[{{1} -> 1}, {k}]]))];
    nQMESetL0[L0];
11  nQMESetJ[J];
    nQMESetRandomVariables[vars];
    nQMESetTraceFunction[TraceFunction];
    ));
```

According to the developed procedure (cf. chapter 3-4) the following matrices
are calculated

$$\hat{\mathcal{W}}(z) = \left\langle \hat{\mathcal{W}}_n(z) \right\rangle = \begin{pmatrix} W_{\Pi 1} & W_{\Pi 2} & W_{\Pi 3} & \dots & W_{\Pi K} \\ 0 & 0 & 0 & & 0 \\ 0 & 0 & 0 & & \vdots \\ \vdots & & & \ddots & 0 \\ 0 & 0 & \dots & 0 & 0 \end{pmatrix} \quad (5.116)$$

$$\hat{\mathcal{P}}(z) = \left\langle \hat{\mathcal{P}}_n(z) \right\rangle = \begin{pmatrix} P_1 & 0 & 0 & \dots & 0 \\ W_1 P_2 & P_2 & 0 & & 0 \\ W_1 W_2 P_3 & W_2 P_3 & P_3 & & \vdots \\ \vdots & & & \ddots & 0 \\ \frac{W_{\Pi 1} P_K}{W_K} & \frac{W_{\Pi 2} P_K}{W_K} & \dots & W_{K-1} P_K & P_K \end{pmatrix} \quad (5.117)$$

$$\hat{\mathcal{T}}^k(z) = \langle Tnz \rangle = \frac{1}{k!} \left(\frac{1}{1 - \frac{1}{W_{\Pi 1}}} \right)^k \begin{pmatrix} 1 & \frac{W_{\Pi 2}}{W_{\Pi 1}} & \frac{W_{\Pi 3}}{W_{\Pi 1}} & \dots & \frac{W_K}{W_{\Pi 1}} \\ 0 & 0 & 0 & & 0 \\ 0 & 0 & 0 & & \vdots \\ \vdots & & & \ddots & 0 \\ 0 & 0 & \dots & 0 & 0 \end{pmatrix} \quad (5.118)$$

with $W_i = \left\langle \frac{\Gamma_i}{z + \Gamma_i} \right\rangle$, $P_i = \left\langle \frac{1}{z + \Gamma_i} \right\rangle$ and $W_{\Pi i} = \prod_{j=i}^{K} W_j$. Thus, the Moment
Generating Function reads

$$\text{Moment Generating Function} \quad \hat{M}(\mathrm{i}\chi) = \frac{\sum\limits_{i=1}^{K} \prod\limits_{k=1}^{i} P_k}{1 - e^{\mathrm{i}\chi} W_{\Pi}}. \quad (5.119)$$

Current and Fano factor

The current becomes

$$\boxed{\langle I_\infty \rangle = \frac{1}{\langle \tau_\Sigma \rangle}} \quad (5.120)$$

with $\langle \tau \rangle_\Sigma = \sum\limits_{i=1}^{K} \langle \tau \rangle_i$, $\langle \tau \rangle_i = \left\langle \frac{1}{\Gamma_i} \right\rangle$

and the Fano factor evaluates to

$$\boxed{\langle F_\infty \rangle = \frac{\sum\limits_{i=1}^{K} \left(\langle \tau_i \rangle - 2 \langle \tau_i^2 \rangle \right)}{\langle \tau_\Sigma \rangle}} \quad (5.121)$$

with $\langle \tau_\Sigma \rangle = \sum\limits_{i=1}^{K} \langle \tau_i \rangle$, $\langle \tau_i \rangle = \left\langle \frac{1}{\Gamma_i} \right\rangle$.

Furthermore, it can be shown that

$$\langle F_\infty \rangle \geq \frac{1}{K}. \quad (5.122)$$

A proof can be developed in the same style as for the Single Quantum Dot (cf. proposition 6). One possibility is to use the multinomial coefficient (see e.g. [Comtet, 1974]).

One can express the Fano factor in central moment representation.

$$\langle F_\infty \rangle = \frac{\sum\limits_{i=1}^{K}(\langle \tau_i \rangle^2 - 2\langle \tau_i^2 \rangle)}{\langle \tau_\Sigma \rangle^2} = \frac{\sum\limits_{i=1}^{K}(\langle \tau_i \rangle^2 + 2\mathrm{Var}(\tau_i))}{\langle \tau_\Sigma \rangle^2} \qquad (5.123)$$

$\mathrm{Var}(\tau_i) \geq 0$, which is minimal for the clean case. Afterwards it is basic mathematics to prove that

$$\frac{\sum_{i=1}^{k} a_k^2}{\left(\sum_{i=1}^{K} a_k\right)^2} \geq \frac{1}{K} \quad \forall a_k \in \mathbb{R}^+. \qquad (5.124)$$

The detailed prove is given in proposition 7.

Expressions for the higher order cumulants can be derived in the same style.

5.4 Double Quantum Dot

In the following the **D**ouble-**Q**uantum-**D**ot **(DQD)** is taken into account. The Double Quantum Dot consists of two coupled Quantum Dots. In this special case the particles can jump from one side to the other and backwards. In contrast to the former example the Double Quantum Dot involves internal system dynamics. This internal dynamics depends on two parameter:

- ϵ : specifies the difference between the energy levels of the dots

- T_C: defines the strength of the coupling of the dots (Tunneling is allowed in both directions.)
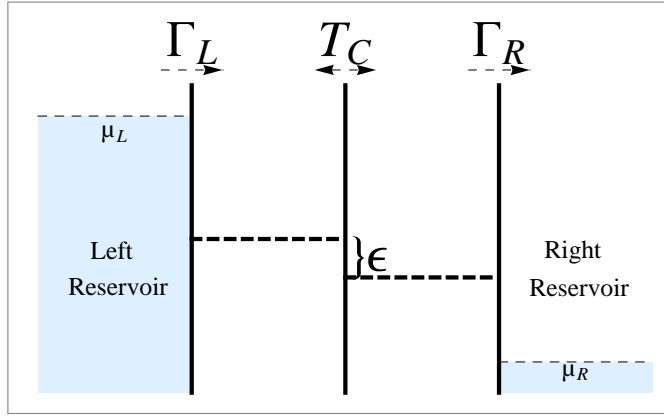
Figure 5.9: Scheme of a Double Quantum Dot. A realistic view can be seen in figure 1.1.

It is simple to derive the System Hamiltonian from figure 5.10 (see also [Emary, 2009, 7.29])

$$\mathrm{H}_S = \epsilon_L \left|L\right\rangle\!\left\langle L\right| + \epsilon_R \left|R\right\rangle\!\left\langle R\right| + T_C(\left|L\right\rangle\!\left\langle R\right| + \left|R\right\rangle\!\left\langle L\right|)$$
$$\mathrm{H}_S = \frac{\epsilon}{2}(\left|L,L\right\rangle\!\rangle - \left|R,R\right\rangle\!\rangle) + T_C(\left|L,R\right\rangle\!\rangle + \left|R,L\right\rangle\!\rangle) \tag{5.125}$$

To write down the System Liouvillian one has to choose an appropriate base[9]. As there is no coherence with the empty state $\left|0\right\rangle$, only the states $\left|0,0\right\rangle\!\rangle \equiv \left|0\right\rangle\!\left\langle 0\right|$, $\left|L,L\right\rangle\!\rangle, \left|R,R\right\rangle\!\rangle, \left|L,R\right\rangle\!\rangle, \left|RL\right\rangle\!\rangle$ have to be regarded.

$$\mathcal{L}_S = \mathrm{i}\mathrm{H}_S.\boxed{x} - \mathrm{i}\boxed{x}.\mathrm{H}_S = \mathrm{i}\sum_{kij}(\mathrm{H}_{Sik}\left|kj\right\rangle\!\rangle - \mathrm{H}_{Skj}\left|ik\right\rangle\!\rangle)\langle\!\langle i,j| \tag{5.126}$$

$$= \mathrm{i}\begin{pmatrix} 0 & 0 & 0 & 0 & 0 \\ 0 & 0 & 0 & T_C & -T_C \\ 0 & 0 & 0 & -T_C & T_C \\ 0 & T_C & -T_C & -\epsilon & 0 \\ 0 & -T_C & T_C & 0 & \epsilon \end{pmatrix}_{\left|00,LL,RR,LR,RL\right\rangle\!\rangle} \tag{5.127}$$

---

[9]This is required to transform the density operator (matrix) to a state of the Liouville Space (vector). For details see appendix B.3 and notebook NB:Ham2Lio

It has to be remarked that the first column and row of the System Liouvillian are (as expected) empty, because the internal system dynamics does not involve the empty state $|0\rangle$. To get rid of all the complex numbers a simple base-
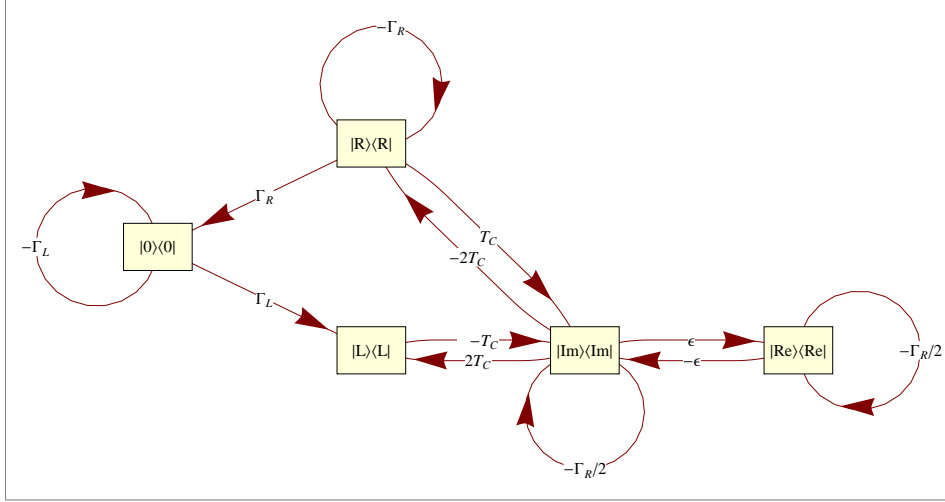
Figure 5.10: Functional graph of Double Quantum Dot, with Re=$\Re$ - real Im=$\Im$-complex part of $|R\rangle\langle L|$.

There are similarities to the Single Quantum Dot. On the left lead is exactly the same setup as in the Single Quantum Dot. So one expects nothing new compared to the single resonant level. This is confirmed in the calculation, where only the average waiting time from the left lead occurs in the current. In the middle there is a system with a structural similarity to the Single Quantum Dot if on neglects the connections to $|L\rangle\langle L|$ and $|R\rangle\langle R|$. The current would be equivalent to the current of a Single Quantum Dot similar system with the pseudo Liouvillian $\mathcal{L} = \begin{pmatrix} -\Gamma_R/2 & -\Gamma_R/2 \\ \epsilon & -\epsilon \end{pmatrix}$. The current for that pseudo subsystem evaluates (with nQME package) to $\langle I_\infty \rangle = \frac{4\epsilon^2 \Gamma_R}{(\Gamma_R + 2\epsilon)^2}$.

transformation to
$\{|00\rangle\rangle, |LL\rangle\rangle, |RR\rangle\rangle, \Re|RL\rangle\rangle, \Im|RL\rangle\rangle\}$ can be performed

$$\mathcal{L}_S = \begin{pmatrix} 0 & 0 & 0 & 0 & 0 \\ 0 & 0 & 0 & 0 & 2T_C \\ 0 & 0 & 0 & 0 & -2T_C \\ 0 & 0 & 0 & 0 & -\epsilon \\ 0 & -T_C & T_C & \epsilon & 0 \end{pmatrix}_{|00,LL,RR,\Re RL,\Im RL\rangle\rangle} . \tag{5.128}$$

Indeed the DQD is coupled to the environment. This works equally to the already seen Single Quantum Dot. Thus, one has a jump in process on the left side with the Liouvillian

$$\mathcal{L}_L = \Gamma_L \mathcal{D}(j_L), \quad \mathcal{L}_R = \Gamma_R \mathcal{D}(j_R) \tag{5.129}$$

with the left jump operator $j_L = |0L\rangle\!\rangle$, $j_R = |R0\rangle\!\rangle$ and the Lindblad Superoperator $\mathcal{D}(j)\boxed{x} = j\boxed{x}j^\dagger - \frac{1}{2}\left\{\boxed{x}, j^\dagger j\right\}$. Thus, the full 'clean' Hamiltonian reads

$$\mathcal{L} = \begin{pmatrix} -\Gamma_L & 0 & \Gamma_R & 0 & 0 \\ \Gamma_L & 0 & 0 & 0 & 2T_C \\ 0 & 0 & -\Gamma_R & 0 & -2T_C \\ 0 & 0 & 0 & -\frac{1}{2}\Gamma_R & -\epsilon \\ 0 & -T_C & T_C & \epsilon & \frac{1}{2}\Gamma_R \end{pmatrix}_{10}. \qquad (5.130)$$

With n-dependent rates and the nQME (3.1) reads

$$\partial_t \rho^{(n)}(t) = \mathcal{L}_0^{(n)} \rho^{(n)}(t) + \mathcal{J}^{(n)} \rho^{(n-1)}(t) \qquad (5.131)$$

$$\mathcal{L}_0^{(n)} = \mathcal{L}_S + \Gamma_L^{(n)} \mathcal{D}(j_L) + \frac{\Gamma_R^{(n)}}{2}\left\{\boxed{x}, j_R j^\dagger{}_R\right\} \quad \mathcal{J}^{(n)} = \Gamma_R^{(n-1)} j_R \boxed{x} j^\dagger. \qquad (5.132)$$

Experimentally, the coupling strength is replaced through an n-dependent version $T_C \to T_C^{(n)}$, although this was not derived microscopically. In matrix notation this looks like

$$\mathcal{L}_0^{(n)} = \begin{pmatrix} -\Gamma_L^{(n)} & 0 & 0 & 0 & 0 \\ \Gamma_L^{(n)} & 0 & 0 & 0 & 2T_C^{(n)} \\ 0 & 0 & -\Gamma_R^{(n)} & 0 & -2T_C^{(n)} \\ 0 & 0 & 0 & -\frac{\Gamma_R^{(n)}}{2} & -\epsilon \\ 0 & -T_C^{(n)} & T_C^{(n)} & \epsilon & -\frac{\Gamma_R^{(n)}}{2} \end{pmatrix}, \quad \mathcal{J}^{(n-1)} = \begin{pmatrix} 0 & 0 & \Gamma_R^{(n-1)} & 0 & 0 \\ 0 & 0 & 0 & 0 & 0 \\ 0 & 0 & 0 & 0 & 0 \\ 0 & 0 & 0 & 0 & 0 \\ 0 & 0 & 0 & 0 & 0 \end{pmatrix}. $$

$$(5.133)$$

For this example the procedure works exactly equal. As the calculation effort is very big, this step was done by a Mathematica Program. This program executes exactly the steps, described in chapter 4 (cf. appendix D.1, p. 147 for the source code).

Figure 5.10 visualizes the Liouvillian for the clean case.

Constant rates

With this Mathematica Package the known results [Stoof and Nazarov, 1996, Gurvitz and Prager, 1996] were reproduced. The handling of the Mathematica Package is simple. Inserting the Liouvillian and jump operator leads to long-time current, Fano factor and higher cumulants. Which variables are said to be random, can be specified individually. The example, which was used to generate the findings below, can be found in appendix D.2, p.149.

For the current one derives

$$\langle I_\infty \rangle = \left(\tau_L + \tau_R \left(\epsilon^2 \tau_T^2 + 2 \right) + \frac{\tau_T^2}{4\tau_R} \right)^{-1}. \qquad (5.134)$$

---

[10] From now on $|00, LL, RR, \Re RL, \Im RL\rangle\!\rangle$ is assumed as default base.

In the standard tunneling rates representation this reads

$$\langle I_\infty \rangle = \frac{4\Gamma_L \Gamma_R \mathcal{T_C}^2}{\Gamma_L \left(\Gamma_R{}^2 + 8\mathcal{T_C}^2 + 4\epsilon^2\right) + 4\Gamma_R \mathcal{T_C}^2}. \tag{5.135}$$

This current looks slightly different from the examples investigated before. A composition of two Single Quantum Dots with unidirectional tunneling would have a waiting time in the middle of

$$\tau_M = \tau_R \left(1 + \epsilon^2 \tau_T^2 + \left(\frac{\tau_T}{2\tau_R}\right)^2\right). \tag{5.136}$$

The Fano factor becomes

$$\langle F_\infty \rangle = \frac{16\tau_L^2 \tau_R^2 + 8\tau_R^2 \tau_T^2 \left(12\epsilon^2 \tau_R^2 - 1\right) + \tau_T^4 \left(4\epsilon^2 \tau_R^2 + 1\right)^2 + 64\tau_R^4}{\left(4\tau_R \left(\tau_L + \tau_R \left(\epsilon^2 \tau_T^2 + 2\right)\right) + \tau_T^2\right)^2} \tag{5.137}$$

or

$$= \frac{\Gamma_L{}^2 \left(\Gamma_R{}^4 - 8\Gamma_R{}^2 \left(\mathcal{T_C}^2 - \epsilon^2\right) + 16 \left(4\mathcal{T_C}^4 + 6\mathcal{T_C}^2\epsilon^2 + \epsilon^4\right)\right) + 16\Gamma_R{}^2\mathcal{T_C}^4}{\left(\Gamma_L \left(\Gamma_R{}^2 + 8\mathcal{T_C}^2 + 4\epsilon^2\right) + 4\Gamma_R\mathcal{T_C}^2\right)^2}$$
$$\tag{5.138}$$

with tunneling rates. The long-time limit for $\frac{c_3(t)}{c_1(t)}$ is a rather long expression. Therefore, nominator and denominator were written down apart from each other.

$$\lim_{t\to\infty} \frac{c_3(t)}{c_1(t)} Z^4 = \Gamma_L{}^4 \left(\Gamma_R{}^8 + 8\Gamma_R{}^6 \left(2\epsilon^2 - 5\mathcal{T_C}^2\right) + 96\Gamma_R{}^4 \left(8\mathcal{T_C}^4 - \mathcal{T_C}^2\epsilon^2 + \epsilon^4\right)\right)$$
$$- 128\Gamma_R{}^2\Gamma_L{}^4 \left(32\mathcal{T_C}^6 + 48\mathcal{T_C}^4\epsilon^2 - 9\mathcal{T_C}^2\epsilon^4 - 2\epsilon^6\right)$$
$$+ 256\Gamma_L{}^4 \left(16\mathcal{T_C}^8 + 32\mathcal{T_C}^6\epsilon^2 + 48\mathcal{T_C}^4\epsilon^4 + 14\mathcal{T_C}^2\epsilon^6 + \epsilon^8\right)$$
$$- 8\Gamma_L{}^3\Gamma_R\mathcal{T_C}^2 \left(\Gamma_R{}^6 + 12\Gamma_R{}^4 \left(\epsilon^2 - \mathcal{T_C}^2\right) + 48\Gamma_R{}^2 \left(2\mathcal{T_C}^2\epsilon^2 + \epsilon^4\right)\right.$$
$$\left. + 64 \left(8\mathcal{T_C}^6 + 24\mathcal{T_C}^4\epsilon^2 + 9\mathcal{T_C}^2\epsilon^4 + \epsilon^6\right)\right)$$
$$+ 96\Gamma_L{}^2\Gamma_R{}^2\mathcal{T_C}^4 \left(\Gamma_R{}^4 + 8\Gamma_R{}^2 \left(\epsilon^2 - \mathcal{T_C}^2\right) + 16 \left(4\mathcal{T_C}^4 + 6\mathcal{T_C}^2\epsilon^2 + \epsilon^4\right)\right)$$
$$- 128\Gamma_L\Gamma_R{}^3\mathcal{T_C}^6 \left(\Gamma_R{}^2 + 8\mathcal{T_C}^2 + 4\epsilon^2\right) + 256\Gamma_R{}^4\mathcal{T_C}^8 \tag{5.139}$$

with the denominator $Z = \Gamma_L \left(\Gamma_R{}^2 + 8\mathcal{T_C}^2 + 4\epsilon^2\right) + 4\Gamma_R\mathcal{T_C}^2$.

5.4.1 Moment Generating Function

Assuming that the system starts in an empty state, what means that $\rho_0 = |0\rangle\langle 0|$,[11]the **moment generating function** can be calculated as[12]

$$
\hat{M}(\mathrm{i}\chi) = \frac{-\left\langle \frac{\Gamma_L}{\Gamma_L+z} \right\rangle_{\Gamma_L} \left\langle \mathcal{T_C}^2 \left\langle \frac{\Gamma_R+2z}{(\Gamma_R+2z)^2(z(\Gamma_R+z)+4\mathcal{T_C}^2)+4z\epsilon^2(\Gamma_R+z)} \right\rangle_{\Gamma_R} \right\rangle_{\mathcal{T_C}}}{e^{\mathrm{i}\chi}\left\langle \frac{\Gamma_L}{\Gamma_L+z} \right\rangle_{\Gamma_L} \left\langle \mathcal{T_C}^2 \left\langle \frac{\Gamma_R(\Gamma_R+2z)}{(\Gamma_R+2z)^2(z(\Gamma_R+z)+4\mathcal{T_C}^2)+4z\epsilon^2(\Gamma_R+z)} \right\rangle_{\Gamma_R} \right\rangle_{\mathcal{T_C}} - \frac{1}{4}}
$$

$$
+ \frac{\left\langle \left\langle \frac{(\Gamma_R+2z)\left((\Gamma_R+z)(\Gamma_R+2z)+4\mathcal{T_C}^2\right)+4\epsilon^2(\Gamma_R+z)}{(\Gamma_R+2z)^2(z(\Gamma_R+z)+4\mathcal{T_C}^2)+4z\epsilon^2(\Gamma_R+z)} \right\rangle_{\Gamma_R} \right\rangle_{\mathcal{T_C}} - \frac{1}{4}\left\langle \frac{1}{\Gamma_L+z} \right\rangle_{\Gamma_L}}{e^{\mathrm{i}\chi}\left\langle \frac{\Gamma_L}{\Gamma_L+z} \right\rangle_{\Gamma_L} \left\langle \mathcal{T_C}^2 \left\langle \frac{\Gamma_R(\Gamma_R+2z)}{(\Gamma_R+2z)^2(z(\Gamma_R+z)+4\mathcal{T_C}^2)+4z\epsilon^2(\Gamma_R+z)} \right\rangle_{\Gamma_R} \right\rangle_{\mathcal{T_C}} - \frac{1}{4}} .
$$

$$(5.140)$$

The calculation is quite long. This is similar to the case of the Single Quantum Dot. Here, this calculation was done with the help of the Mathematica Program (cf. appendix (D.1), p.147). This lengthy expression can be represented in shorter form

$$
\hat{M}(\mathrm{i}\chi) = \frac{\langle A_{R,T}(z)\rangle - W_L(z)\langle B_{R,T}(z)\rangle - \frac{1}{4}P_L(z)}{e^{\mathrm{i}\chi}W_L(z)\langle \Gamma_R B_{R,T}(z)\rangle}
$$

$$(5.141)$$

by the use of

$$
A_{R,T}(z) \equiv \frac{(\Gamma_R+2z)\left((\Gamma_R+z)(\Gamma_R+2z)+4\mathcal{T_C}^2\right)+4\epsilon^2(\Gamma_R+z)}{(\Gamma_R+2z)^2\left(z(\Gamma_R+z)+4\mathcal{T_C}^2\right)+4z\epsilon^2(\Gamma_R+z)}
$$

$$(5.142)$$

$$
B_{R,T}(z) \equiv \mathcal{T_C}^2 \frac{\Gamma_R+2z}{(\Gamma_R+2z)^2\left(z(\Gamma_R+z)+4\mathcal{T_C}^2\right)+4z\epsilon^2(\Gamma_R+z)} .
$$

$$(5.143)$$

In contrast to the former examples, the Double Quantum Dot involves terms of the form $\langle f(\Gamma_R,\mathcal{T_C})\rangle_{\Gamma_R,\mathcal{T_C}}$. Consequently, the series expansion of the kernel becomes more complicated.

---

[11]This is a sensitive assumption, because the long-time values should not depend on the initial state. The Moment Generating Function was also calculated with an arability initial density operator. But this a very long equation, where the effort to print out the equation in LaTeX is much larger than the effort to calculate. However, if one is interested in the full form, one can use the Mathematica Package and enjoy it on the screen.

[12]Notation advice: $\langle y\rangle_x$ means exception value of expression y here with respect to random variable x.

5.4.2   Current

In section 5.4 the clean limit for the Double Quantum Dot was discussed. It was found out that the current in the long-time limit, which we call $I_{\infty,\text{cln}}$, is given by

$$I_{\infty,\text{cln}} \equiv \langle I_{\infty} \rangle (\tau_t^2, \tau_L, \tau_R) = \left(\tau_L + \tau_R \left(\epsilon^2 \tau_T^2 + 2 \right) + \frac{\tau_T^2}{4\tau_R} \right)^{-1}. \qquad (5.144)$$

We remind that this result can be obtained by taking (5.135) and replace $\Gamma_L \rightarrow \frac{1}{\tau_L}, \Gamma_R \rightarrow \frac{1}{\tau_R}, T_C \rightarrow \frac{1}{\tau_T}$. Now we expect the tunneling rates on the left side Γ_L and on the right side Γ_R, as well as the coupling in the middle T_C, to be random. Furthermore, it is assumed that the distribution of the waiting times is known. (The expectation values of the tunneling rates $\langle \Gamma_\alpha \rangle$ can be calculated via the relationship (4.8).) The random results include the clean limit, if a delta distribution is assumed as Probability Density Function (PDF). The calculation with random Γ_L, Γ_R and T_C leads to

$$\langle I_{\infty} \rangle \equiv \langle I_{\infty} \rangle (\langle \tau_T^2 \rangle, \langle \tau_L \rangle, \langle \tau_R \rangle, \langle \Gamma_R \rangle) = \left(\langle \tau_L \rangle + \langle \tau_R \rangle \left(\epsilon^2 \langle \tau_T^2 \rangle + 2 \right) + \tfrac{1}{4} \langle \Gamma_R \rangle \langle \tau_T^2 \rangle \right)^{-1}. \qquad (5.145)$$

One remarks that there is only one additional parameter ($\langle \Gamma_R \rangle$) in the random current. The concrete realization of the PDF for Γ_L and T_C do not affect the result. Only the expectation value of τ_L (namely $\langle \tau_L \rangle$) and the second moment of τ_T (namely $\langle \tau_T^2 \rangle$) influence the current. This is equivalent to the situation in the former sample setups. For τ_R the situation looks slightly different. In this context two properties of the distribution of τ_R affect the current ($\langle \tau_R \rangle, \langle \Gamma_R \rangle$). In the classical case the product of these values would be 1. For a general PDF this does not hold true. Therefore, we introduce a parameter α, which is defined via

$$\langle \tau_R \rangle \langle \Gamma_R \rangle = \langle \tau_R \rangle \left\langle \frac{1}{\tau_R} \right\rangle =: 1 + \alpha. \qquad (5.146)$$

Now it is possible to interpret (5.145) as function of α

$$\langle I_{\infty} \rangle (\langle \tau_T^2 \rangle, \langle \tau_L \rangle, \langle \tau_R \rangle, \alpha) := \langle I_{\infty} \rangle (\langle \tau_T^2 \rangle, \langle \tau_L \rangle, \langle \tau_R \rangle, \frac{1+\alpha}{\langle \tau_R \rangle}). \qquad (5.147)$$

According to that, the relationship between random and clean current can be written as

$$\boxed{\frac{I_{\infty,\text{cln}}}{\langle I_{\infty} \rangle} = 1 + \alpha \frac{\tau_T^2}{4\tau_R \left(\tau_L + \tau_R \left(\epsilon^2 \tau_T^2 + 2 \right) \right) + \tau_T^2} \geq 1.} \qquad (5.148)$$

That means that the current in the clean case cannot be boosted by a random distribution if the corresponding parameter are the same, i.e. ($\tau_L = \langle \tau_L \rangle, \tau_R = \langle \tau_R \rangle, \tau_T = \langle \tau_T^2 \rangle$). Regarding for example the Maxwell Distribution with the PDF $f(\sigma) = \frac{\sqrt{\frac{2}{\pi}} x^2 e^{-\frac{x^2}{2\sigma^2}}}{\sigma^3}$. It is connected with some mathematical effort to

calculate $\langle \tau_R \rangle = 2\sqrt{\frac{2}{\pi}}\sigma$ and $\langle \Gamma_R \rangle = \frac{\sqrt{\frac{2}{\pi}}}{\sigma}$. The use of Mathematica helps to save some time. With these quantities it is simple to derive

$$\langle \tau_R \rangle \langle \Gamma_R \rangle = \frac{4}{\pi} \quad \Rightarrow \alpha = \frac{4}{\pi} - 1. \tag{5.149}$$

Plotting that, leads to figure 5.11, where one can examine that the difference between clean and random current is especially relevant in the case for small ϵ. This is in accordance with (5.148).
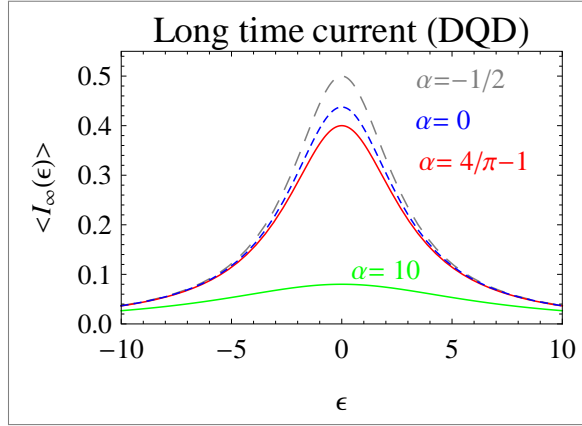
Figure 5.11: random (red) and clean current (blue) with $\langle \tau_L \rangle = 1, \langle \tau_T^2 \rangle = 1, \langle \tau_R \rangle = 1/4$ for the Maxwell Distribution and a pathologic, negative value for α. In the real world the current will always decay. The parameter $\alpha < 0$ (the gray line) does not occur in reality.

Further examples are discussed below in connection with the Fano factor.

5.4.3   Fano factor

Taking (5.137) and replacing $\Gamma_L \to \frac{1}{\tau_L}, \Gamma_R \to \frac{1}{\tau_R}, T_C \to \frac{1}{\tau_T}$ leads to

$$F_{\infty,\text{cln}} = \frac{16\tau_L^2\tau_R^2 + 8\tau_R^2\tau_T^2\left(12\epsilon^2\tau_R^2 - 1\right) + \tau_T^4\left(4\epsilon^2\tau_R^2 + 1\right)^2 + 64\tau_R^4}{\left(4\tau_R\left(\tau_L + \tau_R\left(\epsilon^2\tau_T^2 + 2\right)\right) + \tau_T^2\right)^2}, \tag{5.150}$$

which can be rewritten as

$$F_{\infty,\text{cln}} = \frac{16\tau_L^2 + 16\epsilon^4\tau_R^2\tau_T^4 + 96\epsilon^2\tau_R^2\tau_T^2 + \frac{\tau_T^4}{\tau_R^2} + 64\tau_R^2 + 8\epsilon^2\tau_T^4 - 8\tau_T^2}{\left(4\tau_L + 4\tau_R\left(\epsilon^2\tau_T^2 + 2\right) + \frac{\tau_T^2}{\tau_R}\right)^2}. \tag{5.151}$$

In the random case the Fano factor evaluates to

$$\begin{aligned}
\langle F_\infty \rangle / \langle I_\infty \rangle^2 &= 2\langle \tau_L^2 \rangle - \langle \tau_L \rangle^2 - \langle \tau_R \rangle^2\left(\epsilon^2\langle \tau_T^2 \rangle + 2\right)^2 \\
&\quad - \tfrac{1}{2}\langle \Gamma_R \rangle \langle \tau_R \rangle \langle \tau_T^2 \rangle\left(\epsilon^2\langle \tau_T^2 \rangle + 2\right) + 2\langle \tau_T^4 \rangle\left(\langle \Gamma_R^{-2} \rangle + 8\epsilon^2\right) \\
&\quad + 2\langle \tau_R^2 \rangle\left(\epsilon^4\langle \tau_T^4 \rangle + 5\epsilon^2\langle \tau_T^2 \rangle + 4\right) + \langle \tau_T^2 \rangle\left(8 - \langle \Gamma_R \rangle^2\langle \tau_T^2 \rangle\right). \tag{5.152}
\end{aligned}$$

This is a quiet long expression. The most interesting observations can be made in the right lead. Therefore, one takes the clean limit for the left rate $\langle \tau_L^2 \rangle = \tau_L$ and the coupling $\langle \tau_T^2 \rangle = T_C{}^{-1} \equiv \tau_T$. In addition to that, it is reasonable to make use of the parameters as already done in the former section.

Therefore, we introduce the parameters α, β, which are defined via

$$\langle \tau_R \rangle \langle \Gamma_R \rangle = \langle \tau_R \rangle \left\langle \frac{1}{\tau_R} \right\rangle =: +\alpha \tag{5.153}$$

$$\langle \tau_R^2 \rangle \langle \Gamma_R^{-2} \rangle = \langle \tau_R^2 \rangle \left\langle \frac{1}{\tau_R^2} \right\rangle =: \beta + (1+\alpha)^2. \tag{5.154}$$

The definition of β is a guess. The attempt to improve this parameters ended in negative success. Especially the attempt to get a short expression for the Fano factor, by choosing $\langle \tau_R^2 \rangle \langle \Gamma_R^{-2} \rangle =: (1 + \frac{1}{2}\beta + \alpha + \frac{1}{2}\alpha^2)$, does not produce physically reasonable independent parameter. In that case a negative Fano factor can be generated for a combination of non-negative parameters, which is not the desired behavior. A motivation for the guess (5.154) is that in the clean limit β should become 0 and that this expression is linked to the square of $(1+\alpha)$. However, it is difficult to show that this is a good parameter, as long as there is no formal criteria for evaluating a parameter. The positivity of β is proved in the appendix (A.1.1 p. 129).

The full Fano factor reads

$$\langle F_\infty \rangle = \frac{16\langle \tau_R \rangle^4 \left(\epsilon^4 \left(-\langle \tau_T^2 \rangle^2 \right) + 2\epsilon^4 \langle \tau_T^4 \rangle + 6\epsilon^2 \langle \tau_T^2 \rangle + 4 \right)}{\left(4\langle \tau_R \rangle \left(\langle \tau_L \rangle + \langle \tau_R \rangle \left(\epsilon^2 \langle \tau_T^2 \rangle + 2 \right) \right) + (\alpha+1)\langle \tau_T^2 \rangle \right)^2}$$
$$+ \frac{2(\alpha(\alpha+2) + \beta + 2)\langle \tau_T^4 \rangle - (\alpha+1)^2 \langle \tau_T^2 \rangle^2}{\left(4\langle \tau_R \rangle \left(\langle \tau_L \rangle + \langle \tau_R \rangle \left(\epsilon^2 \langle \tau_T^2 \rangle + 2 \right) \right) + (\alpha+1)\langle \tau_T^2 \rangle \right)^2} \tag{5.155}$$
$$- \frac{8\langle \tau_R \rangle^2 \left(2\langle \tau_L \rangle^2 - 4\langle \tau_T^2 \rangle + \langle \tau_T^2 \rangle \left((\alpha+1)\epsilon^2 \langle \tau_T^2 \rangle + 2\alpha - 20\nu\epsilon^2 + 1 \right) \right)}{\left(4\langle \tau_R \rangle \left(\langle \tau_L \rangle + \langle \tau_R \rangle \left(\epsilon^2 \langle \tau_T^2 \rangle + 2 \right) \right) + (\alpha+1), \langle \tau_T^2 \rangle \right)^2}$$
$$+ \frac{8\langle \tau_R \rangle^2 \left(2\epsilon^2 \left(2\nu\epsilon^2 + 1 \right) \langle \tau_T^4 \rangle + 16\nu \right)}{\left(4\langle \tau_R \rangle \left(\langle \tau_L \rangle + \langle \tau_R \rangle \left(\epsilon^2 \langle \tau_T^2 \rangle + 2 \right) \right) + (\alpha+1), \langle \tau_T^2 \rangle \right)^2}$$

which becomes in the half clean limit a function of $(\alpha, \beta, \nu, \tau_L, \tau_T^2, \langle \tau_R \rangle)$ which can be displayed simply by multiplying with the squared current.

$$\langle F_\infty \rangle \langle I_\infty \rangle^2 = \alpha \left(\frac{1}{8}\alpha\tau_T^2 \left(-8 + \left(-4\epsilon^2 + \frac{1}{\tau_R^2} \right) \tau_T^2 \right) + \alpha \frac{\tau_T^4}{16\tau_R^2} \right)$$
$$+ \beta \frac{\tau_T^4}{8\tau_R^2}$$
$$+ 2\nu \left(4 + 5\epsilon^2\tau_T^2 + \epsilon^4\tau_T^4 \right) \tag{5.156}$$
$$+ \tau_L^2 + \frac{3\tau_T^4}{16\tau_R^2} + \frac{1}{2}\tau_T^2 \left(-1 + \epsilon^2\tau_T^2 \right) + \tau_R^2 \left(4 + 6\epsilon^2\tau_T^2 + \epsilon^4\tau_T^4 \right)$$

The full form reads

$$
\langle F_\infty \rangle = \frac{-2\alpha\tau_T^2\left(\epsilon^2\tau_T^2+2\right)+\beta\frac{\tau_T^4}{\langle\tau_R\rangle^2}+8\nu\left(\epsilon^4\tau_T^4+5\epsilon^2\tau_T^2+4\right)}{\left(\tau_L+\tau_T^2\left(\frac{\alpha+1}{4\langle\tau_R\rangle}+\epsilon^2\langle\tau_R\rangle\right)+2\langle\tau_R\rangle\right)^2}
$$

$$
+\frac{4\tau_L^2+\frac{\tau_T^4\left(4\epsilon^2\langle\tau_R\rangle^2+1\right)^2}{4\langle\tau_R\rangle^2}+2\tau_T^2\left(12\epsilon^2\langle\tau_R\rangle^2-1\right)+16\langle\tau_R\rangle^2}{\left(\tau_L+\tau_T^2\left(\frac{\alpha+1}{4\langle\tau_R\rangle}+\epsilon^2\langle\tau_R\rangle\right)+2\langle\tau_R\rangle\right)^2}. \quad (5.157)
$$

The form above allows to describe the Fano factor with three additional parameters. Setting all that parameters to zero leads to the clean case. The restriction that α is always positive was already discussed before. Even though, the exact mathematical prove is an open point. There are strong arguments that almost every PDF leads to a positive value of alpha. From the physical point of view, negative alpha parameters do not make sense, as this would be in connection to a raise of the current. The parameter ν is the variance of the distribution. It is well known that the variance is always positive. The parameter β has never been discussed before. A prove of the positivity of beta can be imagined in the same style as the prove for the positivity of α. Due to the fact that even the exact prove for α is a mathematically project, no attempt of proving the positivity of β is done in this thesis. In the following it is simply assumed that all three parameters are positive. The sensitivity of that assumption is underlined by the fact that it holds true for all investigated PDFs.

5.4.4 Distributions

As a first step some combinations for the parameter α, β and ν are plotted to demonstrate possible situation. In a second step the situation is discussed for some sample distributions. In the following picture on can see how the parameters influence the Fano factor. The dashed blue line is the reference case for the clean limit. For that case the accordance to [Pöltl, 2008] was verified.

In figure 5.12 the α-dependence of Fano factor is visualized. It is to observe that the Fano factor decays if α raises. For a certain value of α the Fano factor at $\epsilon = 0$ gets minimal and the minima split of.

Afterwards, the minimal points for the Fano factor move away from $\epsilon = 0$. The zero of $\partial_\alpha \langle F_\infty \rangle (\epsilon = 0)$ is

$$
\alpha = \frac{8\tau_R^2\left(\tau_L^2+2\tau_L\tau_R+8\left(\nu+\tau_R^2\right)\right)-2\tau_R\left(\tau_L+2\tau_R\right)\tau_T^2+(1+\beta)\tau_T^4}{2\tau_R\left(\tau_L+4\tau_R\right)\tau_T^2}. \quad (5.158)
$$

For the parameter β the situation is different. As one can see in figure 5.14, the growth of parameter β is connected to a growth in the Fano factor.

The investigation of the parameter ν (see figure 5.15) does not lead to astonishing result. This is intuitive if one thinks about the current fluctuation that is
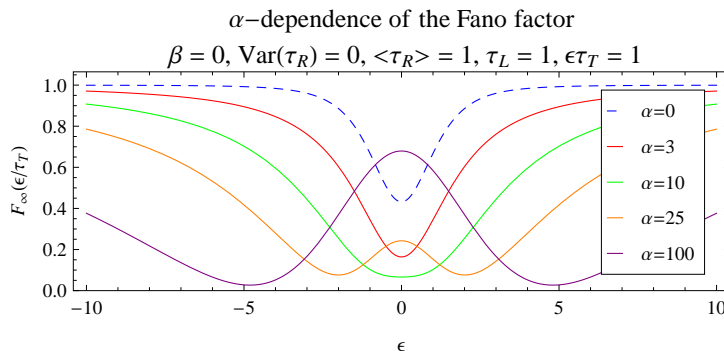
Figure 5.12: α-dependence of Fano factor for certain parameter
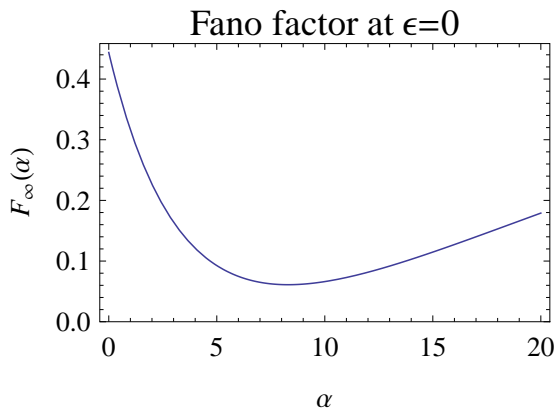
Figure 5.13: α-dependence of the Fano factor for $\epsilon = 0$ with parameters from figure 5.12

implied by the randomness of the rates. Combining this parameters in arbitrary way leads to the astonishing investigation that the Fano factor can decay (see e.g. figure 5.16). It is not to estimate that with the introduction of random tunneling rates the Fano factor can raise, except for the case that the current is suppressed. Therefore, both parameters, Fano factor and current, have to be investigated together.

On the following six pages three PDFs are investigated in detail. The results were obtained by the Mathematica Program in appendix E. Thus, this analysis can be done for all normed positive PDF, where the integrals for the first two negative moments and the variance can be defined. Interesting parameters can be found by an user interactive formula, where the parameters can be set with sliders. Unfortunately, this cannot be put in a portable document or a paper version up to now.

The random Fano factor had originally nine parameter ($\langle \tau_L \rangle$, $\langle \tau_L^2 \rangle$, $\langle \tau_T^2 \rangle$, $\langle \tau_T^4 \rangle$, $\langle \tau_R \rangle$, α, β, σ, ϵ). By regarding a given PDF the number of parameters reduces to
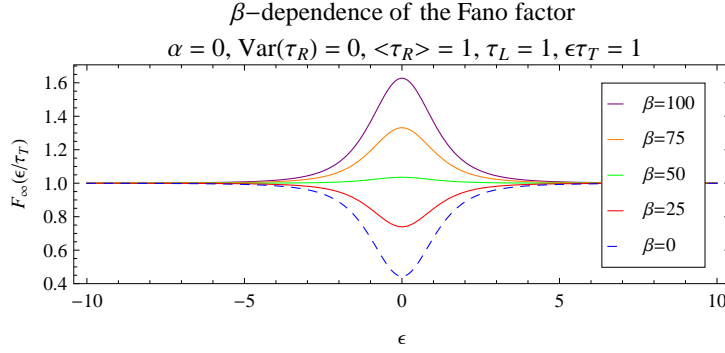
Figure 5.14: β-dependence of Fano factor
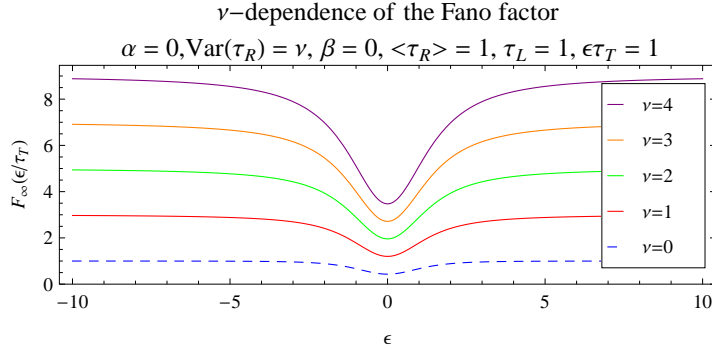
Figure 5.15: ν-dependence of Fano factor

two plus the number of parameters of the PDF $(p_1, p_s, \ldots p_M)$. Thus, there are three plus M parameters, namely $\langle \tau_L \rangle$, $\langle \tau_T \rangle$, ϵ, p_i in the investigated situations $M = 1$ for the Maxwell Distribution and $M = 2$ for the other distributions. Even four parameters are hard to handle. Similar to [Pöltl, 2008], we fix $\langle \tau_L \rangle = 1$ and regard the ratio T_C/Γ_L[13]. As the other distributions discussed here, have one more parameter, we have to eliminate a further parameter to display the information within the three dimensions of space. Therefore, we restrict the situation to two setups.

Situation a $\langle \tau_L \rangle = 1, \langle \tau_T \rangle = 1$

> In that situation the clean case long-time Fano factor is always smaller than one and decays in the region of $\epsilon = 0$ with a global minimum at $\epsilon = 0$. For large values $\lim_{|\epsilon| \to \infty} F_{\infty,\text{cln}} = 1$.

Situation b $\langle \tau_L \rangle = 1, \langle \tau_T \rangle = 5$

> In that situation the Fano factor has two additional maxima and is greater than one at the maxima and smaller than one for the minimum. For large

---

[13][Pöltl, 2008] used T_C/Γ_R. But by doing that interesting information about the current is lost. In our case, where the rate on the right lead is n-dependent, this might be of interest. (For comparison with the same was also calculated with T_C/Γ_R for the clean case. The comparison was successful.)
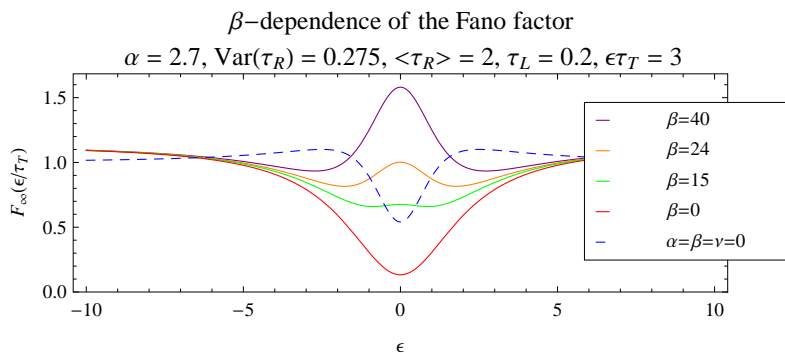
Figure 5.16: β-dependence of Fano factor for some other values of $\alpha, \mathrm{Var}\tau_R = \nu$

values of ϵ the Fano factor converges to $\{1|\}$[14]. A detailed discussion is to find in [Gurvitz and Prager, 1996].

Maxwell Distribution

As an example for a distribution with only one parameter, we take the Maxwell Distributions. As the treatment of many degrees of freedom is not always simple, this is a comfortable starting point.

As a first step we modify the normal Maxwell Distribution, which is given by $\tilde{f}(\sigma) = \frac{\sqrt{\frac{2}{\pi}}x^2 e^{-\frac{x^2}{2\sigma^2}}}{\sigma^3}$ and change the parameter σ by a multiplication with a constant value. In that way this parameter takes the value of the average waiting time and the modified PDF reads

$$f(\sigma) = \frac{32x^2 e^{-\frac{4x^2}{\pi\sigma^2}}}{\pi^2\sigma^3}. \tag{5.159}$$

With the Mathematica Program we obtain the values of interest:

$$\langle\tau_R\rangle \equiv \sigma, \qquad\qquad \langle\tau_R^2\rangle = \frac{3\pi\sigma^2}{8} \tag{5.160}$$

$$\langle\Gamma_R\rangle = \frac{4}{\pi\sigma}, \qquad\qquad \langle\Gamma_R{}^2\rangle = \frac{8}{\pi\sigma^2} \tag{5.161}$$

$$\alpha = \frac{4}{\pi} - 1, \qquad\qquad \beta = 3 - \frac{16}{\pi^2}, \qquad \nu = \frac{1}{8}(3\pi - 8)\sigma^2 \tag{5.162}$$

Thereby, no further limitation to the waiting times was made. The only restriction is, that the waiting times cannot be ≤ 0. Due to the physical interpretation, this is fulfilled automatically.

An interesting observation is that α, β are constant in that case. This is visualized in figure 5.17. Only the variance is dependent of the parameter $\sigma = \langle\tau_R\rangle$.

---

[14]A gentle tool are surreal numbers [Knuth, 1974]. e.g. $\{|1\} < 1 < \{1|\}$
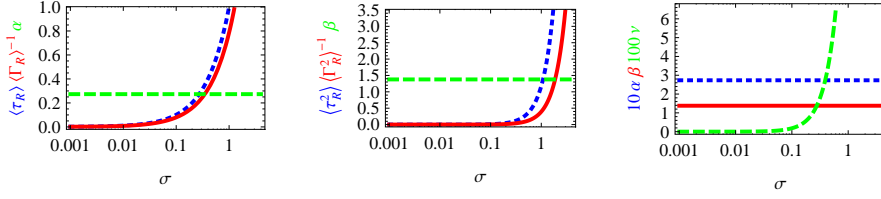
Figure 5.17: left: α-parameter green dashed, $\langle \tau_R \rangle$ blue dotted and solid red line $\frac{1}{\langle \Gamma_R \rangle}$.
center: β-parameter green dashed, $\langle \tau_R^2 \rangle$ blue dotted, solid red line $\frac{1}{\langle \Gamma_R^2 \rangle}$.
right:α blue dotted line, β red line, variance (ν) green dashed line

In that case current and Fano factor read

$$\left\langle I_\infty^{\mathrm{MW}} \right\rangle (\epsilon, \sigma, \tau_T, \tau_L) = \frac{\pi \sigma \tau_L}{\pi \sigma \left(\tau_L + \sigma \left(\epsilon^2 + 2 \right) \right) + \tau_T^2} \tag{5.163}$$

$$\left\langle F_\infty^{\mathrm{MW}} \right\rangle (\epsilon, \sigma, \tau_T, \tau_L) = \frac{\pi^2 \left(\tau_L^2 \left(4\sigma^2 + 30\pi\sigma^4\epsilon^2 \right) + \tau_L^4 \left(6\pi\sigma^4\epsilon^4 + 8\sigma^2\epsilon^2 + 3 \right) + 24\pi\sigma^4 \right)}{8 \left(\tau_L^2 \left(\pi\sigma^2\epsilon^2 + 1 \right) + \pi\sigma \left(2\sigma + \tau_T \right) \right)^2}$$

$$+ 1 - \frac{2 \left(\tau_L^2 \left(\pi\sigma^2\epsilon^2 + 1 \right) + 2\pi\sigma^2 \right)}{\tau_L^2 \left(\pi\sigma^2\epsilon^2 + 1 \right) + \pi\sigma \left(2\sigma + \tau_T \right)}. \tag{5.164}$$

A formal analysis of this expression leads to the following observations. The boundary values evaluate to

$$\lim_{\sigma \to 0} \left\langle I_\infty^{\mathrm{MW}} \right\rangle (\epsilon, \sigma, \tau_t, \tau_L) = \lim_{\sigma \to \infty} \left\langle I_\infty^{\mathrm{MW}} \right\rangle (\epsilon, \sigma, \tau_t, \tau_L) = 0 \tag{5.165}$$

$$\lim_{\sigma \to 0} \left\langle F_\infty^{\mathrm{MW}} \right\rangle (\epsilon, \sigma, \tau_t, \tau_L) = \frac{3\pi^2}{8} - 1 \tag{5.166}$$

$$\lim_{\sigma \to \infty} \left\langle F_\infty^{\mathrm{MW}} \right\rangle (\epsilon, \sigma, \tau_t, \tau_L) = \frac{3\pi \left(\tau_L{}^4\epsilon^4 + 5\tau_L{}^2\epsilon^2 + 4 \right)}{4 \left(\tau_L{}^2\epsilon^2 + 2 \right)^2} - 1. \tag{5.167}$$

Physically spoken that mean that very small waiting times, which corresponds to infinite rates, leads to a fixed Fano factor. However, at this point the current is zero. Therefore, the relevance of that information is little. In addition to that the Fano factor has three zeros. The interesting zero is at $\sigma = 0$. The other two zeros appear if the Fano factor has an local maximum at $\sigma = 0$.

As no interesting results are expected, the exact behavior of this extrema is not treated in detail. For larger values the position of these extreme values is far away from $\epsilon = 0$, so that the current at that place is very little. A brief discussion is to find in the Mathematica Notebook NB:autoMW.

The major interest is in the extreme point at $\sigma = 0$. In figure 5.18 the current and Fano factor are plotted for $\epsilon = 0$. For the two situations a,b we investigate this in detail.

Plotting the Fano factor in a normal (non logarithmic) scale leads to 5.19. In that picture some points are exemplary chosen and then plotted for a range from $-10 \ldots 10$.
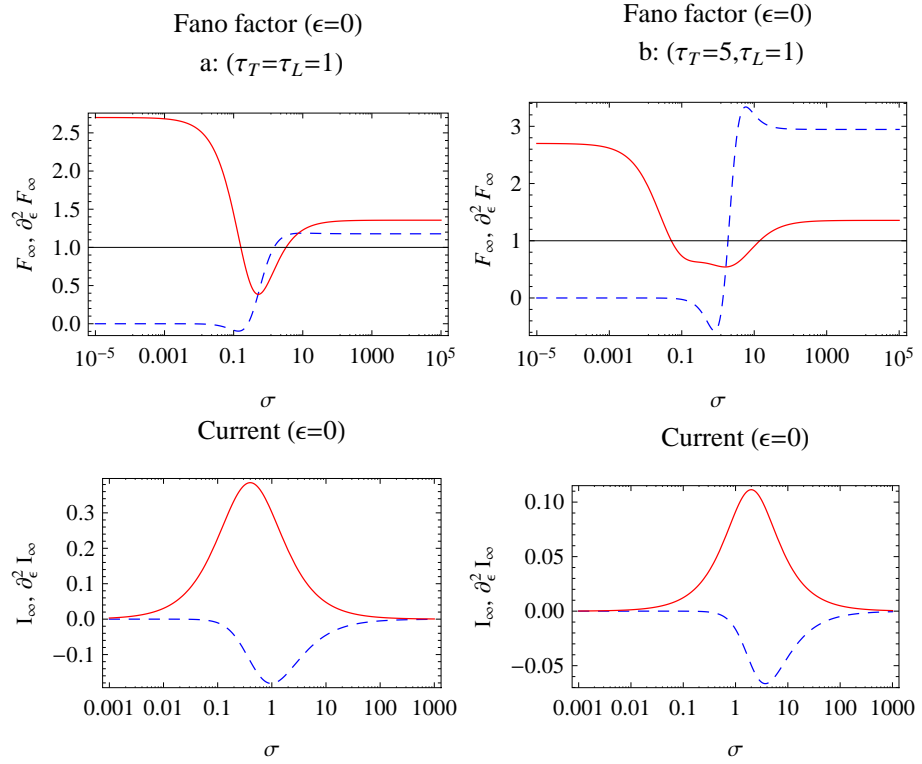
Figure 5.18: Whole range of the Fano factor and Current in logarithmic scale. The Fano factor for a large waiting time or tunneling rate on the right lead $\langle \tau_R \rangle = \sigma \to 0 : \langle F_\infty \rangle = \frac{3\pi^2}{8} - 1$ and respectively $\sigma \to \infty : \langle F_\infty \rangle = \frac{3\pi}{4} - 1$. The current gets 0 as well. The red line is Fano factor or current and the dotted blue line is its second derivative. In the upper right picture the second derivative has been scaled at factor 10.
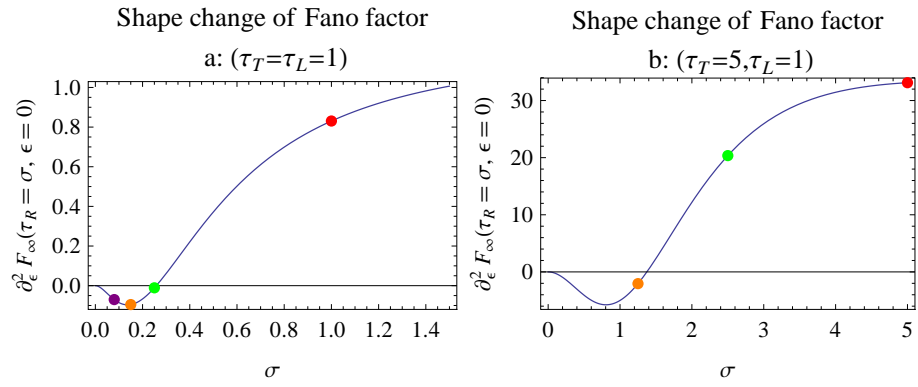
Figure 5.19: The shape of the Fano factor changes at the point $\sigma = \left\langle \tau_R^2 \right\rangle = .26$ for Situation one and at $\sigma = 1.37$
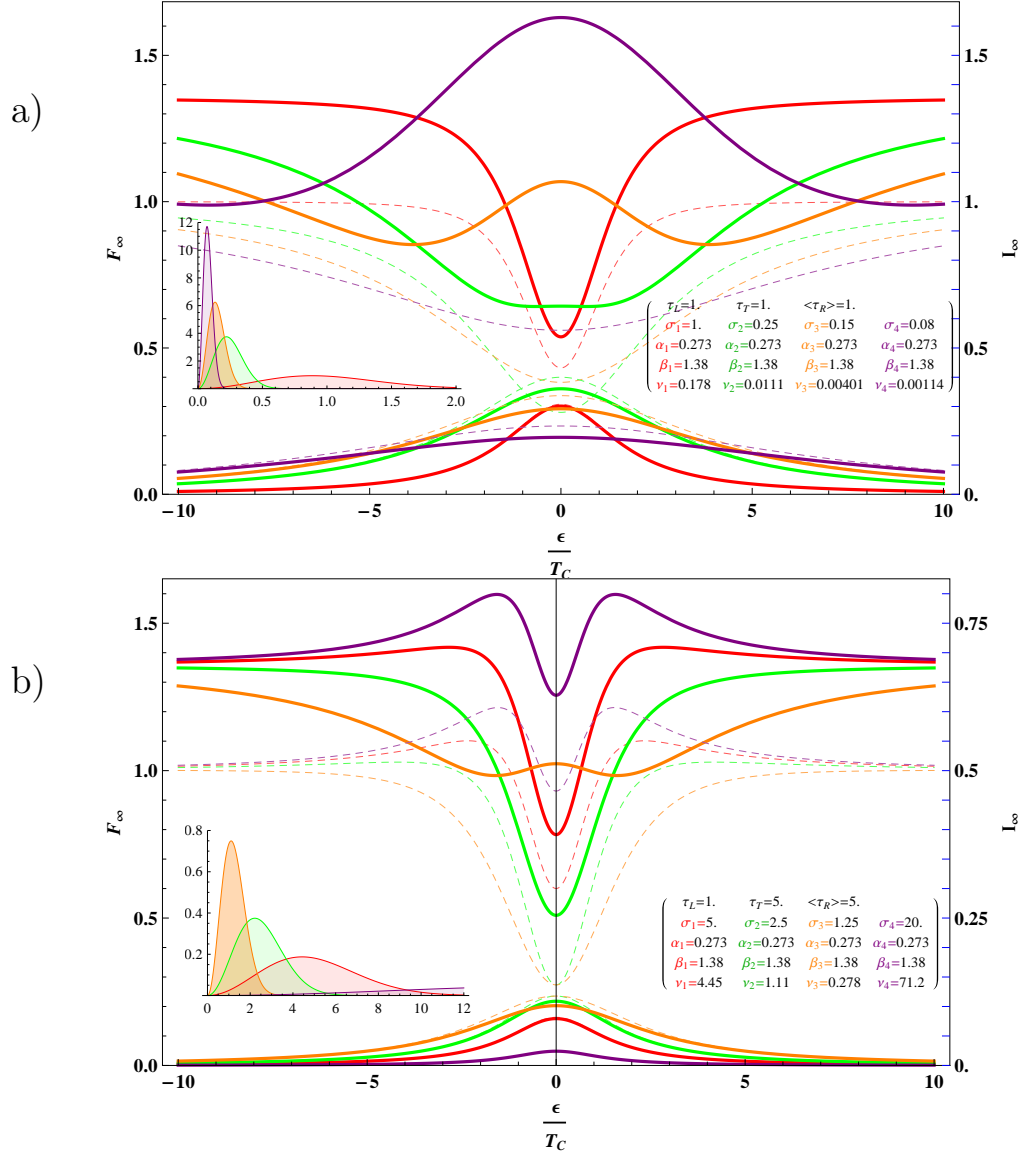
Figure 5.20: Fano factor for case a and b for some exemplary values compare to 5.19
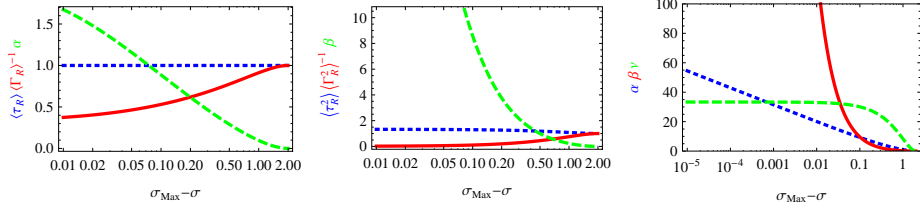
Figure 5.21: **Uniform Distribution**
left: α-parameter green dashed, $\langle \tau_R \rangle$ blue dotted, solid red line $\frac{1}{\langle \Gamma_R \rangle}$.

center: β-parameter green dashed, $\langle \tau_R^2 \rangle$ blue dotted, solid red line $\frac{1}{\langle \Gamma_R^2 \rangle}$.

right: α blue dotted line, β red line, variance (ν) green dashed line
For a Uniform Distribution with mean at 1 and width σ. The maximum width is $\sigma_{Max} < 2$ ($\sigma_{Max} - \sigma = 2$ means sharp delta distribution at $\tau_R = 1$).
α becomes (linear) infinite, β gets (exponential) infinite and ν gets the constant value $\frac{1}{3}$ for $\sigma_{Max} - \sigma \to 0$.

Uniform Distribution

The easiest PDF with two parameters is the Uniform Distribution. After having made experience with the Maxwell distribution, the Uniform Distribution is the point of interest. The Probability Density Function of the Uniform Distribution reads

$$f(x) = \begin{cases} \frac{1}{\sigma} & -\frac{\sigma}{2} + \tau_R \leq x \leq \frac{\sigma}{2} + \tau_R \\ 0 & \text{else} \end{cases}. \tag{5.168}$$

Here, τ_R is the mean of the PDF and σ is the width. This is in contrast to the former example, where only one parameter existed. The parameter of the Maxwell distribution could be chosen freely. In this case, there are some restrictions for the parameter. The minimum for parameter $\sigma = 2$. Otherwise, the integral for the calculation of the negative moments, does not converge. One can see that the expectation value for the waiting time becomes infinity for $\sigma \to 2$. The parameter α and β do not depend on σ, which is an indicator that the choice of the parameter was well.

By integration over that range one obtains (with Mathematica)

$$\langle \tau_R \rangle \equiv \tau_R, \quad \langle \tau_R^2 \rangle = \frac{1}{12} \left(12 \tau_R^2 + \sigma^2 \right) \tag{5.169}$$

$$\langle \Gamma_R \rangle = \frac{\log \left(-\frac{4\tau_R}{\sigma - 2\tau_R} - 1 \right)}{\sigma}, \quad \langle \Gamma_R^2 \rangle = \frac{4}{4\tau_R^2 - \sigma^2} \tag{5.170}$$

$$\alpha = \frac{\tau_R \log \left(-\frac{4\tau_R}{\sigma - 2\tau_R} - 1 \right)}{\sigma} - 1 \tag{5.171}$$

$$\beta = \frac{12\tau_R^2 + \sigma^2}{12\tau_R^2 - 3\sigma^2} - \frac{\tau_R^2 \log^2 \left(-\frac{4\tau_R}{\sigma - 2\tau_R} - 1 \right)}{\sigma^2} \quad \nu = \frac{\sigma^2}{12}. \tag{5.172}$$
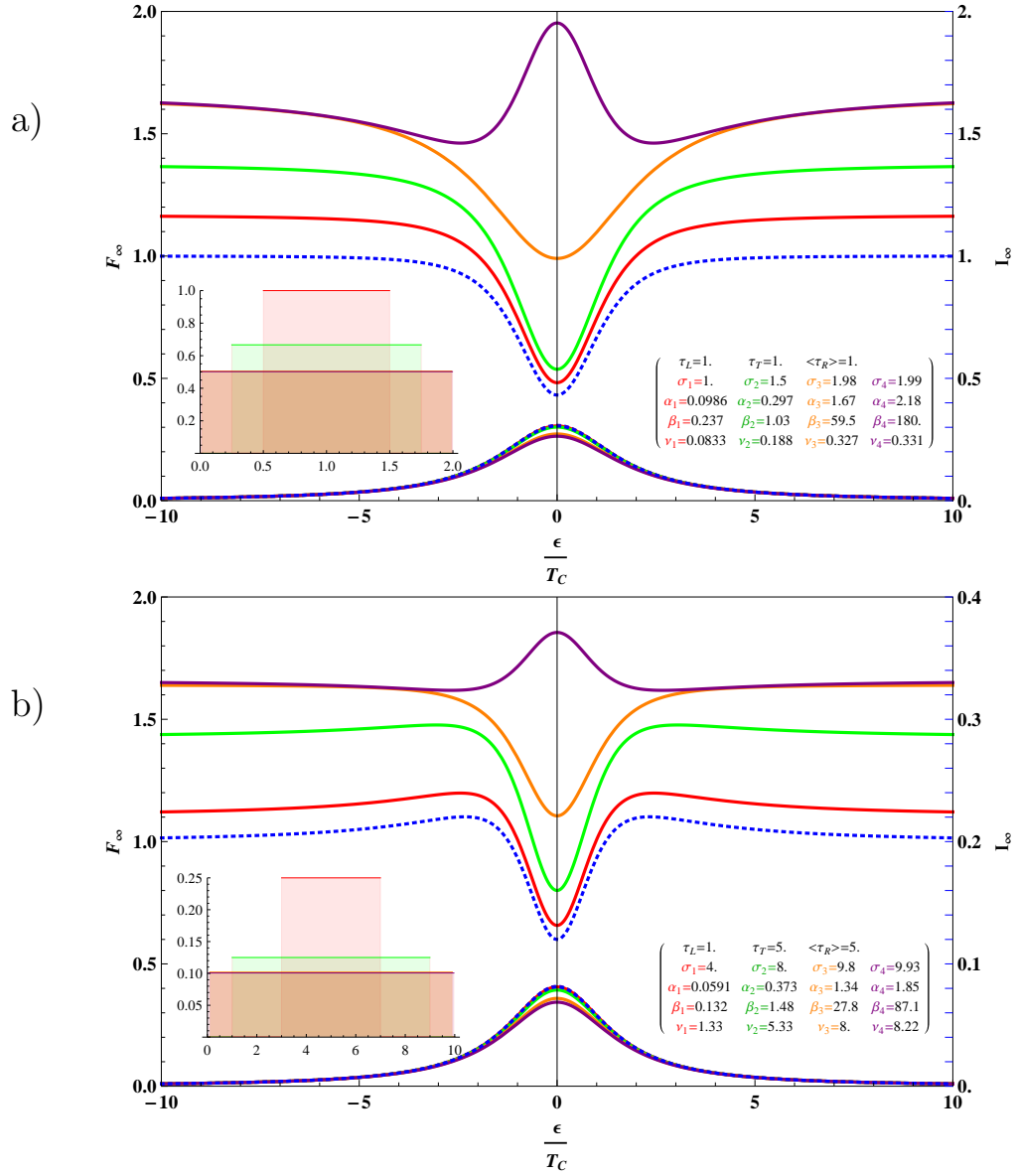
Figure 5.22: Current and Fano factor for a Uniform Distribution as function of energy gap ϵ

Weibull Distribution
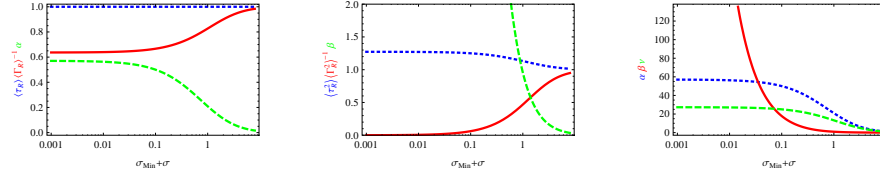
Figure 5.23: *Weibull Distribution*

left: α-parameter green dashed, $\langle \tau_R \rangle$ blue dotted, solid red line $\frac{1}{\langle \Gamma_R \rangle}$.

center: β-parameter green dashed, $\langle \tau_R^2 \rangle$ blue dotted, solid red line $\frac{1}{\langle \Gamma_R{}^2 \rangle}$.

right:α blue dotted line, β red line, variance (ν) green dashed line

For a Weibull Distribution the absolute minimum for parameter $\sigma = 2$. Otherwise, the integral for the calculation of the negative moments does not converge. For $\sigma \to \sigma_{\mathrm{Min}} = 2$, $\langle \Gamma_R^2 \rangle$ becomes infinite, which leads to an infinite β-parameter as well. In the right graph one can see that α, ν become sable for $\sigma \to 2$.

Another example is the Weibull Distribution. As simplification, the default parameter were changed, so that one parameter is the mean of the distribution. This was done with regard to the clean case. In the clean case the mean becomes the waiting time for the right side

$$f(\sigma, \tau_R) = \frac{\sigma e^{-\left(\frac{x \Gamma\left(1 + \frac{1}{\sigma}\right)}{\tau_R} \right)^{\sigma}} \left(\frac{x \Gamma\left(1 + \frac{1}{\sigma}\right)}{\tau_R} \right)^{\sigma}}{x}, \tag{5.173}$$

where Γ is no rate rather than the mathematical gamma function.

The output of Mathematica can be seen in the following equation:

$$\langle \tau_R \rangle = \tau_R, \qquad\qquad \langle \tau_R^2 \rangle = \frac{\tau_R^2 \Gamma\left(\frac{\sigma+2}{\sigma}\right)}{\Gamma\left(1 + \frac{1}{\sigma}\right)^2} \tag{5.174}$$

$$\langle \Gamma_R \rangle = \frac{\pi \csc\left(\frac{\pi}{\sigma}\right)}{\sigma \tau_R}, \qquad\qquad \langle \Gamma_R{}^2 \rangle = \frac{\Gamma\left(1 + \frac{1}{\sigma}\right)^2 \Gamma\left(\frac{\sigma-2}{\sigma}\right)}{\tau_R^2} \tag{5.175}$$

$$\alpha = \frac{\pi \csc\left(\frac{\pi}{\sigma}\right)}{\sigma} - 1, \qquad\qquad \beta = \frac{\pi \left(2\sigma \csc\left(\frac{2\pi}{\sigma}\right) - \pi \csc^2\left(\frac{\pi}{\sigma}\right)\right)}{\sigma^2} \tag{5.176}$$

$$\nu = \frac{\tau_R^2 \left(\Gamma\left(1 + \frac{2}{\sigma}\right) - \Gamma\left(1 + \frac{1}{\sigma}\right)^2 \right)}{\Gamma\left(1 + \frac{1}{\sigma}\right)^2} \tag{5.177}$$

b)
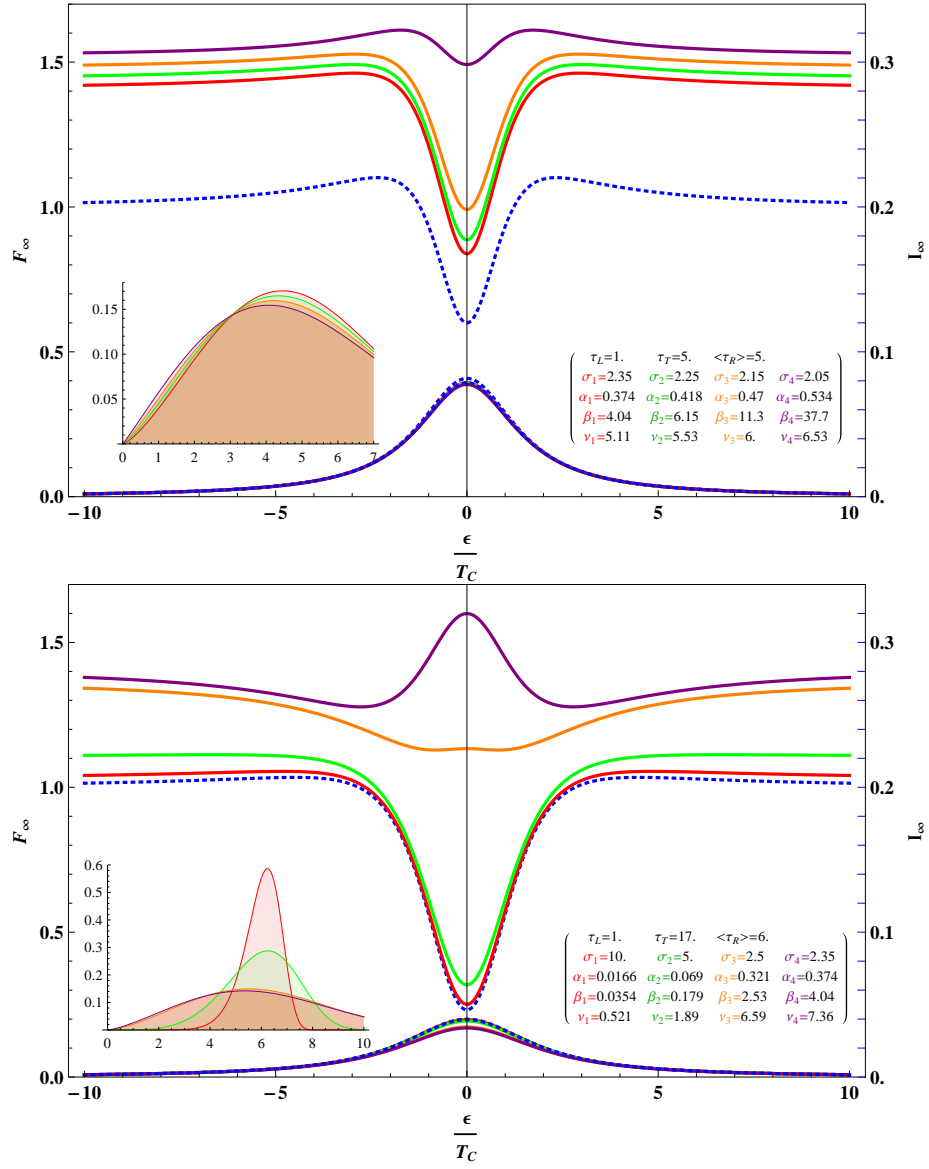
Figure 5.24: Fano factor for some values for the Weibull Distribution

5.4.5   Visual current calculation*

An attempt to guess the current directly from the Hamiltonian in analogy to
the transitions in a ring, was misleading. With regard to the scheme of DQD
in figure 5.10 it was assumed that it is possible that the current for the DQD
could be retrieved directly from the diagram. Some calculations on that are to
find in the mathematic notebook NB:QuasiClassical.

$$\langle I_\infty \rangle = \frac{\pm 4 \langle \tau_R \rangle}{(\langle \tau_\epsilon \rangle + 2 \langle \tau_R \rangle)^2} = \frac{4\epsilon^2 \Gamma_R}{(\Gamma_R + 2\epsilon)^2}.$$

Chapter 6

Summary [1]

6.1 Model and derivation of Quantum Master Equation

Considering the situation, where electrons are transported from a source reservoir on the left side (formally a N_L-fermion Hilbert Space $\mathcal{H}^{\otimes N_L}$), through a system, to a target reservoir on the right side. Without external particle exchange, the number of transported particles n defines a fixed relation for the particle numbers on the left side $N_L(n)$ and the right side $N_R(n)$. The complete system dynamics is described by the Liouville-von Neumann Equation $\partial_t \varrho = \mathcal{L}\varrho$.

ϱ is the complete density operator and $\mathcal{L}$ the superoperator acting on

$$\mathcal{H} = \mathcal{H}_S \otimes \left(\bigoplus_{N_L} \mathcal{H}^{\otimes N_L} \oplus \bigoplus_{N_R} \mathcal{H}^{\otimes N_R} \right) \equiv \mathcal{H}_S \otimes \bigoplus_n \mathcal{H}_B^{(n)}. \qquad (6.1)$$

This Hilbert Space is very large for mesoscopic systems. The majority of this Hilbert Space describes the dynamics of the bath. As only the system part and the number of particles are taken into account in this article, this bath reservoir is not relevant. Therefore, we apply the method of Nakajima and Zwanzig [Kühne and Reineker, 1978, Zwanzig, 1960, Nakajima, 1958] and define a projector $\mathsf{P}\varrho = \bigoplus_n \mathrm{Tr}_\mathrm{B}^{(n)}(\varrho) \otimes \varrho_{B,0}^{(n)}$, which projects on the subspace of relevant information. $\mathrm{Tr}_\mathrm{B}^{(n)}(\varrho)$ is the trace over the bath with a fixed number of particles $N_L(n), N_R(n)$. In the standard approach [Lambert, 2005], one traces out the n-information and reconstructs them later. In contrast to that the n-resolved Quantum Master Equation can be directly obtained with the approach presented in this article. With the short hand notation $\mathsf{Q} = 1 - \mathsf{P}$, the Liouville-von Neumann Equation reads

$$\frac{d}{dt} \begin{pmatrix} \mathsf{P} \\ \mathsf{Q} \end{pmatrix} \varrho = \begin{pmatrix} \mathsf{P} \\ \mathsf{Q} \end{pmatrix} \mathcal{L} \begin{pmatrix} \mathsf{P} \\ \mathsf{Q} \end{pmatrix} \varrho + \begin{pmatrix} \mathsf{P} \\ \mathsf{Q} \end{pmatrix} \mathcal{L} \begin{pmatrix} \mathsf{Q} \\ \mathsf{P} \end{pmatrix} \varrho. \qquad (6.2)$$

---

[1]This chapter is a summary of the former chapter 2-5. This summary is planned to be published in a paper and addresses the advanced reader.

Thereby, the Liouvillan was split with respect to the projection

$$\mathcal{L} = (\mathsf{P}+\mathsf{Q})\mathcal{L}(\mathsf{P}+\mathsf{Q}) = \underbrace{\underbrace{\mathsf{P}\mathcal{L}\mathsf{P}}_{\mathcal{L}_S} + \underbrace{\mathsf{Q}\mathcal{L}\mathsf{Q}}_{\mathcal{L}_B}}_{\mathcal{L}_0} + \underbrace{\mathsf{P}\mathcal{L}\mathsf{Q} + \mathsf{Q}\mathcal{L}\mathsf{P}}_{\mathcal{L}_I}. \tag{6.3}$$

The solution of equation (6.2) is discussed in [Breuer and Petruccione, 2002]. Using a factorizing initial condition and the Born-Markov Approximation, leads to a first order differential equation for $\partial_t \mathsf{P}\varrho$. That differential equation is transformed to the interaction picture with regard to $\mathcal{L}_I$. Furthermore, a perturbative expansion up to the second order is performed. After the back transformation to the Schrödinger Picture it reads

$$\partial_t \mathsf{P}\varrho = \left(\mathsf{P}\mathcal{L} + \int_{t_0}^{t} \mathsf{P}\tilde{\mathcal{L}}_I(t-t')\mathcal{L}_I \right) \mathsf{P}\varrho. \tag{6.4}$$

The Interaction Liouvillian can be split up to a sum of tensor products of a bath and a system part.

$$\mathcal{L}_I \varrho = i \left[\varrho, \sum_{k,n'} S_k \otimes B_k^{(n')} \right] \tag{6.5}$$

Inserting this split Interaction Liouvillian to (6.4) leads to an integral kernel, which consists of a tensor product of system and bath operators. The next step is to apply the projector. For the bath part one can make use of the bath correlation functions. Thereby, one has to take into account that the bath operators of the Interaction Liouvillian might change the number of particles in the bath reservoir, and thereby n. For example

$$\mathrm{Tr}_{\mathrm{B}}^{(\mathrm{n})} \left(\mathrm{b}_k \varrho_{B,0}^{(n')} \mathrm{b}_{\bar{k}}^\dagger \right) = \delta_{k,\bar{k}} \delta_{n',n-1} f(\epsilon_k) \tag{6.6}$$

reduces the number of particles in the left reservoir and increases the number of particles in the right reservoir. Thus, it was assumed that one has a fermionic bath and $f(\epsilon_k)$ is the Fermi Function.

Finally, equation (6.4) can be simplified to

$$\partial_t \rho^{(n)}(t) = \mathcal{L}_S \rho^{(n)}(t) - \sum_{n',l',l} \underline{\Gamma}(n',l',l) \cdot \left[\left[\rho^{(n')}(t), S_{l'} \right], S_l \right]. \tag{6.7}$$

In this notation $\rho^{(n)}(t)$ stands for $\mathrm{Tr}_{\mathrm{B}}^{(\mathrm{n})}(\varrho)$ and $\underline{\Gamma}(n',l',l)$ is a four component vector, which is multiplied with the components of the double commutator.

Explicit Interaction Hamiltonian

The next topic is the investigation of an explicit given Interaction Hamiltonian of the form

$$V = \mathrm{H}_{S,B} = \sum_{k,n} \left(T_{k,n} \mathrm{b}^\dagger{}_k \mathrm{s} + T_{k,n}^* \mathrm{s}^\dagger \mathrm{b}_k \right). \tag{6.8}$$

After the application of the proceedings described above, one obtains our Master Equation

$$
\begin{aligned}
\partial_t \rho^{(n)}(t) \quad &= \mathcal{L}_S \rho^{(n)}(t) \\
&+ \frac{\Gamma_L^{(n)}}{2}\{\rho^{(n)}(t), \mathrm{ss}^\dagger\} - \Gamma_L^{(n)} \mathrm{s}^\dagger \rho^{(n)}(t)\mathrm{s} \\
&+ \frac{\Gamma_R^{(n)}}{2}\{\rho^{(n)}(t), \mathrm{s}^\dagger\mathrm{s}\} - \Gamma_R^{(n-1)} \mathrm{s}\rho^{(n-1)}(t)\mathrm{s}^\dagger \\
&\equiv \mathcal{L}_0^{(n)} \rho^{(n)}(t) + \mathcal{J}^{(n-1)} \rho^{(n-1)}(t)
\end{aligned}
\tag{6.9}
$$

in the infinite bias limit with constant tunneling densities for each n in the Markovian Limit.

6.2 Disorder average

As a first approach, it is physically reasonable that the tunneling rates are independent, statistical distributed and uncorrelated to each other. In the following the mean value of the conditioned density matrix $\langle \rho^{(n)}(t) \rangle$ is in focus of interest. Thereby, $\langle \ldots \rangle$ denotes the disorder average over the random tunneling rates.

As $\langle \partial_t \rho^{(n)}(t) \rangle = \left\langle \mathcal{L}_0^{(n)} \rho^{(n)}(t) + \mathcal{J}^{(n-1)} \rho^{(n-1)}(t) \right\rangle$ involves two different tunneling rates (namely rates depending on n and $n-1$), the Fourier and Laplace transformed form of this equation $\hat{\rho}_\chi(z) = \int_0^\infty \mathrm{d}t e^{-zt}\left(\sum_{n=0}^\infty e^{\mathrm{i}n\chi}\rho^{(n)}(t)\right)$ is preferred. With the short hand notation for the propagator $\hat{\mathcal{P}}_n(z) := \left[z - \mathcal{L}_0^{(n)}\right]^{-1}$ the n-dependent density operator in Laplace Space reads

$$
\hat{\rho}_n(z) = \hat{\mathcal{P}}_n(z)\mathcal{J}^{(n-1)}\ldots\mathcal{J}^{(1)}\hat{\mathcal{P}}_1(z)\mathcal{J}^{(0)}\hat{\mathcal{P}}_0(z)\rho_0.
\tag{6.10}
$$

From now on, $[\ldots]^{-1}$ stands for the inverted operator. In addition to that, scalar factors, (e.g. z), have to be multiplied by the identity-operator. It is being assumed that the rates factorize. Therefore, it is sensible to collect terms with the same n. Thus, all these terms have the same expectation value. This aspect leads to the definition $\hat{\mathcal{W}}(z) = \left\langle \hat{\mathcal{W}}_n(z) \right\rangle, \hat{\mathcal{P}}(z) = \left\langle \hat{\mathcal{P}}_n(z) \right\rangle$. Accordingly, the expectation value for the system density matrix in Laplace Space reads $\langle \hat{\rho}_n(z) \rangle = \hat{\mathcal{W}}(z)^n \hat{\mathcal{P}}(z)\rho_0$. This equation is formally equivalent to the constant rate equation. Thus, it is intuitive to introduce the counting field by a Fourier Sequence Transformation $(\rho_\chi(t) = \sum_n \rho^{(n)}(t)e^{\mathrm{i}n\chi})$ and obtain the expectation value of $\hat{\rho}_\chi(z)$:

$$
\langle \hat{\rho}_\chi(z) \rangle = \left[1 - e^{\mathrm{i}\chi}\hat{\mathcal{W}}(z)\right]^{-1} \hat{\mathcal{P}}(z)\rho_0.
\tag{6.11}
$$

From this representation one can directly obtain the moments in Laplace Space, defined as $\langle \hat{m}_k(z) \rangle \equiv \mathrm{i}^{-k}\mathrm{Tr}\partial_\chi^k \langle \hat{\rho}_\chi(z) \rangle \big|_{\chi \to 0}$. The long-time limit for the current in disorder average is defined as $\langle I_\infty \rangle \equiv \langle \lim_{t\to\infty} \partial_t m_1(t) \rangle$. As well as the moments the current can be obtained directly in Laplace Space via

$$
\langle I_\infty \rangle = \lim_{z\to 0} z^2 \hat{m}_1(z).
\tag{6.12}
$$

Therefore, the property that the limit $\lim_{t \to \infty} f(t)$ in time domain corresponds to $\lim_{z \to 0} z\hat{f}(z)$ in Laplace Space, is used. Thereby, the hat on the letter denotes that the quantity was Laplace transformed, i.e. $\hat{f}(z) = \int_0^\infty dt e^{-zt} f(t)$.

More effort is needed to obtain the long-time value of the Fano factor, whereas the calculation in the Laplace Space can not be efficiently executed. Thus, the approach is to transform the shares of the moments, which become relevant in the long-time limit, back to the time domain and calculate the Fano factor via

$$\langle F_\infty \rangle \equiv \frac{m_2(t) - m_1(t)^2}{m_1(t)}. \tag{6.13}$$

Fortunately, the Laplace Transformation has the convenient property that terms of the order z^{-k} in Laplace Space correspond to terms $\frac{t^{n-1}}{n!}$ in time space. Thus, it is intuitive to derive the Fano factor in the following order. At first, one performs a Taylor Series Approximation of the moments in Laplace Space up to the z^0 order. After that the Inverse Laplace Transformation is applied. Finally, the long-time limit is executed. This proceeding can also be applied to higher cumulants. An efficient way of computing that is presented in the appendix. In the following this method is being applied to simple quantum systems.

6.2.1 Tunneling contact

The simplest imaginable system is a tunneling contact. The first measurements on that setup have been made by [Levitov et al., 1996]. In that case the left, source, reservoir is connected to the right, target reservoir, but there is no system in between. With the discussed assumptions our Quantum Master Equation reads ($\mathcal{L}_0^{(n)} = -\Gamma^{(n)}, \mathcal{J}^{(n-1)} = \Gamma^{(n-1)}$)

$$\partial_t \rho^{(n)}(t) = -\Gamma^{(n)} \rho^{(n)}(t) + \Gamma^{(n-1)} \rho^{(n-1)}(t). \tag{6.14}$$

Straight forward, one calculates by making use of the Laplace Transformation $\hat{\rho}_n(z) = \left(\prod_{k=n}^{1} \frac{\Gamma^{(k)}}{z+\Gamma^{(k)}} \right) \frac{1}{z-\Gamma^{(0)}}$. Following the described procedure one obtains $\hat{\mathcal{P}}(z) = \left\langle \frac{1}{z+\Gamma} \right\rangle, \hat{\mathcal{W}}(z) = 1 - z\hat{\mathcal{P}}(z)$. Finally, $\langle \hat{\rho}_\chi(z) \rangle$ reads

$$\langle \hat{\rho}_\chi(z) \rangle = \frac{\hat{\mathcal{P}}(z)}{1 + e^{\mathrm{i}\chi} \left(z\hat{\mathcal{P}}(z) - 1 \right)}. \tag{6.15}$$

Starting with the calculation of the first moment, which evaluates to $\langle \hat{m}_1(z) \rangle := \frac{1}{z^2 \hat{\mathcal{P}}(z)} - \frac{1}{z}$. The long-time limit of the current is therefore

$$\langle I_\infty \rangle = \frac{1}{\hat{\mathcal{P}}(0)} = \frac{1}{\left\langle \frac{1}{\tau} \right\rangle} \equiv \langle \tau \rangle^{-1}. \tag{6.16}$$

The connection between the Probability Density Functions (PDF) for $\Gamma \equiv \tau^{-1}$ is given by the following relationship

$$\langle \Gamma \rangle = \int d\Gamma \Gamma f(\Gamma) = \int d\tau \frac{1}{\tau} \tilde{f}(\tau), \quad \tilde{f}(\tau) \equiv \frac{1}{\tau^2} f\left(\frac{1}{\tau} \right) \tag{6.17}$$

and the other way round.

To calculate the Fano factor according to our approach, firstly the second moment $(\langle \hat{m}_2(z) \rangle = -\text{Tr}\partial_\chi^2 \langle \hat{\rho}_\chi(z)\rangle|_{\chi \to 0})$ has to be derived.

$$\hat{m}_2(z) = \frac{2}{z^3 \hat{\mathcal{P}}(z)^2} - \frac{3}{z^2 \hat{\mathcal{P}}(z)} + \frac{1}{z} \tag{6.18}$$

A Series Approximation of $\hat{\mathcal{P}}(z)$ leads to a polynomial of waiting times. The connection between $\hat{\mathcal{P}}(z), \langle \tau \rangle$ is given by $\langle \tau^{k+1} \rangle = (-1)^k \frac{\partial_z^k \hat{\mathcal{P}}(z)}{(k)!}$. In that manner the first three terms of $\hat{\mathcal{P}}(z)$ read $\hat{\mathcal{P}}(z) \approx \langle \tau \rangle - z \langle \tau^2 \rangle + z^2 \langle \tau^3 \rangle + O^3(z)$. Inserting that in (6.18) and $\hat{m}_1(z)$, leads to the approximated moments. The order of the next steps is important. After the Inverse Laplace Transformation the moments are combined $m_2(t) - (m_1(t))^2 [m_1(t)]^{-1}$ to the Fano factor. After that the execution of the long-time limit is performed.

Finally, the Fano factor evaluates to

$$\langle F_\infty \rangle = \frac{2\langle \tau^2 \rangle}{\langle \tau \rangle^2} - 1 = 1 + 2\frac{\text{Var}(\tau)}{\langle \tau \rangle^2}, \tag{6.19}$$

where $\text{Var}(\tau)$ is the variance of τ. This Fano factor is always greater than one, as the variance is always positive.

6.2.2 Single Quantum Dot and ring

This example can be generalized if one combines several Tunneling Junctions. Two Tunneling Junctions are formally equal to a Single Quantum Dot. On this system detailed measurements exists as well [Gustavsson et al., 2005].

A sequence of K tunneling contacts can be interpreted as ring (cf. [Brandes, 2008]) The transitions between K states, $1 \to 2 \ldots \to K \to 1$ at rates $\Gamma_i^{(n)}$ are interpreted as nojump superoperator. The step $K \to 0$ is interpreted as jump process in that case, which leads to a change in the rates. So Liouvillian and jump operator read

$$\mathcal{L}_0^{(n)} = \begin{pmatrix} -\Gamma_1^{(n)} & 0 & 0 & \ldots & 0 \\ \Gamma_1^{(n)} & -\Gamma_2^{(n)} & 0 & & 0 \\ 0 & \Gamma_2^{(n)} & -\Gamma_3^{(n)} & & \vdots \\ \vdots & & & \ddots & 0 \\ 0 & 0 & \ldots & \Gamma_{K-1}^{(n)} & -\Gamma_K^{(n)} \end{pmatrix}$$

$$\mathcal{J}^{(n-1)} = \Gamma_K^{(n-1)} |1\rangle\!\rangle \langle\!\langle K|, \tag{6.20}$$

with $\langle\!\langle K| = (0, \ldots, 1)$ and $|1\rangle\!\rangle = (1, 0, \ldots)^T$. For $K = 2$, which is the Single Quantum Dot in infinite bias limit, one obtains the following Quantum Master Equation

$$\partial_t \rho^{(n)}(t) = \begin{pmatrix} -\Gamma_L^{(n)} & 0 \\ \Gamma_L^{(n)} & -\Gamma_R^{(n)} \end{pmatrix} \rho^{(n)} + \begin{pmatrix} 0 & \Gamma_R^{(n-1)} \\ 0 & 0 \end{pmatrix} \rho^{(n-1)}. \tag{6.21}$$

In contrast to the case of the Tunnel Junction, where the operators could be expressed as scalars, in these case the operators become $K \times K$-matrices

$$
\hat{\mathcal{W}}(z) = \begin{pmatrix}
W_{\Pi 1} & W_{\Pi 2} & W_{\Pi 3} & \dots & W_{\Pi K} \\
0 & 0 & 0 & & 0 \\
0 & 0 & 0 & & \vdots \\
\vdots & & & \ddots & 0 \\
0 & 0 & \dots & 0 & 0
\end{pmatrix}
\tag{6.22}
$$

$$
\hat{\mathcal{P}}(z) = \begin{pmatrix}
P_1 & 0 & 0 & \dots & 0 \\
W_1 P_2 & P_2 & 0 & & 0 \\
W_1 W_2 P_3 & W_2 P_3 & P_3 & & \vdots \\
\vdots & & & \ddots & 0 \\
\frac{W_{\Pi 1} P_K}{W_K} & \frac{W_{\Pi 2} P_K}{W_K} & \dots & W_{K-1} P_K & P_K
\end{pmatrix}
$$

with scalar parameters $W_i = \left\langle \frac{\Gamma_i}{z+\Gamma_i} \right\rangle, P_i = \left\langle \frac{1}{z+\Gamma_i} \right\rangle$ and $W_{\Pi i} = \prod_{j=i}^{K} W_j$. Thus, the disorder averaged *Moment Generating Function*, which is defined as $\hat{M}(\mathrm{i}\chi) \equiv \mathrm{Tr}\langle \hat{\rho}_\chi(z) \rangle$, reads

$$
\hat{M}(\mathrm{i}\chi) = \frac{\sum_{i=1}^{K} \prod_{k=1}^{i} P_k}{1 - e^{\mathrm{i}\chi} W_\Pi}.
\tag{6.23}
$$

The moments can be obtained by differentiation from this Moment Generating Function, according to the counting filed variable χ. After back transformation to the time space and the execution of the long-time limit, current and Fano factor read

$$
\langle I_\infty \rangle = \frac{1}{\langle \tau_\Sigma \rangle}, \quad \langle F_\infty \rangle = \frac{\sum_{i=1}^{K} (\langle \tau_i \rangle - 2\langle \tau_i^2 \rangle)}{\langle \tau_\Sigma \rangle},
\tag{6.24}
$$

with $\langle \tau_\Sigma \rangle = \sum_{i=1}^{K} \langle \tau_i \rangle$ and $\langle \tau_i^m \rangle = \left\langle \frac{1}{\Gamma_i^m} \right\rangle$. It is possible to express the Fano factor as $\langle F_\infty \rangle = \frac{\sum_{i=1}^{K} (\langle \tau_i \rangle^2 + 2\mathrm{Var}(\tau_i))}{\langle \tau_\Sigma \rangle^2}$, where $\mathrm{Var}(\tau_i)$ denotes the variance of the inverse tunneling rates, which is always positive. Therefore, one can simply prove that $\langle F_\infty \rangle \geq K^{-1}$. In the special case of the Double Quantum Dot one obtains $\langle I_\infty \rangle = \frac{1}{\langle \tau_L \rangle + \langle \tau_R \rangle}$ for the current and $\langle F_\infty \rangle = \frac{2\langle \tau_L^2 \rangle - \langle \tau_L \rangle^2 + 2\langle \tau_R^2 \rangle - \langle \tau_R \rangle^2}{(\langle \tau_R \rangle + \langle \tau_L \rangle)^2}$ for the Fano factor.

6.2.3   Double Quantum Dot

In contrast to the former examples the Double Quantum Dot is a system that cannot be obtained by a combination of several Tunneling Junctions. In that cases bidirectional tunnelling is allowed, as well as the occurrence of coherent states. [Gurvitz and Prager, 1996].

The nojump and jump operator of the Double Quantum Dot in the basis $\rho = (\rho_0, \rho_L, \rho_R, \Re\rho_{RL}, \Im\rho_{RL})$ have the form

$$\mathcal{L}_0^{(n)} = \begin{pmatrix} -\Gamma_L^{(n)} & 0 & 0 & 0 & 0 \\ \Gamma_L^{(n)} & 0 & 0 & 0 & 2\mathcal{T}_C^{(n)} \\ 0 & 0 & -\Gamma_R^{(n)} & 0 & -2\mathcal{T}_C^{(n)} \\ 0 & 0 & 0 & -\frac{\Gamma_R^{(n)}}{2} & -\epsilon \\ 0 & -\mathcal{T}_C^{(n)} & \mathcal{T}_C^{(n)} & \epsilon & -\frac{\Gamma_R^{(n)}}{2} \end{pmatrix},$$

$$\mathcal{J}^{(n-1)} = \Gamma_R^{(n-1)}|0\rangle\!\rangle\langle\!\langle R|. \tag{6.25}$$

Thereby $\mathcal{T}_C^{(n)}$ stands for the coupling strength to the coherent states and ϵ for the energy difference between the left and right dot level. The Moment Generation Function reads

$$\hat{M}(\mathrm{i}\chi) = \frac{\langle A_{R,T}(z)\rangle - W_L(z)\langle B_{R,T}(z)\rangle - \frac{1}{4}P_L(z)}{e^{\mathrm{i}\chi}W_L(z)\langle\Gamma_R B_{R,T}(z)\rangle} \tag{6.26}$$

with

$$A_{R,T}(z) = \frac{(\Gamma_R + 2z)\left((\Gamma_R + z)(\Gamma_R + 2z) + 4\mathcal{T}_C^2\right) + 4\epsilon^2(\Gamma_R + z)}{(\Gamma_R + 2z)^2\left(z(\Gamma_R + z) + 4\mathcal{T}_C^2\right) + 4z\epsilon^2(\Gamma_R + z)},$$

$$B_{R,T}(z) = \mathcal{T}_C^2 \frac{\Gamma_R + 2z}{(\Gamma_R + 2z)^2\left(z(\Gamma_R + z) + 4\mathcal{T}_C^2\right) + 4z\epsilon^2(\Gamma_R + z)}. \tag{6.27}$$

According to the method proposed, a Mathematica Program was developed to derive that function. This program can also be used to calculate the Full Counting Statistics for a given jump and nojump operator automatically. It becomes obvious that combinations of the scalar objects P_i, W_i are no longer sufficient to describe the cumulants. The description in terms of P_L, W_L is only possible for the left lead. The current evaluates to

$$\langle I_\infty\rangle = \left((\langle\tau_L\rangle + \langle\tau_R\rangle)\left(\epsilon^2\langle\tau_T^2\rangle + 2\right) + \frac{1}{4}\langle\Gamma_R\rangle\langle\tau_T^2\rangle\right)^{-1}. \tag{6.28}$$

It is to observe that this current depends on the average tunnelling rate, as well as on the average waiting time. A comparison to [Gurvitz and Prager, 1996], leads to

$$\frac{I_{Cln}}{\langle I_\infty\rangle} = 1 + \alpha\frac{\tau_T^2}{4\tau_R\left(\tau_L + \tau_R\left(\epsilon^2\tau_T^2 + 2\right)\right) + \tau_T^2} \geq 1, \tag{6.29}$$

with the short hand notation $\langle\tau_R\rangle\langle\Gamma_R\rangle \equiv 1 + \alpha$. That means that the current always decays. Plotting the current as function of ϵ, leads to the observation that the difference to the clean case becomes sufficient for the case of small ϵ. This is the case, as the current denominator involves a ϵ^2 term.

Fano factor

The Fano factor becomes a quite long term.

$$
\begin{aligned}
\frac{\langle F_\infty\rangle}{\langle I_\infty\rangle^2} =& -\langle\tau_L\rangle^2 + 2\langle\tau_L^2\rangle \\
& + \langle\tau_T^2\rangle\left(-4\epsilon^2\langle\tau_R\rangle^2 + 10\epsilon^2\langle\tau_R^2\rangle - \langle\Gamma_R\rangle\langle\tau_R\rangle + \frac{1}{2}\right) \\
& - \langle\tau_T^2\rangle^2\left(\epsilon^4\langle\tau_R\rangle^2 + \frac{1}{2}\epsilon^2\langle\Gamma_R\rangle\langle\tau_R\rangle + \frac{1}{16}\langle\Gamma_R\rangle^2\right) \\
& + \langle\tau_T^4\rangle\left(2\epsilon^4\langle\tau_R^2\rangle + \frac{1}{8}\langle\Gamma_R^{-2}\rangle + \epsilon^2\right) \\
& - 4\langle\tau_R\rangle^2 + 8\langle\tau_R^2\rangle
\end{aligned}
\tag{6.30}
$$

However, the most interesting investigations can be made concerning the distribution of the right lead. Therefore, the distribution of $T_C^{(n)}$ and $\Gamma_L^{(n)}$ are assumed to be a delta distributions. This is equivalent to the case of constant rates. In that case, the Fano factor is given by

$$
\begin{aligned}
\langle F_\infty\rangle Z^2 =& 8\langle\tau_R\rangle^2\left(2\tau_L^2 + 16\nu + \epsilon^2\tau_T^4\left(-\alpha + 4\nu\epsilon^2 + 1\right)\right) \\
& + 8\langle\tau_R\rangle^2\left(\tau_T^2\left(-2\alpha + 20\nu\epsilon^2 - 1\right)\right) \\
& + 16\langle\tau_R\rangle^4\left(\epsilon^4\tau_T^4 + 6\epsilon^2\tau_T^2 + 4\right) \\
& + \left((\alpha+1)^2 + 2\beta\right)\tau_T^4 \\
Z =& 4\langle\tau_R\rangle\left(2\langle\tau_R\rangle + \tau_L\right) + \tau_T^2\left(4\epsilon^2\langle\tau_R\rangle^2 + \alpha + 1\right)
\end{aligned}
\tag{6.31}
$$

with $\langle\tau_R^2\rangle\langle\Gamma_R^{-2}\rangle \equiv (1+\alpha)^2 + \beta$, with $\alpha, \beta \geq 0$.

Sample distributions

As example the Maxwell Distribution is taken into account. For convenience the distribution is normed in the way that the parameter of the Probability Density Function is the average. Thus, the Probability Density Function is $f(x) = \frac{32x^2 e^{-\frac{4x^2}{\pi\sigma^2}}}{\pi^2\sigma^3}$. In that case current and Fano factor read

$$
\langle I_\infty^{\mathrm{MW}}\rangle(\epsilon, \sigma, \tau_T, \tau_L) = \frac{\pi\sigma\tau_L}{\pi\sigma\left(\tau_L + \sigma\left(\epsilon^2 + 2\right)\right) + \tau_T^2}
\tag{6.32}
$$

$$
\begin{aligned}
\langle F_\infty^{\mathrm{MW}}\rangle(\epsilon, \sigma, \tau_T, \tau_L) =& \frac{\pi^2\tau_L^2\left(4\sigma^2 + 30\pi\sigma^4\epsilon^2\right)}{8\left(\tau_L^2\left(\pi\sigma^2\epsilon^2 + 1\right) + \pi\sigma\left(2\sigma + \tau_T\right)\right)^2} \\
& + \frac{\pi^2\tau_L^4\left(6\pi\sigma^4\epsilon^4 + 8\sigma^2\epsilon^2 + 3\right) + 24\pi^3\sigma^4}{8\left(\tau_L^2\left(\pi\sigma^2\epsilon^2 + 1\right) + \pi\sigma\left(2\sigma + \tau_T\right)\right)^2} \\
& + 1 - \frac{2\left(\tau_L^2\left(\pi\sigma^2\epsilon^2 + 1\right) + 2\pi\sigma^2\right)}{\tau_L^2\left(\pi\sigma^2\epsilon^2 + 1\right) + \pi\sigma\left(2\sigma + \tau_T\right)}.
\end{aligned}
\tag{6.33}
$$

The investigation of current and Fano factor at $\epsilon = 0$, where the current is maximal, leads to the following observations. The current gets zero for $\sigma \to 0, \infty$. And the Fano factor converges to the fixed value of $\frac{3\pi^2}{8} - 1$ for σ to 0. For σ to ∞ the Fano factor converges to $\frac{3\pi}{4} - 1$.

6.2.4 Interpretation

In the case of examples without internal dynamics (transitions in a ring) it was shown that the formula for the current of the clean case can be used if one replaces the waiting times by their means. This result is quite intuitive. If one thinks of a classical process, which consists of several sequential subprocesses, the expected time for the whole process is the expected subprocesses. A calculation of that times in terms of average transition rates is not possible.

The Fano factor for the transitions in a ring systems raises in dependence of the variance of the distribution of the waiting times. Thus, quantum mechanic and classical uncertainness are summed up. This is a plausible result.

The situation changes in the case of the Double Quantum Dot, because the internal dynamics of that system is no sequential process. The current depends on tunneling rates and waiting times as well and decays in dependence of the parameter α. In the case of the investigated Maxwell distribution, this parameter has a fixed value. In general, this parameter depends on the parameters of the distribution. There are distributions, for example the Uniform Distribution, where the parameter α tends to infinity if very small tunneling rates become possible. This causes a very strong suppression of the current, which is also an traceable result.

The Fano factor for the Double Quantum Dot, which only depends on the variance ν of the waiting time distribution for the Maxwell Distribution, raises in contrast to the Fano factor for constant rates. The detailed behavior of the Fano factor strongly depends on the investigated distribution. Therefore, the most important next step in this research is to find out, which distribution of waiting times or tunneling rates is physically reasonable.

Part III

Beyond randomness: Special setups

Chapter 7

Impurity case

The first special case discussed here is the impurity case.

We consider a Tunneling Junction with constant rates except for rate n_0.

$$\Gamma^{(n)} = \begin{cases} \Gamma & n \neq n_0 \\ \Gamma' & n = n_0 \end{cases} \tag{7.1}$$

In this special situation the standard approach is applied with $\mathcal{J}^{(n)} = \Gamma^{(n)}, \mathcal{L}_0 = -\Gamma^{(n)}$.

After the $\underset{t \to z}{\mathrm{LT}}$, $\hat{\rho}_n(z)$ reads

$$\hat{\rho}_n(z) = \frac{\Gamma^n}{(z + \Gamma)^{n+1}} \begin{cases} 1 & n < n_0 \\ \frac{z+\Gamma}{z+\Gamma'} & n = n_0 \\ \frac{z+\Gamma}{z+\Gamma'} \frac{\Gamma'}{\Gamma} & n > n_0 \end{cases} . \tag{7.2}$$

Applying the $\underset{n \to \chi}{\mathrm{FST}}$ to $\hat{\rho}_n(z)$ leads to[1]

$$\hat{\rho}_\chi(z) = \frac{1}{z + \Gamma\left(e^{\mathrm{i}\chi} - 1\right)} \left(1 + \frac{(\Gamma' - \Gamma)\left(e^{\mathrm{i}\chi} - 1\right)\Gamma^{n_0} e^{\mathrm{i}n_0\chi}}{(\Gamma' + z)(\Gamma + z)} \right) . \tag{7.3}$$

This is a quite simple function, where the Inverse Laplace Transformation $\underset{z \to t}{\mathrm{LT}}{}^{-1}$ is known[1]

$$\rho_\chi(t) = \frac{1}{\Gamma\left(e^{\mathrm{i}\chi} - 1\right) + \Gamma'} \left[e^{\Gamma t\left(e^{\mathrm{i}\chi} - 1\right)} \left(\Gamma^*\left(e^{\mathrm{i}\chi} - 1\right) \frac{\mathbf{\Gamma}(n_0, \Gamma t e^{\mathrm{i}\chi})}{(n0 - 1)!} + \Gamma' e^{\mathrm{i}\chi} \right) \right.$$

$$\left. + \frac{\Gamma^{n_0}\left(e^{\mathrm{i}\chi} - 1\right)}{\Gamma^{*n_0 - 1}} e^{-\Gamma' + \mathrm{i}n_0\chi} \left(1 - \frac{\mathbf{\Gamma}(n_0, \Gamma^* t)}{(n_0 - 1)!} \right) \right] \tag{7.4}$$

with $\Gamma^* \equiv \Gamma - \Gamma'$ and the **incomplete gamma function $\mathbf{\Gamma}$**. It is quite simple to show that the long-time limit does not change. If one regards an infinite number of transitions, the finite set of impurities is a null set.

---

[1]using Mathematica

Thus, the point of interest is in the time resolved current and Fano factor (see figure 7.1), as well as in the higher cumulants (see figure 7.2).
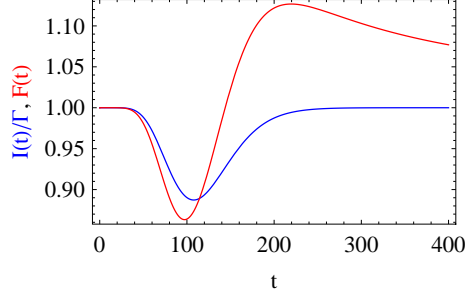
Figure 7.1: Current/Γ and Fano factor for $n_0 = 10$ at rates $\Gamma = 0.1, \Gamma' = 0.01$
It becomes obvious that the current is disordered for a short time and the Fano factor needs some longer time to regenerate.

It has to be investigated that higher cumulants are disordered during a significant longer time than smaller cumulants.[2] Additionally, it can be remarked that impurities for larger n_0 have less impact to the current. This aspect is not visualized, but can be imagined by thinking of the decaying maximal amplitude of $\rho^{(n)}(t)$.

In the situation of feedback control, this would not be the case, because the amplitude is fixed there [Brandes, 2010].

Apart from this results, which leaded to the cumulants, the Inverse Laplace Transform of $\hat{\rho}_n(z)$ (7.2) is know[1] as

$$\rho^{(n)}(t) = \begin{cases} \frac{(\Gamma t)^n}{n!} e^{-\Gamma t} & n < n_0 \\ \frac{\Gamma^{n_0} e^{-\Gamma' t}}{(\Gamma - \Gamma')^{n_0}} \left(1 - \frac{\mathbf{\Gamma}_{(n_0,(\Gamma - \Gamma')t)}}{(n_0 - 1)!}\right) & n = n_0 \\ \frac{\Gamma' \Gamma^{n-1} e^{-\Gamma' t}}{(\Gamma - \Gamma')^n} \left(1 - \frac{\mathbf{\Gamma}_{(n,(\Gamma - \Gamma')t)}}{(n-1)!}\right) & n > n_0 \end{cases} . \qquad (7.5)$$

This result offers directly the possibility to show the probability for n passed electrons [2], it is quite pleasant (figure 7.2, $P_n(t) = \rho^{(n)}(t)$).

At this point the different representation of Full Counting Statistics can be easily seen next to each other (compare section 3.2).

---

[2]With respect to the logarithmic time scale in the plot
[1]not obtained with Mathematica
[2]The trace of a 1x1-matrix is the identity.
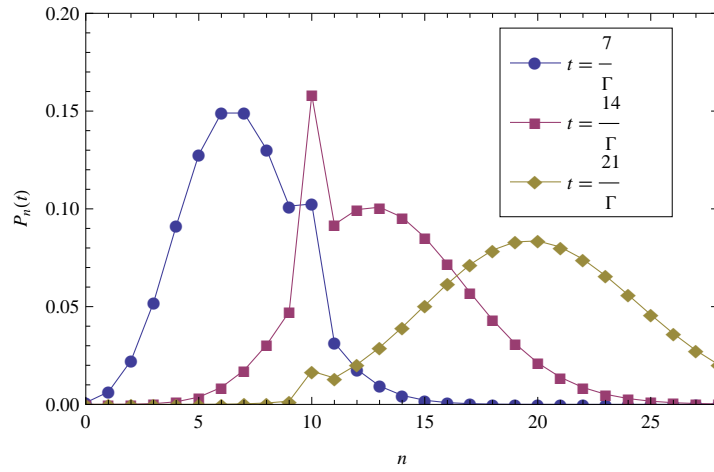
(a) Probability distribution for n passed electrons
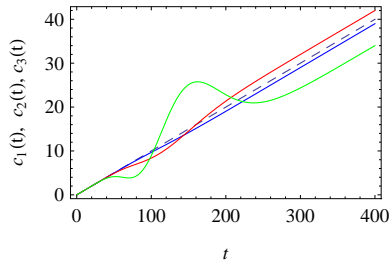
(b) cumulants 1 to 3
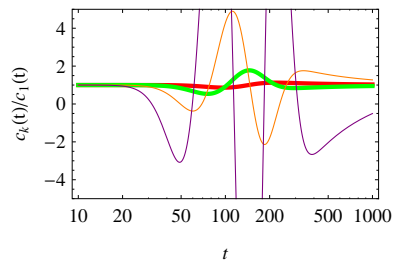
(c) cumulants 2 to 5 normed by cumulant 1 (logarithmic time-scale)

Figure 7.2: Full Counting Statistics: Tunneling Junction with an impurity at $n_0 = 10$ at rates $\Gamma = .1, \Gamma' = .01$.

7.1   Discrete time step approach

In the former section the simplest imaginable system was discussed. The complete system could be calculated analytically, but the expressions were quite complex. Therefore, it seems imaginable that there are systems, where the analytic expression becomes more complex or even unknown. A computational implementation is easy to produce after the proceeding of (5.2). The idea is similar to the heuristically derivation of the Quantum Master Equation of the Single Quantum Dot, which was presented in the Single Quantum Dot example (5.59). The nQME

$$\partial_t \rho^{(n)}(t) = \mathcal{L}_0^{(n)} \rho^{(n)}(t) - \mathcal{J}^{(n-1)} \rho^{(n-1)}(t) \tag{7.6}$$

is formally replaced by

$$\partial_t \rho(n,s) = \mathcal{L}_0 \rho(n,s) + \mathcal{J}^{(n-1)} \rho(n-1,s) \tag{7.7}$$

$$\rho(n,s) = \rho(n,s-1) + \Delta_t \partial_t \rho(n,s-1). \tag{7.8}$$

In that context $\partial_t \rho(n,s)$ is a symbolic variable[3]. For the tunneling contact it is more convenient to insert (7.7) in (7.8).

Listing 7.1: Simulation for impurity case with variables `g=`Γ`,gd=`Γ', $t = \Delta_t$ `s`

```
 1  Clear[p];(*delets all values in connection with p*)

    p[n_,s_,g_,gd_,n0_]  :=     0/;n<0||s<0
    p[0,0,g_,gd_,n0_]    :=     0
    p[1,1,g_,gd_,n0_]    :=     g
 6  p[0,1,g_,gd_,n0_] :=    1-g

    p[n_,s_,g_,gd_,n0_] :=
        p[n,s,g,gd,n0] =(*this stores the result in memory*)
        If[ n==n0,
11          g p[n-1,s-1,g,gd,n0]+(1-gd) p[n,s-1,g,gd,n0],
          If[ n==n0+1,
              gd p[n0,s-1,g,gd,n0]+(1-g) p[n,s-1,g,gd,n0],
              g p[n-1,s-1,g,gd,n0]+(1-g) p[n,s-1,g,gd,n0]
            ]
16        ]
```

Apart from the distribution, $\rho_\chi(t)$ can be approximated by an $\underset{n\to\chi}{\text{FST}}$, which is cut at large n.

For figure 7.3 the following approximation was done

$$\rho_\chi(t) \approx \Gamma \Delta_t \sum_{n=0}^{n_{0,\text{Offset}} + t\frac{\Delta_\infty}{\Delta_t}} e^{in\chi} \rho\left(n, \frac{t}{\Delta_s}, \Gamma, \Gamma', n_0\right). \tag{7.9}$$

Afterwards, the cumulants were derived by the default procedure. The critical parameter in this plot (figure 7.3) is Δ_t. Lowering this parameter produces better results (cf. figure 7.4), but consumes more computation power.

---

[3]This variable is called `dtRnt` in the source code.
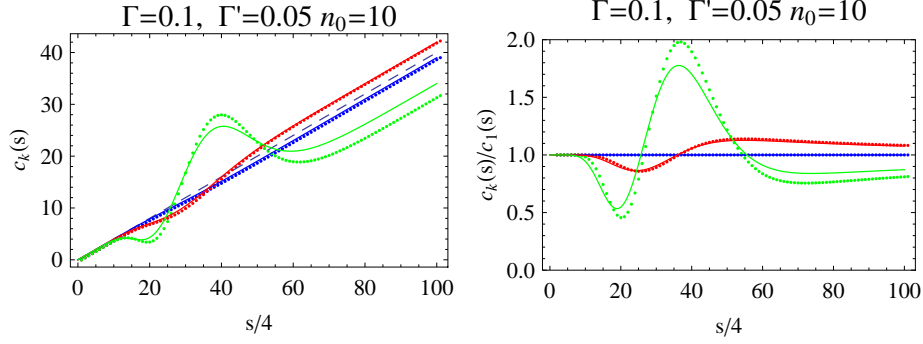
Figure 7.3: Simulated results for the first three cumulants (current: blue, Fano factor: red, 3rd cumulant: green) for the case already discussed in the former section. $n_0 = 10, \Gamma = .1, \Gamma' = .05$ with simulation parameter $n_{0,\text{Offset}} = 7, \Delta_\infty = \frac{1}{5}, \Delta_t = 4.$, comparison to the analytical result (solid lines)
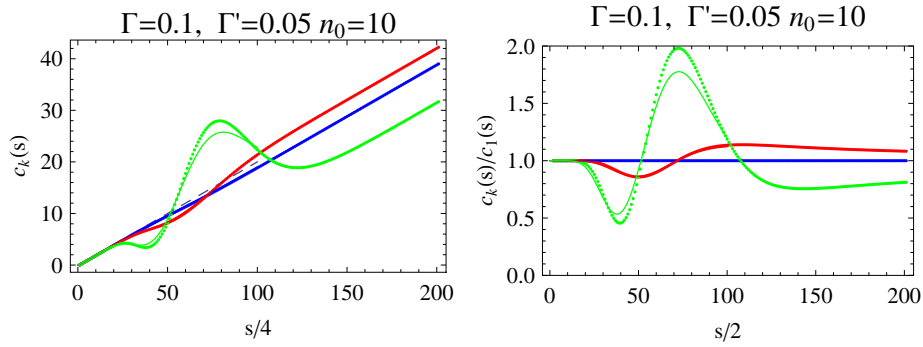
Figure 7.4: Improved results for the first three cumulants (current: blue, Fano factor: red, 3rd cumulant: green) for the case as already discussed in the former section. $n_0 = 10, \Gamma = .1, \Gamma' = .05$ with simulation parameter $n_{0,\text{Offset}} = 7, \Delta_\infty = \frac{1}{5}, \Delta_t = 2.$, comparison to the analytical result (solid lines).

A detailed investigation ot the occupation (of the conditioned density matrix) points to a recursive formula for $P(n,s)$.

$$P(n,s) = \begin{cases} \binom{s}{n}(\Gamma\Delta_t)^n(1-\Gamma\Delta_t)^{s-n} & n < n_0 \\ (\Gamma\Delta_t)^{n_0}\sum_{j=1}^{s-1}\binom{j}{n_0-1}(1-\Gamma\Delta_t)^{j+1-n_0}(1-\Gamma'\Delta_t)^{s-j+1} & n = n_0 \\ \frac{\Gamma'}{\Gamma}(\Gamma\Delta_t)^n\sum_{j=1}^{s-1}\binom{j}{n-1}(1-\Gamma\Delta_t)^{j+1-n}(1-\Gamma'\Delta_t)^{s-j+1} & n > n_0 \end{cases}$$

(7.10)

Calculating the limit $\Delta_t \to 0$ $\left(\frac{\Gamma t}{s} \to \Gamma t\right)$ leads to

$$P(n,t) = \begin{cases} \frac{(\Gamma t)^n}{n!}e^{-\Gamma t} & n < n_0 \\ \left(\frac{\Gamma^2 t}{\Gamma-\Gamma'}\right)^{n_0}\left[e^{-\Gamma' t} - e^{-\Gamma t}\left(1+\sum_{\alpha=1}^{n_0-1}\frac{((\Gamma-\Gamma')t)^\alpha}{\alpha!}\right)\right] & n = n_0 \\ \frac{\Gamma'}{\Gamma}\left(\frac{\Gamma^2 t}{\Gamma-\Gamma'}\right)^n\left[e^{-\Gamma' t} - e^{-\Gamma t}\left(1+\sum_{\alpha=1}^{n-1}\frac{((\Gamma-\Gamma')t)^\alpha}{\alpha!}\right)\right] & n > n_0 \end{cases}$$

(7.11)

$$= \begin{cases} \frac{(\Gamma t)^n}{n!}e^{-\Gamma t} & n < n_0 \\ \left(\frac{\Gamma^2}{\Gamma-\Gamma'}\right)^{n_0}\left[e^{-\Gamma' t}\left(\frac{(n0-1)!-\boldsymbol{\Gamma}(n_0,(\Gamma-\Gamma')t)}{(n_0-1)!}\right)\right] & n = n_0 \\ \frac{\Gamma'}{\Gamma}\left(\frac{\Gamma^2}{\Gamma-\Gamma'}\right)^n\left[e^{-\Gamma' t}\left(\frac{(n-1)!-\boldsymbol{\Gamma}(n,(\Gamma-\Gamma')t)}{(n-1)!}\right)\right] & n > n_0 \end{cases}$$

(7.12)

which is in accordance to the analytical result.

7.2 Comparison and alternatives*

In this section the known result of the clean limit is reproduced in a very brief way. An idea for an alternative approach to treat this problem, is outlined in the second subsection. This addresses readers, who want to the work on similar systems.

Reference system barrier*

With the method discussed in the former section, the graphic [Flindt, 2007, 4.1] can be reproduced by setting $\Gamma' = \Gamma = 0.1$. As expected the same result is obtained.

Considering particles transmitted to a barrier with a transmission rate Γ and finite time-steps dt with $s = t/dt$. The probability to have n particles after s time-steps is obviously

$$P_{n,s} = \Gamma dt P_{n-1,s-1} + (1-\Gamma dt)P_{n,s-1}.$$

(7.13)

Solving this recurrence equation yields to a binomial distribution

$$P_{n,s} = \binom{s}{n}(\Gamma dt)^n(1-\Gamma dt)^{s-n}.$$

(7.14)

For the limit $dt \to 0$, $\left(\frac{\Gamma t}{s} \to \Gamma t\right)$, (7.14) becomes a Poisson Distribution

$$P_n(t) = \frac{(\Gamma t)^n}{n!} e^{-\Gamma t}.$$ (7.15)

This function is well known. Another way to derive this result, is to change the order of time limit and the solution of the function.

$$\partial_t P_{n,t} = \Gamma \left(P_{n,t}(n-1,t) - P_{n,t} \right)$$ (7.16)

$t \to z$

$$z P_{n,z} - P_{n,t}(n,0) = \Gamma \left(P_{n,z}(n-1,t) - P_{n,z} \right)$$ (7.17)

$n \to \chi$ and $P_{n,t}(n,0) = \delta_{n,0}$

$$z P_{\chi,z} - 1 = \Gamma \left(e^{i\chi} - 1 \right) P_{\chi,z}$$ (7.18)

$z \to t$

$$P_{\chi,t} = e^{-\Gamma t (1 - e^{i\chi})}$$ (7.19)

The Cumulant Generating Function is

$$S_p(\chi) = (\Gamma t)(e^{i\chi} - 1).$$ (7.20)

[Flindt, 2007, 4.8] $\chi \to t$.

$$P_{n,t} = \frac{1}{2\pi} \int_0^{2\pi} e^{-in\chi - \Gamma t(1 - e^{i\chi})} \, d\chi = \frac{(\Gamma t)^n}{n!} e^{-\Gamma t}$$ (7.21)

Alternative approach*

Another approach: $\Gamma^* = \Gamma - \Gamma'$

$$\partial_t \rho^{(n)}(t) = \Gamma \left(\rho^{(n)}(t)(n-1,t) - \rho^{(n)}(t) \right) + \Gamma^* \left(\delta_{n0,n} \rho^{(n)}(t) - \delta_{n0-1,n} \rho^{(n)}(t)(n_0 - 1, t) \right)$$ (7.22)

With the series Fourier Transformation and the short notation $\rho_\chi(t) = \sum_n \rho^{(n)}(t) e^{in\chi}$ one gets

$$\partial_t \rho_\chi(t) = \Gamma \left(e^{i\chi} - 1 \right) \rho_\chi(t) + \Gamma^* \left(e^{in\chi} \rho^{(n)}(t)(n_0, t) - e^{i(n_0+1)\chi} \rho^{(n)}(t)(n_0 - 1, t) \right)$$ (7.23)

cf [Emary, 2009, 9.15].

The Fourier Representation of $\rho^{(n)}(t)$ is

$$\rho^{(n)}(t) = \frac{1}{2\pi} \int e^{-in\chi} \rho_\chi(t) d\chi,$$ (7.24)

which evaluates to

$$\partial_t \rho_\chi(t) = \Gamma\left(e^{i\chi} - 1\right)\rho_\chi(t)$$
$$+ \Gamma^*\left(\int_0^{2\pi} e^{-i(n_0)(\chi-\chi')}\rho_\chi(t)(\chi',t)\,d\chi' + \int_0^{2\pi} e^{-i(n_0-1)(\chi-\chi')}\rho_\chi(t)(\chi',t)\,d\chi'\right).$$

$$(7.25)$$

For convenience, this is transformed to the Laplace Space by using

$$\hat{\rho}_\chi(z) = \int_0^\infty \rho_\chi(t)e^{(-zt)}\,dt. \tag{7.26}$$

This leads to

$$z\hat{\rho}_\chi(z) - \rho_\chi(t)(\chi,0) = \Gamma\left(e^{i\chi} - 1\right)\rho_\chi(t) + \Gamma^*(e^{n_0} + e^{n0-1})\left(\int_0^{2\pi} e^{-i(\chi-\chi')}\rho_\chi(t)(\chi',t)\,d\chi'\right)$$

$$(7.27)$$

$$\hat{\rho}_\chi(z) = \frac{1}{z - (e^{i\chi} - 1)}\left(1 + \Gamma^*(e^{n_0} + e^{n0-1})\int_0^{2\pi} e^{-i(\chi-\chi')}\rho_\chi(t)(\chi',t)\,d\chi'\right).$$

$$(7.28)$$

This equation can be expanded as a Dyson Series [Brandes, 2007, 1.2.7]

$$\hat{\rho}_\chi(z)^{(0)} = \frac{1}{z - (e^{i\chi} - 1)}1 \tag{7.29}$$

$$\hat{\rho}_\chi(z)^{(1)} = \frac{1}{z - (e^{i\chi} - 1)}\left(1 + \Gamma^*(e^{n_0} + e^{n0-1})\int_0^{2\pi} e^{-i(\chi-\chi')}\rho_\chi(t)(\chi',t)\,d\chi'\right)$$

$$(7.30)$$

$$\dots$$

Chapter 8

Simulated
Single Quantum Dot

Instead of random rates or constant rates with impurities, one can think about alternating rates. All systems, which are a special type of the ring case, can be modelled with this approach.

The aim of this chapter is only to explain the idea. It is meant to do an all-embracing and general research on that idea. Therefore, the Single Quantum Dot will be taken as an example. In terms of the graphical scheme 5.5, the two dimensional process is uncompressed to a linear process.

Defining $n = 2m + i$ with $\{n, m, i\} \in \mathbb{N}, i < 2$ and

$$\Gamma^{(n)} = \begin{cases} \Gamma_L & i(n) = 0 \\ \Gamma_R & i(n) = 1, \end{cases} \tag{8.1}$$

makes the barrier becoming a Single Quantum Dot. This means for collecting the terms after i, m leads to

$$\partial_t \begin{pmatrix} \rho_{n=2m+0}(t) \\ \rho_{n=2m+1}(t) \end{pmatrix} = \begin{pmatrix} -\Gamma_L & 0 \\ \Gamma_L & -\Gamma_R \end{pmatrix} \begin{pmatrix} \rho_{n=2m+0}(t) \\ \rho_{n=2m+1}(t) \end{pmatrix} + \begin{pmatrix} 0 & \Gamma_R \\ 0 & 0 \end{pmatrix} \begin{pmatrix} \rho_{n=2(m-1)+0}(t) \\ \rho_{n=2(m-1)+1}(t) \end{pmatrix} \tag{8.2}$$

with a new definition for $\rho^{(n)}(t)^{dot}$, as vector

$$\rho_{n=m}(t)^{dot} := \begin{pmatrix} \rho_{n=2m}(t) \\ \rho_{n=2m}(t) \end{pmatrix} \tag{8.3}$$

and

$$\mathcal{L}_0 = \begin{pmatrix} -\Gamma_L & 0 \\ \Gamma_L & -\Gamma_R \end{pmatrix}, \mathcal{J} = \begin{pmatrix} 0 & \Gamma_R \\ 0 & 0 \end{pmatrix}. \tag{8.4}$$

Disregarding the $\boxed{x}^{dot}$ index, makes (8.2) become the known n-resolved Liouville-von Neumann Equation for constant rates

$$\partial_t \rho^{(n)}(t) = \mathcal{L}_0 \rho^{(n)}(t) + \mathcal{J} \rho_{n-1}(t). \tag{8.5}$$

The physical interpretation was already discussed:

$\mathcal{J}$: particles leaving the system

$\mathcal{L}_0$: the rest

Tunneling Junction interpretation

The next step is to find out, what happens if one regards the system with its original interpretation as Tunneling Junction?

Remembering equation (3.10)

$$\hat{\rho}_n(z) = \hat{\mathcal{P}}_n(z) \left(\prod_{k=n-1}^{0} \hat{\mathcal{W}}_k(z) \right) \rho_0. \tag{8.6}$$

In our case, with commuting 1x1-matrices, it becomes

$$\hat{\rho}_n(z) = \hat{\mathcal{P}}_n(z) W_L(z)_\delta \left(\prod_{k=m-1}^{0} \hat{\mathcal{W}}_{2k}(z) \hat{\mathcal{W}}_{2k+1}(z) \right) \rho_0 \tag{8.7}$$

$$= \hat{\mathcal{P}}_n(z) W_L(z)_\delta \left(W_L(z) W_R(z) \right)^m, \tag{8.8}$$

where $W_L(z)_\delta = 1 + i(n)(W_L(z) - 1)$, $\rho_0 = 1$, $\hat{\mathcal{P}}_n(z) = \frac{1}{z - \Gamma^{(n)}}$, $\hat{\mathcal{W}}_n(z) = \frac{\Gamma^{(n)}}{z - \Gamma^{(n)}}$, $\Gamma^{(n)} = \Gamma^{(i(n))\mathbf{1}}$.

This forces us to split the sum of the $\underset{n \to \chi}{\text{FST}}$ into two parts. One for the even part and one for the odd part.

$$\underset{n \to \chi}{\text{FST}} \hat{\rho}_n(z) = \sum_{m=0}^{\infty} \left(\hat{\mathcal{P}}_L(z) \left(\hat{\mathcal{W}}(z) \right)^m e^{\mathrm{i}2m\chi} + \hat{\mathcal{P}}_R(z) W_L(z) \left(\hat{\mathcal{W}}(z) \right)^m e^{\mathrm{i}(2n+1)\chi} \right) \tag{8.9}$$

$$= \left(\hat{\mathcal{P}}_L(z) + \hat{\mathcal{P}}_R(z) W_L(z) e^{\mathrm{i}\chi} \right) \sum_{n=0}^{\infty} \left(\hat{\mathcal{W}}(z) \right)^n e^{\mathrm{i}2n\chi} \tag{8.10}$$

$$= \frac{\hat{\mathcal{P}}_L(z) + \hat{\mathcal{P}}_R(z) W_L(z) e^{\mathrm{i}\chi}}{1 - e^{2\mathrm{i}\chi} \hat{\mathcal{W}}(z)} \tag{8.11}$$

It is quite simple to derive the current from this point by inserting the definitions $(\hat{\mathcal{W}}(z) = W_L(z) W_R(z))$.

$\lim_{z \to 0} z^2 \hat{m}_1(z)$ leads to

$$\langle I_\infty \rangle = 2 \frac{1}{\tau_L + \tau_R} = 2 \frac{\Gamma_L \Gamma_R}{\Gamma_L + \Gamma_R}, \tag{8.12}$$

which is the double of the clean case current. Using the known method to derive the Fano factor, leads to [2]

$$\langle F_\infty \rangle = 2 \frac{\Gamma_L{}^2 + \Gamma_R{}^2}{(\Gamma_L + \Gamma_R)^2} = 2 \frac{\tau_L^2 + \tau_R^2}{(\tau_L + \tau_R)^2}, \tag{8.13}$$

---

[1] $i(n) = i(i(n))$ can be interpreted as projector in this case

[2] In this (special) case the expression in terms of waiting times and tunneling rates are **formally equivalent**.

which is also the double of the Fano factor (5.97). (8.12, 8.13) are expected results. In the simulation, the current passing through the right and the left Tunneling Junction, is transported through one Tunneling Junction. This Tunneling Junction can then be interpreted as alternatingly right or left tunneling contact.

Chapter 9

Feedback control simulation

In a former step a classical feedback look for the nQME could be used. Therefore, the principle of [Brandes, 2010] is applied to the n-dependent tunneling rates.

In this thesis the view is restricted to the simulation of the Tunneling Junction. The nQME now reads

$$\partial_t \rho^{(n)}(t) = \Gamma^{(n-1)} f(q_{n-1}(t)) \rho^{(n-1)}(t) - \Gamma^{(n)} f(q_n(t)) \rho^{(n)}(t) \qquad (9.1)$$

with $f(x) = 1 + gx$ and $q_n = \langle I_\infty \rangle t - n$. In [Brandes, 2010] the following observations were done for the clean case:

- The FCS charge distribution $P(n,t)$ converges rapidly into a stationary distribution with a fixed shape, which moves with a constant speed to larger n.

- Even cumulants have finite values in the long-time limit.[1]

Clean case

At first the result for constant waiting times is being reproduced with the simulation method explained in chapter 7.1.

Listing 9.1: Simulation for clean feedback case with variables $\mathtt{gm}{=}\Gamma\Delta_t$, $\mathtt{G}{=}g$, $\mathtt{I0}{=}I_\infty$, $t = \Delta_t$ $\mathtt{s}$ and rate restriction to $\mathtt{gFB}{=}\Delta_t\Gamma_{\mathrm{eff}} \in [0.001\ldots0.999]$

```
    (*initial values*)
    Clear[pFB,gFB];
    pFB[n_,s_] :=     0/;n<0||s<0
 4  pFB[n_,0] :=    DiscreteDelta[n]
    (*rates*)
    cFB[n_,s_] :=
       Min[Max[G (I0 s-n),(.001-gm)/gm],(.999-gm)/gm] (*numerical restriction*)
    gFB[n_,s_] :=
 9     gFB[n,s] = gm (1+cFB[n,s])
    (*density operator*)
    pFB[n_,s_] :=
       pFB[n,s] = N[gFB[n-1,s-1] pFB[n-1,s-1]+(1-gFB[n,s-1]) pFB[n,s-1]]
```

---

[1]In the case without feedback they become infinite. The constant values were current and Fano factor.
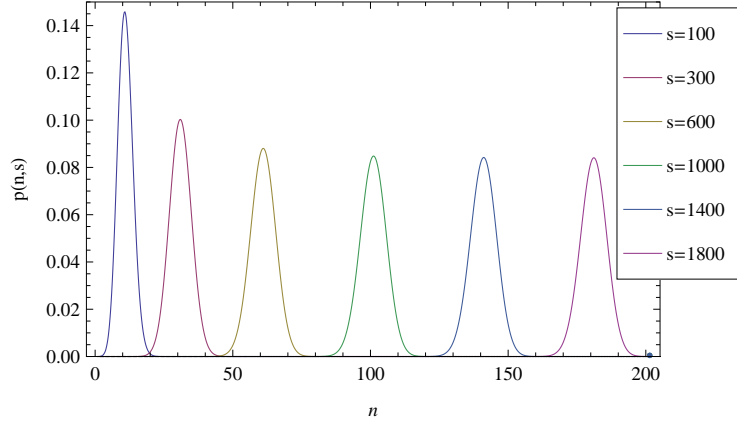
(a) FCS charge distribution
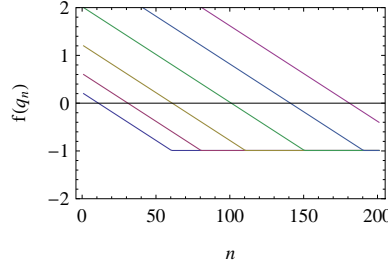
(b) feedback parameter
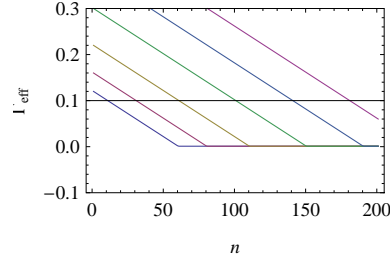
(c) effective rate

Figure 9.1: Simulation for the distribution of the FCS charge distribution $p(n, s)$ with $\Gamma = 1, \Delta_t = 0.1, g = 0.02$ on the left. On the right feedback parameters. g_{eff} was restricted to the range between 0 and one. With a time-step of 0.1 this restricts $f(q_n)$ in the area of $0 \ldots 10$.

This leads to good results despite the finite control strength (cf. figure 9.1). This finite control strength had to be introduce to keep the trace of the system density matrix equal to one[2]. A more intuitive explanation for the finite strength is that the probability for an event has to be in the range from zero to one.

Random case

Analogically to the clean case, a simulation for the random case was designed. To get a reference a simulation without feedback is done at first. As in the clean case without feedback (not shown), the distribution for the random case splits up. In that case the parameter α is the parameter of a Uniform Distribution with the width $\sigma = 1.8$ the mean $\Gamma = 1$

$$\alpha = \alpha_{\mathrm{Uniform}} = \frac{\log\left(-\frac{4}{\Gamma\sigma - 2} - 1\right)}{\Gamma\sigma} - 1 \approx 0.63, \qquad (9.2)$$

which implies a decay in the current to $\langle I_\infty \rangle = \langle \Gamma \rangle \frac{1}{1+\alpha} \approx .61 \langle \Gamma \rangle$.

---

[2]In that one dimensional example that measure keep $1 = 1$.

This fact can also be observed by comparing figure 9.1 with 9.2. For example the maximum at $s = 1800$ is slowed down from 180 to about 110 (see also (5.24)). Due to the fact that the shape of the distribution for the random rates is unknown as function of time (see 5.1), a simulation was performed with 20 independent sets of random rates. Averaging over the probability for that rates, approximates the charge distribution. Thus, only the rates are simulated and the charge distribution for every set of random rates is derived analytically. In 9.2 it can be observed that the shape of the distribution runs in a fixed state apart from the random fluctuations.
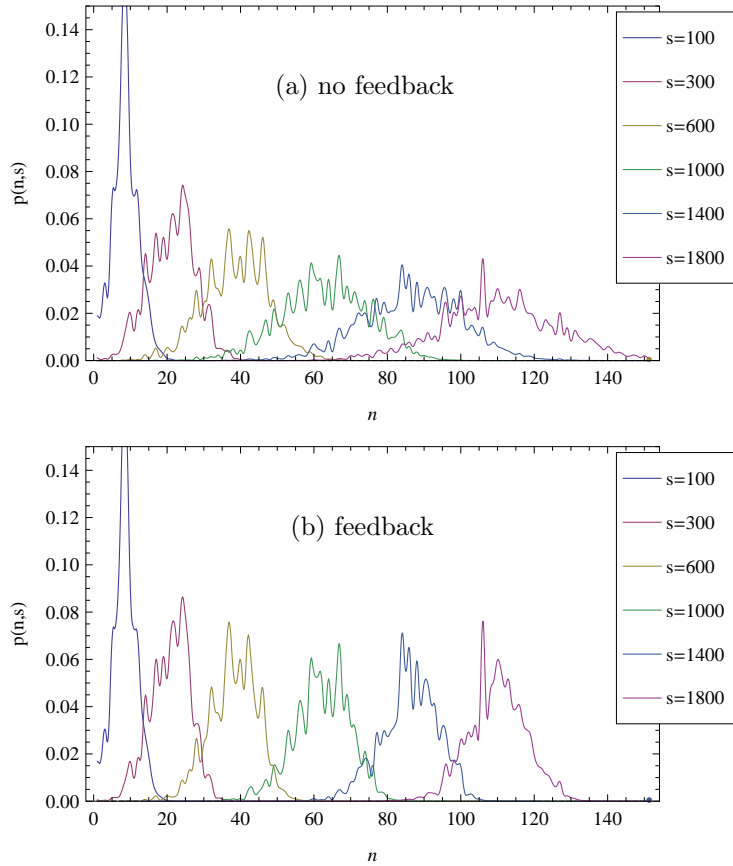
Figure 9.2: Simulation for the distribution of the FCS charge distribution $p(n, s)$ for a **Uniform Distribution** with mean at $\Gamma = 1$ and width $\sigma = 1.8$. This distribution was calculated based on just 20 samples. Therefore, the shape is not smooth. The upper picture shows the situation without feedback and the lower picture with feedback at feedback strength $g = 0.02$. The time step width was set to $\Delta_t = 0.1$ again. As in the clean case the shape of the distribution is conserved. Thereby, the same rates were used for the case with and without feedback.

To clarify the situation one single time step is taken into account in figure 9.3. In that figure one can see that the feedback controls the randomness like a
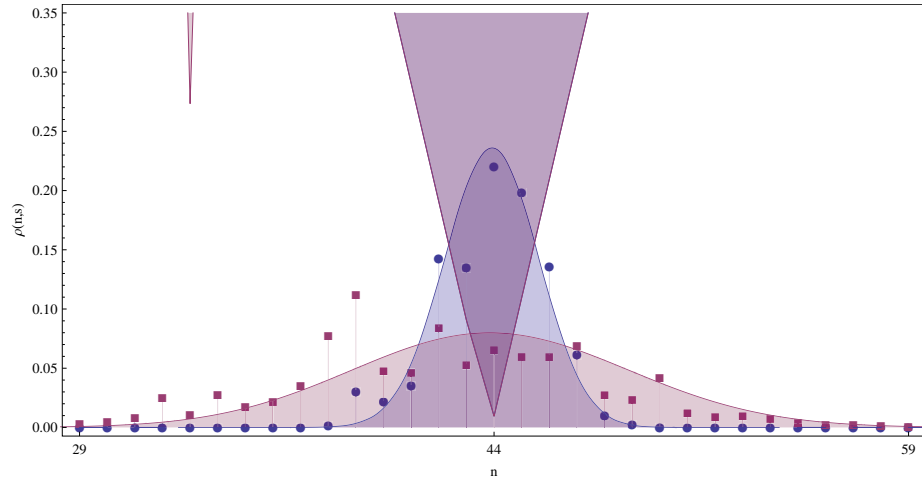
Figure 9.3: Simulation for the distribution of the number of particles p_n over n after
$s = 101$ steps of simulation

red line : for constant rates $\Gamma = \left(\int_{.1}^{.9} x^{-1} t_{.5}(x) dx \right)^{-1} = 0.434$, where $t_{.5}(x)$ is
the PDF of a triangular distribution with mean at 0.5 and width 0.8
blue line : for the same rate with feedback $g = .1$
red squares : one realization of random rates for the former distribution $t_{.5}(x)$.
blue dots : same realization with feedback $g = .1$. One can see
blue+red area (top) The outer boarder is the absolute value of the additional
feedback rate for random rates
red area (top) : additional feedback rate for random case.
For the simulation with a discrete time step approach the rate has to get a
value between 0 and 1, in contrast to the analytical calculation, where the
control part can becomes any value. As this gets affected for very large
or small rates, the feedback was bordered for the simulation.

moving potential. At this point it has to be mentioned that it was not proven
that the average random rate has the same shape as the clean rate with the
same waiting time. This facts implicate a discussion, which is handled in the
following outlook.

Chapter 10

Conclusion and Outlook

In this thesis the wide range of applications of the n-resolved Quantum Master Equation with variable tunneling rates was demonstrated.

It was shown that a microscopic derivation of the nQME is possible. A further step in this direction is to check if this derivation can be generalized to time resolved methods. In this context it should be possible to consider non Markovian effects. Therefore, a budding approach is the TCL[1]-method, which is discussed in [Breuer and Petruccione, 2002].

In a further step it was shown that the formalism for constant rates can be generalized for random distributed tunneling rates as well. The known results were reproduced for as special case in the clean limit, where a sharp distribution was investigated. It was pointed out that the mean of the inverse tunneling rates, the waiting times are the fundamental variables to describe random distributed current for systems without internal dynamics. The expected result that random rates lead to a decrease of the current and an increase of the Fano factor could be confirmed for all investigated sample setups. For a conclusion of these results see 6.2.5 on page 102. A software was developed to investigate arability setups. Thus, it would be simple to derive the current, Fano factor and higher order cumulants for Triple Quantum Dots etc. The next step is to investigate, which distributions occur in reality. A detailed research on a large number of PDFs without experimental background might be misleading.

The next step is to investigate, which distributions occur in reality. A detailed research on a large number of PDFs without experimental background might be misleading.

The FCS for shorter times were not investigated in detail. One approach was the small bandwidth approach. With this approach one is able to determine the shape of the average distribution for random rates. However, the precondition for that is that the derivation of the nQME is compatible with the investigated time scales.

Another point to continue the research is to connect the quantum mechanical

---

[1]time-convolution-less

waiting times [Brandes, 2008] with the (negative moment) waiting times of this thesis. By doing that, a gentle tool for experimental examinations could be created.

It was also shown that there are many other options to apply the nQME beyond randomness. For further investigations, especially the approach of combining Feedback Control with the random is an interesting topic.

Overall there are many possible connotations. Some of them are adumbrated in the * chapter.

However, if this research is being continued, the overall next step is to get a close relationship to the experiments and to compare the theoretical calculations with experimental data.

Appendix

Appendix A

Mathematical definitions and propositions

The following chapter contains the mathematical definitions and propositions, which were used in this thesis. As it concerns very simple mathematical sentences, it seems to be easier to formulate a fitting statement and proof it, instead of doing a literature research. Even so the sentences can be probably found in the appropriate books.

A.1 Basic statistic

Definition 5 $\langle \boxed{x} \rangle := \int_S \boxed{x}(\Gamma) f(\Gamma) \, d\Gamma$

Definition 6 (expected value) $\langle \boxed{x} \rangle$ *is the expected value with regard to all rates in expression* $\boxed{x}$*, where*

- *S is the region of all possible rates* [1]*,*
- *$\Gamma \in S$ is a vector, representing a set of rates Γ_α and*
- *f is the Probability Density Function (PDF).*

The Probability Density Function f has the following properties

- $\int_S f(\Gamma) \, d\Gamma = 1$
- $\forall \Gamma \in S : f(\Gamma) \geq 0$

Proposition 4 (separable case) *In the special case, when*

- *$S = \prod_\alpha S_\alpha$ is the Cartesian power of subsets S_α and*
- *the expression $\boxed{x} = \prod_\alpha \boxed{x}_\alpha$ is separable with respect to S_α,*

the expected value $\langle \boxed{x} \rangle_\Gamma = \prod_\alpha \langle \boxed{x}_\alpha \rangle_{\Gamma_\alpha}$*.*

---

[1] S was chosen with regard to the word Sample space

Proof

$$\langle \boxed{x} \rangle_S = \int_S \boxed{x}(\Gamma) f(\Gamma)\, d\Gamma$$

$$= \int_{S_1, S_2, \ldots} \cdots \int a_1(\Gamma_1) a_2(\Gamma_2) \ldots f_1(\Gamma_1) f_2(\Gamma_2) \ldots d\Gamma_1 d\Gamma_2 \ldots$$

$$= \underbrace{\int_{S_1} a_1(\Gamma_1) f_1(\Gamma_1)\, d\Gamma_1}_{\langle \boxed{x}_1 \rangle_{\Gamma_1}} \underbrace{\int_{S_2} a_2(\Gamma_2) f_2(\Gamma_2)\, d\Gamma_2}_{\langle \boxed{x}_2 \rangle_{\Gamma_2}} \ldots \tag{A.1}$$

Assumption 1 *Due to physical reasons, all rates are said to be positive real numbers.*

That means for S_α

$$S_\alpha \subset\,]0, \infty\, [. \tag{A.2}$$

For convenience we extend f_α to the whole range of reals

$$f_\alpha(x) := \begin{cases} 0 & x \leq 0 \vee x = \infty \\ f_\alpha(x) & \text{else (old definition).} \end{cases} \tag{A.3}$$

Cumulants

The relationship between moments and cumulants is [Wikipedia, 2010b]

$$c_n = m_n(t) - \sum_{k=1}^{n-1} \binom{n-1}{k-1} c_k m_{n-k}(t). \tag{A.4}$$

Special regard has to be taken to the displacement law, which was used in (3.50) and is a special case of the formula (A.4)

Proposition 5 (displacement law) *The variance of any random variable $\boxed{x}$:* $\left\langle (\boxed{x} - \langle \boxed{x} \rangle)^2 \right\rangle$ *can be rewritten by*

$$\left\langle (\boxed{x} - \langle \boxed{x} \rangle)^2 \right\rangle = \langle \boxed{x}^2 \rangle - \langle \boxed{x} \rangle^2. \tag{A.5}$$

Proof

$$\left\langle (\boxed{x} - \langle \boxed{x} \rangle)^2 \right\rangle = \langle \boxed{x}^2 - 2\boxed{x}\langle \boxed{x} \rangle)^2 + \langle \boxed{x} \rangle^2 \rangle = \langle \boxed{x}^2 \rangle - 2\langle \boxed{x}\langle \boxed{x} \rangle\rangle + \left\langle \langle \boxed{x} \rangle^2 \right\rangle = \langle \boxed{x}^2 \rangle - \langle \boxed{x} \rangle^2 \tag{A.6}$$

Proposition 6 (variance and Fano factor (Single Quantum Dot))

$$\forall \{a, b\} \in \mathbb{R}^+ : \frac{a^2 + b^2}{(a+b)^2} \geq \frac{1}{2} \tag{A.7}$$

Proof

$$\frac{a^2 + b^2}{a^2 + b^2 + 2ab} \geq \frac{1}{2} \tag{A.8}$$

$$\Leftrightarrow 2(a^2 + b^2) \geq a^2 + b^2 + 2ab \tag{A.9}$$

$$\Leftrightarrow a^2 + b^2 \geq 2ab \tag{A.10}$$

Without loss of generality we write $b > a \rightarrow b = a + \epsilon, \epsilon \geq 0$

$$\Leftrightarrow 2a^2 + 2a\epsilon + \epsilon^2 \geq 2a^2 + 2a\epsilon \tag{A.11}$$

$$\Leftrightarrow \epsilon^2 \geq 0. \tag{A.12}$$

Proof *Alternative* $(a - b)^2 \geq 0 \Rightarrow a^2 + b^2 \geq 2ab \Rightarrow 2(a^2 + b^2) \geq (a + b)^2$.

Proposition 7 (variance and Fano factor (ring))

$$\forall \{a_k\} \in \mathbb{R}^+ : \frac{\sum_{k=1}^{K} a_k^2}{(\sum_{k=1}^{K} a_k^2} \geq \frac{1}{K} \tag{A.13}$$

Proof *This sum can be rewritten to*

$$K \sum_{k=1}^{K} a_k^2 \geq \left(\sum_{k=1}^{n} a_k\right)^2 = \sum_{k=1}^{K} a_k^2 + 2 \sum_{\substack{i,j=1 \\ i \neq j}}^{K} a_i a_j \tag{A.14}$$

$$\Leftrightarrow (K - 1) \sum_{k=1}^{K} a_k^2 \geq +2 \sum_{\substack{i,j=1 \\ i \neq j}}^{K} a_i a_j. \tag{A.15}$$

Assuming, without loss of generality, $a_K \geq a_{K-1} \cdots > a_1$, *leads to* $a_k^2 \geq a_k a_j$, *with* $k \geq j$. *So it is sufficient to show that the n inequalities*

$$(K - 1)a_k \geq \sum_{j=1}^{k-1} a_j \tag{A.16}$$

are valid. This is obvious, because $K \geq k \geq j$.

Remark: Proposition 6 is a special case of proposition 7.

A.1.1 Positivity of Fano factor parameters

According to the Jenson inequality for every convex function $f(x)$, we have

$$f(\langle x \rangle) \leq \langle f(x) \rangle. \tag{A.17}$$

That means that

$$\langle x \rangle^{-k} \leq \langle x^{-k} \rangle. \tag{A.18}$$

Especially $k = 1$ leads to the fact that $\alpha \geq 0$. In the same style, one can show that $\langle x^2 \rangle \geq \langle x \rangle^2$ and $\langle x^{-2} \rangle \geq \langle x \rangle^{-2}$. The multiplication of these two inequalities leads to

$$\left\langle \frac{1}{x^2} \right\rangle \langle x^2 \rangle \geq \left\langle \frac{1}{x} \right\rangle^2 \langle x^2 \rangle = (1 + \alpha)^2. \tag{A.19}$$

Thus $\beta \geq 0$.

A.2   Features of Laplace Space

If there is no way to derive $m_k(t)$ analytically, one can use a Taylor Series at $z = 0$ if the long-time limit is in focus of interest. Due to the following proposition, it is sufficient to develop up to order $O(z)^0$.

Proposition 8 (order of Taylor Series for long-time limit) *The Inverse Laplace Transformation of z^k for $k > 0$ is $\underset{z \to t}{LT^{-1}}\{z^k\} = 0$ for $t \neq 0$.*

Proof

$$\underset{z \to t}{LT^{-1}}\{z^k\} = \frac{1}{2\pi i} \lim_{c_2 \to \infty} \int_{c_1 - ic_2}^{c_1 + ic_2} e^{zt} z^k \, dz, \tag{A.20}$$

which is a so called Bromwich Integral that can be calculated via the residual theorem. Obviously, the function $e^{zt}z^k$ has no residuals. Thus, the Bromwich integral evaluates to 0.

Proposition 9 *For a complex function $\hat{m}_1(z)$ that has no singularities in the region, where $Re(z) > 0$ and $\underset{z \to t}{LT^{-1}}\hat{m}_1(z) = m_1(t)m$, we have*

$$\lim_{t \to \infty} \partial_t m_1(t) = \lim_{z \to 0} z^2 \hat{m}_1(z). \tag{A.21}$$

Proof

$$\lim_{t \to \infty} \partial_t m_1(t) = \int_0^\infty \partial_t^2 m_1(t) dt + \partial_t m_1(0) \tag{A.22}$$

$$= \lim_{z \to 0} \int_0^\infty \partial_t^2 m_1(t) e^{-zt} dt + \partial_t m_1(0)$$

$$= \lim_{z \to 0} z^2 \hat{m}_1(z) - \lim_{z \to 0} z m_1(0)$$

$$= \lim_{z \to 0} z^2 \hat{m}_1(z)$$

A.3   Series Approximations

For a sharp distribution a series expansion at the mean value is possible as well.

While calculating the Taylor Series, the following proposition was used.

Proposition 10 (series of a product of function) *The Taylor Series of a product of two functions $f(z), g(z)$ of order k can be calculated as the first k orders of the product of the Taylor Series of order $k+1$ of f and g*

$$T_{k,fg}z = T_{k,f}(z) \cdot T_{k,g}(z) + O(z)^{k+1}. \tag{A.23}$$

Proof *The Taylor Polynomial (at point $a = 0$ of order k of function f) is defined as*

$$T_{k,f}(z) = \sum_{j=0}^{k} \frac{f^{(j)}(z)}{j!} z^j. \tag{A.24}$$

The product rule is

$$(f(z)g(z))^{(j)} = \sum_{l=0}^{j} \binom{j}{l} f^{(j-l)}(z) g^{(l)}(z) \tag{A.25}$$

with $\binom{j}{l} = \frac{j!}{l!(j-l)!}$.

Inserting (A.25) into (A.24) leads to

$$T_{k,f}(z) = \sum_{j=0}^{k} \frac{\sum_{l=0}^{j} \binom{j}{l} f^{(j-l)}(z) g^{(l)}(z)}{j!} z^j = \sum_{j=0}^{k} \sum_{l=0}^{j} \frac{f^{(j-l)}(z) g^{(l)}(z)}{l!\,(j-l)!} z^j. \tag{A.26}$$

Comparing with

$$T_{k,f}(z) \cdot T_{k,g}(z) = \left(\sum_{j=0}^{k} \frac{f^{(j)}(z)}{j!} z^j \right) \left(\sum_{j=0}^{k} \frac{g^{(j)}(z)}{j!} z^j \right) = \sum_{j=0}^{k} \sum_{l=0}^{j} \frac{f^{(j-l)}(z)}{(j-l)!} \frac{g^l(z)}{l!} z^j + O(z)^{k+1} \tag{A.27}$$

and collecting the terms of the same z^k, shows the result.

Proposition 11 (permutability of mean and series) *Let g be a function of Γ, z and $\langle g \rangle = \langle g(z, \Gamma) \rangle_\Gamma$ with $\partial_z(\Gamma) = 0$. Then it is possible to permute the calculation of mean and series.*

$$T_{k,\langle g \rangle}(z) = \langle T_{k,g}(z) \rangle \tag{A.28}$$
$$\tag{A.29}$$

Proof

$$
\begin{aligned}
T_{k,\langle g \rangle}(z) &= \sum_{j=0}^{k} \frac{\langle g^{(j)}(\Gamma, z) \rangle}{j!} z^j \\
&= \sum_{j=0}^{k} \frac{\int g^{(j)}(\Gamma, z) f(\Gamma) \, d\Gamma}{j!} z^j \\
&= \int \sum_{j=0}^{k} \frac{g^{(j)}(\Gamma, z)}{j!} z^j f(\Gamma) \, d\Gamma \qquad = \langle T_{k,g}(z) \rangle \tag{A.30}
\end{aligned}
$$

A.4 Special derivates

Proposition 12 (derivative of inverse matrices) *Let $A = A(x)$ be an invertible matrix, which only depends on x. Then one can calculate the derivative of the inverse matrix (A^{-1}) via*

$$\partial_x A^{-1} = -A^{-1}.\partial_x(A).A^{-1}. \tag{A.31}$$

Proof

$$
\begin{aligned}
\partial_x A^{-1} &= \partial_x(A^{-1}.A.A^{-1}) \\
&= \partial_x(A^{-1}).A.A^{-1} + A^{-1}.\left(\partial_x(A).A^{-1} + A.\partial_x A^{-1}\right) \\
&= 2\partial_x A^{-1} + A^{-1}.(\partial_x A).A^{-1} \\
&= -A^{-1}.(\partial_x A).A^{-1} \tag{A.32}
\end{aligned}
$$

Appendix B

Basic physic

In this chapter standard methods from quantum mechanics and statistics are repeated.

B.1 Liouville-von Neumann Equation

In this section the Liouville-von Neumann Equation will be derived from the Schrödinger Equation and expressed in superoperator form.

B.1.1 Schrödinger Equation

The well known time dependent Schrödinger Equation [Brandes, 2009, 1.30]

$$i\partial_t \Psi = H\Psi \tag{B.1}$$

can be expressed in bra- or ket-notation

$$\langle i\partial_t \Psi | = \langle H\Psi | \tag{B.2}$$

$$|i\partial_t \Psi \rangle = |H\Psi \rangle . \tag{B.3}$$

By using the hermitian property of the scalar product $\langle \alpha\Psi | \beta\Phi \rangle = \alpha^* \beta \langle \Psi | \Phi \rangle$ [Brandes, 2009, 2.72], it is possible to derive the time derivative of the state in bra- or ket-notation.

$$\partial_t |\Psi \rangle = -iH |\Psi \rangle \tag{B.4}$$

$$\partial_t \langle \Psi | = i \langle \Psi | H \tag{B.5}$$

B.1.2   Density matrix and Liouville-von Neumann Equation

The *density matrix* is defined as

$$\varrho_S := \sum_n p_n \, |n\rangle \, \langle n| \quad [Brandes, 2009, 3.43] \tag{B.6}$$

with the general properties:

$$\mathrm{Tr}\varrho_S = 1 \qquad\qquad \text{traceclass 1} \tag{B.7}$$

$$\varrho_S^\dagger = \varrho_S \qquad\qquad \text{Hermitian} \tag{B.8}$$

$$\varrho_S \geq 0 \qquad\qquad \text{positv semidefinit} \tag{B.9}$$

The time development is

$$\varrho = \varrho_H := \mathrm{U}\varrho_S\mathrm{U}^\dagger, \tag{B.10}$$

described via the *time-development-operator* [Brandes, 2009, 3.71]

$$\mathrm{U} = e^{-\mathrm{i}\mathrm{H}t} \tag{B.11}$$

$$\Rightarrow \partial_t\mathrm{U} = -\mathrm{i}\mathrm{H}\mathrm{U}. \tag{B.12}$$

$$\Rightarrow \partial_t\mathrm{U}^\dagger = \mathrm{i}\mathrm{U}^\dagger\mathrm{H}. \tag{B.13}$$

With the time derivatives and straight forward algebra, one computes [Brandes, 2009, 3.75]

$$\boxed{\partial_t\varrho = \mathrm{i}\,[\varrho, \mathrm{H}]\,, \qquad \textit{Liouville-von Neumann Equation.}} \tag{B.14}$$

B.1.3   Motivation: n-dependent tunneling rates
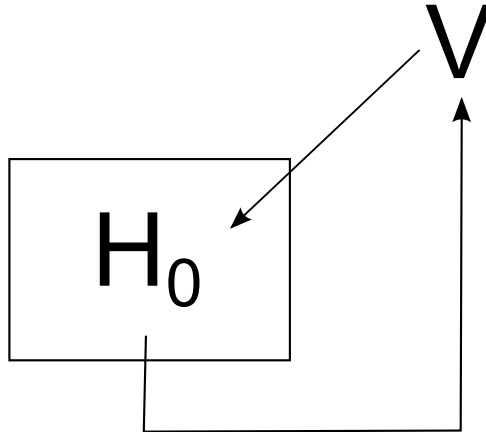
Figure B.1: Idea of n-dependent rates

The derivation of the full n-resolved Quantum Master Equation with n-dependent tunneling rates is quite long.

As a first simplification we start to derive n-dependent [1] tunneling rates after standard quantum mechanics methods (QMII Schöll,Brandes). Starting with a Hamiltonian, which depends on scalar function $n(t)$ and can be split into two parts

$$H(n(t)) = H_0 + V(n(t)), \tag{B.15}$$

where one depends on $n(t)$ and the other one not.

Assuming that $n(t)$ is a step-function, leads to the following form for $V(n(t))$ and can be written as

$$V(n(t)) = \begin{cases} V^{(1)} & 0 < t \leq t_1 \\ V^{(2)} & t_1 < t \leq t_2 \\ \dots \\ V^{(n)} & t_{n-1} < t \leq t_n \\ \dots \end{cases} \tag{B.16}$$

It has to be remarked that the t_i are completely unknown. Writing $V(n(t))$ stands for the expectation value of all possible realization, where n-1 steps happened after the time t ($\langle V(t_1, t_2, \dots, t_N, t) : t_{n-1} < t \leq t_n \rangle$). Thus, the (**??**) becomes

$$\partial_t \varrho(n(t)) = i[\varrho(n(t)), H(n(t))]. \tag{B.17}$$

With the assumption that the solution for H_0 is known, it is nearby to transform to an effective interaction picture

$$U_0 = e^{-iH_0 t} \tag{B.18}$$

$$\tilde{\varrho}(t, n(t)) := U^\dagger{}_0 \varrho(n(t)) U_0. \tag{B.19}$$

So with the product rule and the derivative for U, one becomes

$$\partial_t \tilde{\varrho}(t, n(t)) = -i\left[\tilde{\varrho}(n(t)), H_0\right] + U^\dagger{}_0 \left(\partial_t \varrho(n(t))\right) U_0 \tag{B.20}$$

$$= -i\left[\tilde{\varrho}, H_0\right] + U^\dagger{}_0 \left(i\left[\varrho, H_0 + V(n(t))\right]\right) U_0 \tag{B.21}$$

$$= -i\left[\tilde{\varrho}, H_0\right] + iU^\dagger{}_0 \left[\varrho, V\right] U_0 + iU^\dagger{}_0 \left[\varrho, H_0\right] U_0 \tag{B.22}$$

$$= -i\left[\tilde{\varrho}, H_0\right] + i\left[\tilde{\varrho}, \tilde{V}\right] U_0 + i\left[\tilde{\varrho}, H_0\right] \tag{B.23}$$

$$= i\left[\tilde{\varrho}(t, n(t)), \tilde{V}(t, n(t))\right], \tag{B.24}$$

where

$$\tilde{V}(t, n(t)) = e^{iH_0 t} V(n(t)) e^{-iH_0 t}. \tag{B.25}$$

The notations $,\tilde{\varrho}' := \tilde{\varrho}(t', n(t'))$ and the same for V ($\tilde{V} := \tilde{V}(t, n(t)), \tilde{V}' := \tilde{V}(t', n(t'))$) [2], as well as the definition $\int' = \int_{t_{n-1}}^{t} dt'$, helps to keep the text

---

[1] n has no physical interpretation yet. It does not stand for the number of particles, which have been transported through a Quantum Dot yet.

[2] In the literature s is sometimes used instead of t'

readable.

If one regards $\tilde{V}$ as a perturbation, it is self-evident that a perturbative expansion makes sense

$$\tilde{\varrho} = \tilde{\varrho}(t_{n-1}) + \mathrm{i} \int{}' \left[\tilde{\varrho}', \tilde{V}' \right], \tag{B.26}$$

$$\tag{B.27}$$

where $\tilde{\varrho}(t_{n-1})$ is the state, when the last jump process happened.

$$\tilde{\varrho} = \tilde{\varrho}(t_{n-1}) + \mathrm{i} \int{}' \left[\varrho(t_{n-1}), \tilde{V}' \right] + O(\tilde{V})^2 \tag{B.28}$$

$$\partial_t \tilde{\varrho} = \mathrm{i} \left[\varrho(t_{n-1}), \tilde{V} \right] - \int{}' \left[\left[\tilde{\varrho}', \tilde{V}' \right], \tilde{V} \right] \tag{B.29}$$

If we write the former equation in the basis-representation $\varrho_{a,b} = \langle a | \varrho | b \rangle$, it looks like this

$$\varrho_{a,b} = \varrho_{a-,b-} + \mathrm{i} \int{}' \left[\varrho_{a-,b-}, \tilde{V}' \right] + O(\tilde{V})^2. \tag{B.30}$$

B.2   Fermi's Golden Rule

To be consisted with the standard notation of Fermi's Golden Rule, the state notation is used instead of the density matrix notation for the next steps.

We start with

$$|\tilde{\psi}(t)\rangle = |\tilde{\psi}_0\rangle - \mathrm{i} \int_0^t dt' \, \tilde{V}(t') |\tilde{\psi}(t')\rangle. \tag{B.31}$$

For our problem we call the system-state at time $t = t_n : \psi_n$ (B.30)

$$|\tilde{\psi}(t)\rangle = |\tilde{\psi}_{n-1}\rangle - \mathrm{i} \int{}' \tilde{V}' |\tilde{\psi}_{n-1}\rangle + O(\tilde{V}')^2. \tag{B.32}$$

Assuming that the system is in the pure state $|\psi_{n-1}\rangle = |i\rangle$ at time $t = t_n$. The probability for a change from $|i\rangle$ to $|f\rangle$ with $i \neq f$ in the time region t_n $(t_{n-1} > t > t_{n+1})$ is given by

$$P_{n,i \to f}(t) := \left| \langle f | \tilde{\psi} \rangle \right|^2 = \left| \langle f | U_0{}^\dagger \psi \rangle \right|^2 = \underbrace{\left| e^{\mathrm{i}(\epsilon_f - \epsilon_i)t} \right|^2}_{1} |\langle f | \psi \rangle|^2 \tag{B.33}$$

$$= \left| \int{}' \langle f | \tilde{V}' | i \rangle \right|^2 = \left| \langle f | V^{(n)} | i \rangle \right|^2 \left| \int{}' e^{\mathrm{i}(\epsilon_f - \epsilon_i)t'} \right|^2 \tag{B.34}$$

$$= \left| V_{fi}^{(n)} \right|^2 \sin^2 \left(\frac{(t - t_{n-1})\Delta\epsilon}{2} \right) \left(\frac{2}{\Delta\epsilon} \right)^2 {}^3. \tag{B.35}$$

The rate is defined as $\Gamma_{i \to j} := \lim_{t \to \infty} \frac{1}{t} P_{i \to j}$.

$$\Gamma_{n,i \to j} = \lim_{t \to \infty} \frac{1}{t} P_{n,i \to j} = \lim_{t \to \infty} \frac{1}{t} \left| V_{fi}^{(n)} \right|^2 \sin^2 \left(\frac{(t - t_{n-1})\Delta\epsilon}{2} \right) \left(\frac{2}{\Delta\epsilon} \right)^2 \quad \text{(B.36)}$$

$$= \left| V_{fi}^{(n)} \right|^2 \lim_{t \to \infty} \frac{1}{t} \sin^2 \left(\frac{t\Delta\epsilon}{2} \right) \left(\frac{2}{\Delta\epsilon} \right)^2 = \left| V_{fi}^{(n)} \right|^2 \lim_{t \to \infty} t \operatorname{sinc}^2 \left(\frac{t\Delta\epsilon}{2} \right)$$
$$\text{(B.37)}$$

$$= \left| V_{fi}^{(n)} \right|^2 2\pi \lim_{2\gamma \to 0} \frac{1}{\pi 2\gamma} \operatorname{sinc}^2 \left(\frac{\Delta\epsilon}{2\gamma} \right) \quad \text{(B.38)}$$

$$= \left| V_{fi}^{(n)} \right|^2 2\pi \delta(\Delta\epsilon) \quad \text{(B.39)}$$

In the second line the definition of the rate hides a physical problem. When every real number t_{n-1} can be neglected in comparison to t, which is going to ∞, this question has to discussed on finite timescales. This problem is ignored at this point, because $\Gamma_{n,i \to j}$ will be derived from the waiting time distribution for experimental data.

In the last step $\pi^{-1} \operatorname{sinc}^2$ was used as normalized L^2 function for a dirac-series[4].

Thus, the definition for the n-dependent tunneling rates reads

Definition 7 $\Gamma_k^{(n)} := \sum_f \lim_{t \to \infty} \frac{1}{t} P_{n,k \to f} = 2\pi \sum_f \left| V_{fi}^{(n)} \right|^2 \delta(\epsilon - \epsilon_f)$

Replacing the rate in the QME with this n-dependent rates leads to the nQME.
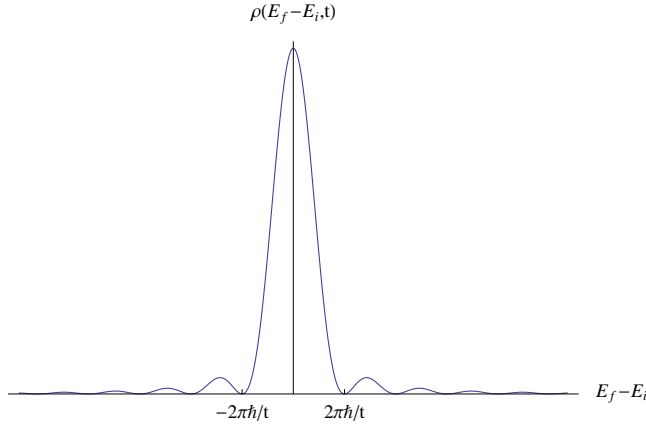
Figure B.2: sinc function

---

[3] $\Delta\epsilon = \epsilon_f - \epsilon_i$

[4] $\int_{-\infty}^{\infty} \operatorname{sinc}^2(x) \, dx = \pi$ and $\lim_{\gamma \to 0} \frac{1}{\gamma} f \left(\frac{x}{\gamma} \right) = \delta(x)$

B.3   Superoperator form

In linear algebra linear mappings from matrices to matrices are expressed by matrices.

$$\mathbb{K}^{n \times n} \times \mathbb{K}^{n \times n} \to \mathbb{K}^{n \times n} \tag{B.40}$$

This is done by expressing source and target of the matrices as vectors by choosing an appropriate basis and write the linear mapping as matrix concerning this basis. In this style the same can be done with linear operations from operators to operators called superoperators.

As an example, one regards the density matrix of a two level system as linear combination of *Pauli Matrices*.

$$\rho = \begin{pmatrix} x_1 \\ x_2 \\ x_3 \end{pmatrix}_\sigma = \begin{pmatrix} a & b \\ c & d \end{pmatrix}_{\rho_{i,j}} \tag{B.41}$$

$$\rho = \frac{1}{2} \sum_{i=0}^{4} x_i \sigma_i \tag{B.42}$$

$$\sigma_0 = \begin{pmatrix} 1 & 0 \\ 0 & 1 \end{pmatrix}, \quad \sigma_1 = \begin{pmatrix} 0 & 1 \\ 1 & 0 \end{pmatrix}, \quad \sigma_2 = \begin{pmatrix} 0 & -i \\ i & 0 \end{pmatrix}, \quad \sigma_3 = \begin{pmatrix} 1 & 0 \\ 0 & -1 \end{pmatrix}. \tag{B.43}$$

Obviously, $x_0 = 1$. Otherwise the trace (B.7) of the density-matrix would not be one. The formula $x_i = \mathrm{Tr}\sigma_i\rho$ helps to compute explicitly the basis-change. [5]

For the Liouville-von Neumann Equation this means (B.14)

$$\partial_t \varrho = \mathcal{L}\varrho, \tag{B.44}$$

where $\mathcal{L}$ is called Liouvillan, which is discussed in detail below.

B.3.1   Effective interaction picture

Regarding the case that the Hamiltonian is given in the form

$$\mathrm{H} = \mathrm{H}_0 + \lambda\mathrm{V}, \tag{B.45}$$

where $\lambda\mathrm{V}$ is a small perturbation for the Hamiltonian H_0 .

With the *free-time-evolution-operator* $\mathrm{U}_0 := e^{-i\mathrm{H}_0 t}$ for the unperturbed system (H_0) and its hermitian conjugate (h.c) $\mathrm{U}^\dagger_0 := e^{i\mathrm{H}_0 t}$, one defines $\tilde{\varrho} := \mathrm{U}_0 \varrho \mathrm{U}^\dagger_0$.

Thus, the Liouville-von Neumann Equation in the interaction picture reads

$$\partial_t \tilde{\varrho} = \lambda \tilde{\mathcal{L}} \tilde{\varrho} \tag{B.46}$$

---

[5]An Mathematica Program concerning Pauli Matrices can be found at `http://homepage.cem.itesm.mx/lgomez/quantum/v7pauli.pdf`

with $\tilde{\mathcal{L}} := \mathrm{i}\left[\boxed{x}, \tilde{V}\right]$ [6]. With $\tilde{\varrho}_0 = \tilde{\varrho}(t=0), \tilde{\mathcal{L}}' := \mathrm{i}\left[\boxed{x}, \tilde{V}(t')\right]$ [7], as well as the definition $\int' = \int_0^t dt'$, which helps to keep the text readable, $\tilde{\varrho}$ reads

$$\tilde{\varrho} = \tilde{\varrho}_0 + \int' \tilde{\mathcal{L}}' \tilde{\varrho}'. \tag{B.47}$$

---

[6]H_0 disappears, because of the product-rule $\partial_t \tilde{\varrho} = \partial_t(U^\dagger{}_0)\varrho U_0 + U^\dagger{}_0 \varrho \partial_t(U_0) + U^\dagger{}_0(\partial_t \mathcal{L}\varrho)U^\dagger{}_0 = -\mathrm{i}[\varrho, H_0] + \mathrm{i}[\varrho, H_0] + \mathrm{i}\lambda[\varrho, U^\dagger{}_0 V U_0]$

[7]In the literature s is sometimes used instead of t'

Appendix C

Calculations

C.1 Higher moments

As this is a quiet long expression even for the first moment, the following short hand notation makes sense for higher moments. The superoperator

$$\hat{\mathcal{T}}(z) := \left(\lim_{i\chi \to 0} e^{i\chi} \hat{\mathcal{W}}(z) \cdot \frac{1}{1 - e^{i\chi} \hat{\mathcal{W}}(z)} \right) = \left(\hat{\mathcal{W}}(z) \cdot \hat{\mathcal{G}}_0(z) \right) . \tag{C.1}$$

$$\tag{C.2}$$

Therefore, one defines a custom trace function with the short hand notation

$$\mathrm{TrC}\boxed{x} = \mathrm{Tr}\boxed{x} \cdot \hat{\mathcal{P}}(z) \cdot \hat{\mathcal{G}}_0(z) \cdot \rho_0. \tag{C.3}$$

The coefficients $c(n, k)$ can be calculated as a nested sum of the first k integer numbers. The iteration step looks for example like this $1 + 2 + 3 \to 1 + 2(1 + 2) + 3(1 + 2 + 3)$. These numbers comes from the derivative.

With the help of the standard differentiation rules and the incremental use of (A.31), the first six moments evaluate to

$$\hat{m}_1(z) = \mathrm{CTr}\left(\hat{\mathcal{T}}(z) \right) \tag{C.4}$$

$$\hat{m}_2(z) = \mathrm{CTr}\left(\hat{\mathcal{T}}(z) + 2! \, \hat{\mathcal{T}}^2(z) \right) \tag{C.5}$$

$$\hat{m}_3(z) = \mathrm{CTr}\left(\hat{\mathcal{T}}(z) + 3 \cdot 2! \, \hat{\mathcal{T}}^2(z) + 3! \, \hat{\mathcal{T}}^3(z) \right) \tag{C.6}$$

$$\hat{m}_4(z) = \mathrm{CTr}\left(\hat{\mathcal{T}}(z) + 7 \cdot 2! \, \hat{\mathcal{T}}^2(z) + 6 \cdot 3! \, \hat{\mathcal{T}}^3(z) + 4! \, \hat{\mathcal{T}}^4(z) \right) \tag{C.7}$$

$$\hat{m}_5(z) = \mathrm{CTr}\left(\hat{\mathcal{T}}(z) + 15 \cdot 2! \, \hat{\mathcal{T}}^2(z) + 25 \cdot 3! \, \hat{\mathcal{T}}^3(z) + 10 \cdot 4! \, \hat{\mathcal{T}}^4(z) + 5! \, \hat{\mathcal{T}}^5(z) \right) \tag{C.8}$$

$$\hat{m}_6(z) = \mathrm{CTr}\left(\hat{\mathcal{T}}(z) + 31 \cdot 2! \, \hat{\mathcal{T}}^2(z) + 90 \cdot 3! \, \hat{\mathcal{T}}^3(z) + 65 \cdot 4! \, \hat{\mathcal{T}}^4(z) + 15 \cdot 5! \, \hat{\mathcal{T}}^5(z) + 6! \, \hat{\mathcal{T}}^6(z) \right) \tag{C.9}$$

In that way even higher moments look quite simple.

The kernel of higher moments has been calculated with the help of the Mathematica function `nQMEMomMatGen`.

Listing C.1: General form of the moments.

```
    (* ::Package:: *)

  3 (*Define a custom matrix product with standard attributes*)
    Attributes[SmallCircle] = {Flat, OneIdentity};(*SmallCircle is something like a matrix product (.)*)
    SmallCircle /: a_o(b_ + c_) := aob + aoc;
    SmallCircle /: a_o(k_Integer*b__) := k*aob;
    SmallCircle /: (k_Integer*a_ob__)oc_ :=  k*aoboc;
  8
    (*D[_,χ]-->d*)
    d::usage = "Someting like a differential-operator for matrices concerning χ";
    d[R] := Rod[W]oR (*see AA EqRefRWR ZZ *)
    d[W] = W;(*W does not depend on chi*)
 13 (*Standard differntiation rules*)
    d[x_oy_] := d[x]oy + xod[y];
    d[k_Integer*b__] := k*d[b];
    d[a_ + b_] := d[a] + d[b]
    d[1, b__] := d[b];
 18 d[n_, b__] := d[d[n - 1, b]];
    (*rewrite Rules to keep the result short*)
    TzRul := {WoR -> Tz[1], Tz[n_]oTz[k_] -> Tz[n + k]} (*find WR*)
    CTrace1Rul := RoTz[k_] -> 1/k! Tz[k] (*Replace with Tz*)

 23 (*the exported function*)
    nQMEMomMatGen[k_] := nQMEMomMatGen[k] = Expand[d[k, R]]//. TzRul  /. CTrace1Rul;(*keep the evaluated
        values*)
```

Taking a look to the coefficients of $\hat{\mathcal{T}}^k(z)$ leads to the following observations.

- The derivative produces terms in the form $k! \left(\hat{\mathcal{W}}(z).\hat{\mathcal{G}}_0(z) \right)^k$. Therefore, $\hat{\mathcal{T}}^k(z)$ was defined in the way it is.

- The coefficients $c(n,k)$ can be calculated as a nested sum of the first k integer numbers. The iteration step looks for example like this $1 + 2 + 3 \rightarrow 1 + 2(1+2) + 3(1+2+3)$. These numbers comes from the derivative

$$c(n,k) = \tilde{c}(n-k+1, k) \tag{C.10}$$

$$\text{with} \quad \tilde{c}(s,k) = \begin{cases} \sum_{i=1}^{k} i\tilde{c}(s-1, i) & s > 1 \\ 1 & \text{else} \end{cases} \tag{C.11}$$

Following the general formula reads

$$\hat{m}_n(z) = \text{CTr} \sum_{k=1}^{n} c(n,k) k! \, \hat{\mathcal{T}}^k(z)^k. \tag{C.12}$$

So one can calculate high cumulants in a very short time.

Listing C.2: Improved algorithm. First 100 moments in less than 1 second.

```
    Coeff[s_, k_] :=  Coeff[s, k] = If[s > 1, Sum[i*Coeff[s - 1, i], {i, 1, k}], 1];
    Coeffn[n_, k_] := Coeff[n - k + 1, k];
    nQMEMomMatGen[n_] := nQMEMomMatGen[n] = Sum[Coeffn[n, k]*Tz[k], {k, 1, n}];
```

C.1.1 Single Quantum Dots

For the Single Quantum Dot the higher cumulants read

$$\hat{m}_1(z) = \frac{W_R(z)(P_L(z) + P_R(z)W_L(z))(\rho_{00}W_L(z) + \rho_{01})}{(W_L(z)W_R(z) - 1)^2} \tag{C.13}$$

$$\hat{m}_2(z) = -\frac{W_R(z)(W_L(z)W_R(z) + 1)(P_L(z) + P_R(z)W_L(z))(\rho_{00}W_L(z) + \rho_{01})}{(W_L(z)W_R(z) - 1)^3} \tag{C.14}$$

$$\hat{m}_3(z) = \frac{W_R(z)(W_L(z)W_R(z)(W_L(z)W_R(z) + 4) + 1)(P_L(z) + P_R(z)W_L(z))(\rho_{00}W_L(z) + \rho_{01})}{(W_L(z)W_R(z) - 1)^4} \tag{C.15}$$

$$\hat{m}_4(z) = -\frac{W_R(z)(W_L(z)W_R(z) + 1)(W_L(z)W_R(z)(W_L(z)W_R(z) + 10) + 1)(P_L(z) + P_R(z)W_L(z))}{(W_L(z)W_R(z) - 1)^5}$$

$$\cdot (\rho_{00}W_L(z) + \rho_{01}) \tag{C.16}$$

$$\hat{m}_5(z) = \frac{(W_L(z)W_R(z)(W_L(z)W_R(z)(W_L(z)W_R(z)(W_L(z)W_R(z) + 26) + 66) + 26) + 1)}{(W_L(z)W_R(z) - 1)^6}$$

$$\cdot (P_L(z) + P_R(z)W_L(z))W_R(z)(\rho_{00}W_L(z) + \rho_{01}) \tag{C.17}$$

$$\hat{m}_6(z) = -\frac{(W_L(z)W_R(z)(W_L(z)W_R(z)(W_L(z)W_R(z)(W_L(z)W_R(z) + 56) + 246) + 56) + 1)}{(W_L(z)W_R(z) - 1)^7}$$

$$\cdot W_R(z)(W_L(z)W_R(z) + 1)(P_L(z) + P_R(z)W_L(z))(\rho_{00}W_L(z) + \rho_{01}) \tag{C.18}$$

C.2 Alternatives

C.2.1 Vector-Notation*

One idea was to use the vector notation. The disadvantage of this approach is that one has to deal with vectors of infinite length. Starting from [Emary, 2009, 9.12] in vector notation with

$$\partial_t \rho^{(n)}(t) = \mathcal{L}_0 \rho^{(n)}(t) + \mathcal{J} \rho^{(n)}(t)(n - 1, t). \tag{LvN.n}$$

For convenience the short notation $\boxed{x}_i = \begin{cases} \boxed{x}_L & i \text{ Odd} \\ \boxed{x}_R & i \text{ Even} \end{cases}$ and $\boxed{x}_{\bar{i}} = \begin{cases} \boxed{x}_R & i \text{ Odd} \\ \boxed{x}_L & i \text{ Even} \end{cases}$

is used.

$$\sigma_i = \begin{cases} \rho^{(n)}(t)_{,0}(i/2, t) & i \text{ Even} \\ \rho^{(n)}(t)_{,1}(\frac{i-1}{2}, t) & i \text{ Odd} \end{cases}$$

$$\mathcal{K}_{i,j} = \delta_{i-1,j}\Gamma_{\bar{i}} - \delta_{i,j}\Gamma_i$$

$$\partial_t \sigma = \mathcal{K}\sigma$$

Hence, the propagator

$$G = \frac{1}{z - \mathcal{K}}$$

yields to a lower triangle matrix,

we introduce $k_R = \mathfrak{L}_R(z)\Gamma_L$ and $k_L = \mathfrak{L}_L(z)\Gamma_R$ [1]

- The diagonal-elements are $G_{i,i} = \mathfrak{L}_i$

- The off-diagonal-elements can be calculated recursively by
  $G_{i,j} = \theta_0(i - j)G_{i-1,j}k_i$

... to be continued (see Mathematica Notebooks)

---

[1] If Γ becomes n-dependent, only the definition of k has to be changed.

C.2.2 The other dimension of randomness*

A further step is to calculate the variance of $\hat{\rho}_n(z)$ as well.

$$\left\langle (\hat{\rho}_n(z) - \langle \hat{\rho}_n(z) \rangle)^2 \right\rangle \tag{C.19}$$

Definition 8 $V_{n,n';z,z'} := \langle \hat{\rho}_n(z) \rho_{n'z'} \rangle$

For this model $V_{n,n';z,z'}$ is with (5.7)

$$V_{n,n';z,z'} = \left\langle \left(\frac{1}{z + \Gamma^{(n)}} \prod_{k=0}^{n-1} \frac{\Gamma^{(k)}}{z + \Gamma^{(k)}} \right) \left(\frac{1}{z + \Gamma^{(n')}} \prod_{k'=0}^{n'-1} \frac{\Gamma^{(k')}}{z + \Gamma^{(k')}} \right) \right\rangle. \tag{C.20}$$

It is no restriction to assume $n \geq n'$. That means

$$V_{n,n';z,z'} = \left\langle \prod_{k=0}^{n'-1} \frac{\Gamma^{(k)2}}{(z + \Gamma^{(k)})(z' + \Gamma^{(k)})} \prod_{k=n'+1}^{n-1} \frac{\Gamma^{(k)}}{z + \Gamma^{(k)}} \frac{\Gamma^{(n')}}{(z'+\Gamma^{(n')})(z+\Gamma^{(n')})(z+\Gamma^{(n)})} \right\rangle$$

$$V_{n,n';z,z'} = \left\langle \prod_{j=0}^{n'-1} \frac{\Gamma^{(j)2}}{(z + \Gamma^{(j)})(z' + \Gamma^{(j)})} \right\rangle \left\langle \prod_{j=n'}^{n-2} \frac{\Gamma^{(j)}}{z + \Gamma^{(j)}} \right\rangle \left\langle \frac{\Gamma^{(n-1)}}{(z'+\Gamma^{(n-1)})(z+\Gamma^{(n-1)})} \right\rangle \left\langle \frac{1}{z+\Gamma^{(n)}} \right\rangle$$

$$\tag{C.21}$$

with

$$\left\langle \prod_{j=0}^{n'-1} \frac{\Gamma^{(j)2}}{(z + \Gamma^{(j)})(z' + \Gamma^{(j)})} \right\rangle = \left(1 + \frac{z^2}{z' - z} L(z) + \frac{z'^2}{z - z'} L(z') \right)^{n'} \tag{C.22}$$

(sign change!!)

$$\left\langle \frac{\Gamma^{(n-1)}}{(z' + \Gamma^{(n-1)})(z + \Gamma^{(n-1)})} \right\rangle = \frac{z}{z - z'} L(z) + \frac{z'}{z' - z} L(z'). \tag{C.23}$$

$V_{n,n';z,z'}$ evaluates to

$$V_{n,n';z,z'} = \left(1 + \frac{z^2}{z' - z} L(z) + \frac{z'^2}{z - z'} L(z') \right)^{n'} (1 + zL(z))^{n-n'-1} \left(\frac{z}{z - z'} L(z) + \frac{z'}{z' - z} L(z') \right) L(z). \tag{C.24}$$

However, as no application for this variance could be found, this approach was not being continued.

Appendix D

Software

D.1 Mathematica Package nQME

Download The package can be downloaded at

`https://fcs.physikerwelt.de/wiki/nQME-Package`

Installation After having downloaded, the software has to be decompressed into the folder `$UserBaseDirectory/Applications`, where `$UserBaseDirectory` can be obtained by typing `$UserBaseDirectory` into a blank Mathematica Notebook. Afterwards, there should be a file `$UserBaseDirectory/Applications/nQME/Ramdom.m`.

Initialization `Needs["nQME`Random`"]` initializes the package

source The full source code from the main package

Listing D.1: Source of the main package.

```
     (* ::Package:: *)

     (* Mathematica Package *)

  5  (* Created by the Wolfram Workbench Feb 23, 2010 *)

     BeginPackage["nQME`Random`"]
     (* Exported symbols added here with SymbolName::usage *)
     (*Put here unprotect clear*)
 10  nQMESetL0::usage="The Liouvillian"
     nQMESetJ::usage="The Jump-Operator"
     nQMESetTraceFunction::usage="The trace function."
     nQMESetAssumptions::usage="Assumptions used for to simplify the trace"
     nQMESetRandomVariables::usage="The variables assumed to be random"
 15  nQMESetMethod::usage="Set Method to \"matrix\" or MGF"


 20  nQMEMomMatGen::usage="Gives a general expression for the matrices of the moments. The moments are
            obtained by tracing that matrix."
     Tz::usage="Def .."
     Tau::usage="Def .."
     Mu::usage="Def .."
     Cum::usage="Def .."
 25  Kurt::usage="Def .."
     Scrw::usage="Def .."
     nQMEILt::usage="Gives the current for the long time limit"
     nQMEFanoLt::usage="Fano Factor"
     nQMECumLt::usage="Fano Factor"
```

147

```
30  CleanLimit::usage="CleanLimit"
    CleanLimitG::usage="CleanLimit concerning tunnel rates"

    CentralMomentForm::usage="Central Moments"
    CumulantForm::usage="Cumulants"
35  DistNamedForm::usage="Central Moments with Scrwness and Kurt"
    GenTex::usage="Generates Latex Code"
    \[Tau]::usage="waiting time"
    \[CapitalGamma]::usage="tunnel rate"
    GenTexMom::usage=""
40  MGenFkt::usage=""
    z::usage=""
    χ::usage=""
    Erw::usage=""

45
    Begin["`Private`"]


50  Clear[R,W,P,WE,PE,RE];
    (*Set initial conditions*)
    nQMESetL0[Mat_]:=(s=SessionTime[];L0:=Mat);
    nQMESetJ[Mat_]:=(s=SessionTime[];J:=Mat);
    nQMESetTraceFunction[Mat_]:=(s=SessionTime[];TraceFunction:=Mat);
55  nQMESetAssumptions[Mat_]:=(s=SessionTime[];TraceKond:=Mat);
    nQMESetRandomVariables[Mat_]:=(s=SessionTime[];nDependent:=Mat);
    nQMESetMethod[Meth_]:=(s=SessionTime[];method:=Meth);
    (*general Form for Moments in z-space*)
    Print["Load moment function"];
60  Get["nQME`momGenImp`"];
    (*Seperation aproach*)
    Seperate[Expression_, Var_] :=
      Module[{Dep = 1, InDep = 1, Fkt, Exp = Factor[Expression]},
        Fkt[subexp_] :=
65       If[Or[MemberQ[subexp, Var, Infinity], MatchQ[subexp, Var]],
          Dep *= subexp, InDep *= subexp];
        If[ ! (Head[Exp] === Times), Fkt[Exp],
         Map[Fkt, Exp]]; Return[{Dep, InDep}]];


70
    (*rules for ERW*)
    Erw[gl_^n_Integer, gl_] := Tau[-n, gl];(* /; n < 0*)
    (*Erw[gl_,gl_]:=Tau[-1,gl]*)

75  Erw /: D[Erw[x_, y_], z_] := Erw[D[x, z], y]
    Erw /: Series[Erw[x_, y_], z__] := Erw[Series[x, z], y]
    Erw[a_ + b_, z_] := Erw[a, z] + Erw[b, z]

    Erw[k_Integer, x_] := k
80  Erw[k_Integer*y_, x_] := k*Erw[y, x]
    ErwRul0 := Erw[x_, y_] :> Erw[ExpandAll[x], y];
    ErwRul1 := {Erw[s_*Erw[x_, y_Symbol], z_Symbol] :>
      Erw[s*Erw[x, y] /. ErwRul, z],
     Erw[Erw[x_, y_], z_] :> Erw[Erw[x, y] /. ErwRul, z]}
85  ErwRul2 :=
     Erw[x_, y_Symbol] :>
      Module[{Sep = Seperate[x, y]}, Sep[[2]]*Erw[Sep[[1]], y]];

    ErwRul3:= Erw[gl_,gl_]->Tau[-1,gl];
90  (*Transformation function for expectation value*)
    TF1[e_] := e /. ErwRul0 /. ErwRul1 /. ErwRul2 /.ErwRul3(**)


    Ser[e_, k_] := e /. Erw[x_, y_] :> NewErw[x, y, k]
95
     (*claculation of the expectation value with seperation of x*)
    NewErw[x_, y_, k_] :=
     TF1@Normal@
      Module[{},(*Print["Called with "];Print[{x,y,k}];*)
100     If[MemberQ[x, Erw[_, _], Infinity] || MatchQ[x, Erw[_, _]],
          Module[{Erg = Seperate[x, Erw[_, _]], Dep = 1,
           InDep = 2},(*Print[Erg[[Dep]]];*)

           If[MemberQ[Erg[[InDep]], z, Infinity],
105          If[MatchQ[Erg[[Dep]], Erw[_, _]],
             If[Erg[[Dep, 2]] =!= y,
               (*Print["case1"];*)
               Erw[Ser[Erw[Erg[[Dep, 1]]*Erg[[InDep]], Erg[[Dep, 2]]], k],
                y],
110            Throw["not implemented one" + Erg]
               ],
              Throw["not implemented two" + Erg]
              ],
           (*Print["no z dep"];*)
115
             Erw[Erg[[InDep]]*Ser[Erg[[Dep]], k], y]]],
          TF1@Normal@Erw[Series[x, {z, 0, k + 1}], y] + O[z]^(k + 1)]];

    SepErw[Exp_, Var_] :=
120  Module[{Seperated = Seperate[Exp, Var]},
     Erw[Seperated[[1]], Var]*Seperated[[2]]]


    ErwGen[Exp_] := Erw[Exp, nDependent];
125  MatErw[L_] := Map[ErwGen[#] &, L, {2}]
    ErwExpFkt[e_] :=
     Collect[Simplify@e /.
       Erw[Exp__, Dep_List] :> Fold[SepErw[#1, #2] &, Exp, Dep], z]
```

```
       ctSer1[n_] :=
130  ctSer1[n,s] =
       Simplify[mtSer[[n]] -
         Sum[Binomial[n - 1, k - 1] ctSer1[k] mtSer[[n - k]], {k, n - 1}]]


135  Clear[dim];
     dim:=pDim[s]=Dimensions[L0][[1]]

     PSpc  := PSpci[s] = FullSimplify[Inverse[z IdentityMatrix[dim] - L0]];
     WSpc  := WSpci[s] = J.PSpc;
140  (*R=Inverse[IdentityMatrix[dim]-W];*)
     WE := WEi[s]= MatErw[WSpc];
     PE := PEi[s]= MatErw[PSpc];
     RE := REi[s]= Inverse[IdentityMatrix[dim] - WE];
     REchi := REchii[s]= Inverse[IdentityMatrix[dim] -Exp[I χ] WE];
145
     MomMatSpc[k_] := MomMatSpc[k,s]= nQMEMomMatGen[k] /. Tz[l_] -> l!*PE.RE.MatrixPower[WE.RE, l];
     MGenFkt:= ErwExpFkt@((TraceFunction@((PE.REchi))));
     mzSer[k_] := mzSer[k,s]= If[TrueQ[method=="matrix"], Ser[Limit[D[MGenFkt,{χ,k}],χ->0]/I^k, k + 1];
     ,mzSer[k,s]= Ser[ErwExpFkt@((TraceFunction@ MomMatSpc[k])), k +1]]; (*gives a Series aproximation with
             O[z]^k term*)
150  mzSer0[k_]:= mzSer[k,s]=Simplify@Collect[1/z*Normal[z*mzSer[k]+O[z]],z]; (*this is speed*)
     mtSer[k_] :=mtSer[k,s]= Simplify[InverseLaplaceTransform[mzSer0[k], z, t],
         t > 0 && TraceKond];


     ctSer[n_] :=
155  ctSer[n,s] =
       Simplify[mtSer[n] - Sum[Binomial[n - 1, k - 1] ctSer[k] mtSer[n - k], {k, n - 1}]];


     nQMEFanoLt := Simplify@
       Limit[Simplify[ctSer[2]/ctSer[1], TraceKond], t -> Infinity];
160  nQMECumLt[k_] :=
      Simplify@
        Limit[Simplify[ctSer[k]/ctSer[1], TraceKond],
         t -> Infinity]


165  nQMEILt := m1LT[s]=Simplify[Limit[z^2*mzSer[1], z -> 0], TraceKond];


     REP[Ord_]:=Table[Tau[n,x_]->Sum[Binomial[n,k]Mu[k,x] Tau[1,x]^(n-k),{k,0,n}],{n,Ord,1,-1}]; (*Replaces
             moments of the waiting time distribution by central Momements.*)
     Tau[0,x_]:=1;
170  Mu[0,x_]:=1;
     Mu[1,x_]:=0;
     REPC[Ord_]:=Table[Tau[n,x_]->Cum[n,x]+Sum[Binomial[n-1,k-1]Cum[k,x] Tau[n-k,x],{k,1,n-1}],{n,Ord
             ,1,-1}];
     sRep:=Mu[3,x_]->Scrw[x] Mu[2,x]^(3/2);
     kRep:=Mu[4,x_]->Kurt[x] Mu[2,x]^2;
175  CleanLimit[x_]:=((x/.Tau[n_,y_]->Subscript[\[Tau],y]^(n)));
     CleanLimit[x_,s_]:=((x/.Tau[n_,s]->Subscript[\[Tau],s]^(n)));
     CleanLimitG[x_]:=((x/.Tau[n_,y_]->Subscript[\[CapitalGamma],y]^(-n)));
     CleanLimitG[x_,s_]:=((x/.Tau[n_,s]->Subscript[\[CapitalGamma],s]^(-n)));
     CentralMomentForm[x_,o_]:=x/.REP[o];
180  CumulantForm[x_,o_]:=x/.REPC[o];
     DistNamedForm[x_,o_]:=CentralMomentForm[x,o]/.kRep/.sRep
     TexRulesLog := {RegularExpression[
         "\\\\text\\{Erw\\}(\\\\left)?\\((.*?),(.*?)(\\\\right)?\\)"] ->
       "\\Erw{$2}_{$3}",RegularExpression["\\\\text\\{Tau\\}(\\\\left)?\\((.*?),(.*?)(\\\\right)?\\)"] ->
185    "\\TAU{$2}_{$3}",
       RegularExpression["\\\\text\\{SmallTau\\}(\\\\left)?\\((.*?)(\\\\right)?\\)"] ->
         "\\tau_{$2}"}
     TexRules := {"\\Gamma _L" -> "\\GL", "\\Gamma _R" -> "\\GR",
       " i " -> "\\I ", "\\Gamma _T" -> "\\GT",
190    "\\text{Tz}("~~x_~~")"->"\\Tz["~~x~~"]",
         "\\TAU{" ~~ x_ ~~ "}_{"~~y_~~"}" :> "\\TAU" ~~IntegerString[ToExpression[x], "Roman"]~~"{"~~y~~"}
             ",
         "\\TAU{-" ~~ x_ ~~ "}_{"~~y_~~"}" :> "\\TAUm" ~~IntegerString[ToExpression[x], "Roman"]~~"{"~~y~~
             "}" };


      GenTex[tex_] :=
195    StringReplace[StringReplace[StringReplace[ToString[TeXForm[tex]], TexRulesLog], TexRulesLog],
       TexRules];


     GenTexMom[n_]:=Module[ {out=""},
     For[i=1,i<=n,i++,
200  out=out~~ "\\mz"~~ToString[i]~~" &=& \\MyTrace {\\left("~~GenTex[nQMEMomMatGen[i]]~~ "\\right)} \\\\ \
             n";
     ]out];

     End[]

205  EndPackage[]
     Print["nQME`Random was loaded."];
```

D.2   Double Quantum Dot

As a demonstration, the application of the program to the Double Quantum Dot example is listed below.

For convenience the output is set as TEX equations.

Listing D.2: Sample for use of nQME for DQD.

```
(* ::Package:: *)

Needs["nQME`Random`"](*Initialize tha package*)
nQMESetL0[Transpose[{{-L,L,0,0,0},{0,0,0,0,-T},{0,0,-R,0,T},{0,0,0,-1/2R,\[Epsilon]},{0,2T,-2T,-\[
        Epsilon],-1/2R}}]];  (*specify the DQD Liouvillian. Here just the subscript of \[CapitalGamma]
        is given*)
5 nQMESetJ[Normal[SparseArray[{{1,3}->R},{5,5}]]];(*and the jump part*)
nQMESetRandomVariables[{L,R,T}]; (*Specify variables that should be treated as random*)
TraceFunction[Mat_]:=Tr[((Mat.{p00,p11,p22,p12,p21}))[[1;;3]]]; (*The tracefunction of the
        Superoperator*)
nQMESetTraceFunction[TraceFunction];
nQMESetAssumptions[p00+p11+p22==1];(*Toal density matrix at t=0 shold have Tr 1*)
10 ILt=nQMEILt(*Calculate the current*)
GenTex[ILt]  (*pass output to latex*)
CleanLimit[ILt](*Calculate the clean limit with waiting times*)
GenTex[%](*pass output to latex*)
FanoLt=FullSimplify@CleanLimit[#,L]&@CleanLimit[#,T]&@nQMEFanoLt (*calculate the FanoFactor with clean
        (L,T)*)
15 GenTex[FanoLt]  (*pass to latex out...with some special mods\]*)
FanoLtG=FullSimplify@CleanLimitG[#,L]&@CleanLimitG[#,T]&@nQMEFanoLt (*FanoFactor with Gamma istead of
        t*)
GenTex[FanoLtG] (*pass to latex out...with some special mods\]*)
FCl=FullSimplify@CleanLimit[FanoLt] (*clean limit for fano factor*)
GenTex[FCl](*pass output to latex*)
```

First the system is specified. After the evaluation of the system, the variable
ILT has the value of long-time current

$$\langle I_\infty \rangle = \frac{4}{4\langle \tau_L \rangle + 4\langle \tau_R \rangle \left(\epsilon^2 \langle \tau_T^2 \rangle + 2\right) + \langle \Gamma_R \rangle \langle \tau_T^2 \rangle}. \tag{D.1}$$

The clean limit one can get via CleanLimit[ILt]

$$\langle I_\infty \rangle_{cln} = \frac{4}{4\tau_L + 4\tau_R \left(\epsilon^2 \tau_T^2 + 2\right) + \frac{\tau_T^2}{\tau_R}} \tag{D.2}$$

Modifing the Random variables to nQMESetRandomVariables[{R}]; FanoLt = nQMEFanoLt // FullSimplify;

$$\langle F_\infty \rangle_{,rnd,R} =$$
$$\frac{\Gamma_L{}^2 \left(-\left(4\left(2T_C{}^2 + \epsilon^2\right)\langle \tau_R \rangle + \langle \Gamma_R \rangle\right)^2 + 32\left(T_C{}^2 + \epsilon^2\right)\left(4T_C{}^2 + \epsilon^2\right)\langle \tau_R^2 \rangle + 2\langle \Gamma_R^{-2} \rangle\right)}{\left(4\left(\Gamma_L\left(2T_C{}^2 + \epsilon^2\right)\langle \tau_R \rangle + T_C{}^2\right) + \Gamma_L\langle \Gamma_R \rangle\right)^2}$$
$$+ 8\frac{\left(\Gamma_L{}^2\left(T_C{}^2 + 2\epsilon^2\right) + 2T_C{}^4\right)}{\left(4\left(\Gamma_L\left(2T_C{}^2 + \epsilon^2\right)\langle \tau_R \rangle + T_C{}^2\right) + \Gamma_L\langle \Gamma_R \rangle\right)^2} \tag{D.3}$$

$$\langle F_\infty \rangle_{,rnd,R} \left(\tau_T^2\left(4\epsilon^2\langle \tau_R \rangle + \langle \Gamma_R \rangle\right) + 8\langle \tau_R \rangle + 4\tau_L\right)^2 =$$
$$8\tau_T^2\left(20\epsilon^2\langle \tau_R^2 \rangle -\right.$$
$$2\langle \tau_R \rangle \left(4\epsilon^2\langle \tau_R \rangle + \langle \Gamma_R \rangle\right) + 1\right) + \tau_T^4\left(-\left(-32\epsilon^4\langle \tau_R^2 \rangle + \left(4\epsilon^2\langle \tau_R \rangle + \langle \Gamma_R \rangle\right)^2 - 2\langle \Gamma_R^{-2} \rangle - 16\epsilon^2\right)\right)$$
$$- 64\left(\langle \tau_R \rangle^2 - 2\langle \tau_R^2 \rangle\right) + 16\tau_L^2$$

$$\langle F_\infty \rangle = \frac{8\tau_R^2\left(2\Gamma_L{}^2\tau_R^2\left(4T_C{}^4 + 6T_C{}^2\epsilon^2 + \epsilon^4\right) + \Gamma_L{}^2\left(\epsilon^2 - T_C{}^2\right) + 2T_C{}^4\right) + \Gamma_L{}^2}{\left(4\tau_R\left(\Gamma_L\tau_R\left(2T_C{}^2 + \epsilon^2\right) + T_C{}^2\right) + \Gamma_L\right)^2}$$

$$\tag{D.4}$$

$$= \frac{16\tau_L^2\tau_R^2 + 8\tau_R^2\tau_T^2\left(12\epsilon^2\tau_R^2 - 1\right) + \tau_T^4\left(4\epsilon^2\tau_R^2 + 1\right)^2 + 64\tau_R^4}{\left(4\tau_R\left(\tau_L + \tau_R\left(\epsilon^2\tau_T^2 + 2\right)\right) + \tau_T^2\right)^2} \tag{D.5}$$

D.3   Sample Notebooks

List of sample notebooks that can be downloaded at `https://fcs.physikerwelt.de/wiki/SampleNotebooks`. In the text the following notebooks where referenced explicitly.

`https://fcs.physikerwelt.de/wiki/NB:SmallBWBar`   (NB:SmallBWBar)

`https://fcs.physikerwelt.de/wiki/NB:SimSD`   (NB:SimSD)

`https://fcs.physikerwelt.de/wiki/NB:Ham2Lio`   (NB:Ham2Lio)

`https://fcs.physikerwelt.de/wiki/NB:autoMW`   (NB:autoMW)

`https://fcs.physikerwelt.de/wiki/NB:QuasiClassical`
(NB:QuasiClassical)

Lists and References

List of Figures

List of Tables

Bibliography

[BMB, 2011] (2011). Nanotechnologie - eine Zukunftstechnologie mit Visionen.

[Bagrets and Nazarov, 2003] Bagrets, D. A. and Nazarov, Y. V. (2003). Full counting statistics of charge transfer in Coulomb blockade systems. *Physical Review B*, 67(8).

[Belzig, 2005] Belzig, W. (2005). Full Counting Statistics of Mesoscopic Electron Transport. *AIP Conference Proceedings*, pages 480–483.

[Brandes, 2007] Brandes, T. (2007). *Statistische Mechanik I - Computergestützte Methoden*.

[Brandes, 2008] Brandes, T. (2008). Waiting Times and Noise in Single Particle Transport. *Ann. Phys. (Berlin)*, Ann.:Phys.17,No.7,477–496(2008).

[Brandes, 2009] Brandes, T. (2009). *Quantenmechanik (I) Vorlesung*.

[Brandes, 2010] Brandes, T. (2010). Feedback Control of Quantum Transport. *Physical Review Letters*, 105(6):1–4.

[Breuer and Petruccione, 2002] Breuer, H.-P. and Petruccione, F. (2002). *The Theory of Open Quantum Systems*. Oxford University Press, USA.

[Büttiker, 1992] Büttiker, M. (1992). Scattering theory of current and intensity noise correlations in conductors and wave guides. *Physical Review B*, 46(19):12485–12507.

[Comtet, 1974] Comtet, L. (1974). *The Art of Finite and Infinite Expansions*.

[Datta, 1995] Datta, S. (1995). *Electronic Transport in Mesoscopic Systems*. Cambridge Studies in Semiconductor Physics and Microelectronic Engineering. Cambridge University Press.

[Datta, 1997] Datta, S. (1997). *Electronic transport in mesoscopic systems*. Cambridge University Press.

[Emary, 2009] Emary, C. (2009). *Theory of Nanostructures*.

[Fano, 1947] Fano, U. (1947). Ionization Yield of Radiations. II. The Fluctuations of the Number of Ions. *Physical Review*, 72(1):26–29.

[Flindt, 2007] Flindt, C. (2007). *Electrons in Nanostructures*. PhD thesis, Technical University of Denmark.

[Flindt et al., 2010a] Flindt, C., Novotný, T., Braggio, A., and Jauho, A.-P. (2010a). Counting statistics of transport through Coulomb blockade nanostructures: High-order cumulants and non-Markovian effects. *Physical Review B*, 82(15):1–25.

[Flindt et al., 2010b] Flindt, C., Novotný, T., Braggio, A., and Jauho, A.-P. (2010b). Counting statistics of transport through Coulomb blockade nanostructures: High-order cumulants and non-Markovian effects. *Physical Review B*, 82(15).

[Flindt et al., 2008] Flindt, C., Novotný, T., Braggio, A., Sassetti, M., and Jauho, A.-P. (2008). Counting Statistics of Non-Markovian Quantum Stochastic Processes. *Physical Review Letters*, 100(15):1–4.

[Flindt et al., 2004] Flindt, C., Novotný, T., and Jauho, A.-P. (2004). Current noise in a vibrating quantum dot array. *Physical Review B*, 70(20):1–21.

[Flindt et al., 2005] Flindt, C., Novotný, T., and Jauho, A.-P. (2005). Full counting statistics of nano-electromechanical systems. *Europhysics Letters (EPL)*, 69(3):475–481.

[Fujisawa et al., 2004] Fujisawa, T., Hayashi, T., Hirayama, Y., Cheong, H. D., and Jeong, Y. H. (2004). Electron counting of single-electron tunneling current. *Applied Physics Letters*, 84(13):2343.

[Gardiner et al., 1986] Gardiner, C. W., Bhat, U. N., Stoyan, D., Daley, D. J., Kutoyants, Y. a., and Rao, B. L. S. P. (1986). Handbook of Stochastic Methods for Physics, Chemistry and the Natural Sciences. *Biometrics*, 42(1):226.

[Gurvitz and Prager, 1996] Gurvitz, S. and Prager, Y. (1996). Microscopic derivation of rate equations for quantum transport. *Physical Review B*, 53(23):15932–15943.

[Gustavsson et al., 2005] Gustavsson, S., Leturcq, R., Simovic, B., Schleser, R., Ihn, T., Studerus, P., Ensslin, K., Driscoll, D. C., and Gossard, A. C. (2005). Counting statistics of single-electron transport in a quantum dot. *Solid State Physics*, 1:1–5.

[Hanson et al., 2006] Hanson, R., Kouwenhoven, L. P., Petta, J. R., Tarucha, S., and Vandersypen, L. M. K. (2006). Spins in few-electron quantum dots. *Applied Physics*, page 52.

[Herbort, 2008] Herbort, G. A. P. D. (2008). Analysis III.

[Jäckle, 1978] Jäckle, J. (1978). *Einfürung in die Transporttheorie*. Vieweg.

[J.Jacack, 1998] J.Jacack (1998). *Quantum Dots*, volume 268. Wiley-VCH.

[Kambly et al., 2010] Kambly, D., Flindt, C., and B, M. (2010). Factorial cumulants reveal interactions in counting statistics.

[Kato, 2004] Kato, A. (2004). On reduced dynamics of quantum-thermodynamical systems.

[Knuth, 1974] Knuth, D. E. (1974). Surreal Numbers. *American Mathematical Monthly*, 82(10):1023.

[Kühne and Reineker, 1978] Kühne, R. and Reineker, P. (1978). Nakajima-Zwanzig's generalized master equation: evaluation of the kernel of the integro-differential equation. *Z Physik B*, 31(1):105–110.

[L et al., 1966] L, Y. L., Roberts, G. E., and Kaufman, H. (1966). Table of Laplace Transforms. *Mathematics of Computation*, 20(96):631.

[Lambert, 2005] Lambert, N. (2005). *Critical Entanglement and Noise in Mesoscopic Systems*. PhD thesis, University ofManchester.

[Lenstra, 1982] Lenstra, D. (1982). Photon-number statistics in resonance fluorescence. *Physical Review A*, 26(6):3369–3377.

[Levitov et al., 1996] Levitov, L. S., Lee, H., and Lesovik, G. B. (1996). Electron counting statistics and coherent states of electric current. *Journal of Mathematical Physics*, 37(10):4845.

[Lindblad, 1979] Lindblad, G. (1979). Non-Markovian quantum stochastic processes and their entropy. *Communications in Mathematical Physics*, 65(3):281–294.

[Lu et al., 2003] Lu, W., Ji, Z., Pfeiffer, L., West, K. W., and Rimberg, A. J. (2003). Real-time detection of electron tunnelling in a quantum dot. *Nature*, 423(6938):422–425.

[Ming-Kuei, 1962] Ming-Kuei, H. (1962). Visual pattern recognition by moment invariants. *IEEE Transactions on Information Theory*, 8(2):179–187.

[Nakajima, 1958] Nakajima, S. (1958). On Quantum Theory of Transport Phenomena. *Progress of Theoretical Physics*, 20(6):948–959.

[Nazarov, 1993] Nazarov, Y. (1993). Quantum interference, tunnel junctions and resonant tunneling interferometer. *Physica B: Condensed Matter*, 189(1-4):57–69.

[Nazarov and Blanter, 2009] Nazarov, Y. and Blanter, Y. (2009). *Quantum transport: introduction to nanoscience*. Cambridge university press.

[Nazarov and Division, 2003] Nazarov, Y. V. and Division, N. A. T. O. S. A. (2003). *Quantum noise in mesoscopic physics*. Springer.

[Pöltl, 2008] Pöltl, C. (2008). Dunkelzustände im Transport durch gekoppelte Quantenpunkte. Master's thesis, Technische Universität Berlin.

[Reulet et al., 2003] Reulet, B., Senzier, J., and Prober, D. E. (2003). Environmental Effects in the Third Moment of Voltage Fluctuations in a Tunnel Junction. *Physical Review Letters*, 91(19):1–4.

[Schaller et al., 2009] Schaller, G., Kiesslich, G., and Brandes, T. (2009). Transport Statistics of Interacting Double Dot Systems: Coherent and Non-Markovian Effects. *Physical Review B*, 80(24):24.

[Schöll, 1998] Schöll, E. (1998). *Theory of Transport Properties of Semiconductor Nanostructures (Electronic Materials Series)*. Springer.

[Skobel'tsyn and Wood, 1972] Skobel'tsyn, D. and Wood, J. (1972). *Quantum Electronics in Lasers and Masers: Pt. 2 (Lebedev Physics Institute)*. Plenum Publishing Corporation.

[Sohn et al., 1997] Sohn, L. L., Schön, G., and Kouwenhoven, L. P. (1997). *Mesoscopic Electron Transport (NATO Science Series E: (closed))*. Springer.

[Stoof and Nazarov, 1996] Stoof, T. and Nazarov, Y. (1996). Time-dependent resonant tunneling via two discrete states. *Physical Review B*, 53(3):1050–1053.

[Thomsen and Gumlich, 2008] Thomsen, C. and Gumlich, H.-E. (2008). *Ein Jahr für die Physik*. Wissenschaft + Technik Verlag.

[Weisstein,] Weisstein, E. W. Moment-Generating Function – from Wolfram MathWorld.

[Weisstein, 2010a] Weisstein, E. W. (2010a). Central Moment. From MathWorld–A Wolfram Web Resource.

[Weisstein, 2010b] Weisstein, E. W. (2010b). Raw Moment. From MathWorld–A Wolfram Web Resource.

[Wikipedia, 2010a] Wikipedia (2010a). Fermis Goldene Regel — Wikipedia{,} Die freie Enzyklopädie.

[Wikipedia, 2010b] Wikipedia (2010b). Kumulante — Wikipedia{,} Die freie Enzyklopädie.

[Wilczek, 2007] Wilczek, F. (2007). Fundamental Constants. page 20.

[Zedler et al., 2009] Zedler, P., Schaller, G., Kiesslich, G., Emary, C., and Brandes, T. (2009). Weak-coupling approximations in non-Markovian transport. *Physical Review B*, 80(4):1–8.

[Zwanzig, 1960] Zwanzig, R. (1960). Ensemble Method in the Theory of Irreversibility. *The Journal of Chemical Physics*, 33(5):1338.

The bibliography has become quite long during the work phase. Most of the entries below have influenced this thesis peripherally. Special regard has to be taken to [Pöltl, 2008] or [Brandes, 2007], [Emary, 2009, Flindt, 2007, Breuer and Petruccione, 2002] and [Brandes, 2008, Brandes, 2010].

Index

Glossary

any object ($\boxed{\text{x}}$) Any object, TEX-Command: `Any`, Occurrence: 59
        Arguments: $[x]$

bath annihilation operator (b_k) , TEX-Command: `bk`, Occurrence: 10
        Arguments: $[k]$
bath creation operator ($b_k^\dagger$) , TEX-Command: `bkD`, Occurrence: 11
        Arguments: $[k]$
bbra ($\langle\!\langle\boxed{1}|$) , TEX-Command: `bbra`, Occurrence: 5
        Arguments: $\boxed{1}$
binominal ($\left(\boxed{\genfrac{}{}{0pt}{}{1}{2}}\right)$) , TEX-Command: `Choose`, Occurrence: 18
        Arguments: $\boxed{1}\boxed{2}$

commutator ($\left[\boxed{1},\boxed{2}\right]$) , TEX-Command: `Comm`, Occurrence: 58
        Definition: $\left[\boxed{1},\boxed{2}\right] \equiv \boxed{1}\boxed{2} - \boxed{2}\boxed{1}$
        Arguments: $\boxed{1}\boxed{2}$
ct ($c_n(t)$) , TEX-Command: `ct`, Occurrence: 16
        Arguments: $[n]$
   ctLt ($c_{n,\infty}$) , TEX-Command: `ctLt`, Occurrence: 5
        Arguments: $[n]$
   ctSer ($\bar{c}_n(t)$) , TEX-Command: `ctSer`, Occurrence: 6
        Arguments: $[n]$
   cz ($\hat{c}_{\boxed{x}}(z)$) , TEX-Command: `cz`, Occurrence: 3
        Arguments: $\boxed{x}$
custom trace (CTr) Categorie: **Operator**, custom trace function, TEX-Command:
        `MyTrace`, Occurrence: 8
        Definition: $\text{CTr} \equiv \text{Tr}\hat{\mathcal{P}}(z).\hat{\mathcal{G}}_0(z).\boxed{x}.\rho_0$
        Description: Definition for CTr applied to $\boxed{x}$

dagger ($\boxed{1}^{\dagger}$) Categorie: **Suffix**, , TEX-Command: `Dagger`, Occurrence: 85

Arguments: $\boxed{1}$

. 18, 20–23, 58, 59, 75, 96, 97, 134–136, 138, 139, 166, 169, 172, 173

den ($\mathfrak{L}$) , TEX-Command: `den`, Occurrence: 4

. 144, 166

denL ($\mathfrak{L}_L(z)$) , TEX-Command: `denL`, Occurrence: 2

. 144, 166

denR ($\mathfrak{L}_R(z)$) , TEX-Command: `denR`, Occurrence: 2

. 144, 166

density matrix (ϱ) Categorie: **Operator**, without index full density matrix, TEX-Command: `DMat`, Occurrence: 259

. 12–23, 95, 96, 134–136, 138, 139, 166

density matrix ($\hat{\rho}_\chi(z)$) , TEX-Command: `rxz`, Occurrence: 43

Definition: $\hat{\rho}_\chi(z) \equiv \sum_{n=0}^{\infty} \hat{\rho}_n(z)e^{\mathrm{i}n\chi}$

. 28–31, 33, 44, 49, 50, 55, 56, 62, 97–100, 107, 114, 166

density matrix of bath ($\varrho_{B,0}^{(N')}$) , TEX-Command: `DMatBN`, Occurrence: 16

Arguments: $[N']$

. 18, 22, 95, 96, 166

density matrix of bath ($\varrho_{B,0}^{(n)}$) , TEX-Command: `DMatBn`, Occurrence: 3

Arguments: $[n]$

. 95, 96, 166

DMatT ($\tilde{\varrho}$) , TEX-Command: `DMatT`, Occurrence: 22

Definition: $\tilde{\varrho} \equiv \mathrm{U}_0 \varrho \mathrm{U}^{\dagger}_0$

. 14–17, 19, 138, 139, 166

DMatTS ($\tilde{\varrho}'$) , TEX-Command: `DMatTS`, Occurrence: 15

Definition: $\tilde{\varrho}' \equiv \tilde{\varrho}(t', n(t'))$

. 15–17, 19, 23, 139, 166

initial density matrix ($\hat{\rho}_0(z)$) Categorie: **operator**, , TEX-Command: `rNz`, Occurrence: 3

. 31, 166

irrelevant propagation initial system density matrix ($\hat{\rho}_{0,\mathrm{SD}}(z)$) Categorie: **Operator**, , TEX-Command: `rNzSD`, Occurrence: 8

Definition: $\hat{\rho}_{0,\mathrm{SD}}(z) \equiv \begin{pmatrix} P_L(z) & \frac{P_L(z)}{W_L(z)} \\ P_R(z)W_L(z) & P_R(z) \end{pmatrix} \rho_0$

. 62, 63, 166

n-t ($\rho^{(n)}(t)$) conditioned density operator in n, time space, TEX-Command: `rnt`, Occurrence: 123

Arguments: $[n]$

. 9, 10, 17, 22, 23, 26–28, 31, 33, 44, 47, 59–61, 75, 96–98, 100, 108, 110, 113, 115, 119, 143, 166, 167, 172

n-z ($\hat{\rho}_n(z)$) , TEX-Command: `rnz`, Occurrence: 53

Definition: $\hat{\rho}_n(z) \equiv \mathop{\mathrm{LT}}_{t \to z} \rho^{(n)}(t) = \int_0^{\infty} e^{-zt}\rho^{(n)}(t)\,\mathrm{d}t, \quad z \in \mathbb{C}$

Arguments: $[n]$

. 28–30, 44, 48–50, 55, 61, 62, 66, 97, 98, 107, 108, 116, 145, 166, 173

rntA ($\rho_{\boxed{1}}(t)$) , TEX-Command: `rntA`, Occurrence: 11

Arguments: $\boxed{1}\boxed{2}$

Gxz $(\hat{\mathcal{G}}_\chi(z))$, TEX-Command: `Gxz`, Occurrence: 21

Definition: $\hat{\mathcal{G}}_\chi(z) \equiv \left(1 - e^{i\chi}\hat{\mathcal{W}}(z)\right)^{-1}$

. 28–31, 34, 35, 44, 62, 169, 170

HB (H_B) , TEX-Command: `HB`, Occurrence: 4

. 20, 169

heaviside theta $(\Theta\,(\boxed{1}))$ Categorie: **Distribution**, , TEX-Command: `DistU`,
Occurrence: 2

Arguments: $\boxed{1}$

. 55, 169

HI $(H_{S,B})$, TEX-Command: `HI`, Occurrence: 5

. 20, 96, 169

HN (H_0) Categorie: **Operator**, , TEX-Command: `HN`, Occurrence: 20

. 135, 138, 139, 169, 173

ILt $(\langle I_\infty\rangle)$, TEX-Command: `ILt`, Occurrence: 43

Definition: $\langle I_\infty\rangle \equiv \lim_{t\to\infty}\partial_t m_1(t)$

Arguments: $[]$

. 33, 39, 49–53, 63, 71, 74–76, 78–80, 85, 94, 97, 98, 100–102, 116, 119,
120, 150, 169

    ILtCl $(I_{\infty,\mathrm{cln}})$, TEX-Command: `ILtCl`, Occurrence: 7

Definition: $I_{\infty,\mathrm{cln}} \equiv \lim_{t\to\infty}\partial_t m_1(t)$

. 51, 63, 78, 169

imagninar unit (i) Categorie: **constant**, , TEX-Command: `I`, Occurrence:
191

. 16, 21, 22, 28–31, 33–35, 37–39, 44, 49, 50, 54–56, 59, 62, 71, 73, 77,
97, 98, 100, 101, 107, 113, 114, 116, 130, 133–136, 138, 139, 141, 166,
167, 169, 170, 172, 173

initial density matrix (ρ_0) , TEX-Command: `rN`, Occurrence: 74

. 26–31, 35, 36, 44, 48, 61–64, 66, 77, 97, 116, 141, 143, 165, 166, 169

Interaction Hamiltonian (V) , TEX-Command: `V`, Occurrence: 93

. 16, 17, 20, 21, 96, 135, 136, 138, 139, 169, 170, 173, 174, *see* HI

Irrelevant (Q) Categorie: **Projector**, Projects on irrelevant part of Hilbert
space, TEX-Command: `pQ`, Occurrence: 51

Definition: $Q \equiv 1 - P$

. 12–14, 95, 96, 169, 173

ja (j_α) , TEX-Command: `ja`, Occurrence: 4

Definition: $j_\alpha \equiv \begin{cases} \sqrt{\Gamma_L}\,|1\rangle\langle 0| & \alpha = L \\ \sqrt{\Gamma_R}\,|0\rangle\langle 1| & \alpha = R \end{cases}$

. 59, 169

jan $(j_\alpha^{(n')})$, TEX-Command: `jan`, Occurrence: 3

Definition: $j_\alpha^{(n')} \equiv \begin{cases} \sqrt{\Gamma_L^{(n')}}\,|n';1\rangle\langle 0;n'| & \alpha = L \\ \sqrt{\Gamma_R^{(n')}}\,|n'+1;0\rangle\langle 1;n'| & \alpha = R \end{cases}$

. 59, 169

    jad $(j^\dagger{}_\alpha)$, TEX-Command: `jad`, Occurrence: 3

. 59, 169

    jand $(j^\dagger{}_\alpha{}^{(n'')})$, TEX-Command: `jand`, Occurrence: 3

. 59, 169

Definition: $U_0 \equiv e^{-iH_0 t}$
. 138, 139, 166, 172, 173

UND $(U^{\dagger}_0)$, TEX-Command: `UND`, Occurrence: 8
Definition: $U^{\dagger}_0 \equiv e^{iH_0 t}$
. 138, 139, 166, 173

Time development $(\mathcal{U}^{\dagger}(t, t'))$ Categorie: **Superoperator**, , TEX-Command: `SOUD`, Occurrence: 6
Definition: $\mathcal{U}^{\dagger}(t, t') \equiv T_{\leftarrow} e^{\int_{t'}^{t} ds Q\mathcal{L}(s)}$
Arguments: $[t']$
. 13, 173

SOUN $(\mathcal{U}_0(t, t_0))$, TEX-Command: `SOUN`, Occurrence: 2
Arguments: $[t_0]$
. 15, 173

SOUND $(\mathcal{U}^{\dagger}_0(t, t_0))$, TEX-Command: `SOUND`, Occurrence: 9
Arguments: $[t_0]$
. 14, 15, 173

TMean $(\langle \tau \rangle)$, TEX-Command: `TMean`, Occurrence: 4
Definition: $\langle \tau \rangle \equiv \langle \tau \rangle$
. 71, 173

Trace (Tr) Categorie: **Multilinear Operator**, , TEX-Command: `Tr`, Occurrence: 31
. 26, 27, 33–36, 44, 48, 62, 63, 97, 99, 100, 134, 138, 141, 165, 170, 173

Bath $(\mathrm{Tr}_B \, [\![\underline{x}]\!])$, TEX-Command: `TrB`, Occurrence: 6
Definition: $\mathrm{Tr}_B \, [\![\underline{x}]\!] \equiv \sum \langle B| \, H \, |B\rangle$
Arguments: $\underline{x}$
. 16, 18, 173

Custom (TrC) , TEX-Command: `CTr`, Occurrence: 2
. 141, 173

relevant $(\mathrm{Tr}_B^{(N)} \, (\underline{x}))$, TEX-Command: `TrBN`, Occurrence: 17
Definition: $\mathrm{Tr}_B^{(N)} \, (\underline{x}) \equiv \sum \langle N_\alpha; k_{\alpha 1}, \ldots, k_{\alpha N}| \, \underline{x} \, |N_\alpha; k_{\alpha 1}, \ldots, k_{\alpha N}\rangle$
Arguments: $[N]\underline{x}$
. 16, 18, 21–23, 173

relevant (subspace) $(\mathrm{Tr}_B^{(n)} \, (\underline{x}))$, TEX-Command: `TrBn`, Occurrence: 17
Definition: $\mathrm{Tr}_B^{(n)} \, (\underline{x}) \equiv \sum_\alpha \langle N(n, \alpha) k_{\alpha 1}, \ldots, k_{\alpha N}| \, \underline{x} \, |N(n, \alpha); k_{\alpha 1}, \ldots, k_{\alpha N}\rangle$
Arguments: $\underline{x}$
. 16, 17, 20, 95, 96, 173

Tz $(\hat{\mathcal{T}}^k(z))$ Categorie: **Superoperator**, , TEX-Command: `Tz`, Occurrence: 28
Definition: $\hat{\mathcal{T}}^k(z) \equiv \left(\lim_{i\chi \to 0} e^{i\chi \hat{\mathcal{W}}(z)} . \frac{1}{1 - e^{i\chi} \hat{\mathcal{W}}(z)} \right)^k = \left(\hat{\mathcal{W}}(z) . \hat{\mathcal{G}}_0(z) \right)^k$
Arguments: $[k]$
. 52, 71, 141, 142, 173

Var (Var) , TEX-Command: `Var`, Occurrence: 11
. 38, 65, 72, 84, 99, 100, 173

var $(V_{n,n';z,z'})$, TEX-Command: `var`, Occurrence: 7
Definition: $V_{n,n';z,z'} \equiv \langle \hat{\rho}_n(z) \rho_{n'z'} \rangle$
. 145, 173

VT $(\tilde{V})$, TEX-Command: `VT`, Occurrence: 21
Definition: $\tilde{V} \equiv \tilde{V}(t, n(t))$

VTS ($\tilde{V}'$) , TEX-Command: `VTS`, Occurrence: 7

Definition: $\tilde{V}' \equiv \tilde{V}(t', n(t'))$

waiting time ($\left\langle \tau^{\boxed{x}} \right\rangle$) expectation value of first negative moment, TEX-Command: `TAU`, Occurrence: 261

Definition: $\left\langle \tau^{\boxed{x}} \right\rangle \equiv \int \tau^{\boxed{x}} \tilde{f}(\tau) d\tau = \left\langle \Gamma^{-\boxed{x}} \right\rangle$

Arguments: $[]\boxed{x}$

TAUII ($\left\langle \tau^2_{\boxed{x}} \right\rangle$) , TEX-Command: `TAUII`, Occurrence: 50

Definition: $\left\langle \tau^2_{\boxed{x}} \right\rangle \equiv \left\langle \tau^2_{\boxed{x}} \right\rangle$

Arguments: $\boxed{x}$

TAUIV ($\left\langle \tau^4_{\boxed{x}} \right\rangle$) , TEX-Command: `TAUIV`, Occurrence: 7

Definition: $\left\langle \tau^4_{\boxed{x}} \right\rangle \equiv \left\langle \tau^4_{\boxed{x}} \right\rangle$

Arguments: $\boxed{x}$

TAUmI ($\left\langle \Gamma_{\boxed{x}} \right\rangle$) , TEX-Command: `TAUmI`, Occurrence: 23

Definition: $\left\langle \Gamma_{\boxed{x}} \right\rangle \equiv \left\langle \frac{1}{\tau_{\boxed{x}}} \right\rangle$

Arguments: $\boxed{x}$

TAUmII ($\left\langle \Gamma^{-2}_{\boxed{x}} \right\rangle$) , TEX-Command: `TAUmII`, Occurrence: 8

Definition: $\left\langle \Gamma^{-2}_{\boxed{x}} \right\rangle \equiv \left\langle \frac{1}{\tau^2_{\boxed{x}}} \right\rangle$

Arguments: $\boxed{x}$

TI ($\langle \tau_\Sigma \rangle$) , TEX-Command: `TI`, Occurrence: 9

Definition: $\langle \tau_\Sigma \rangle \equiv \langle \tau_R \rangle + \langle \tau_L \rangle$

TII ($(\langle \tau^2_R \rangle + \langle \tau^2_L \rangle)$) , TEX-Command: `TII`, Occurrence: 4

Definition: $(\langle \tau^2_R \rangle + \langle \tau^2_L \rangle) \equiv \langle \tau^2_R \rangle + \langle \tau^2_L \rangle$

TLI ($\langle \tau_L \rangle$) , TEX-Command: `TLI`, Occurrence: 30

Definition: $\langle \tau_L \rangle \equiv \langle \Gamma^{-1}_L \rangle$

TLII ($\langle \tau^2_L \rangle$) , TEX-Command: `TLII`, Occurrence: 12

Definition: $\langle \tau^2_L \rangle \equiv \langle \Gamma^{-2}_L \rangle$

TRI ($\langle \tau_R \rangle$) , TEX-Command: `TRI`, Occurrence: 28

Definition: $\langle \tau_R \rangle \equiv \langle \Gamma^{-1}_R \rangle$

TRII ($\langle \tau^2_R \rangle$) , TEX-Command: `TRII`, Occurrence: 12

Definition: $\langle \tau^2_R \rangle \equiv \langle \Gamma^{-2}_R \rangle$